ARMY PROJECT ORDER NO: 88PP8863

TITLE: FATE OF COLORED SMOKE DYES

PRINCIPAL INVESTIGATOR: Arthur W. Garrison
AUTHORS: George L. Baughman, Eric J. Weber, Rebecca L. Adams, Mary Sue Brewer

CONTRACTING ORGANIZATION: U.S. Environmental Protection Agency
Environmental Research Laboratory
Athens, Georgia 30613-0801

REPORT DATE: January 1992

TYPE OF REPORT: Final Report

PREPARED FOR: U.S. ARMY MEDICAL RESEARCH AND DEVELOPMENT COMMAND
Fort Detrick, Frederick, Maryland 21702-5012

REPORT DOCUMENTATION PAGE

Form Approved
OMB No. 0704-0188

1. AGENCY USE ONLY (Leave blank)	2. REPORT DATE	3. REPORT TYPE AND DATES COVERED
	January 1992	Final Report (9/15/88 - 12/14/91)

4. TITLE AND SUBTITLE

FATE OF COLORED SMOKE DYES

5. FUNDING NUMBERS

Army Project Order
88PP8863

62720A ✓
3E162720A835.00.014
WUDA315649

6. AUTHOR(S)

Arthur W. Garrison; George L. Baughman; Eric J. Weber;
Rebecca L. Adams*; Mary Sue Brewer*

7. PERFORMING ORGANIZATION NAME(S) AND ADDRESS(ES)

U.S. Environmental Protection Agency
Environmental Research Laboratory
Athens, Georgia 30613-0801

8. PERFORMING ORGANIZATION REPORT NUMBER

9. SPONSORING/MONITORING AGENCY NAME(S) AND ADDRESS(ES)

U.S. Army Medical Research and Development Command
Fort Detrick
Frederick, Maryland 21702-5012

10. SPONSORING/MONITORING AGENCY REPORT NUMBER

11. SUPPLEMENTARY NOTES

*Rebecca L. Adams, Technology Applications, Inc., c/o Environmental Research Lab.
*Mary Sue Brewer, University of Georgia, Athens, Georgia

12a. DISTRIBUTION/AVAILABILITY STATEMENT

Approved for public release; distribution unlimited

12b. DISTRIBUTION CODE

13. ABSTRACT *(Maximum 200 words)*

Smokes dyes are used by military personnel for s.jnalling and marking purposes. Because dissemination of smoke dyes results in deposition on vegetation, soil and surface waters there is a need to determine their potential environmental impact. The present study was designed to provide part of the data necessary for environmental assessment.

The project consisted of seven tasks addressing three basic goals: 1) purification and characterization of study compounds, 2) measurement of reaction rates and identification of products for the most probable transformation products as typified by the anilines. Five pathways or processes were identified that were expected to be important for the environmental fate of the smoke dyes: 1) partitioning from water to soil/sediment and biota, (Tasks 2, 3, and 4), 2) assessment of metal complexation (Task 5), 3) photolysis on soil (Task 6), 4) transformation in anaerobic sediments (Task 7), and 5) transformation of aeromatic amines (Task 8).

14. SUBJECT TERMS	15. NUMBER OF PAGES
Environmental Fate; Colored Smokes; Dyes; RAIII; PO	16. PRICE CODE

17. SECURITY CLASSIFICATION OF REPORT	18. SECURITY CLASSIFICATION OF THIS PAGE	19. SECURITY CLASSIFICATION OF ABSTRACT	20. LIMITATION OF ABSTRACT
Unclassified	Unclassified	Unclassified	Unlimited

TABLE OF CONTENTS

Executive Summary

Smoke dyes are used by military personnel for signalling and marking purposes. Because dissemination of smoke dyes results in deposition on vegetation, soil and surface waters there is a need to determine their potential environmental impact. The present study was designed to provide part of the data necessary for environmental assessment.

The project consisted of seven tasks addressing three basic goals: 1) purification and characterization of study compounds, 2) measurement of reaction rates and identification of products for the most probable transformation pathways, and 3) elucidation of the fate of expected aromatic amine transformation products as typified by the anilines. Five pathways or processes were identified that were expected to be important for the environmental fate of the smoke dyes: 1) partitioning from water to soil/sediment and biota, (Tasks 2, 3, and 4), 2) assessment of metal complexation (Task 5), 3) photolysis on soil (Task 6), 4) transformation in anaerobic sediments (Task 7), and 5) transformation of aromatic amines (Task 8).

Tasks 2, 3, and 4. The water solubility, octanol-water partition coefficient and entropy of fusion were measured for the smoke dyes and other disperse and solvent dyes. Based on these data, three regression approaches were examined for use in estimating water solubilities and octanol-water partition coefficients. The approaches included regression of solubility against partition coefficient, determination of the product of solubility and partition coefficient, and application of an equation from Yalkowsky and Valvani [4.9]. In addition, an experimental method based on capacity factors from high performance liquid chromatography was examined. The measured capacity factors were used in regression equations to estimate water solubilities and octanol-water partition coefficients. The resulting equations can be used to estimate the octanol-water partition coefficient from solubility, or vice versa, with sufficient accuracy for environmental assessment. The chromatographic method provides similar accuracy, but can be applied to dyes that are impure or of unknown structure. These data also show that the smoke dyes will partition strongly to sediments and soils and that they have potential bioconcentration factors that range from 100 to well over a million.

Task 5. The goal of this task was to determine if sufficient data exist to assess whether complexation of the smoke dyes is probable. Based on a literature search, it was concluded that Solvent Yellow 33 is a good complexing agent for divalent metals and probably undergoes cation exchange with sediments. Given the available data, however, the extent of metal complexation by either Solvent Yellow 33 or Solvent Red 1 could not be predicted. Based on fundamental chemical considerations and the absence of data for metal complexes, it was concluded that complexation of Disperse Red 9, Disperse Violet 1, and Disperse Red 11 in the environment would likely be insignificant.

Task 6. Photolysis studies on soil indicated that all of the dyes were readily photodegraded to some extent. Because of light attenuation by soil particles, however, none of the dyes were completely photolyzed. The magnitude of mean depths of photolysis measured for the dyes, the dependence of the mean depth of photolysis on soil depth, and solution phase photolysis studies

suggested that photodegradation of the dyes was occurring primarily through photoxygenation via reaction with singlet oxygen. Except for Solvent Green 3, none of the dyes gave photolysis products that are expected to be persistent in the environment.

Task 7. Disappearance rate constants were measured for the dyes in anaerobic sediments. The half-lives for the dyes varied from 0.1 to 140 days or about 1000 fold. Only Disperse Blue 3, Disperse Blue 14, and Solvent Yellow 33 had half-lives greater than a few days. Solvent Yellow 33 was the least reactive but is predicted to have a half-life in anaerobic sediments of approximately six months. Products studies of the azo dyes, Disperse Red 5 and Solvent Red 1, showed that reduction of the azo linkages and the nitro group resulted in the formation of substituted anilines. Reduction of Disperse Red 9 resulted in the formation of anthrones. The hydrogen bonded isomer was found to be the most stable anthrone. The 1,4-diaminoanthraquinones, Disperse Violet 1 and Disperse Red 11, undergo more complex reactions. It is probable that multiple products result from reduction and replacement of the amino groups with OH. Demethylation of Disperse Red 11 also occurs, resulting in the formation of a product that accumulates.

Task 8. To determine the mechanisms by which aromatic amines sorb to soil and sediment surfaces, the sorption kinetics of a series of 2- and 4-substituted anilines were measured in a sediment-water system. In general, the rate and extent of sorption were found to increase with the pKa of the aniline. Decreasing pH enhanced the sorption of the 4-substituted anilines in a silt-clay. In other studies, however, the sorption of aniline was pH independent in a resaturated pond sediment. Sequential extraction studies with ^{14}C-aniline suggested that reversible cation exchange processes do not contribute significantly to aniline sorption in this natural sediment-water system and that irreversible covalent binding to the organic matter of the sediment matrix dominates the sorption process. On the other hand, in similar experiments with ^{14}C-pyridine, a nitrogen containing heterocycle, the dominant sorption process was determined to be cation exchange. To gain further insight into the mechanism(s) by which the anilines covalently bind to sediments, a sediment-water system was treated with chemicals known to form stable adducts with carbonyl groups. Treatment of a sediment-water system with 2 4-DNP or hydroxylamine 24 hours prior to the addition of 4-methoxy-aniline effectively blocked the sorption of the aniline, suggesting the importance of covalent binding through nucleophilic addition to carbonyl groups in the sediment matrix. To provide direct spectroscopic evidence for this type of sorption mechanism, ^{15}N NMR was used to analyze fulvic acid that had been treated with ^{15}N-aniline. INEPT and ACOUSTIC ^{15}N NMR spectra exhibited resonances for imine, anilide, anilino-quinone, and anilino-hydroquinone nitrogens in the ^{15}N-aniline-reacted fulvic acid, providing further evidence for covalent binding through nucleophilic addition to carbonyl moieties. Although the number of anilines examined was small, the results strongly suggest that such compounds will be rendered highly immobile in soil or sediment systems.

List of Tables

Note: All Tables appear at the end of the text.

List of Figures

Note: All Figures appear at the end of the text.

Note: All Figures appear at the end of the text.

1. Introduction and Background

The U.S. Army uses munitions to create colored smoke as signals and markers in both training and combat exercises. The smoke is developed and dissipated by the combustion of chemical mixtures containing, or forming, dyes as the colorant. As a consequence of the use of smoke devices, troops, equipment and the environment are exposed to dye that is deposited as very fine particles. Interest in the environmental behavior of dyes is prompted primarily by concern over their possible toxicity and carcinogenicity. This concern is heightened by the fact that many dyes formerly were made from known carcinogens such as benzidine, an aromatic amine, which may be reformed as a result of dye transformation. Because of human health and ecological concerns, there is a need to examine the potential environmental impact of the smoke dyes, which are largely deposited on vegetation, soil, or surface waters. This, in turn, requires data on the behavior (fate) of dyes and their products in the environment.

The present study was designed to provide part of the data necessary for environmental assessment. The approach taken was to study selected dyes and develop data and methods that can be applied to other materials or conditions.

The project consisted of seven tasks addressing three basic goals: (1) purification and characterization of study compounds, (2) measurement of reaction rates and identification of products for the most probable transformation pathways, and (3) elucidation of the fate of expected aromatic amine transformation products as typified by the anilines.

Dyes that produce colored smoke are either the same compounds that are used on textiles or they are closely related structures. The common names of textile dyes, given by the Color Index (C. I.) [1.1], reveal their mode of application to textiles. This is reflected in the names of the main dyes for this study: (C. I.) Disperse Violet 1, C. I. Disperse Red 5, C. I. Disperse Red 9, C. I. Disperse Red 11, C. I. Solvent Red 1, C. I. Solvent Green 3, and C. I. Solvent Yellow 33. These names immediately identify the compounds as non-ionic, hydrophobic, organic dyes, the structures of which can be obtained by use of the Color Index Constitution Number (C.I. No.). Dye structures are given in Figures 1-1.

Dyes also are classified by their chemical structures, the largest group of which is the azo dyes, represented by Disperse Red 5 and Solvent Red 1. The second most important group is the anthraquinone dyes, represented by Disperse Violet 1, Disperse Red 9, Disperse Red 11 and Solvent Green 3. Solvent Yellow 33 belongs to the small group of quinoline dyes which includes the commercially important Disperse Yellows 54 and 64. It should be noted that Disperse Red 5 is not a smoke dye but was included in this study as another example of the azo dyes. Also, there are other smoke dyes that were not included in this study.

Because the selected dyes have been known for decades, it is reasonable to assume that there would be significant literature on their basic physical and chemical properties. Unfortunately, few such data have been published, as indicated by exhaustive computer and manual searches of Chemical Abstracts.

Data from environmental studies or data that are directly useful for environmental assessment are almost nonexistent. An exception is the data from waste treatment studies, which shows dyes to be resistant to aerobic biological degradation.

In the absence of actual measurements, fundamental considerations of data for close structural analogs can provide estimates of some parameters. Unfortunately, data are usually not available for dye analogs that are close enough in structure to permit reliable estimates. Thus, there were few estimated data on soil/sediment-water or n-octanol-water partition coefficients (K_{oc} and K_{ow}). Similarly, there were few data on water solubility and none on environmental transformation.

These facts, together with considerations of expected environmental chemistry, led to identification of five pathways as most likely to be important in the fate of smoke dyes: (1) partitioning from water to soil/sediment and biota (Tasks 2, 3, and 4), (2) complexation with metals (Task 5), (3) photolysis on soil (Task 6), (4) transformation in anaerobic sediments (Task 7), and (5) transformation of aromatic amine products (Task 8).

Task 8 was included because the dyes and their expected transformation products are all aromatic amines, many of which are known to be toxic and/or carcinogenic. Also, environmental transformation of several azo dyes and munitions components is known to result in anilines.

In this report, tasks related to water solubility and partitioning (Tasks 2, 3, and 4) are treated as a unit. Results from these tasks and part of Task 7 have been published in the scientific literature. Thus, the final report includes only data that are complementary to the papers and essential for a coherent summary. (Other tasks are treated individually.)

2. Materials and methods

Chemicals. Samples of the seven dyes selected for study were obtained from several sources. Disperse Red 9, 1-methylaminoanthraquinone, was provided by Atlantic Industries (lot #N03267). Disperse Violet 1, 1,4-diaminoanthraquinone, was provided by Atlantic Industries (lot #N03267) and commercially obtained from Aldrich Chemical (Milwaukee, WI). Disperse Red 11, 1,4-diamino-2-methoxyanthraquinone, was provided by Atlantic Industries (lot #NP501), as well as by the Pine Bluff Arsenal (lot #01195-001). Solvent Yellow 33, 2-(2'-quinolinyl)-1,3-indandione, was obtained from Aldrich Chemical (Milwaukee, WI) and Dr. Dennis Burton of Johns Hopkins. Solvent Green 3, 1,4-di-p-toluidino-9,10-anthraquinone, was supplied by Atlantic Industries (lot #N901), and commercially obtained from Aldrich Chemical (Milwaukee, WI). Solvent Red 1, 1-methoxybenzenazo-2-naphthol, was supplied by the Pine Bluff Arsenal (lot #N9501) and by Atlantic Industries (lot #N9501). Disperse Red 5, 2-chloro-2'-methyl-4-nitro-4'-N,N-*bis*(2-hyroxyethyl)azobenzene, was provided by Crompton and Knowles. All other chemicals were reagent grade and were used without purification.

The EPA soils used in Tasks 6 and 8 were collected from various locations in the midwestern United States [2.1]. Their characteristics are given in

Table 6-3. The Cherokee Park sediment used in Task 8 was collected from a local pond in the Athens, Georgia area. After decanting the overlying water, the sediment was air dried on a Buchner Funnel for 72 hr. The sediment was passed through a 1mm sieve and homogenized with a mortar and pestle.

High performance liquid chromatography with isocratic elution from C18 columns at 1 to 1.5 ml/min was used for measurement of dye solubility and kinetics. Columns were 4.6 mm in diameter and either 25 cm or 12.5 cm in length with guard columns and inline prefilters. Columns with 30 percent carbon loading (Phenomenex ultracarb 5 ODS) were used for quantifying some of the anthraquinone dyes.

In estimating the solubility of Solvent Green 3 and developing solubility-retention volume relationships, the mobile phase was methanol/water. For all other work, the mobile phase was acetonitrile/water (ACN/H_2O) with ACN content between 60 and 100 percent, depending on the dye.

Several different HPLC pumps and detectors were used. The pumps were a ABI Kratos Spectroflow 400, a Varian model 5020, a Perkin-Elmer series 100 and a Gilson 302. Detectors included a Waters model 990 diode array detector, ABI Spectroflow 757 and model 783 absorbance detectors, and Perkin-Elmer LS40 fluorescence detector.

Quantitation was done by using the electronically integrated signals from standards (in ACN) to develop calibration curves. Detection was at the visible wavelength maximum of the dye. Because standards of the transformation product of Disperse Red 11 were unstable, standards were used to determine the ratio of dye to product absorbance at 568 nm. Both dye and product were detected at 568 nm, on each injection, and product was quantified based on the ratio. The anthrone from Disperse Red 9 was detected at 426 nm, on each injection, along with the dye, by using a detector that switched wavelengths at the appropriate time.

Dye standards were prepared by weight of dye that had been purified as described (Section 3). Occasionally it was necessary to use commercial dye, in which case, standards of the commercial dye were used to verify linearity over the concentration range of interest.

GC-MS was usually performed with a Hewlett Packard Gas Chromatograph 5890 equipped with a Hewlett Packard Mass Selective Detector 5970. The chromatographic column was a Hewlett Packard (12 m x 0.22 mm i.d.) fused silica capillary column with a bonded HP-1 phase.

For other work, full-scan electron impact mass spectra were acquired at 70 eV on either a VG 70-SEQ high resolution, hybrid mass spectrometer, equipped with the VAX-based OPUS data system and a Hewlett Packard model 5890A GC, or a Finnigan model 4500 quadrupole mass spectrometer, equipped with the INCOS data system and Finnigan GC. The VG instrument was operated at 8 kV accelerating voltage and at resolutions of 1000 and 7000 for low and high resolution mass spectrometry (HRMS), respectively. The Finnigan mass spectrometer was operated at a resolution of 1000. High resolution EI masses were within 2 milli-mass units of theoretical masses calculated for molecular ions

and fragments. Perflucrokerosene was used as the mass calibrant over the 40 to 500 mass range. Both GC and probe sample introduction techniques were used. When GC introduction was used, a J&W Scientific DB-5 capillary column (30 m length, 0.25 mm i.d., 0.25 μm film thickness) was employed with a temperature program consisting of an initial temperature of 40°C, which was held for 2 min, followed by an increase at a rate of 8°C/min to 290°C, where it was held for 30 min. Transfer lines were held at 250°C, and the injection port was controlled at 230°C. The linear velocity of the helium carrier gas was approximately 25 cm/s. When probe sample introduction was used, the probe temperature was manually increased from ambient temperature to 300°C.

GC-FTIR analyses were performed with a Digilab model FTS-60 spectrometer equipped with a Digilab model 3200 workstation and a Hewlett Packard model 5890 GC and split/splitless injector. The FTIR spectrometer has a model GC/C 32 light pipe-based interface and a narrow band mercury-cadmium telluride detector. Generated spectra had 8 cm^{-1} resolution with a useful range of 4000 to 700 cm^{-1}. The GC contained a J&W Scientific, DB-5, 30 m, Megabore® column (1.5 μm film thickness). Helium carrier gas had a linear velocity of 22 cm/s. The FTIR interface was held at 280°C for the light pipe and transfer lines. The initial column temperature was 100°C for 3 min after which it was programmed upward at 10°C/min to 280°C where it was held.

NMR spectra were obtained with a Bruker AC 250 spectrometer equipped with a 5 mm ^{1}H, ^{13}C dual probe. The C-H two dimensional heteronuclear correlations were obtained on a Bruker AMX 400 MHz instrument with an inverse probe. The software used was the standard software supplied by Bruker.

3. Purification and Characterization (Task 1)

3A. Introduction

Commercial dyes are products standardized for their end use and are typically not homogeneous chemical compounds. Analysis of presscake samples of the smoke dyes by liquid chromatography (HPLC) and thin-layer chromatography (TLC) indicated the presence of numerous components. The inhomogeneity of the dyes required that the dyes be purified before meaningful characterization and kinetic studies could be performed.

3B. Materials and Methods

3B.I. Purification Method

All of the dyes were initially recrystallized from ethanol/water solutions. The recrystallized samples were then flash-chromatographed on silica gel (32-63 μm, Universal Adsorbents) [3.1]. The dyes were eluted with mixtures of high purity ethyl acetate and hexane (Burdick and Jackson). Purified dyes were analyzed by HPLC and thin layer chromatography. Thin layer chromatography was performed with Analtech Silica Gel G 250 μm plates. Elutions were made with mixtures of high purity solvents (Burdick and Jackson).

The absorption spectra were measured on a Carey Model 210 from Varian.

Infrared spectra were recorded on a Digilab FTIR FTS-60, with a TGS detector using KBr pellets as the sample matrix. Mass spectra and gas chromatogram/mass spectra were recorded on a Finnigan 4500 GC/MS using a DB-5 (30 mm x 0.25 mm) capillary column. The GC conditions were: 40°C for 2 minutes, 12°C/min, final temperature of 280°C.

3C. Results and Discussion

The percent recovery of the dyes after purification by flash chromatography ranged from 40 to 80%. The purified dyes were determined to be homogeneous by HPLC and TLC. The dyes were characterized by mass spectrometry (Appendix A), infrared (Appendix B) and uv-visible spectrometry (Appendix C). TLC R_f values, HPLC retention times, and lambda max values for the purified dyes are summarized in Table 3-1. Dye purities, which were measured by scanning differential calorimetry, ranged from >96% to >99% (Table 4.4).

4. Water solubility and partition coefficient measurement and estimation (Tasks 2, 3 and 4)

4A. Background

Water solubility and the octanol/water partition coefficient (K_{ow}) are fundamental equilibrium constants that are used to predict other partition equilibria. Among the more widespread uses of these constants is prediction of bioconcentration and environmental distribution of uncharged organic compounds in aquatic systems. Unfortunately, both parameters are very difficult to measure accurately when values are extreme for a particular chemical--i.e., if K_{ow} is greater than about 10^4 or if water solubility is less than 0.1 mg/L. Consequently, few reliable values are available for hydrophobic dyes like the smoke dyes.

Available data for solubility of disperse and solvent dyes has been compiled by Baughman and Perenich [4.1], who also found that there were no octanol-water partition coefficients for the dyes. Their review provides water solubilities for three of the smoke dyes--Disperse Red 9, Disperse Red 11, and Disperse Violet 1--as well as Disperse Red 5. The water solubility of Solvent Yellow 33 has recently been published [4.2], which leaves Solvent Green 3 and Solvent Red 1 as the only smoke dyes for which there are no water solubility data.

The need for water solubilities and K_{ow}'s for environmental assessment has spurred interest in methods for estimating these parameters. This is partly because, for many purposes, a reliable approximation is sufficient and the measurements are expensive. Also, estimation methods, in principle, are applicable to compounds that have heretofore been unstudied. Thus, one not only needs data for the smoke dyes in use, but also needs to be able to evaluate alternative dyes as necessary.

The above circumstances have led to attempts to predict these parameters by *a priori* computational methods [4.3, 4.4], regression equations relating solubility to K_{ow} (see Isnard and Lambert [4.5] for a survey), and chromatographic methods [4.6 through 4.8]. All of these methods are essentially

empirical, but each has important features that are independent of data quality. *A priori* methods are the most flexible but, as will be seen, are often unconvincing for compounds very different from those for which they were developed. Regression equations, including that of Yalkowsky and Valvani [4.9], simply relate solubility to K_{ow}. The chromatographic method is an experimental approach and thus must be calibrated against known materials.

Baughman and Perenich [4.1] suggested that methods of predicting K_{ow} gave unsatisfactory results when applied to disperse dyes. They concluded that a widely used computer program CLOGP [4.3] and the frequently used equation of Yalkowsky and Valvani [4.9] gave low values of log K_{ow} for these materials. Problems with the latter method were attributed to possible errors in entropy of fusion, ΔS_f. Recently published K_{ow} and solubility data [4.10] confirm that both methods can yield significant underestimates.

Chromatographic methods do not permit direct measurement of either solubility or K_{ow}, but both reverse phase thin layer chromatography [4.11] and reverse phase high performance liquid chromatography (HPLC) [4.6, 4.8, 4.12, 4.13] have been applied to their estimation. This approach has the advantages of sensitivity and of not requiring high purity and known structures. Recently, an OECD test guideline based on HPLC was subjected to an interlaboratory comparison [4.7]. Although the HPLC method was viewed as acceptable, estimated K_{ow}'s for three out of five dyestuffs included in the study were found to be insufficiently accurate.

Because of the above circumstances, three tasks were identified for this work: 1. measure the solubility, octanol-water partition coefficient and entropy of fusion of the smoke dyes and several other dyes, 2. develop regression equations between these parameters that are suitable for predicting these properties for other smoke dyes, and 3. develop an experimental method using reverse phase HPLC for estimating solubility and K_{ow} for other hydrophobic (smoke) dyes.

These three tasks were completed and the results have been published in the open scientific literature [4.14, 4.15]. For that reason, the discussion to follow will include only a summary of findings and results. The published articles should be consulted for more detailed discussion.

4B. Materials and methods

Saturation of water for solubility measurements was performed at 25 ± 0.1 °C by the generator column method, except for Solvent Green 3, as described previously [4.10, 4.16]. For the latter dye, solubility was estimated by the approach of Morris et al. [4.17]. Partition coefficients were measured by the batch method or were estimated as the ratio of measured octanol and water solubilities [4.10]. Dye concentrations were measured by HPLC with absorbance detection.

Melting points and enthalpies were obtained by differential scanning calorimetry (DSC) using a Mettler TA 4000 micro-processor-controlled DSC 20 furnace. The instrument was calibrated against melting point standards from the National Bureau of Standards and against high purity indium, tin, benzoic

acid, and biphenyl. Onset of melting is reported as the melting point. Calibration consistently showed that calorimetric accuracy was better than 5% and melting points are believed to be accurate within 1°C. Entropies of fusion were obtained as the ratio of the enthalpy of fusion to the absolute temperature with entropy units (eu) in Joules per mole degree.

The HPLC method for measuring capacity factors is, in most respects, similar to that of an OECD method tested recently [4.7]. The liquid chromatographic system comprised a Perkin Elmer Series 2000 pump, a Varian Vari-Chrom absorbance detector, and an Alltech Econosil C-18 (10 micrometer) column (4.6 mm X 25 cm with guard column). The mobile phase, HPLC-grade methanol and deionized water (75/25 vol.%), was prefiltered for use at a flow rate of 1.3 ml/min. Detection was at the wavelength of maximum absorbance in the visible spectrum.

Capacity factors, K', ($K'=(t_r-t_o)/t_o$) initially were determined by measuring K' over a range (5% intervals) of four to five mobile phase compositions. Time for an unretained component to move through the system, t_o, was identified by injection of water and measured by strip chart recorder as was retention time, t_r. The data then were interpolated (occasionally extrapolated) by linear regression to zero percent MeOH, K'_0, or 75 percent, K'_{75}. We found, however, that the dyes could usually be measured more easily and accurately with the 75/25 $MeOH/H_2O$. These conditions sometimes necessitated long retention times (up to 90 min) but extrapolation was necessary only for Solvent Green 3 and Disperse Blue 354. All values are reported as the mean of triplicate determinations for which the variability was about 6 percent.

Regressions were all performed with the statistical procedures in Lotus©.

4C. Relationships between solubility and K_{ow}

Basically three methods have been used to relate solubility to partition coefficient. The first is regression of log S versus log K_{ow}. This method is essentially phenomenological and, of itself, implies no theoretical rationale. The second approach is from Miller et al. [4.18], who noted that the product of S and K_{ow} is a pseudo octanol solubility, Q, and hence relatively constant. The third, from ideal solution theory, is the method of Yalkowsky and Valvani [4.9], which incorporates the melting point, mp, and ΔS_f. Each of these three methods is examined below using the data for smoke and other dyes.

4C.I. Regression of Log S with Log K_{ow}

The solubilities and Log K_{ow}'s for the dyes are given in Table 4-1, which is taken from Baughman and Weber [4.14]. Except as noted, the data were measured for this project. The data in Table 4-1 for partition coefficient and water solubility of the crystalline dye, S_c, gave the regressions shown in equations 4-1 through 4-4. Here, S_c is in mol/m^3, mp is in degrees centigrade, R is the correlation coefficient, and sigma is the root mean square deviation between measured and calculated values.

$$\text{Log } K_{ow} = 1.32 - 0.77\text{Log } S_o \qquad (4\text{-}1)$$
$$R^2 = 0.785$$
$$\sigma = 0.67$$

$$\text{Log } K_{ow} = 2.16 - 0.77\text{Log } S_o - 0.0049(mp - 25) \qquad (4\text{-}2)$$
$$R^2 = 0.800$$
$$\sigma = 0.64$$

$$\text{Log } S_o = 0.34 - 1.02\text{Log } K_{ow} \qquad (4\text{-}3)$$
$$R^2 = 0.785$$
$$\sigma = 0.76$$

$$\text{Log } S_o = 1.27 - 1.03\text{Log } K_{ow} - 0.0050(mp - 25) \qquad (4\text{-}4)$$
$$R^2 = 0.797$$
$$\sigma = 0.74$$

The R^2's and root mean square deviations for these equations are not as good as hoped--about a factor of 4 to 6. However, application of other available equations to the same data shows equations 4-1 through 4-4 to give lower root mean square deviations [4.14].

4C.II. Product of solubility and partition coefficient

As noted earlier, Miller et al. [4.18] showed that the product of S and K_{ow} is essentially an octanol solubility, Q, and thus is expected to be relatively constant. Table 4-2 shows the result when Q is calculated using actual solubility, S_o, and subcooled liquid solubilities. The results can be compared with values in Table 4-3.

The geometric mean of Q_t (Table 4-2) is about 20 times greater than the value reported previously [4.1], which is consistent with the conclusion that CLOGP [4.3] predictions of log K_{ow} were too low. This mean value is also more in line with the higher values reported by Miller et al. [4.18]. It is interesting that the root mean square deviation of Q_t is less than that of Q_a, but the range is greater (see Table 4-2 for symbol definition).

4C.III. Regression including melting point and ΔS_f

Equation 4-5, from Yalkowsky and Valvani [4.9] provides the third approach relating K_{ow} and solubility (mol/L):

$$\text{Log } K_{ow} \approx \text{Log } S_o - 0.000194\Delta S_f(mp - 25) + 0.54 \qquad (4\text{-}5)$$

This equation includes terms for the melting point, mp(°C), and the entropy of fusion, ΔS_f (kJ/mol•°k). Entropies of fusion and melting points measured for the dyes in this study are given in Table 4-4. In general, the data are in good agreement with other available values. An exception is the value for Solvent Yellow 33 reported by Krien [4.19] who found both a molecular weight and a dehydration (apparently for technical grade dye) that we did not see. Usually, ΔS_f is approximated by the value 56.5 eu, (i.e., $\Delta S_f = 6.8$), but this has been shown to be too low for disperse dyes and a value of 66 eu. has been

suggested [4.1]. As anticipated, the average ΔS_f value of 78 J/mol*K is significantly greater than the 66 J/mol*K value that was based on previously available data [4.1]. Table 4-4 shows that the anthraquinone dyes (Disperse Violet 1, Disperse Red 60, Disperse Red 9, Disperse Red 11 and Solvent Green 3) have entropies of fusion near 66 J/mol*K as do the other "rigid" structures (Disperse Yellow 54 and Disperse Yellow 33). However, addition of large flexible chains to the anthraquinone ring system raises the ΔS_f to 78 J/mol*K [4.20]. The only ΔS_f that seems unreasonable is the low value of 50.7 J/mol*K for the rigid dye N3. This value almost certainly is too low, but it did not increase with further purification. These data are given by Baughman and Weber [4.14]. If the value of 6.8 for entropy is used in equation 4-5, all but two of the K_{ow}'s in Table 4-1 are over estimated and the root mean square deviation is 1.34 log units. Use of the measured values of ΔS_f and mp (Table 4-4), still produces over-estimates of all but four K_{ow}'s, and the root mean square deviation decreases only to 1.02.

Equation 4-5 and similar derivations are based on the assumption that a term containing the change in heat capacity upon melting, ΔC_p, is small and thus can be omitted. The ΔC_p on melting was measured or obtained from literature for several dyes in this work. They show that the assumption concerning heat capacity is not correct. The changes in heat capacity are probably influenced by some of the factors, discussed later, that also affect solubility and partition coefficient.

This observation is consistent with the considerable improvement obtained when regression of data in Tables 4-1 and 4-4 is used to obtain equation 4-6. Also in this case, the intercept is not different from zero at the 95 percent confidence level.

$$\text{Log } K_{ow} = -0.82 \text{Log } S_o - 1.05\times10^{-4}\Delta S_f(mp-25) - 0.03 \qquad (4\text{-}6)$$
$$R^2 = 0.836$$
$$\sigma = 0.58$$

Because equations 4-1 through 4-6 have low regression coefficients, it is important to examine data on which they are based and to identify possible sources of error. Unfortunately, it is not possible to determine whether partition coefficients or their related solubilities contribute the most error.

A discussion of sources of variability in these approaches is given by Baughman and Weber (4-14). In their work, it was concluded that, for dyes, variability is especially likely to be affected by factors such as purity, polymorphism, tautomerization, hydrogen bonding, and polarization. However, dyes used in this work are purer than usual (Table 4-4). Variability from the last four sources probably can not be eliminated.

4D. Liquid chromatography method

4D.1. Regression equations

Capacity factors of the 20 dyes used for this study are given in Table 4-5. Linear regression analysis provided the three equations shown below.

$$\text{Log } K_{ow} = 2.95 + 2.31 \text{ Log } K'_{75} \qquad R^2 = 0.791,\ \sigma = 0.659 \qquad (4\text{-}7)$$

$$\text{Log } S_l = -3.09 - 2.68 \text{ Log } K'_{75} \qquad R^2 = 0.862,\ \sigma = 0.594 \qquad (4\text{-}8)$$

$$\text{Log } S_o = -5.39 - 2.70 \text{ Log } K'_{75} \qquad R^2 = 0.839,\ \sigma = 0.634 \qquad (4\text{-}9)$$

S_l is the molar solubility of the sub-cooled liquid dye, at 25 degrees centigrade and K'_{75} is the capacity factor for 75 volume percent $MeOH/H_2O$. S_l is defined as $S_o/\exp(\Delta S_f(1\text{-}mp/K)/R)$ [4.18] where ΔS_f is the entropy of fusion, mp is the melting point in degrees K, K is the temperature in degrees Kelvin, and R is the gas constant.

The regression coefficients for these equations are also relatively low. Nevertheless, they are regarded as reasonable, given that four K_{ow}'s and one solubility in Table 4-5 are experimental estimates and that all the compounds have high melting points. Significantly, the equations have deviations and regression coefficients similar to regressions of Log K_{ow} against Log S for the same data in equations 4-1 through 4-6. This is expected since the values for K'_{75} are considerably more precise than those of solubility and K_{ow}.

Regressions of a slightly different form have been used by other workers [4.8]. However, regressions in those forms resulted in regression coefficients [4.15] much lower than given above.

Whitehouse and Cook [4.13] obtained an R^2 of 0.97 for an equation in the form of equation 4-10. This equation fit the data in Table 4-5, with an R^2 = 0.855.

$$\text{Log } S_o = -4.95 - 2.76 \text{Log } K'_{75} - 0.00180[MP(^\circ C)] \qquad (4\text{-}10)$$

Thus, as in the case of regressions of Log S_o against Log K_{ow} (equations 4-3 and 4-4), inclusion of a melting point term results in only a small improvement in regression coefficient. Isnard and Lambert [4.5] made a similar observation. For equation 4-5, the standard error of the prediction actually increases slightly.

Sources of variability in the chromatographic data include those in the solubilities and partition coefficients (Section 4C.III). However, chromatographic methods can be strongly affected by some of the same sources of error--especially those due to solvent interactions. Some that are particularly likely to be important for dyes include hydrogen bonding, polarization and tautomerization. These factors argue strongly against extrapolations in solvent composition to obtain K', even at the expense of long retention times.

As a consequence of the above factors, it is likely that statistical reliability of the chromatographic method will be primarily limited by

availability of accurate dye solubilities and K_{ow}'s. This should not obscure the fact that speciation changes can, and for dyes probably do, result in data that are "chemically " accurate but which may not give statistically desirable, i.e., predictable results.

Whether estimates are adequate must ultimately be determined by the use of the data and, as noted earlier, for environmental purposes the demands for precision are often not great. In the present case, the equations have root mean square deviations from the reference values in Table 4-5 on the order of a factor of 4 to 5.

4D.II. Applications

To illustrate the utility of the method, K'_{ss} was measured for some commercially formulated dyes, and equations 1 and 3 were used to estimate the solubilities and K_{ow}'s (Table 4-6). Few of these dye solubilities and none of the K_{ow}'s have been previously reported. It is noteworthy that the absence of melting points for substances like Indigo that decompose before melting, does not prevent estimation.

Measured (Table 4-5) and predicted values (Table 4-6) were used to calculate the sediment/water partition coefficient, K_{oc}, and potential bioconcentration factor (BCF) for all dyes used in this work (Table 4-7). Specifically, the smoke dyes have BCF's that range from about 100 to almost 10 million and the soil sorption coefficients are also very large. Thus, the data clearly show that some of the dyes have a large potential to partition to sediments and biota. Further, this conclusion would not change even if there were rather large errors in the data. Interestingly, data in Table 4-7 also show that the solubility equations return values of Log BCF that are, on average, about 0.7 log units larger than those from K_{ow}.

4E. Conclusions

Equations in this section provide the most reliable available means of estimating water solubility from the octanol-water partition coefficient or vice versa. The HPLC method is of similar precision and has the advantage that known structure and purity of the dye are not necessary for its use. The accuracy of these estimation approaches is probably on the order of a factor of 4 to 5.

The data on smoke dyes shows them to have potential bioconcentration factors that range from about 100 to well over a million. Similarly, sediment-water partition coefficients show that most of the smoke dyes will migrate very little in the soil or water except in the sorbed state.

5. Assessment of metal complexation (Task 5)

5A. Background

Complexation by metals is an environmental transformation process that has the potential to dramatically alter the fate of organics. This can occur if a large portion of the dye exists in the environment as a metal complex or

if the complex has more reactive transformation pathways than the parent dye. Unfortunately, complexation has received little research attention with regards to its effect on the fate of organics. The purpose of this task was to determine whether there are sufficient data in the literature to determine whether complexation of smoke dyes is probable.

In order for a metal in natural water to form a complex with any significant portion of a dye, it must have several characteristics. First, there must be enough metal present, relative to the dye. Second, the metal must be capable of forming complexes with the dye that are stable enough to offset low environmental concentrations. Third, complexes with naturally occurring ligands, such as water, amino acids or humics, must be such that the dye can compete for the metal. Under environmental conditions, these constraints on the metal are rather severe. Thus the most likely candidates are calcium, magnesium, iron (II) and, perhaps, manganese.

Examination of the dye structures in Figure 3.1 shows that, in principle, all of the dyes except Disperse Red 5 have the potential to chelate with metals. The anthraquinone dyes--Disperse Red 11, Solvent Green 3, and Disperse Violet 1--can function as tetradentate ligands but steric constraints would not permit them to form two chelate rings with the same metal atom. They also should be very weak complexing agents.

Solvent Red 1 and Solvent Yellow 33 would be bidentate ligands expected to form complexes that are potentially quite stable. This conclusion is based on the fact that ortho hydroxy azo compounds are well known to form stable complexes that are used as dyes. Also, both dyes have structures with aromatic OH's and electron donating groups in position to form stable chelate rings. The latter feature is a well known characteristic of many strong complexing agents. The presence of the ionizable proton would make the formation constants a strong function of pH.

5B. Results of literature search

The usual compilations of stability constants had no data on these dyes or on closely related compounds, so exhaustive manual and computer searches were made of Chemical Abstracts (C.A.). The search produced no useful data. Equilibrium constants for Solvent Yellow 33 were also sought by a computer search of the structure in C.A. This search was undertaken because the other literature produced nothing, even for analogous sulfonated food dyes. The computer structure search resulted in 205 "hits," none of which contained equilibrium or solubility data. However, a manual search resulted in several references. Two references had data on metal complexes of Solvent Yellow 33, also called quinophthalone.

Bontchev and coworkers [5.1] reported complexes of the pyridyl analog of Solvent Yellow 33 with copper and also stated that earlier workers had reported complexes of this ligand with divalent ions of copper, nickel, cobalt, iron (II), magnesium, zinc, and manganese. In a more recent paper [5.2], the same authors presented the important result that Solvent Yellow 33 is zwitterionic.

A paper by Cook and Martin [5.3] gives pK_a for both Disperse Yellow 33 and Solvent Yellow 54 in dioxane-water. They also provide an equation relating pK to water content so that the data can be extrapolated to pure water. In addition, they give formation constants for metal complexes of Solvent Yellow 33 with copper, beryllium, nickel, manganese, zinc, magnesium and cobalt in dioxane-water. Another paper by Apsit et al. [5.4] shows that Solvent Yellow 33 is a strong complexing agent for divalent metals and that the equilibria are pH sensitive. However, they did not give data for iron, magnesium, or calcium.

There are no data in the literature for the metal equilibria of Solvent Red 1. Data of Dwivedi et al. [5.5], Manku et al. [5.6] and Yampolski et al. [5.7] are for compounds of closely related structure. Data from these papers suggest that formation constants for Solvent Red 1 are of the same order of magnitude as for Solvent Yellow 33.

5C. Assessment

The absence of data in the chemical literature on aminoanthraquinone metal complexes is indicative of their very weak nature. Thus, complexation of such compounds can not be estimated but is likely to be insignificant. This conclusion is supported by their use on textiles since strong complexation would almost certainly make them very poor textile dyes.

Data from [5.3] permit calculation of an extrapolated pK_a of 9.8 for Solvent yellow 33. It is also clear from [5.3] and [5.4] that Solvent Yellow 33 can complex divalent metals expected in natural waters. However, there are no reliable procedures for conversion of the dioxane-water formation constants to values for water alone or from one metal to another. Consequently, the extent of complexation in water can not be determined. The situation is less favorable for Solvent Red 1 since in this case there are no data on either the pK_a or the formation constants.

As a simple test of complexation with calcium, two abbreviated laboratory experiments were conducted using lanthanide ion spectroscopy and solvent extraction. The first involves the effect of calcium competition for dye on the laser-stimulated fluorescence of Eu^{3+} ions. The second depends on complexation to make the dye unextractable into an organic solvent.

In neither case could evidence of complexation be detected under the experimental conditions. These experiments were inconclusive, but since the calcium concentration was higher than expected in nature, they strongly indicate that complexation with calcium is unlikely.

In view of the reported zwitterionic character of Solvent Yellow 33 [5.2] and its potential importance, we conducted two other simple experiments. In the first, we examined the dye spectrum as a function of pH. In the second, the clay mineral montmorillonite was added to a colorless saturated solution of the dye. The spectral data were characteristic of a compound having only one ionizable functional group. In the second experiment, the white clay was quickly dyed a bright yellow. Montmorillonite is noted for its cation exchange ability.

Based on the above, we concluded that cation exchange causes the extreme variability (and perhaps persistence also) in our kinetic experiments with quinoline dyes.

It is also worth noting that a divalent metal ion containing one of these ligands will be a cation and thus subject to ion exchange by sediment. The above information is insufficient to eliminate this possibility. This situation is one that, to the best of our knowledge, has not been previously reported and could be very important in the fate of both metals and organics.

In conclusion, it can be stated with certainty that Solvent Yellow 33 is a good complexing agent for divalent metals and probably undergoes cation exchange with sediments. The extent of complexation in the environment can not be predicted for either solvent dye, given available data.

6. Photolysis on Soil Surfaces (Task 6)

6A. Background

Smoke dyes are used by military personnel for signalling and marking purposes. Because dissemination of the colored smokes results in deposition on surfaces of soils and vegetation, it was of interest to determine whether the dyes photodegrade on such surfaces, and if so, whether reaction products would form that may be of more concern or be more persistent than the parent. All of the smoke dyes, by design, contain chromophores that strongly absorb visible light. Furthermore, they have low vapor pressures and water solubilities, which suggests that photolysis on soil/plant surfaces may be fast compared to loss by physical processes, such as by volatilization or transport into the soil column.

In recent years, our understanding of photochemical processes on soil surfaces has increased substantially. Herbert and Miller studied the depth dependence of direct and indirect photolysis on soil surfaces [6.1]. They concluded that direct photolysis on soil surfaces will be restricted to approximately the first 0.2 to 0.3 mm of soil due to light attenuation, and that indirect photolysis, i.e. photooxidation by singlet oxygen, may occur at significantly greater depths due to the penetration of singlet oxygen into the soil column. These findings are of importance with respect to the smoke dyes because previous studies have demonstrated that azo [6.2], anthraquinone [6.3] and quinophthalone dyes [6.4] in solution and on fibers are subject to photooxidation by singlet oxygen.

The primary objectives of this task were to measure the photolysis kinetics of the smoke dyes on a soil surface and identify photodegradation products. We also were interested in determining the relative importance of direct versus indirect photolysis and soil column depth on photolysis kinetics.

6B. Materials and Methods

6B.I. Photolysis Method

In all experiments, unless otherwise noted, EPA #3 soil was used as the medium. Reaction vessels for the photolysis studies were prepared by mounting a 1-mm thick glass plate (1 in x 1 in) with a 1/2 in diameter hole in the center, back-to-back with a solid 1-mm-thick glass plate (1 in x 1 in). The aperture was filled with 150 mg of soil, and 25 μl of a 1 x 10^{-3} M solution of each dye was uniformly applied to the soil. For the depth dependence studies, 4-mm-thick plates were prepared as described above. They were filled with 300, 450, or 600 mg of soil, which corresponded to soil depths of 2, 3, and 4 mm, respectively. All studies were performed in duplicate, with unexposed (dark) controls pulled at the end of the experiment. For outdoor studies, which were conducted in Athens, Georgia, between March and June 1990, the glass plates were placed in a glass dish covered with 0.5-mil transparent polyethylene film to minimize disturbances. Indoor studies were performed using a Spectral Energy LH153 Solar Simulator with an Air Mass 1 filter for environmental simulation.

6B.II. Dye Quantitation

Soil samples were transferred from the plates to 15-ml test tubes into which was added 8 ml of a 3:5 solution of acetonitrile/water. The tubes were vortexed for 1 minute and centrifuged (2000 rpm). The supernate was removed and centrifuged again. Analyses were performed by HPLC and GC/MS.

6C. Results and Discussion

6C.I. Photolysis Kinetics

To perform quantitative kinetic studies of the smoke dyes on soils, a means to apply the dyes to soil surfaces in a uniform manner was required. Initially, we attempted to apply the dyes to the soil by evaporating a CH_2Cl_2 solution of the dye in the presence of the soil on a rotary evaporator. Much of the dye, however, sorbed to the glass walls of the round bottom flask and solid clumps of the dye were apparent on the soil surface. Application of the dyes to the soil surface by spraying with a CH_2Cl_2 solution of the dye also was not satisfactory. It was difficult to apply quantitative amounts of the dyes to the soils and to obtain uniform coverage of soil samples. Upon further experimentation, we found that by applying solutions of the dyes, in either acetonitrile or ethyl acetate, via syringe to known quantities and depths of soil resulted in reproducible kinetic results.

The disappearance kinetics for the photolysis of the smoke dyes on EPA-3 soil at a depth of 1 mm in natural and simulated sunlight are illustrated in Figure 6.1. All of the dyes were photodegraded to some extent. Disperse Violet 1, Solvent Yellow 33, and Disperse Red 11 were the least reactive, exhibiting approximately 35 to 40% loss over the period of the experiment. Solvent Red 1, Solvent Green 3, and Disperse Red 9 were somewhat more photolabile, exhibiting losses of 60 to 70%. Dark controls exhibited minimal loss of each dye. Except for Disperse Red 9, the photodegradation kinetics of the

dyes in natural sunlight and solar-simulated sunlight were very similar.

The disappearance kinetics of the dyes can not be described by simple first-order kinetics. In general, rapid loss of dye occurs initially followed by a period during which prolonged irradiation produces an insignificant loss. The same type of disappearance kinetics have been reported for the photolysis of octachlorodibenzo-p-dioxin [6.5] and several agrochemicals [6.1] on soil surfaces, and the photolysis of DDE sorbed to suspended sediments [6.6]. This kinetic behavior is attributed to a bulk light attenuation effect and/or an inner particle light shielding effect [6.1].

6C.II. Mean Depths of Photolysis

Miller et al. [6.5] defined the mean depth of photolysis as the depth of the soil multiplied by the fractional loss of the chemical at the point where further photochemical loss is no longer observed. The magnitude of the mean depth of photolysis may provide some insight into photolysis mechanisms. Herbert and Miller [6.1] found that direct photolysis was restricted to the first 0.2 to 0.4 mm of the soil column because of strong light attenuation by soil particles, whereas depths for indirect photolysis were reported to be significantly deeper.

The mean depths of photolysis for the smoke dyes calculated from the kinetic data in Figure 6-1 are summarized in Table 6-1. Many of the mean photolysis depths for the smoke dyes are significantly below the soil depth where direct photolysis may occur, suggesting indirect photochemical processes play an important role in the photodegradation of the dyes. The large values we measured for the ratio of the indirect to the direct photolysis rate constants for the smoke dyes in aqueous systems (Table 6-2), as well as the results of other studies of 1-aryl-2-naphthol, quinophthalone and anthraquinone dyes demonstrate that photolysis of these types of chemicals in solution occurs primarily through sensitized photo-oxygenation via the reaction with $^1O_2$ [6.7, 6.4, 6.3]. The photo-generation of $^1O_2$ on soil surfaces at environmentally significant rates upon irradiation has been demonstrated previously [6,8]. Furthermore, Herbert and Miller [6.1] suggest that vertical migration of $^1O_2$ into the soil column of depths greater than 2 mm is possible.

In other studies, we determined that the mean depth of photolysis for Disperse Red 9 was dependent on soil depth; the MDPs would be expected to be independent of soil depth if only direct photolysis were occurring (see Figure 6-2). These data suggest that either (1) transport of the dye to the soil surface occurs followed by photolysis or (2) indirect photolysis occurs at depths below the photic depths of the soils. For several reasons, we believe that the latter scenario is operating. Kieatiwong et al. [6.9] have demonstrated that for a series of alkylated quinones, migration in the soil column is not a significant process for the quinones with vapor pressures below 10^{2-} to 10^{3-} torr. In general, vapor pressures for solvent and disperse dyes are several orders of magnitude below this range suggesting that their transport in dry soils will not be significant [6.10, 6.11].

6C.III. Effect of Soil Type on Photolysis Kinetics

In an attempt to determine the effect of soil type on photolysis kinetics, we measured the photolysis kinetics of Disperse Red 9 on two other EPA soils, in addition to EPA-3 (Figure 6-3). The soil characteristics and the measured depths of photolysis are summarized in Table 6-3. After 24 hours of irradiation, little difference in the photolysis kinetics for the three soils was apparent; however, upon prolonged exposure a greater spread in the kinetic data was observed. For this limited data set, there appears to be no clear correlation between the measured depths of photolysis for Disperse Red 9 and soil characteristics. Herbert and Miller also reported that no clear correlation was apparent for the photodegradation of the agrochemical, flumetralin, on various soil types [6.1].

6D. Product Studies

In addition to product studies on soils, the solid state photolysis of the smoke dyes was studied to aide in the identification of reaction products and to determine the effect of the soil matrix on product distribution. Success in detecting and identifying reaction products, however, was limited. In general, anticipated reaction products appear to be more photolabile than the parent dyes. Only in the case of Disperse Red 9, Solvent Green 3 and Solvent Yellow 33 are reaction products detected upon their photolysis on soils or in the solid state.

The major photodegradation pathway for Disperse Red 9 was demethylation, resulting in the formation of 1-aminoanthraquinone (Figure 6-4). This reaction product was observed both on soils and in the solid state. Photochemical N-dealkylation of aminoanthraquinone disperse dyes sorbed to polyester fibers has been reported previously [6.12]. It was hypothesized that dealkylation results from initial attack of an electrophilic reagent on the lone pair of electrons on the nitrogen atom. We propose that demethylation of Disperse Red 9 on soil results from reaction with photochemically generated $^1O_2$. In the case of solid-state photolysis, demethylation most likely results from reaction with $^1O_2$ from a self-sensitized reaction of Disperse Red 9.

Photolysis of Solvent Green 3 resulted in the formation of two stable reaction products. Chin and Borer [6.13] observed the thermal degradation of Solvent Green to proceed by dephenylation, deamination, and lastly the formation of 10,10'-bianthrone from the coupling of the anthrone rings. Several of these products were purchased commercially and compared to products seen from the soil photolysis of Solvent Green 3; however, we determined that none of these compounds corresponded to the photodegradation products. Analysis of the reaction products by HPLC with a photodiode array detector indicated that the absorption maximum in the visible spectrum was almost identical to that of the parent compound, suggesting also that the anthraquinone ring had not been disrupted. We made a substantial effort to isolate the major product by preparative LC and TLC. Analysis of the isolated product by HPLC and solid probe MS showed the major product had reverted back to the parent dye, Solvent Green 3. Based on this observation, we hypothesized that the major photolysis product was the hydroquinone of Solvent Green 3.

Photolysis of Solvent Yellow 33 in the solid state resulted in the formation of 2-carboxyquinoline (Figure 6-5), however, this reaction product could not be detected in photolysis studies on soils. Independent soil photolysis experiments demonstrate the half-life for 2-carboxyquinoline on EPA #3 soil is < 1 hour, suggesting that if 2-carboxyquinoline was formed, it was readily degraded.

Photooxidation of 1-aryl-2-naphthols, such as Solvent Red 1, are known to proceed by reaction of $^1O_2$ with the hydrazone tautomer (Figure 6-6) resulting in the formation of the 1,2-napthoquinone and guaiacol [6.7]. We have been unable to detect either of these potential reaction products in either soil or solid state studies.

In summary, all of the smoke dyes were photoreactive to some extent on soil. Because of light shielding effects, however, none of them were completely photodegraded. The mean depths of photolysis measured for the dyes and the dependence of the MDP on soil depth for Disperse Red 9 suggested that indirect photolysis occurs below the photic depths of the soils. Solution phase studies indicated that indirect photolysis was most likely occurring through photo-oxygenation via reaction with singlet oxygen. Except for Solvent Green 3, none of the dyes gave photolysis products that are expected to be more persistent than their parent compounds.

7. Fate in anaerobic sediments (Task 7)

7A. Background

Prior to this study, there were no published data on the fate of dyes in environmental systems. However, there had been a few reports of disperse dyes detected in aquatic systems [7.1, 7.2]. It had been shown that re-formation of the parent amines could result from *in vivo* metabolism of azo dyes [7.3, 7.4, 7.5] or the action of bacteria in river water and soil [7.6]. It also was known that aerobic biological waste treatment was inefficient [7.7, 7.8, 7.9].

From basic chemical considerations as well as from the chemistry of dyeing, it was known that many dyes are subject to reduction. Potentially very important was the fact that the vat dyes, many of which are anthraquinone analogs, are easily and reversibly reducible [7.10]. Similar considerations strongly suggested that reduction of azo dyes would be irreversible.

Although there were few studies of reduction as an environmental transformation pathway, nitro group reduction on pesticides had been demonstrated. This is significant because many dyes and most munitions are nitrated. Also, reduction of aromatic nitro groups is irreversible and results in formation of an aromatic amine. The potential importance of reduction as a transformation pathway was further supported by the reduction of the dye resazurin to measure dehydrogenase activity of sediments [7.11]. Most bottom sediments are anaerobic.

Few data were in the literature regarding probab[illegible]ctions of the quinoline dyes beyond their existence in water as zwitterions and their role

as complexing agents (See section 5). Studies had found two disperse quinoline dyes to be very stable in sediment.

Recently, studies have shown reduction of aromatic azo compounds [7.12], nitroaromatics [7.13, 7.14], benzidine-based dyes [7.15], and disperse dyes [7.16] by sediments. Thus, it was concluded that the smoke dyes were most likely to be transformed either by photolysis on surfaces or under anaerobic conditions. The potential importance of the latter conclusion was further indicated by the fact that smoke dyes are expected to be transported to bottom sediments because of their strong sorbtion to sediment particles (See section 4D.II).

7B. Materials and Methods

7B.I. Sediment preparation

Sediments were collected by scraping the soft upper surface of a lake bottom (approximately 2 to 5 cm) with a polyethylene or metal container at a depth of 20 to 100 cm. The sediments were sieved (60 mesh, U.S. Standard) at the lake and stored under lake water in completely filled 4-liter jars. Jars were stored at room temperature prior to use. Lake water was always used in sediment experiments and the sediment slurries had pH's of 5 to 6. Sediment samples were analyzed several times to determine their organic carbon content. No attempt was made to obtain a statistically defensible characterization of the different lake sediments. However, three different methods were used for organic carbon determination. The University of Georgia's soils laboratory (where the analyses were performed) basically uses the standard Walkley-Black method [7.25] for organic matter. This was converted to organic carbon by dividing by 1.724. A coulometric combustion method [7.26] was used by the Colorado School of Mines laboratory, which also performed analyses. The EPA laboratory also used a combustion method but with infra-red detection.

Sediments were prepared for product studies by adding known amounts of purified dye in acetonitrile (ACN) to sediment (0.3 - 0.5 kg) that was slowly stirred in large beakers or Mason jars. Dye was added such that the sediment was usually, but not always, undersaturated with respect to dye and ACN was less than 1% by volume.

The sediment-to-water ratio was maintained as high as possible, consistent with good mixing, by an impeller type stirrer. The containers were sealed with aluminum foil or lids and stored in the dark at room temperature until analysis. Under these conditions, the sediment layer was always at least 4 cm thick and had 4 to 8 cm of overlying lake water.

As necessary, some of the sediment was added to several scintillation vials prior to storage. These vials were analyzed by HPLC at various times to determine the approximate amount of dye loss (or dye-to-product ratio) prior to processing the product run for analysis.

For kinetics studies, sediment was treated in a manner similar to that described, in detail, by Yen et al. [7.16]. In general, the sediment was filtered with a Buchner funnel to obtain a known moist weight and to provide a

sample for moisture determination. The sediment was then returned to its water of known volume (after subdividing if desired). The containers were usually 1-pint Mason jars, which were sealed and allowed to remain quiescent for 2 or more days prior to the experiment. The sediment to water ratio ,ρ, was approximately 0.2 to 0.3. This approach allowed preparation of kinetic runs that were as near duplicate as possible.

The sediment samples were stirred under nitrogen before, during and after dye addition (usually less than 20 min). Dye was added in ACN solution that had been sonicated such that all dye was presumably dissolved. The sediment was stirred under nitrogen sparge while 15- to 20-ml portions were pipetted into 20-ml scintillation vials. The vials (15 to 25) then were sealed with aluminum-lined screw caps and stored in the dark until used for analysis.

Most experiments were performed at room temperature (23 - 27°C). Other temperatures were attained by using a constant temperature water bath or a refrigerator.

Samples were prepared by filtering (5.5-cm Buchner funnel with glass fiber filter paper) the sediment for 5 min after the surface of the filter cake appeared dry. Portions of the filter cake, used for moisture determination and analysis, were weighed in 20-ml scintillation vials. The moisture vials were oven dried at 80°C overnight for moisture determination. Sediment, in vials for analysis, was sonicated with ACN (2 ml per g of sediment). The overlying liquid was decanted and filtered through a 0.5-micrometer fluorocarbon membrane filter (13 mm) for analysis by HPLC. This method usually resulted in consistent recoveries that were quite adequate since absolute values of concentration are not necessary for determining first order kinetics.

Solvent Yellow 33 kinetic runs, however, always produced very erratic data, a result that may have been partly due to recovery problems. The same situation was observed with the other quinoline dyes.

Recovery also was checked for the later experiments with Disperse Red 9 and Disperse Red 11. This was necessitated by the kinetics of product formation. In the case of Disperse Red 9, the recoveries of dye and anthrone were found to be in excess of 95% and were not corrected. Recovery of the product of Disperse Red 11 was only 24% and so data for formation of this product were corrected prior to kinetic analysis.

Kinetic data were interpreted according to the model given by equations 7-1 and 7-2 where D is dye and A_1 and A_2 are intermediate products. Only A_1 was measured in the experiments.

$$D \xrightarrow{k_1} A_1 \xrightarrow{k_3} \text{Products} \qquad (7\text{-}1)$$

$$D \xrightarrow{k_2} A_2 \xrightarrow{} \text{Products} \qquad (7\text{-}2)$$

The differential equations describing dye and product, A_1, are given in equations 7-3 and 7-4.

$$-\frac{dD}{dt} = D_1 e^{-k_L t} \qquad (7\text{-}3)$$

$$\frac{dA_1}{dt} = k_1 D - k_3 A_1 \qquad (7\text{-}4)$$

For initial conditions, $D=D_1$ and $A_1=0$ at time zero, where $k_L = k_1 + k_2$, the simultaneous solutions are:

$$D = D_1 e^{-(k_1+k_2)t} = D_1 e^{-k_L t} \qquad (7\text{-}5)$$

$$A_1 = D_1 \left(\frac{k_1}{k_3 - k_L}\right) [e^{-k_L t} - e^{-k_3 t}] \qquad (7\text{-}6)$$

In most cases, kinetic plots were first order over at least two halflives and included eight or more points. The rate constants were extracted in two ways. In all cases, a value for the rate constant for dye disappearance, k_L, was obtained as the slope of a regression of ln dye concentration versus time, i.e., from the logarithmic form of equation 7-5. Whenever possible, the regressions extended over approximately two halflives. When this was not possible, the data either were not used or were taken from a shorter, early part of the plot. In some situations, as few as four or five points were used for comparison purposes.

In a few cases, dye loss, product appearance and product disappearance were all followed, by HPLC, in the same experiment. For these experiments, rate constants k_1, k_2, and k_3 were also extracted individually by curvefitting. This was done by the NLIN procedure of SAS [7.27], which minimizes the least squares function, φ, for all time points, equation 7-7.

$$\varphi = \Sigma(D_1 - D_{predicted})^2 + \Sigma(A_1 - A_{predicted})^2 \qquad (7\text{-}7)$$

k_3 could not be obtained by curvefitting when the appearance of product A_1 was followed but its loss was not. However, single values of k_1 could be estimated as follows.

From equation 7-6, it can be seen that a linear regression of A_1 versus the bracketed term has a slope of $D_i(k_1/(k_3-[k_1+k_2]))$. However, k_1+k_2 is equivalent to k_t (known from regression), k_3 is small compared to k_t, and D_i is known from regression or curvefit. Thus, k_1 can be estimated by equating k_3 to zero or by using an estimated value. The difference between the values returned by these two methods was less than 40 percent in the worst case. Whenever possible, estimated values of were used.

In a few cases, Arrhenius activation energies were estimated from the rate constants at two or three temperatures. This was based on the change in ln k_t with respect to the reciprocal of temperature. The slope was obtained algebraicly for two points or by regression for three.

7B.II. Isolation of products

Sediments were processed to identify products by decanting the overlying water (which was never found to contain more than tiny portions of dye or product). The sediment was then filtered with a Buchner funnel to remove most of the water. This mostly pore water contained only traces of products except in the case of Disperse Red 11.

The filter cake was slurried with a volume (L) of ACN equal to two times the sediment weight (kg). As appropriate, the ACN (actually ACN/water) slurry was either neutralized and made acidic (pH 5-6) with acetic acid or basic (pH 8 - 10) with ammonium hydroxide. The slurry was filtered again to give an ACN/water solution that was rotary evaporated until only water remained. The pH of the water was adjusted again, if necessary, and extracted with methylene chloride. The methylene chloride was rotary evaporated to a volume of less than 2 ml for gel permeation chromatography (GPC).

Product runs were usually made using sediment from Herrick and Kingfisher Lakes (Georgia). Occasionally Beef Pond Lake (Georgia) sediments were used, but in all cases, the detected products were found in at least two different sediments. Products were not quantified, so differences in product composition could not be related to sediment source. Duration of the run was probably a more important factor in product distribution than sediment source.

As expected, ACN extracted a very large amount of a significant number of materials (mostly humics) from the sediment, making product detection virtually impossible by GC-MS and usually by HPLC. This problem was greatly compounded by the fact that usual clean-up methods could not be used since the products were unknown. Consequently, GPC (size exclusion) was tried as a last resort. This technique resulted in removal of the vast majority of naturally occurring materials and produced a much lower, but still substantial, background.

GPC apparatus (Bio-Rad Laboratories) consisted of a glass column (2.5 cm x 75 cm) containing approximately 45 cm (100 g) of 200 to 400 mesh S-X12 Bio-beads®. Methylene chloride was pumped through the column at a rate of 1 to 2 ml/min by a Perkin-Elmer series 100 HPLC pump. Under these conditions, most of the humic components were eluted by a retention volume of 90 ml. The volume between 90 and 135 ml, containing the dyes, was usually collected and rotary evaporated for HPLC or GC-MS. As required, eluates from GPC were dried and taken up in ACN (or ether) for HPLC or methylation with diazomethane. The diazomethane was generated using Diazald® (Aldrich Chemical Co.).

7B.III. Identification

Identification of transformation products was based on the use of one or more of the following techniques--GC-MS, GC-FTIR, NMR, HPLC with diode array spectra, HRMS, TLC or HPLC with more than one stationary or mobile phase. Whenever possible, data for identified chemicals were compared with data for purchased or synthesized compounds.

7B.IV. Synthesis of Transformation Products

Dye/anthraquinone products were synthesized, by dithionite or aluminum reduction, in quantities sufficient for characterization by GC-MS, HPLC, GC-FTIR, NMR, etc. The dithionite and the aluminum metal reductions were based on information from Bradley [7.17] and Hudlický [7.18], respectively.

Aluminum reductions were carried out by addition of a small amount of dye (less than 1 mg) to approximately 20 ml of gently stirred concentrated acid, which contained about 0.5 g of Al filings. The solution was warmed slightly, if necessary, until there was a definite change of color. The reaction mixture was then cooled, poured over ice, neutralized while cooling, and extracted with a small amount of methylene chloride for GC-MS. A portion of the extract was rotary-evaporated and put in acetonitrile (ACN) for HPLC.

For dithionite reductions, less than 1 mg of dye was placed in approximately 10 ml of MeOH or EtOH. To this was added 1 pellet of KOH and 20 to 30 ml of water. The solution was stirred during the reaction and during the addition of sodium dithionite (up to about 0.1 g). More dithionite, base and or gentle warming was used as necessary to bring about a sustained color change. The solution was then cooled, neutralized and treated as with the aluminum reductions.

The methods were convenient because they could be carried out in a small beaker or flask on a hot plate and because isolation/purification of individual components was not necessary. They were also easily scaled-up if needed. Both methods, however, resulted in troublesome amounts of S_8 in the methylene chloride extracts. It is interesting, and perhaps significant, that both methods produced the same major products. Attempts to reduce several anthraquinones with sodium borohydride resulted in products that largely reoxidized to the parent dye on extraction.

7C. Transformation Product Studies

7C.I. Azo Dyes

7C.Ia. Disperse Red 5. Three transformation products--2-chloro-4-nitroaniline, 2-chloro-1,4-phenylenediamine and N,N-*bis*(2-hydroxyethyl)-1,4-phenylenediamine--were found from sediment reduction of Disperse Red 5 [7.16]. All three compounds are anilines, two from cleavage of the azo group and one from both cleavage and nitro group reduction. These products are entirely consistent with expectations. It is almost certain, however, that the nitro compound would not have been found if the product run had been extracted after a longer reaction time.

7C.Ib. Solvent Red 1. Products of Solvent Red 1 were more difficult to identify because the expected products--o-anisidine and 1-amino-2-naphthol--co-eluted by HPLC. Also, GC-MS was not successful until GPC could be used to clean-up the samples. After GPC, each product was detected by GC-MS; both the spectra and the retention times of the products were identical to those of purchased materials.

Several other azo dyes have been studied in sediment systems [7.16, 7.19]. Reaction pathways for the two azo smoke dyes and two other azo dyes that have been studied in sediments are shown in Figure 7-1. In all cases, the primary products are amines resulting from nitro group reduction and/or cleavage of the azo bond. This is consistent with environmental data on Disperse Blue 79 [7.19], in that a cleavage product has been found recently in river water [7.20]. Thus, we conclude that reduction of nitro and azo groups is general in anaerobic environments.

7C.II. Quinoline Dyes

Several different studies were carried out with Solvent Yellow 33 in three different sediments. However, the dye was found to be so unreactive that, initially, no attempts were made to identify products. Late in the project, an attempt was made to identify products by using Herrick Lake (Georgia) sediment that had been standing with dye for about 2 years. This analysis was prompted by the fact that chemical reduction of Solvent Yellow 33 (Mass 273) with sodium dithionite resulted in the formation of a stable product having a molecular weight of 275. GC-MS of the extract after GPC showed the presence of a very small amount of the compound since both retention time and spectrum matched those of the synthetic material. Mass spectra of the synthesized and sediment-extracted products are given in Figure 7-36. Although the product was not identified positively, the expected product is shown in Figure 7-37.

7C.III. Anthraquinone Dyes

7C.IIIa. Disperse Red 9. Twelve different runs were carried out to identify transformation products. Early kinetic and product studies showed the appearance of a product by HPLC having the chromatogram and diode array spectrum shown in Figures 7-2, and 7-3. However, characterization of the

product required GPC for sample clean-up. After clean-up, GC-MS showed the dye with mass 237 and two components having apparent mass 223 (Figure 7-4) that eluted before and after the dye. This was first thought to be 1-amino-anthraquinone resulting from demethylation of the dye but, on close examination, the retention time and spectrum did not match those of the purchased material.

The difference of 14 mass units also suggested an anthrone or an oxyanthrone. A literature search resulted in a paper [7.17] giving the synthesis and properties of one of the two possible anthrone isomers. Reduction of Disperse Red 9 with aluminum metal resulted in material for which the mass chromatogram showed components of mass 223 eluting on either side of the dye. The GC-MS and HPLC retention times and spectra of the peak eluting before the dye matched precisely with those of the compound found in the sediment. The other isomer was found to be much less stable, but both were found in some product runs (Figures 7-4, and 7-5). The diode array spectrum of the second isomer is shown in Figure 7-6.

The compound, ANT, eluting before the dye was synthesized and purified by flash chromatography in sufficient quantity for HRMS, NMR and melting point determination. Figure 7-7 is the HRMS obtained by direct insertion of the solid. The accurate mass, 223.100, was consistent with the formula $C_{15}H_{13}NO$, and the presence of a peak at mass 206.098, due to loss of OH, suggests the hydrogen-bonded isomer. The mass 249 peak is an impurity.

The melting point at 115 to 117°C was higher than the 111 to 113°C mp, for the compound identified as the 1-methylamino(9,10H)anthraceneone [7.17]. Unfortunately, Bradley and Maisey [7.17] gave no basis for their isomer assignment so further work was required to achieve a definitive identification.

The NMR spectra of ANT are shown in Figures 7-8 through 7-11. After the chromatographic runs, there was insufficient sample for ^{13}C NMR so assignment was pursued first by GC-FTIR. However, the ^{13}C NMR and correlations were obtained later with the following results.

The proton NMR spectrum (Figure 7-8) shows a broad NH resonance at 9.51 ppm and singlets at 4.23 and 2.95 ppm for the methylene group at C10 and the methyl group of the amine, respectively. The remaining downfield signals between 6.5 and 8.5 ppm are from the aromatic hydrogens. All 15 signals are present in the ^{13}C spectrum (Figure 7-9) and DEPT 135 (Figure 7-10) indicates the methyl group at 29.4 ppm, the methylene carbon at 33.2 ppm, and 7 CH's between 107 and 134 ppm. The carbonyl carbon is located at 186.8 ppm. The complex pattern of aromatic hydrogens was resolved in a CH correlation experiment into the expected four doublets and three triplets (Figure 7-11). A ^{1}H COSY experiment indicates coupling between the aromatic hydrogens but also shows some coupling between the hydrogens of the methylene group to aromatic hydrogens (Figure 7-12). Based on the above experiments, the following assignments are proposed (ppm)[proton first then carbon]: C1 153.0; C2 doublet 6.58, 107.9; C3 triplet 7.35, 134.3; C4 doublet 6.59, 114.4; C4a 139.4, C5 doublet 7.34, 127.5; C6 triplet 7.49, 131.8; C7 triplet 7.40, 126.6; C8 doublet 8.25 126.8; C9 186.8; C10 33.2; C10a 142.9; C8a 133.1; C9a 114.4,

CH_3 29.4. Carbons 9 and 10 were assigned with the help of data from Tomano and Koketsu [7.28].

A Gram-Schmidt chromatogram from a sediment run extract was obtained by GC-FTIR (Figure 7-13). Spectra of the peaks at 39.8 min (Figure 7-14) 44.1 min and 46.4 min (Figure 7-15) show these components to be ANT, dye, and the second anthrone, respectively. This was confirmed by excellent agreement with spectra of the three components obtained from the extract of an aluminum reduction of the dye. A GC-FTIR chromatogram of the latter is shown in Figure 7-16 along with spectra of the dye and anthrones (Figures 7-17 through 7-19).

Examination of the FTIR spectra shows that Disperse Red 9 has two carbonyl stretching peaks at 1686 and 1643 cm^{-1} corresponding to the free and intramolecularly hydrogen bonded C=O's, respectively. It also has its N-H stretching peak at 3308 cm^{-1}. The spectrum of the first eluting peak, ANT, has only one carbonyl stretching peak at 1642 and an N-H stretching peak at 3306. Combined with the mass spectral data, the infrared spectra provide unequivocal proof that ANT is the hydrogen-bonded isomer, 1-methylamino-(9,10H)anthraceneone. A similar analysis shows that the peak eluting after the dye is the non-hydrogen bonded anthrone, 1-methyl(9H,10)aminoanthraceneone.

Gas chromatographic elution of the hydrogen-bonded isomer before the dye, and the non-hydrogen-bonded isomer afterwards, is entirely as expected. This behavior was also observed for other anthrones. The reaction of Disperse Red 9 is shown in Figure 7-39.

7C.IIIb. Disperse Violet 1. Disperse Violet 1 was initially expected to be reduced to DDA, 1,4-diamino-2,3-dihydroanthraquinone (mass 240),in sediment. This compound is the leuco form of Disperse Violet 1 [7.21]. It was previously used in violet smoke devices where it formed Disperse Violet 1 on combustion. However, DDA is reported [7.22, 7.23] to be unstable toward hydrolysis, the products of which react with ferric ions to produce a fluorescent compound.

Bradley and Maisey also reported that Disperse Violet 1 reduction (followed by aeration) yields quinizarin [7.17]. Quinizarin is also anticipated to undergo metal complexation, or reduction to leuco-quinizarin in sediments. Quinizarin is probably the compound reacting with ferric ions to produce the fluorescent product noted by Salinas et al. [7.23].

Ten product runs were made with Disperse Violet 1 in an attempt to identify products, especially DDA. Unfortunately, only two products were identified with certainty--quinizarin in product runs 4 and 7 and quinizarin and 1-hydroxyanthraquinone in run 8. Both compounds were identified by comparison of retention times and spectra with those of purchased material. In addition, the quinizarin from product run 4 was identified by HPLC with fluorescence detection. In this case, quinizarin eluted at 5.9 min as did the unknown component. Both the sample peak and quinizarin had exitation and emission maxima at 490 nm and at 565 - 570 nm, respectively. In all cases, the product peaks detected were very small.

Other products that were tentatively identified by GC-MS were leuco-quinizarin and 1-aminoanthraquinone. These compounds could not be confirmed. Many anthraquinones and related compounds are difficult to identify at trace levels by GC-MS because the base peak is due to the molecular ion and other peaks often have an intensity of less than 15%.

Reaction of Disperse Violet 1 with dithionite resulted in two major products. These were identified as quinizarin [7.17] and leuco-quinizarin as expected. Identification was based on GC-MS, HPLC and TLC for quinizarin and MS for leuco-quinizarin. GC-MS of the reaction mixture shows quinizarin (mass 240) and the leuco compound (mass 242) (Figure 7-20). High resolution MS of these components resulted in molecular weights of 240.043 and 242.059, corresponding to $C_{14}H_8O_4$ and $C_{14}H_{10}O_4$, respectively.

The above facts strongly suggest that Disperse Violet 1 is reduced in sediment to a product, perhaps DDA, that is converted at least partly to products containing OH groups in place of NH_2. As noted above, such products are likely to react further. Also, complexation by the metals in sediment could adversely affect extraction (recovery) of quinizarin and other alpha hydroxy compounds. It was found, however, that addition of EDTA did not result in increased recovery of quinizarin.

7C.IIIc. Solvent Green 3. No product studies were attempted with Solvent Green 3 for two reasons. First, the dye is so insoluble that it would be difficult to attain levels of dye sufficiently high for measurement. Data from Section 4 can be used to show that, in a sediment with 1% organic carbon, about 0.3 mg of dye would saturate 1 kg of sediment. Second, the dye is expected to be extremely immobile in the environment and to reach sediment only as runoff of particulates. This contention is supported by the large K_{oc} (Section 4).

7C.IIId. Disperse Red 11. Fifteen sediment runs for product identification were conducted for different time periods and at different concentrations. Early in the project, a component that absorbed at the same wavelength as the dye was detected by HPLC. This red compound, HA43, proved extremely difficult to resolve cleanly by HPLC and was not detected by GC-MS. A diode array spectrum is shown in Figure 7-21. The fact that the spectrum was so similar to that of the Disperse Red 11 strongly suggested that the compound was an anthraquinone with a structure similar to that of the parent dye. Importantly, there was no reaction in sediment that had been boiled for 20 minutes.

Because the compound was not amenable to gas chromatography, it was separated from sediment components by HPLC, and its electron impact mass spectrum was obtained by direct insertion. Analysis (Figure 7-22) showed the compound to have a molecular weight of 254 and a typical anthraquinone fragmentation pattern. Realistically, a molecular weight of 254 could result from only two possible anthraquinones--the hydroxymethoxy or the hydroxy-diamino. Since the former compound requires the replacement of one amino group by a proton and another by an OH, it seemed likely that HA43 was the hydroxydiamino-anthraquinone.

To verify the identity of this reaction product, the methyl group was cleaved from the parent dye with cold concentrated sulfuric acid to give a red compound that could not be extracted from basic aqueous solutions. Mass spectra of the sediment reaction product (Figure 7-22) and the synthesis product are essentially the same. The HRMS spectrum in Figure 7-23 is consistent with the empirical formula $C_{14}H_{10}N_2O_3$. The HRMS also confirms the expected fragmentation as M/e 254, molecular ion; M/e 226, M- C=O; and M/e 197, M- NH_2-C_2-OH. Thus, HA43 is the demethylated product, 1,4-diamino-2-hydroxyanthraquinone. This compound has not been reported previously in the chemical literature as indicated by exhaustive searches of Chemical Abstracts and Beilstein.

Because of the importance of transformation products, HA43 was further characterized by its absorbance and fluorescence spectra as follows. The uv-visible maxima in 60/40 acetonitrile/water are at 256-258nm, 528-532nm and 560-564nm. The two peaks in the visible range have about the same extinction coefficient, which is much less than that of the peak near 250nm. The latter two peaks and the relative intensities are characteristic of all anthraquinone dyes that we have examined.

The fluorescence spectrum (uncompensated) was obtained in 60/40 ACN/water with the HPLC detector (Perkin-Elmer model LS-40). In this solvent, the exitation maximum is at 256-260nm and the emission maximum is at 600-610nm. The fluorescence of this product is cherry red, as is that of the parent dye, and is very obvious on TLC plates. Its emission and excitation spectra were identical to those of the sediment product.

As expected, the hydroxy compound was less strongly retained than the parent methyl compound on reverse phase chromatography. However, no solvent composition would shift the peak very far from the solvent front since the Rf would go through a maximum. Nevertheless, it was possible to confirm that the synthesized chemical and the sediment product were the same by both TLC and HPLC.

Synthesized HA43 was examined by NMR (^{13}C and proton). The proton spectrum (Figure 7-24) indicates the presence of an alcohol proton at 11.5 ppm and the remaining aromatic hydrogen of ring C at 6.6 ppm. Two additional sets of aromatic hydrogens are located at 8.2 ppm (C5 and C8 hydrogens) and at 7.7 ppm (C6 and C7 hydrogens). The remaining upfield signals are solvent, water, and ethyl acetate (an impurity). Addition of 100 μl of D_2O causes an immediate exchange of the alcohol hydrogen and loss of the signal in the ^1H spectrum. The hydrogen at C3 is fully exchanged in 7 days, possibly due to keto-enol tautomerization (Figure 7-25).

Only 14 signals are present in the ^{13}C spectrum since the high intensity peak at 125.7 ppm is due to two carbon resonances (Figure 7-26). The carbon containing the hydroxyl group resonates at 153.4 ppm. A DEPT 45 spectrum contains five carbon signals because of the five aromatic C-H's (Figure 7-27).

The parent compound, containing a methoxy group at C2, shows only the aromatic hydrogen and the new methyl signal at 3.1 ppm. There are no

resonances downfield of 8.0 ppm. The NMR results, given in Figures 7-24 to 7-27, unequivocally establish HA43 as the 1,4-diamino-2-hydroxy compound. The FTIR spectrum (Figure 7-28) is entirely consistent with this conclusion.

No other products were verified, either from Disperse Red 11 or from its daughter product, HA43, although many attempts were made. However, it is probable that products are formed from either the dye or HA43 as a result of replacement of one or more of the amino groups with protons or a hydroxy group. For example, quinizarin was tentatively identified in several product runs but at concentrations too low for confirmation.

The above facts are consistent with the observation that dithionite or aluminum reduction of the dye results in formation of 1-amino-2-methoxy anthraquinone as the major product. Similar reduction of HA43 resulted in the analogous 2-hydroxy compound. Our experience with this compound and several other substituted anthraquinones suggests that compounds having a hydroxyl group in the 2 position will probably not be amenable to GC. These observations are based on GC-MS, HRMS and methylation of the products with diazomethane. Methylation of the sediment extracts, prior to GPC, was not attempted because of their complexity.

If the above conclusion is correct, other products may still not have been seen because (1) they are not amenable to GC-MS, (2) they quickly form compounds that are not volatile, (3) they are good complexing agents which could prevent their extraction, or (4) their chromatographic peaks were hidden behind those of the sediment background components.

7C.IIIe. Other Anthraquinones

1-Chloroanthraquinone. Before GPC was available for sample cleanup, a decision was made to look for sediment products of 1-chloroanthraquinone as a test case. It was hoped that the Cl isotope peaks would serve as a tracer and permit us to find the products among the background peaks.

Figure 7-29 shows the GC-MS spectra of an extract from Kingfisher Lake (Georgia) sediment where both anthrones were observed. The peak at 7.4 min is one of the anthrones and the large peak at about 8.3 min is the parent compound at mass 242, which coelutes with the other anthrone. The peak at 8.44 min is the reduction product, mass 244, resulting from addition of two protons. It is probably the dihydroanthraquinone. We have not seen the dihydroanthra-quinones from other anthraquinones.

The chloroanthrones also were synthesized by reduction with dithionite and with aluminum, and both isomers were found in each case. The GC-MS of the synthesis mixture matched the results from sediment except for the absence of one peak. The mass 244 reduction product was not observed in the reductions with dithionite or aluminum.

1-Aminoanthraquinone. This compound reacted in sediment with the formation of one anthrone that eluted at 16.6 min. The other anthrone could not be detected. Reduction of the aminoanthraquinone with aluminum resulted in formation of both anthrones. Figure 7-30 shows the GC-MS data with

anthrones eluting on each side of the parent compound. Both compounds have the molecular ion as the base peak, with loss of 29 mass units causing the second largest peak.

Since the peak at 16.6 min is the first to elute, by analogy with the anthrones from Disperse Red 9, we can assume it is the hydrogen-bonded isomer. This was confirmed by GC-FTIR as shown in Figures 7-31 through 7-34. The reaction is shown in Figure 7-38.

Reduction of 1-hydroxyanthraquinone with dithionite also gave two anthrones as expected. On GC-MS analysis of the reduction product mixture, the anthrones were found to elute on either side of the parent compound. In both cases, the base peak is the molecular ion and the second largest peak is formed by loss of 29 mass units. The hydroxy compound was not studied in sediment.

7C.IIIf. Summary. The present data suggest that mono 1-substituted anthraquinones will probably undergo transformation of the ring system by anthrone formation in sediment. At least in the case of Disperse Red 9, the hydrogen-bonded isomer is the most stable.

The 1,4-diaminoanthraquinones seem to undergo more complicated reactions that lead to extensive degradation and/or products that are not easily recovered. It is probable that multiple products result from replacement of the amino groups with OH and reduction. The presence of an OH or methoxy group in the 2-position results in a demethylated product that accumulates. However, elimination of substituents in the 2 position has been reported [7.21, 7.29] and may lead to products that were not detected. All of the above facts taken together suggest that Disperse Violet 1 and Disperse Red 11 may give difficult-to-detect products by reactions similar to those in Figure 40.

7D. Kinetic Studies

The development of disappearance rate constants for the dyes was the primary goal of the kinetic studies, but the project proved much more complicated than initially envisioned. For example, reactions were usually first order over about two halflives but frequently deviated at longer times, i.e. the rate constants decreased. Thus, delineation of detailed kinetics of the dyes and products was given low priority because of time constraints and because Task 8 was addressing the reactions of products like those from the azo dyes. In addition, the first dyes studied, azo and quinoline, reacted too fast or too slow, respectively, for detailed studies.

Among the factors that might influence reaction rates in sediment, organic carbon content seems likely to be one of the most significant. Therefore, organic carbon content was measured for all of the sediments used in this work (Table 7-1). However, no attempt was made to systematically examine carbon content in sediment as a variable; indeed, the results are not suitable for that purpose. Measurements do show about a factor of three variation in organic carbon for the different sediments. Three factors that affected the design and execution of the kinetic experiments are discussed below.

First, there are few data to guide the handling of sediment or to suggest how addition of solvents might affect reactions. Early in the project, we found that the stirring and mixing required for sediment preparation could affect the kinetics rather erratically. This effect was most pronounced for the fastest reactions--a fortunate fact since kinetics are of little importance for compounds that are quickly transformed.

Second, different reaction time scales for a dye and its products proved to be a major problem. In the cases of Disperse Red 9 and Disperse Red 11, the products had much longer halflives than the parent dyes. Also, time constraints due to sample processing and analysis clearly indicate that halflives less than a few hours must be considered as experimental upper limits. The possibility exists that sediment changes may be important when reaction times are short because then the sediment has no chance to recover from the disturbance of mixing, solvent addition, etc. Similarly, halflives of several months lead to questions about possible changes in the sediment over such long times.

Third, in systems that are so complex, there is always the possibility, perhaps even probability, that there are competitive reaction pathways. This can be indicated by the data in at least three ways: (1) the prepared dye concentration, D_o, is not approximately equal to the extrapolated initial dye concentration, D_i, (2) kinetics are not first order, and (3) rate constants are highly erratic and/or not the same for product appearance and dye loss. All of these indications were seen in one or more experiments.

Detailed data for kinetic runs are given in Table 7-1 and the notes thereto (Table 7-2), although many other augmenting experiments were conducted to help understand the sediment/dye system. Relevant data are included for each run that resulted in useful information. Individual kinetic plots are provided in the text only to illustrate specific points in the discussion to follow. Other relevant plots of kinetic data are included in Appendix D. Since the data in Tables 7-2 and 7-3 are largely self-explanatory, they will be used first to illustrate some of the general problems discussed earlier. Then, kinetics of specific dyes will be discussed in regard to their sediment reactions.

Problems associated with sediment treatment are illustrated by Figure 7-41 for Disperse Red 5 experiments 6c and 6d that were prepared in the presence and absence of air, respectively. The data clearly show that stirring in air reduces the transformation rate. To examine this effect, great care was taken to split and acclimate sediments so that. to the extent possible, the only variable was exposure to air.

Although the data are not shown, experiment 6 was conducted with duplicates that were split so that two were air stirred and two were under nitrogen. In this case, rate constants of the two kept under nitrogen differed by a factor of 4.5 and spanned those of the air-stirred replicates. Thus the variability, although small from the point of view of environmental considerations, is too large to permit rigorous problem identification.

Most experiments to examine the effect of air were conducted with Disperse Red 5, but other dyes also were used. For example, experiments 4 (air) and 5 (N_2) with Disperse Red 9 (Tables 7-2 and 7-3) show the rate constant to be a factor of two less in air. Also, the data for 1-chloroanthraquinone (Tables 7-2 and 7-3) show only a factor of four variation using different sediments. Experiments 24A and 24B only differ by a factor of 2, while 24A was stirred for 1.5 hr in air whereas 24B was under nitrogen. Although many experiments were conducted to define the magnitude of this effect, no definitive results were obtained. It seemed clear, however, that the effect was most severe in the cases where it is least important, i.e., for the fast reactions. Thus, all of the later experiments used acclimated sediments that were prepared under nitrogen. Also because of this, we assume that halflives of less than 0.08 days are an upper limit and are reported that way in Table 7-2 even though rate constants were estimated.

The effect of dye concentration also was difficult to determine because the concentration and nature of reactants in sediment are entirely unknown. Consequently, appropriate initial dye concentrations could only be determined empirically, if at all. This was made difficult by the fact that dye concentrations must be high enough for adequate analytical sensitivity. But, dye concentrations are limited by their low solubility and the need to conduct studies below the system saturation limit.

The effect of exceeding the saturation limit is easily seen in a simulated kinetic experiment Figure 7-35. That figure shows the decrease in initial rate due to presence of solid dye, assuming that dissolution of dye is not rate limiting. Even if dissolution is rate limiting, there will be a reduced initial rate until the excess dye is consumed. Most importantly, the extrapolated initial concentration, D_i, would be greater than the prepared concentration.

For these reasons, the usual systematic studies of variation in rate constant with concentration were not conducted. Although concentrations were varied in a number of experiments, the range in dye concentration was generally not greater than the variability in rate constants between experiments. The following examples will highlight these points.

Disperse Red 9 data in Table 7-2 show about a 10-fold decrease in rate constant for a 3- to 10-fold change in dye concentration, based on experiments 3 and 8. However, most of the points for experiment 3 were not well spaced in time and were late in the reaction. Although experiment 8 had very good data, both 3 and 8 have extrapolated D_i's that are less than D_o. Thus, whatever the cause of the low rates in these two experiments, they were not above the saturation point. Similar observations can be made for the Solvent Yellow 33, Disperse Red 9, and Disperse Red 5 experiments. The latter however, are much more variable.

In three experiments, the sediment was respiked with dye on termination. This guaranteed that the sediment was identical for each spike. In all three cases, Disperse Red 1 (expt. 1), Disperse Red 11 (expt. 12b) and Disperse Red 5 (expt. 1), the respike had a lower rate constant (Table 7-2). This is

consistent with the fact that the rate often decreased with time after about 2 halflives. Nevertheless, the effect is still only about a factor of 2.

Phenol and $NaNO_3$ were added in some experiments to determine the effect of these biological inhibitors. Experiment 12 with Disperse Red 5 contained $NaNO_3$ (replicate 12b, 0.01 M (0.1 mol/kg) and 12c, 0.03 M (0.27 mol/kg)). The higher concentration clearly slowed the reaction but it was still too fast for good measurement.

The same measurement problems were found with phenol and Disperse Red 5 (experiment 11; containing 1 percent phenol). However, the two replicates with phenol reacted faster than the two without phenol. A similar experiment, 24C, with Disperse Red 11 showed the phenol to have only a minor effect on the rate of dye loss (Table 7-2) compared to the control, 24B, but no HA43 product was formed. We also found that heat sterilizing the sediment before dye addition dramatically reduced the rate of loss of Disperse Red 9.

The effect of solvent was examined in experiment 5 with Disperse Red 9. Data in Table 7-2 show that there is no perceptable difference in rate constants over a 10-fold range in ACN concentration. Similar results have been found for other compounds [7.30]. However, this does not guarantee that reactions of other dyes might not be sensitive to solvent.

Examination of Table 7-2 shows considerable scatter in the rate constants. Surprisingly, however, the overall averages have coefficients of variation that are less than 100 percent, except for Disperse Red 5 and Disperse Red 11 loss. As shown in Table 7-4, the variation in the Disperse Red 11 data decreases to 35% when experiments 3 and 12 are eliminated. At one point, there was considerable problem with Disperse Red 11 in Herrick Lake sediment. The reaction seemed to be very erratic and unusually fast. The reason was not determined, but it was suspected to be due to an algal bloom since the extracts at that time were very green. As noted earlier, Disperse Red 5 reacted too fast for accurate measurement and was subject to effects of air on mixing.

Table 7-4 also shows that the halflives of the dyes vary from 0.1 to 140 days or about 1000 fold. Only Disperse Blue 3, Disperse Blue 14, and Solvent Yellow 33 have halflives greater than a few days. Certainly none of the dyes, except possibly Solvent Yellow 33, would be likely to persist very long in anaerobic sediments. The stability of Solvent Yellow 33 is consistent with data [7.16] for two other quinoline dyes, Disperse Yellow 54 and Disperse Yellow 64, which also were found to be very unreactive in sediment. It is possible that the slowness of reaction is due to metal complexation and/or existence as zwitter ions. The latter, and possibly the former, would lead to their sorption by cation exchange (Section 5).

Several extensive experiments with Disperse Red 9 and Disperse Red 11 were interpreted according to the model in Equations 7-1 and 7-2. These data are summarized in Tables 7-5 and 7-6 where data from Table 7-2 are compared with data obtained by curvefitting. In general, the agreement is good. This is shown by Figure 7-42 which includes all of the data points for experiments

8A and 8B with Disperse Red 9. Curves for the other runs gave similar fits but the replicates were not always superimposable.

The data in these tables show that the sum of k_1 and k_2 is similar to k_t for Disperse Red 11, but the sum is 29% lower than k_t in the case of Disperse Red 9. This observation can only be made for the regression data since k_t was not determined by curvefitting. The most important observation from Tables 7-5 and 7-6 relates to the ratio of k_1 to k_t (or $k_1 + k_2$). If the ratio is 1, the rate constant k_2 is zero and products other than A_1 are not formed. The tables show that the ratio is about 0.2 to 0.4 for Disperse Red 9 and about 0.5 to 1.0 for Disperse Red 11, strongly supporting the model. It also shows that most of the Disperse Red 9 that is destroyed does not form the anthrone, ANT. However, the reverse is true for Disperse Red 11 and its product, HA43. No convincing case could be made that the ratio was affected by temperature.

Little is known about temperature effects on sediment transformations so it was decided to estimate activation energies. Time constraints prevented systematic studies to be conducted at multiple temperatures but estimates based on 2 or 3 temperatures were adequate and feasible. The data in Table 7-7 show the activation energies to be in the range of 11 to 19 kcal/mol. This range is typical of many chemical reactions. Such limited data are of little use for mechanistic purposes, but can be used to estimate the effect of temperature differences.

Given all of the above information about products and kinetics, it is possible to tentatively suggest part of the reaction scheme for Disperse Red 11 (Figure 7-43). Inclusion of the mass 253 and 239 structures in the scheme is based on the following logic. The major products isolated from dithionite and aluminum reduction of 1,4-diaminoanthraquinones usually resulted from hydrolysis and or reoxidation during handling. Thus, the products were under thermodynamic rather than kinetic control. This control condition has obvious implications for the products isolated from sediments since much more sample handling is involved. Thus, reduced compounds, which were undetected under synthesis conditions, probably would not survive isolation from sediment. The mass 253 component is the major product of reaction of the parent dye with either Al or dithionite. If reaction B is slow (Figure 7-43) compared to D, then the mass 253 component may not be seen in the sediment extracts. The mass 239 product will not go through the GC and could only be seen after methylation. Although we know that path C (Figure 43) is slow compared to A, it is probable that neither product would be seen in sediments without studies designed specifically for that purpose.

In summary, it can be stated with reasonable certainty that under most environmental conditions, the smoke dyes are unlikely to persist in bottom sediments. The possible exception is Solvent Yellow 33, which is likely to have a half-life of approximately 6 months. The products that were detected from Disperse Red 9 and Disperese Red 11 are significantly more stable than the parent dyes and have halflives of a few months in sediment. Thus, they also are not very persistent at normal temperatures. The halflives will be longer at lower temperatures, but the rate constants can be corrected using the activation energies that were measured.

Task 8: Fate studies of aromatic amines

8.A Introduction

The aromatic amines comprise an important class of environmental contaminants. Aromatic amines can enter the environment from the degradation of textile smoke dyes, various agrochemicals and munitions. The munitions, specifically the polynitrobenzenes, such as TNT and tetryl, are of particular concern to the Department of Defense because of the potential for their reduction to the corresponding aromatic amines and their subsequent migration into groundwaters. Because aromatic amines are building blocks for many high volume industrial chemicals, loss to the environment may also occur from production processes or improper treatment or disposal of industrial waste streams. Therefore, EPA also has a significant interest in aromatic amines. Approximately one-third of the more than 3,000 chemicals reviewed by EPA under the Premanufacture Notice Review Process in the past year were aromatic amines. The ecological assessment of such large numbers of chemicals requires the development of predictive models that will accurately predict their behavior in soils, sediments and natural waters.

The primary focus of this task was to determine how aromatic amines interact with soil and sediment surfaces. Sorption processes that must be considered for aromatic amines in soil- and sediment-water systems include partitioning through hydrophobic interactions, cation or ligand exchange reactions, and chemical reactions leading to the formation of covalent bonds through nucleophilic and/or oxidative processes [8.1,8.2,8.3]. Differentiation between these processes is necessary, because, in general, sorption through the formation of covalent bonds with constituents of the sediment or soil matrix is an irreversible process, as opposed to sorption partitioning or cation exchange that can be described by equilibrium constants. Furthermore, irreversible sorption has important implications with regard to the persistence, bioavailibility and mobility of pollutants.

To gain further insight into sediment- and soil-associated reactions of the aromatic amines, studies with a series of 2-substituted and 4-substituted anilines were performed. These compounds were selected to vary the electron-donating and withdrawing properties of the 2- and 4-position substituents. Variation in this property, in turn, will affect the reactivity of the amino moiety, which is reflected in each aniline's pKa value, oxidation potential and nucleophilicity. The substituted anilines selected for this study and some of their pKa's are shown in Figure 8-1.

8B. Materials and Methods

8B.I. Sorption Kinetics

To a series of 8-ml test tubes was added 200 mg of dried pond sediment and 4 ml of distilled water. The tubes were incubated in a controlled temperature room at 25°C on a variable speed rotator. After an equilibration period of 18 hr, the tubes were spiked with 0.025 ml of a 1.6×10^{-4}M solution of the aniline in MeOH and rotated end-over-end at 25°C. At designated times, the sediment-water slurries were centrifuged, and the supernate was removed

and analyzed by HPLC on a Supelco pK_b-100 4.5 mm x 25 cm column with either 20:80 acetonitrile:water or 40:60 acetonitrile:water at 1.5 ml/min.

8B.II. pH-dependent Experiments

To 0.5 g EPA #11 clay and silt fraction (<105 micrometer) was added 300 ml distilled water. The slurry was continuously agitated with magnetic stirring and maintained at the desired pH by automated control. Sediment was allowed to equilibrate at the desired pH for 30 minutes and then spiked with the desired compounds to give a final concentration of 1.0×10^{-6} M. Samples for centrifugation and HPLC analysis were pulled as 5-ml aliquots at 24-hr intervals.

8B.III. Inhibition Experiments

These experiments were performed using the procedure as described above for the pH-dependent experiments; however, the blocking reagent was added to the slurry prior to the 18-hr equilibration period for resaturation.

8B.IV. Recovery Studies

To a series of 15-ml test tubes was added 1.0 g of dried pond sediment and 10 ml of distilled water. The tubes were spiked with 0.050 ml of 1×10^{-3} M aniline in water and 0.100 ml of 3.2×10^{-6} M aniline-UL-^{14}C-hydrochloride to give a final concentration of 0.005 μCi/ml of label and then rotated end-over-end at 25°C. At designated times, the sediment-water slurries were centrifuged, and the supernate was removed. The sediment plug was washed twice with 2 x 10 ml portions of distilled water for 30 min (tubes rotated end-over-end at 25°C), followed by sequential extraction for 2 hr each with 10 ml of 1.0 M ammonium acetate, and 10 ml of 0.5 M sodium hydroxide. In each case, the solvent was removed by centrifugation. One ml of each solution was then added to 10 ml of scintillation cocktail and counted for 5 min using a sample channel ratio method.

8B. V. Nitrogen-15 NMR Studies

Reaction with Aniline. Aniline was reacted with Suwannee Fulvic Acid (SFA) under two sets of conditions. In the first reaction, 500 mg of SFA (H-saturated) and 200 μl of aniline, 99.2 atom % ^{15}N were dissolved in 50 ml MeOH and refluxed for 3.5 hr. The solvent was then removed with vacuum distillation and the product dissolved in 3 ml of DMSO-d_6 in a 10-mm NMR tube. In the second reaction, 500 mg of SFA (H-saturated) and 200 ul of aniline were added to 100 ml of H_2O, titrated to pH 6 with 1N NaOH, and allowed to react at room temperature for 5 days. The sample was then H-saturated on a cation exchange column and freeze-dried. About 400 mg of the fulvic acid was dissolved in 2.5 ml DMSO-d_6 in a 10-mm NMR tube.

Nitrogen-15 NMR Spectrometry. Liquid phase ^{15}N NMR spectra were recorded on a Varian XL300 NMR spectrometer at an ^{15}N resonant frequency of 30.4 MHz. Refocussed (proton decoupled) INEPT spectra were acquired using a 15,649.5 Hz (515 ppm) spectral window, 0.5 second acquisition time, 2.0 second delay for proton relaxation, and polarization transfer times and refocussing

delays both equal to 2.78 milliseconds. ACOUSTIC spectra were acquired using the pulse sequence of Patt [8-4]. Acquisition parameters included a 15,649.5 Hz spectral window, 90° pulse angle, 2.0 second pulse delay, and tau delay of 0.1 millisecond. The ACOUSTIC spectrum of the SFA reacted with aniline in aqueous solution was recorded with the addition of chromium *tris*-acetylacetonate to obtain quantitative results. Chemical shifts are reported downfield of ammonia taken as 0.0 ppm.

8C. Sorption Kinetics

Initial studies focused on measuring the sorption kinetics of the 2- and 4-substituted anilines in sediment-water systems. The aqueous concentration of each aniline was measured in a resaturated pond sediment (Cherokee Park Pond, Georgia) at 5% solids (pH 6.5) as a function of time (Figure 8-2, data shown for the 4-substituted anilines). Removal of the anilines from the aqueous phase was fast over the first 24-hr period of the experiment followed by a slower rate of removal. This same type of kinetic behavior has been reported by Paris [8.1] and Ononye et al. [8.2] who have studied the binding of aromatic amines to humic material. They concluded that, initially, a rapid equilibrium is established, which may represent formation of imines with carbonyl components in the humic material, followed by a slow irreversible reaction, which may represent Michael-type or 1,4-nucleophilic addition to quinone components. Although our kinetic data may allow us to draw the same conclusion, based on these data we cannot rule out the possibility that cation exchange processes play a role in the sorption of these chemicals to the sediment.

Further analysis of the data in Figure 8-2 indicates that, with the exception of 4-aminobenzotrifluoride, a general trend is observed. As the pK_a of the aniline increases, there is an increase in both the rate and extent of sorption. Subsequent studies with 4-aminobenzotrifluoride determined that aqueous standards of this compound showed substantial loss over the time period that the sediment studies were conducted. 4-Aminobenzotrifluoride was excluded from analysis in subsequent data sets.

A plot of initial disappearance rate constants from Cherokee Park sediment versus pKa for both the 2- and 4-substituted anilines further illustrates the general trend between sorption kinetics and substrate pKa (Figure 8-3). It is obvious from these data that both the 2-methoxy- and 4-methoxyaniline are much more reactive than would be predicted by their pKa's, suggesting that these anilines sorb or react in the sediment-water system in a different manner than the other substituted anilines.

8D. Extraction Studies

Although the kinetics studies provide useful information concerning substrate reactivity, they provide little insight into sorption or binding mechanisms. To differentiate among the fractions of the anilines bound to a sediment by hydrophobic partitioning, cation exchange or covalent binding, we conducted a number of experiments in which Cherokee Park sediment that had been treated with either 4-methoxyaniline or ^{14}C-labeled aniline was extracted with an organic solvent, a salt solution, and a strong base either separately

or sequentially. Extraction of the sediment with an organic solvent, such as acetonitrile or methanol, is expected to remove that fraction of aniline sorbed by hydrophobic interactions. Likewise, the fractions of aniline bound by cation exchange and covalent bonding should be removed, or at least partially removed, by extraction with salt solutions and strong base, respectively. Although the fraction of aniline in the initial aqueous phase, organic extract and salt solution extract could be measured by HPLC, the use of ^{14}C-labeled aniline was necessary to determine the fraction of aniline irreversibly bound to the base-solubilized organic matter. Thus, by analyzing for free aniline by HPLC and counting the ^{14}C-label, it was possible to differentiate between reversibly and irreversibly bound aniline.

Initially, we treated a Cherokee Park sediment-water system at 10% solids with 4-methoxyaniline (initial aqueous phase concentration of 1×10^{-5} M). We determined that the 4-methoxyaniline was completely associated with the sediment phase after a 24 hr equilibration period. Extraction of the sediment phase with either acetonitrile, 0.5 M $CaCl_2$, 1 N HCl, or 1 N NaOH, with and without acetonitrile, resulted in no recovery of 4-methoxyaniline as determined by HPLC. We were also unable to detect any transformation products of 4-methoxyaniline or to detect an increase in the concentration of exchangeable cations in the aqueous phase of the sediment-water system after treatment with 4-methoxyaniline. These observations suggest the importance of irreversible binding and the need to work with radio-labeled chemicals to track the distribution of the bound residue.

Subsequent studies were conducted with aniline containing 0.2% uniformly ring-labeled ^{14}C-aniline. In these experiments, we treated a Cherokee Park sediment (10% solids) with aniline at an initial aqueous concentration of 5.0×10^{-6}M. After 72 hr of continuous shaking, the aqueous layer was removed and the sediment plug was extracted sequentially with methanol, 1.0 M ammonium acetate, and 0.5 N sodium hydroxide. The aqueous layer and each of the extracts were counted for the radioactive ^{14}C, and in select cases, were analyzed for aniline by HPLC. Initial studies indicated that only small amounts (typically 2 to 3%) of the sorbed ^{14}C could be recovered by extraction with methanol, thus, this part of the extraction procedure was eliminated.

Initially, we spent some time improving our method for the sequential extraction of aniline from sediment-water systems. We found that increasing the extraction time from 1 hr to 15 hr had little effect on recovery of ^{14}C-label by extraction with either ammonium acetate or sodium hydroxide. Also, sonicating the sediment during the extraction process had no effect on recoveries. In other experiments, we substituted calcium chloride and paraquat, a divalent organic cation, for ammonium acetate to determine whether these treatments might further disrupt sorption by cation exchange. Recoveries, however, fell significantly in both cases.

Figure 8-4 illustrates the recovery of ^{14}C by sequential extraction of the sediment with 1.0 M sodium acetate and 0.5 N sodium hydroxide over a period of 1 week. These data demonstrate that there is a relatively rapid disappearance of the ^{14}C-aniline from the initial aqueous phase of the sediment-water system over the first 48 hr at which time a plateau is reached. The rate constant for the initial disappearance of aniline, calculated from

the ln concentration versus time plot, was $(4.72 + 0.29) \times 10^{-2}$ h^{-1}. The concentration of the ^{14}C, which accounts for 5 to 10% of the initial concentration of ^{14}C-labeled aniline in the sediment-water system, remains nearly constant for the remainder of the experiment. The fraction of ^{14}C recovered by extraction with ammonium acetate reaches a maximum in approximately 10 hr accounting for roughly 15% of the label and then decreases slowly over the following week, further demonstrating that cation exchange processes do not contribute significantly to the sorption of aniline in the sediment-water system. The fraction of ^{14}C recovered by extraction with strong base reached a plateau after approximately 2 days, accounting for nearly 40% of the initial concentration of the ^{14}C. The total recovery of the ^{14}C decreased steadily over the first 3 days and then remained constant for the remainder of the experiment.

These observations indicate that the extent of sorption through cation exchange processes is not significant, even at short reaction times, and sorption through covalent binding becomes increasingly significant with time. The decrease in total recovery with time is explained by the probability that only the most labile fraction of the organic matter is being solubilized by base extraction; thus, as more of the ^{14}C becomes associated with the organic matter its recovery would be expected to drop.

A significant effort was also given to comparing the sorptive behavior of pyridine to aniline in sediment-water systems. The pKa of pyridine is 5.25, compared to aniline, which has a pKa of 4.60, and although it is a slightly stronger base, unlike aniline, pyridine cannot undergo nucleophilic addition with carbonyl moieties. Accordingly, we would predict that pyridine would sorb to sediments primarily through cation exchange mechanisms, and thus, the fraction of pyridine that sorbs should be recovered by extraction with ammonium acetate.

Figure 8-5 illustrates the recovery of ^{14}C-labeled pyridine by sequential extraction as a function of time in a Cherokee Park sediment-water system. This experiment was performed in an identical manner to the experiment with ^{14}C-aniline discussed above. As expected, pyridine behaved quite differently than aniline in the Cherokee Park sediment-water system. First, the fraction remaining in the aqueous phase of the sediment-water system reached a plateau in only 2 to 3 hours, accounting for approximately 40% of the ^{14}C initially added. Second, of the fraction of ^{14}C associated with the sediment phase, nearly 90% could be recovered by treatment of the sediment with 1.0 M ammonium acetate, while less than 10% could be recovered by treatment with strong base. Finally, the total recovery of the ^{14}C remained high (90% or greater) over the 24 hr period of the experiment. These data suggest that cation exchange processes dominate the sorption of pyridine in this sediment-water system.

In preliminary experiments with ^{14}C-pyridine, we did observe that the total recovery of ^{14}C-label fell to less than 50% after 72 hr. However, after a period of 120 hr in autoclaved sediments, the total recovery of ^{14}C-label remained above 90%, indicating that pyridine is susceptible to microbial degradation. We had previously determined that autoclaving had no or little effect on the reaction kinetics of aniline.

To determine the sorption capacity for aniline and pyridine in the Cherokee Park sediment-water system (10% solids), we measured the distribution of aniline and pyridine in independent experiments over a concentration range of 5×10^{-6} to 5×10^{-4}M. The log-log plots of sediment concentration versus aqueous concentration for aniline and pyridine are illustrated in Figure 8-6. For these experiments, a 98 to 2 mixture of unlabeled and labeled compound was used at each concentration studied. The distribution of aniline between the sediment and aqueous phases was measured after a period of 72 hr, assuring that the aqueous concentration of aniline had reached a plateau. For the experiment with pyridine, we selected an equilibration period of 8 hr. The linearity of the log-log plots in Figure 8-6 indicates that over the concentration range studied, the sorption capacity of the Cherokee Park sediment-water system at 10% solids was not exceeded by either aniline or pyridine. We concluded that this system has a significant number of binding sites for aniline and cation exchange sites for pyridine.

8E. Effect of pH on Sorption

Because pH can affect the speciation of aromatic amines and can also affect the properties of soil and sediment surfaces, we felt that an understanding of how pH affects sorption was important. Initial studies focused on determining the effect of pH on the irreversible sorption of 4-substituted anilines in a sediment-water system. In these experiments, the fraction of substrate remaining in the aqueous phase of an EPA #11 silt-clay system (3% solids) was measured as a function of pH for 6 of the 4-substituted anilines (Figure 8-7). These experiments were performed by spiking the sediment-water system with the 4-substituted anilines of interest at pH 8.0, which was the natural pH of the silt-clay-water system. After a 24 hr period, an aliquot was removed for analysis and the pH of the sediment-water system, which was controlled by a pH stat, was lowered to pH 7.0. This process was repeated every 24 hr until pH 4.0 was reached. The data in Figure 8-7 demonstrate that the sorption or binding of the anilines to the sediment phase is pH dependent and that the anilines with higher pKa values are readily removed from the aqueous phase as the pH of the sediment-water system is lowered. Only 4-cyanoaniline (pKa=1.74) and 4-aminoacetophenone (pKa=2.19) persisted in the aqueous phase at pH 4.0.

To study the effects of pH on sorption in greater detail, we measured the disappearance kinetics of 4-methoxyaniline over the pH range of 4.0 to 8.0 (Figure 8-8). These data demonstrate that sorption kinetics of 4-methoxyaniline are extremely sensitive to changes in pH. Dropping the pH below 7 significantly enhances the irreversible sorption of the aniline to the sediment. Although the initial rates for the disappearance of 4-methoxyaniline over the pH range of 3.0 to 6.5 appear not to vary much, an effect on the binding capacity of the sediment was observed. This effect is more clearly observed when the binding or distribution coefficients, Kd, which were calculated from the portion of the curves in Figure 8-8 that had reached a plateau, is plotted against pH (Figure 8-9). Maximal sorption occurs at pH 5.0 and decreases at pH values below and above this point. It was somewhat surprising to observe that a decrease in sorption occurs at the lower end of the pH range. Although one would predict that nucleophilic addition to

carbonyl moieties would be impeded due to protonation of the amino group at acidic pH values, it seemed likely that formation of the organic cation would result in enhanced sorption through cation exchange processes. One explanation for this type of behavior is that protons are able to effectively compete for cation exchange sites on the sediment surface. These results are an indication that we need to take into account the effects of pH on the sediment surface in addition to the effect of pH on the speciation of the anilines in the aqueous phase.

We also studied the effect of varying pH on the sorption of aniline and its recovery by sequential extraction from the Cherokee Park sediment (Figure 8-10). We were somewhat surprised to find that the sorption and recovery of aniline, in general, were independent of pH. Only at the lower end of the pH range studied (pH 3.0) was there a significant decrease (a factor of 2 fold) in the amount of aniline associated with the sediment phase. The recoveries of ^{14}C by extractions with ammonium acetate and sodium hydroxide were fairly constant over the pH range studied. In contrast, we had previously observed that the sorption of aniline in the EPA #11 silt-clay-system was pH dependent; the fraction of aniline associated with the sediment phase increased with decreasing pH.

8F. Effect of Carbonyl Blocking Groups on Sorption

To elucidate the mechanism(s) by which the anilines irreversibly bind to sediments, we studied the sorption of 4-methoxyaniline in EPA #11 silt-clay systems that had been treated with carbonyl blocking groups such as 2,4-dinitrophenylhydrazine (DNP), hydroxylamine (NH_2OH) and sodium bisulfite ($NaHSO_3$). These chemicals are expected to react with carbonyl moieties in the organic material by nucleophilic addition to form hydrazones, oximes and bisulfite adducts, respectively (Figure 8-11). Although formation of the bisulfite adduct is readily reversible, the hydrazones and oximes should be stable adducts, thus effectively blocking the binding of the anilines to the sediment through nucleophilic addition to carbonyl moieties in the organic matrix [8.4].

In these experiments, sediment-water systems were treated with NH_2OH, DNP or $NaHSO_3$ 24 hr prior to the addition of 4-methoxyaniline. In each case, prior treatment of the sediment-water systems with these chemicals inhibited sorption of 4-methoxyaniline (Figure 8-12). At 5.0×10^{-6}M hydroxylamine, approximately 70% loss of 4-methoxyaniline (initial aqueous concentration of 1×10^{-6}M) was observed after 24 hr compared to 100% loss of 4-methoxyaniline after 5 hr without prior treatment with hydroxylamine. At 1.0×10^{-5}M hydroxylamine, a 30% loss of 4-methoxyaniline was observed after 24 hr. Treatment of the silt-clay suspension with 2,4-DNP at a concentration of 1.0×10^{-5} M prior to the addition of 4-methoxyaniline resulted in complete blockage of the binding of the aniline to the solid matrix. We observed only a 10% loss of 4-methoxyaniline after 24 hr. These observations indicate that a signifi-cant fraction of 4-methoxyaniline is binding to the sediment through nucleo-philic addition to carbonyl groups in the sediment matrix.

8G. Reaction of Aniline with Dissolved Organic Matter

As part of our effort to elucidate the mechanisms by which anilines sorb irreversibly to soil and sediments, we used ^{15}N NMR techniques to provide direct spectroscopic evidence for the nature of the binding of the humic materials. These studies focused on dissolved organic materials because of the experimental difficulties associated with solid state NMR. The results of these studies, however, should be applicable to our studies in soils and sediments. The ^{15}N NMR studies were performed in conjunction with Dr. Kevin Thorn at the U.S. Geological Survey in Arvada, Colorado.

The ^{15}N NMR spectra of the aniline-reacted fulvic acid are illustrated in Figures 8-13, 8-14, 8-15, and 8-16. The peaks centered at about 327 ppm, 128 ppm, 104 ppm, and 76 and 64 ppm in these spectra were assigned to imine, anilide, anilino-quinone, and anilino-hydroquinone nitrogens, respectively. These assignments were based on the chemical shifts of model compounds (Figure 8-17). The INEPT spectra (Figures 8-13 and 8-14) show only protonated nitrogens; the anilide, anilino-quinone, and anilino-hydroquinone peaks are more clearly resolved in these spectra compared to the ACOUSTIC spectra (Figures 8-15 and 8-16). The negative inversion of peaks in the ACOUSTIC spectrum in Figure 8-15 is due to negative nuclear Overhauser enhancement. This is the only spectrum in which the imine nitrogen is clearly present. The ACOUSTIC spectrum recorded with addition of paramagnetic relaxation reagent (Figure 8-16) represents the quantitative distribution of nitrogens in the fulvic acid reacted with aniline under aqueous conditions. The resonances downfield of about 130 ppm in this spectrum are quantitatively significant but remain unassigned. They probably represent heterocyclic forms of nitrogen resulting from both intra- and intermolecular condensation reactions of aniline with the fulvic acid molecules.

The ^{15}N NMR studies provide direct spectroscopic evidence for imine, anilide, anilino-quinone, and anilino-hydroquinone nitrogens in the aniline-reacted fulvic acid indicating the significance of binding through the formation of covalent bonds. Of interest is the lack of imine nitrogen in the reaction of the fulvic acid with aniline in water at 25°C for 5 days. This result may be a reflection of the thermodynamic instability of the imine.

9. Assessment of expected environmental fate and recommendations for further work

9A. Assessment

The solubilities and partition coefficients demonstrate that, with the exception of Disperse Violet 1, all of the dyes examined in this project will be very strongly sorbed by soil. Migration of particulate dye, either as deposited particles or sorbed, will be the major transport route to and through water bodies. The same data indicate that Disperse Red 11, Disperse Red 9, and Solvent Yellow 33 have the potential to bioconcentrate about 1000 times. Solvent Red 1 and Solvent Green 3, however, have potential bioconcentration factors of about 10^5 to 10^7, respectively, but because they are large molecules may be biologically accumulated very slowly.

All of the smoke dyes appear to be photo-reactive on soil surfaces initially. In each case, the extent of reaction is 40 to 50 percent within a period of 50 hr exposure to sunlight. The reactions then decrease dramatically due to diffusion or light limitations. Thus, it can be concluded that photolysis alone is insufficient to prevent persistence of the dyes on the surfaces where they are initially deposited. Products of photolysis, to the extent that they could be identified, are much smaller molecules and thus not expected to be persistent. However, products of Solvent Green 3 may be stable since the anthraquinone ring system remains intact.

Reaction in compacted sediments is fast (halflife less than a few days) for all dyes except Disperse Violet 1 (15 days), Disperse Blue 14 (15 days), Disperse Blue 3 (26 days) and Solvent Yellow 33 (about 6 months). Solvent Green 3 could not be studied because of its extreme insolubility and strong sorption to sediment.

Disperse Red 9 and Disperse Red 11 react quickly in sediment to form products that have halflives of 2 to 3 months. The products are an anthrone of Disperse Red 9 and the demethylated dye in the case of Disperse Red 11. Anthrone formation seems to be a probable reaction for 1-monosubstituted aminoanthraquinones. The toxicity of these compounds is not known, but they almost certainly are not very stable under aerobic conditions in sediment. Disperse Violet 1 appears to form products in which amino groups are replaced by hydroxy groups to give compounds like quinizarin. These products seem tc react further by complexation, reduction, etc. In any event, few products were detected and those were at very low concentrations. The demethylated product of Disperse Red 11 probably also undergoes similar reactions.

All azo dyes that have been examined in this study (Disperse Red 1 and Solvent Red 1), or previously, have been found to undergo very rapid cleavage of the azo group with the formation of two primary aromatic amines. Similary, nitro aromatic groups are quickly reduced to primary aromatic amines.

Complexation of the dyes by metals could not be rigorously examined because relevant data were not in the literature. However, it seems clear that only Solvent Red 1 and Solvent Yellow 33 have any possibility of significant complexation. The latter dye is known to complex with divalent metals as are compounds similar to Solvent Red 1. The extent of complexation cannot be determined in the absence of equilibrium constants.

The totality of the above data strongly suggests that if the dyes survive photolysis long enough to enter the water, they will end up in sediments and quickly be transformed. Possible exceptions are Solvent Yellow 33, which is much more stable, and Solvent Green 3 for which kinetic data are not available. Thus, compared to compounds like PCB's, DDT, PAH's, etc., the smoke dyes are not very persistent.

9B. Recommendations

A more rigorous assessment of environmental behavior will require additional information:

1. Data, especially equilibrium constants, for complexation of Solvent Yellow 33 by divalent metals.

2. Data on soil behavior of Solvent Green 3 and other dyes. This could probably best be obtained from field samples. If Solvent Green 3 is found to be persistent in soil, its kinetics should be, at least, estimated in compacted sediment.

3. Use of data of the type presented in this project will always be controversial until sediment, or soil, is characterized as if it were a chemical reactant. Thus, it is necessary to know the amount of reactant per kilogram and how reactivity varies with organic carbon content, inorganic reductants, exposure to air, particle size, etc. The absence of this kind of understanding is the major deficiency to defensible and cost-effective remediation of polluted soil or sediment. This is particularly true when the pollutants are reducible as in the case of most munitions and munition wastes.

4. Product studies, similar to those herein, should be carried out with smoke dyes that were not included in this study. That is because dyes like Disperse Blue 7, Disperse Blue 3 and Disperse Blue 14 are disubstituted in the 1- and 4-positions and/or have functional groups that may lead to stable products. Thus, Disperse Blue 7 has OH groups in the 5- and 8-positions and will almost surely be a very good complexing agent. Kinetics of reaction products should then be measured if major or stable transformation products result from sediment reaction.

10 Acknowledgments

We would like to gratefully acknowledge the following people for valuable contributions to this project: Kevin Clodfelter and Jennifer Buynitsky for their technical assistance in determining sorption processes of aromatic amines; Hadasa Aped for technical assistance in identifying the reduction products of the smoke dyes; Dr. Susan Richardson and Al Thruston for providing MS analysis of the smoke dyes and their reaction products; Linda Exum and Bob Ryans for their assistance in the preparation of this report; Dr. Chad Jafvert, Dr. Wayne Garrison and Dr. Richard Zepp for valuable discussions during this work; Dr. Robert von Tersch for providing ^{1}H and ^{13}C NMR analyses; Dr. Kevin Thorn for providing ^{15}N NMR analyses; and Dr. Tim Collette and Cheryl Trusty for FTIR analyses.

11 References

1.1 *Color Index*, Third ed. Soc. Dyers Colourists, Bradford, U.K. and Am. Assoc. Text. Chem. Colorists, 1971-1982, Research Triangle Park, N.C.

2.1 Hassett, J.J., J.C. Means, W.L. Barnwart, S.G. Woods. Sorption Properties of Sediment and Energy-related Pollutants; EPA 600/3-80-041; U.S. Environmental Protection Agency, Athens, GA 1980.

3.1 Still, W.C., M. Kahn and A. Mitra. *J. Org. Chem.* 1978, *43*, 2923.

4.1 Baughman, G. L., and T.A. Perenich. *Environ. Toxicol. Chem.*, 1988, *7*, 183-199.

4.2 Fisher, D. J., D. T. Burton and M. J. Lenkevich. *Analytical methods for determining the concentration of Solvent Yellow 33, Solvent Green 3, synthetic-HC smoke combustion products and DEGDN in freshwater.* November 1985, AD-A167875, Defense Technical Information Center, Alexandria, Virginia.
4.3 Medicinal Chemistry Project, *Medchem Software Manual-Ver.3.3.2.* 1984. Pomona College, Claremont, CA.
4.4 Rekker, R. F. *The Hydrophobic Fragmental Constant*, 1984, Elsevier, Amsterdam.
4.5 Isnard, P. and S. Lambert. *Chemosphere*, 1989, *18*, (9/10), 1837-1853.
4.6 Veith, G. D., N. M. Austin and R. T. Morris. *Water Res.*, 1979, *13*, 43-47.
4.7 Klein, W. et al. *Chemosphere*, 1988, *17*, 361-386.
4.8 Tomlinson, E. and T. L. Hafkenscheid. in *Partition Coefficient Determination and Estimation.* 1986, Dunn, W. J., J.H. Block and R.S. Pearlman eds., Pergamon, New York.
4.9 Yalkowsky, S. H. and S. C. Valvani. *J. Pharm. Sci.* 1980, *69*, 912-922.
4.10 Yen, C-P. C., T. A. Perenich and G. L. Baughman. *Environ. Toxicol. Chem.* 1989, *8*, (11) 981-986.
4.11 Bruggeman, W.A., J. Van Der Steen and O. Hutzinger. *J. Chrom.* 1982, *238*, 335-346.
4.12 Chin, Y-P., W.J. Weber and T.C. Voice. *Water Res.*, 1986, *20*, 1443-1450.
4.13 Whitehouse, B. G. and R. C. Cook. *Chemosphere*, 1982, *11*, 689-699.
4.14 Baughman, G. L. and E. J. Weber *Dyes and Pigments*, 1991, *16*, 261-271.
4.15 Hou, M., G. L. Baughman and T. A. Perenich. *Dyes and Pigments*, 1991, *16*, 291-297.
4.16 Baughman, G. L. and T. A. Perenich. *Textile Chem. Color.* 1989, *21*, (2) 33-37.
4.17 Morris, K. R. et al. *Chemosphere*, 1989, *17*, (2), 285-289.
4.18 Miller, M. M. et al. *Environ. Sci. Technol.* 1985, *19*, 522-529.
4.19 Krien, G. *Thermochimica Acta*, 1984, *81*, 29-43.
4.20 Foitzik, J.D. and W. Haase. *Mol. Cryst. Liq. Cryst.*, 1987, *149*, 401-416.
4.21 Breitung, B., B. Packebusch, and O. Hutzinger. *Intern. J. Environ. Anal. Chem.* 1988, *32*, 135-144.
4.22 Anliker, R. and P. Moser. *Ecotoxicol. and Environ. Safety*, 1987, *13*, 43-52.
4.23 Shibusawa, T., Y. Ohya and T. Hamayose. *Nippon Kagaku Kaishi*, 1977, *10*, 1536-1542.
4.24 Jones, F. and L. Flores. *J. Soc. Dyers. Colour.* 1972, *88*, 101-106.
4.25 Lyman, W. J., W. F. Reehl and D. H. Rosenblatt. eds. *Handbook of Chemical property Estimation Methods*, 1982, McGraw-Hill, New York.
4.26 Karickhoff, S. W.. *J. Hydraul. Eng.*, 1984, *110*, 707-735.
5.1 Bontchev, P. R., et al. 1983, *J.Prakt. Chemie.*, *325*, 803-810.
5.2 Miterva, M., et al. 1985, *J. Prakt. Chemie.*, *327*, 516-520.
5.3 Cook, J. R. and D. F. Martin. 1964, *J. Inorg. Nucl. Chem.*, *26*, 571-577.
5.4 Apsit, A. A., K. Ya. Dorfman and V. P. Oshkaya. 1974, *Zh. Neorg.Khim.*, *19*, 182-185. Translation in *Russ. J. Inorg. Chem.*, *19*, (1), 1974, 97-99.
5.5 Dwivedi, K.M. Chandra and A.K. Dey. 1976, *Ind. J. Chem. 14A*, 900.
5.6 Manku et al. *J. Inorg. Nucl. Chem.*, *34*, 1091.
5.7 Yampolski, M.Z. et al. 1969, *Trudy Komissii Po Analiticheso i Khimii. 1969*, *17*, 107-115.

6.1 Herbert, V.R., and G. C. Miller. *J. Agric. Food Chem.* 1990. *38*, 913-918.
6.2 Bortolus, P., S. Monti, A. Albini, E. Fasani, and S. Pietra. *J. Org. Chem.* 1980. *54*, 534-540.
6.3 Kuramoto, N. and T. Kitao. *J. Chem. Tech. Biotechnol.* 1980. *30*, 129-135.
6.4 Kuramoto, N. and T. Kitao. *J. Chem. Soc. Chem. Comm.* 1979. 379.
6.5 Miller, G.C. and V.R. Herbert. *Chemosphere.* 1989. *18*, 1265-1274.
6.6 Zepp, R.G. and P.F. Schlotzhauer. *Chemosphere.* 1981. *10*, 453-460.
6.7 Griffiths, J. and C. Hawkins. *J. Chem. Soc. Perkins Trans. II.* 1977. 747-752.
6.8 Gohre, K. and G.C. Miller. *J. Agric. Food Chem.* 1983. *31*, 1104-1108.
6.9 Kieatiwong, S. and G.C. Miller. In press in *Environ. Sci. Technol.* 1990. *24*, 1575-1580.
6.10 Krien, G. *Thermochimica Acta.* 1984. *81*, 29-43.
6.11 Shimizu, T., S. Ohkubo, M. Kimura, I. Tabata, and T. Hori. *J.S.D.C.* 1987. *103*, 132-137.
6.12 Giles, C.H. and R.S. Sinclair. *J.S.D.C.* 1972. *88*, 109-113.
6.13 Chin, A. and L. Borer. *Propellants, Explosives and Pyrotechnics.* 1983. *8*, 112-118.

7.1 Jensen, S. and O. Pettersson. *Environ. Pollut.*, 1971, *2*, 145-155.
7.2 Tincher, W. *Survey of the Coosa Basin for Organic Contaminants from Carpet Processing.* 1978. Final Report, Project E-27-630. Textile Engineering Department, Georgia Institute of Technology, Atlanta, Ga.
7.3 Nony, C.R., et. al., *J. Anal. Toxicol.*, 1980, 4, 132-140.
7.4 Lynn, R.K., et. al., *Toxicol. Appl Pharmacol.*, 1980, *56*, 248-258.
7.5 Bos, R.P., et. al., *Toxicology*, 1984, *31*, 271-282.
7.6 Yoshida, O., et. al., in *Decomposition of Toxic and Nontoxic Organic Compounds in Soils*, 1981, Overcash, M. R. Ed., Ann Arbor Science, Ann Arbor, MI.
7.7 Porter, J.J. and E.H. Snider. *J. Water Poll. Cont. Fed.*, 1976 *48*, 2199.
7.8 Shaul, G.M., et. al. *Chemosphere*, 1991 *22* (1-2), 107-119.
7.9 Clarke, E.A., and R. Anliker, in *Handbook of Environmental Chemistry, Vol. 3, Part A, Anthropogenic Compounds*; 1980, Hutzinger, O., Ed., Springer-Verlag: Berlin and Heidelberg, pp. 181-215.
7.10 Zollinger, H. *Color Chemistry: Syntheses, Properties and Applications of Organic Dyes and Pigments VCH*, 1987, Weinheim, New York.
7.11 Liu, D. and W.M.J. Strachan. *Arch. Hydrobiol. Beiheft. Ergeb. Limnol.*, 1979, *12*, 24-31.
7.12 Weber, E.J. and N.L. Wolfe. *Environ. Toxicol. Chem.*, 1987, *6*, 911-919.
7.13 Willis, G.H., R.C. Wander and L.M. Southwick. *J. Environ. Quality*, 1974, *3*(3), 262-264.
7.14 Wolfe, N.L., et. al. *Environ. Toxicol. Chem.*, 1986, *5*, 1019-1026.
7.15 Weber, E.J. ibid., 1991, *10*, 609-618.
7.16 Yen, C-P.C., T.A. Perenich and G.L. Baughman. *ibid.* 1991, *10*, 1009-1017.
7.17 Bradley, W., and R.F. Maisey. 1954, *J. Chem. Soc.* (London) 274-278.
7.18 Hudlický, M. *Reduction in Organic Chemistry*, 1984, Ellis Harwood, Chichester, U.K.
7.19 Weber, E.J. *Fate of Textile Dyes in the Aquatic Environment: Degradation of Disperse Blue 79 in Anaerobic Sediment-Water Systems.* 1988, EPA 600/X-88-146, U.S. Environmental Protection Agency, Athens, Ga.
7.20 Maguire, R.J. and R.J. Tkacz, in press, *Water Pollution Research J. Canada.*
7.21 Coffey, S. *Chemistry and Industry*, 1953, 1068-1074.

7.22 Salinas, F., C. Genestar and F. Grases. *Analytica Chimica Acta*, **1981**, *130*, 337-344.
7.23 Salinas, F., F. Garcia-Sanchez and C. Genestar. *Analytical Letters*, **1982**, *15*(A9), 747-756.
7.24 Price, R. in *Comprehensive Coordination Chemistry: The Synthesis, Reactions, Properties & Applications of Coordination Compounds*. **1987**, Vol. *6*, Applications, G. Wilkinson ed. Pergamon, Oxford, NY.
7.25 Walkley, A. and I. A. Black. *Soil Sci.*, **1934**, *37*, 29.
7.26 Lee, C. M. and D. L. Macalady. *Intern. J. Environ. Anal. Chem.*, **1989**, *35*, 219-225.
7.27 *SAS Users Guide: Statistics*, **1985**, Ver. 5, SAS Institute Inc. Carey, N.C.
7.28 Tamano, M. and J. Koketsu. *Nippon, Kagaku Kaishi*, **1983**, *(7)*, 1028-1034.
7.29 Bredereck, K., M. Diamantoglou and J. Sommermann. *Chem. Ber.*, **1970**, *103*, 1748-1758.
7.30 N. L. Wolfe, personal communication

8.1 Paris, G.E. *Environ. Sci. Technol.*, **1980**, *14*, 1099.
8.2 Ononye, A.I.; Graveel, J.G.; Wolt, J.D. *Environ. Toxicol. Chem.*, **1989**, *8*, 303.
8.3 Bollag, J.M.: Minard, R.D.; Liu, S. *Environ. Sci. Technol.* **1983**, *17*, 72-80.
8.4 Sollenberger, P.Y.; Martin, R.B. *Carbon-Nitrogen and Nitrogen-Nitrogen Double-Bond Condensation Reactions, In The Chemistry of the Amino Group*, Patai, S., ed. Interscience Publishers: New York, **1968**; pp. 367-392.
8.5 Pratt, *J. Mag. Res.*, **1982**, *49*, 161.
8.5 Lowry, T.H.; Richardson, K.S. *Mechanism and Theory in Organic Chemistry*, Harper and Row: New York, **1976**; pp. 432-439.

Table 3-1. Analytical Data and Spectral Characterisitics of Army Smoke Dyes

Dye	R_t (min)[a]	R_f[b] (EtoAc:Hex)	λ_{max}(log ϵ)
Disperse Red 5	7.5[c]	0.19 (80:20)	292 (4.49) 509 (4.96)
Disperse Red 9	4.1[d]	0.25 (10:90)	243 (4.58) 503 (3.86)
Disperse Red 11	4.8[c]	0.26 (75:25)	254 (4.68) 528 (4.18)
Disperse Violet 1	4.1[c]	0.19 (30:70)	250 (4.50) 525 (4.11)
Solvent Green 3	4.9[d]	0.23 (5:95)	254 (4.59) 654 (4.27)
Solvent Red 1	5.9[d]	0.18 (10:90)	230 (4.50) 495 (4.32)
Solvent Yellow 33	4.2[d]	0.22 (25:75)	289 (4.73) 412 (4.79)

[a]HPLC, ODS-3 reverse phase column

[b]TLC, silica gel G-250 micron

[c]60:40/acetonitrile:water

[d]90:10/acetonitrile:water

Table 4-1. Water solubilities and partition coefficients of dyes

Dye Name (Color Index No.)	Mol Wt.	Sol. (mole/L)	(%CV)/N	$LogK_{ow}$ (meas)	(%CV)/N	Note
N1	546	1.3E-09		5.4		a
N2	362	2.0E-07		3.4		a
N3	363	2.8E-10		5.8		a,b
N5	449	1.3E-09		5.5		a
N7	427	3.7E-08		5.4		a
N9	374	7.4E-07		4.0		a
Ra	438	1.8E-08		3.0		a
Disperse Blue 79 (11345)	625	8.3E-09		4.8		a
Disperse Yellow 54 (47020)	289	2.6E-09		5.0		a
Disperse Red 60 (60756)	331	1.9E-09		6.2		a,b
Disperse Red 1 (11110)	314	5.1E-07		4.3		c
Disperse Yellow 42 (10338)	369	5.4E-07		4.6		d
Disperse Red 274	501	9.0E-09	(14)/19	3.8	(32)/9	
Disperse Red 5 (11215)	378	2.7E-07	(10)/26	4.3	(19)/5	
Disperse Violet 1 (61100)	238	1.4E-06	(19)/22	3.0	(9)/10	
Disperse Red 11 (62015)	268	1.8E-06	(17)/18	3.5	(6)/5	
Disperse Red 9 (60505)	237	5.1E-07	(12)/20	4.1	(15)/5	
Solvent Yellow 33 (47000)	273	6.2E-07		4.1		e
Solvent Red 1 (12150)	278	1.2E-09	(18)/16	7.5		a,b
Solvent Green 3 (61565)	418	2.2E-13		9.3		b

a. Solubility and K_{ow} from (4-1).
b. Underlined values are estimated -- see text.
c. Solubility from (4-16).
d. Solubility from (4-21). Log K_{ow} from (4-21) is 4.3.
e. Solubility from (4-2).

Table 4-2. Product, Q, of K_{ow} and S

	Q^1	Q_m^2	Q_t^3
Geometric mean (mol/m^3)	1.8	91	310
σ^4	0.76	0.77	0.66
range	0.06-39	2.8-1500	8.8-5500

1. Based on solubility of crystal, S_c
2. Based on solubility of sub cooled liquid with $\Delta S_f/R = 6.8$. see (4-18)
3. Based on solubility of sub cooled liquid using meaured ΔS_f and mp.
4. Root mean square deviation in log Q.

Table 4-3. Measured dye solubilities in octanol and water

Dye	Octanol/w[1]				Water/o[3]		
	M	%CV	N	M[2]	M	%CV	N
N1	1.6E-4	7	5	1.5E-4*	7.5E-10	49	4
	3.1E-4*						
N2	3.1E-4	8	4	2.8E-4*	1.6E-7	4	4
N3	1.9E-4*	10	3	3.3E-4*			
N5	3.9E-4	3	4	9.1E-4*	1.2E-9	13	8
N7				2.2E-3*			
N9	1.7E-4	12	5	5.6E-3*	1.7E-7	14	3
Ra	1.3E-4	3	7		5.4E-9	29	4
	1.0E-4*	23	3				
Dis. B. 79	2.6E-4	3	3		3.7E-9	26	4
Dis. Y. 54	7.6E-4	3	4		7.8E-9	60	3
Dis. R. 60	3.2E-3	10	4				
Dis. R. 1	8.4E-3	8	4		7.0E-7	4	4
Dis. Y. 42	4.6E-3	9	3		9.9E-8	32	5
Dis. R. 274	1.7E-4	16	10		2.6E-8	27	9
Dis. R. 5	5.9E-3	6	5		3.4E-7	29	5
Dis. V. 1	7.6E-3	8	4		6.7E-6	25	10
Dis. R. 11	3.2E-3	5	5		1.1E-6	10	5
Dis. R. 9	1.8E-3	16	4				
Sol. Y. 33	2.4E-3	24	5		1.7E-7	21	5
Sol. R. 1	3.9E-2	5	3				
Sol. G. 3	4.0E-3	8	4				

* Solubility in dry octanol
1. Solubility in octanol saturated with water (M)
2. From [4.22]
3. Solubility in water saturated with octanol

Table 4-4. Entropies of fusion of hydrophobic dyes

Dye	Transitions(°C) mp	Other	Purity Mol %	ΔS_f J/mol*K(%CV)	Ref.
N1	192		95	127(1.3)	*
N2	227		>99	70.3(1.8)	*
N3	217	182	>99	50.7(4.1)	*
N5	151		>99	89.3(3.1)	*
N7	198	155,179,191	98	82.5(2.4)	*
N9	155	127	99	61.4(2.2)	*
Disperse Red 60	185		>99	67.2(1.3)	*
Disperse Blue 79	148		95	136(2.0)	*
Disperse Yellow 54	266	211	>99	57.3(2.1)	*
Disperse Red 274	196		>99	111(1.6)	*
Ra			97	90.4(2.0)	*
Disperse Red 1	167	140	97	66.0(1.3)	*
				71.5	†
Disperse Yellow 42	159	155	---	82.4(1.0)	*
				86.1	†
Disperse Red 5	192	158,167	99	69.8(1.3)	*
				65.4	†
Disperse Violet 1	268		98	56.5(3.0)	*
				37.0	†
				51.8	†
				50.0	†
				52.3	†
Disperse Red 11	237	235	---	65.9(7.0)	*
				68.1	†
Disperse Red 9	170	156	96	65.0(1.0)	*
				60.7	†
				66.1	†
Solvent Yellow	33	241	99	56.8(2.8)	*
				21.9	†
Solvent Red 1	183		98	77.3(2.0)	*
				61.9	†
Solvent Green 3	218		99	74.5(1.7)	*

* This Work
† See ref. 4-14

Table 4-5. Dye properties

Dyes	Mole Wt.	Melting Point(°C)	logKow	logSc (M)	logK'75
N 1	546.4	192	5.4	-8.90	0.967
N 2	361.8	227	3.4	-6.69	0.554
N 3	363.4	217	5.8	-9.56	1.651
N 5	449.5	151	5.5	-8.88	1.017
N 7	426.3	198	5.4	-7.43	1.161
N 9	373.8	155	4.0	-6.13	0.462
Disperse Red 60	438.5	185	6.2	-8.71	1.176
Disperse Blue 79	625.4	148	4.8	-8.08	0.964
Disperse Yellow 54	289.3	266	5.0	-8.59	1.083
Disperse Red 274	331.3	196	3.8	-8.05	0.834
Ra	314.4	171	4.6	-7.74	0.525
Disperse Red 1	369.4	167	4.3	-6.29	0.650
Disperse Yellow 42	501.5	159	4.6	-6.27	0.262
Disperse Red 5	378.8	192	4.3	-6.57	0.688
Disperse Violet 1	238.3	268	3.0	-5.85	-0.076
Disperse Red 11	268.3	237	3.5	-5.76	0.097
Disperse Red 9	237.3	170	4.1	-6.30	0.774
Solvent Yellow 33	273.3	241	4.1	-6.21	0.598
Solvent Red 1	278.3	183	7.5	-8.90	1.236
Solvent Green 3	418.5	218	9.3	-12.65	2.519

Table 4-6. K_{ow}'s and Solubilities Predicted from Measured K'_{75}

Disperse Dye	K_{75}'	Log K_{ow}[1]	Solubility(M) Calc.[2]	Solubility(M) Lit.[3]
Orange 25	3.8	4.3		
Orange 30	4.0	4.3		
Brown 1	3.5	4.5		
Orange 29	9.3	5.2		
Blue 14	4.5	4.4	7.1E-8	(1.4, 2.8)E-7 4.1E-6
Blue 56	7.6	5.0		
Blue 7	1.1	3.0		
Yellow 64	27.3	6.3		
Blue 3	1.4	3.3	1.6E-6	1.2E-7, 4.7E-5
Yellow 23	17.8	5.8		
Violet 8	0.50	2.2		
Blue 165	10.4	5.3		
Yellow 3	3.9	4.3	1.0E-7	1.2E-7, 4.4E-6
Blue 354	120	7.8		
Indigo	2.1	3.6		

Notes:

1. calculated from equation 4-7
2. calculated from equation 4-9
3. from ref. 4.1

Table 4-7. Sediment/water and Biota/water Partition Coefficients

	Calculated		
Reference dyes	logKoc[1]	logBCF[2]	logBCF[3]
N 1	5.5	3.9	4.8
N 2	3.8	2.4	3.8
N 3	5.9	4.2	5.1
N 5	5.7	4.0	4.8
N 7	5.0	3.9	4.1
N 9	4.0	2.8	3.5
Disperse Red 60	5.8	4.5	4.7
Disperse Blue 79	5.1	3.4	4.4
Disperse Yellow 54	5.1	3.6	4.6
Disperse Red 274	4.6	2.7	4.4
Ra	4.8	3.3	4.2
Disperse Red 1	4.2	3.0	3.6
Disperse Yellow 42	4.2	3.0	3.6
Disperse Red 5	4.2	3.0	3.7
Disperse Violet 1	3.3	2.1	3.4
Disperse Red 11	3.5	2.4	3.3
Disperse Red 9	4.1	2.9	3.6
Solvent Yellow 33	3.9	2.9	3.5
Solvent Red 1	6.4	5.5	4.8
Solvent Green 3	8 5	6.8	6.6
Commercial dyes			
Disperse Orange 25	4.3	3.0	3.9
Disperse Orange 30	4.3	3.1	3.9
Disperse Brown 1	4.4	3.0	3.8
Disperse Orange 29	5.0	3.7	4.4
Disperse Blue 14	4.4	3.2	4.0
Disperse Blue 56	4.9	3.6	4.3
Disperse Blue 7	3.3	2.1	3.2
Disperse Yellow 64	5.9	4.5	5.0
Disperse Blue 3	3.5	2.3	3.3
Disperse Yellow 23	5.5	4.2	4.7
Disperse Violet 8	2.6	1.5	2.8
Disperse Blue 165	5.1	3.8	4.4
Disperse Yellow 3	4.3	3.0	3.9
Disperse Blue 354	7.2	5.7	5.8
Indigo	3.8	2.6	3.6

1. Average of value from eqs. 4-5, 4-7, 4-9 of ref. 4.5 and eqs. 15 and 22 of ref. 4.26.
2. Based on K_{ow} from eq. 4-7 and eq. 5-1 of ref. 4.25.
3. Calculated from S_e using eq. 5-3 of ref. 4.25.

Table 6-1. Estimated Mean Depth of Photolysis for the Smoke Dyes

	Mean Photolysis Depth, mm	
Dye[a]	Outdoor	Indoor
Disperse Red 9	0.50	0.77
Solvent Red 1	0.68	0.73
Disperse Red 11	0.33	0.46
Solvent Green 3	0.56	0.62
Solvent Yellow 33	0.42	0.45
Disperse Violet 1	0.37	0.42

a. Sorbed on EPA #3 soil, 1.0 mm deep

Table 6-2. Solution Photolysis of the Smoke Dyes

Dye	log K_{ow}[a]	k_i/k_d[b]
Solvent Red 1	7.50	25.71
Disperse Violet 1	1.25	5.58
Solvent Yellow 33	4.09	18.64
Solvent Green 3	9.30	1.58
Disperse Red 9	2.87	4.64
Disperse Red 11	1.29	4.02

a. Baughman, C.L., and T.P. Perenich. *Environ. Tox. Chem.* 1988. 7:183-199.

b. Ratio of indirect to direct photolysis rate constants measured in 50:50 MeOH:H_2O; dye, 3.0 μM; sensitizer, 1.5 μM Rose Bengal.

Table 6-3. Characteristics of EPA Soils selected for study[a]

EPA Soil	pH (1:1)	% Organic Carbon	% Silt	% Sand	% Clay	Photolysis Depth(mm)[b]
# 3	6.65	1.53	33.5	2.4	24.1	0.77
# 9	8.34	0.11	75.6	7.1	17.4	0.56
#13	6.90	3.04	27.1	20.3	52.6	0.46

a. Hassett, J.J. *Sorption Properties of Sediments and Energy-Related Pollutants*. 1980. USEPA, Athens, GA. Report No. EPA 600/3-80-041.

b. For Disperse Red 9, 1 mm soil depth

Table 7-1. Organic Carbon Content of Sediments

Lake	Lab	%O.C.*	n
Beef Pond			
	Soils	2.71 ± 10	4
	EPA	3.22	2
	Macalady	2.59 ± 12	3
	average	3.05 ± 14	9
Herrick			
	Soils	1.79 ± 51	14
	EPA	1.58 ± 77	6
	Macalady	1.17 ± 39	12
	average	1.52 ± 56	31
Kingfisher			
	Soils	8.34 ± 38	8
	EPA	3.94	2
	average	7.46 ± 45	10
Oglethorpe			
	Soils	2.09	2
	Macalady	1.96 ± 55	5
	Average	1.99 ± 48	7

* ± coefficient of variation

Table 7-2. Data from kinetic experiments

Dye Run/Lake[a]	D_0[b] mg/kg	k hr^{-1}	$t_{1/2}$[c] days	D_i[d] mg/kg	t_r[e] days	n	r^2	Date[f]	t^0_{ex} days	Notes
Disperse Red 9 loss										
#2/H	3.56	4.52E-2	0.64	3.07	1.25	8	0.947	3/90	11	
#3/H	4.02	3.6E-3	8.1	3.81	14	18	0.966	4/90	14	
#4	5.01	1.49E-2	1.9	3.1	3.1	11	0.78	5/90		
#5A	10.6	2.84E-2	1.0	10.8	1.3	12	0.994	2/91	33	+0.12% ACN
#5B	10.7	2.46E-2	1.2	10.8	1.2	8	0.985	2/91	43	+1.5% ACN
#5C	10.1	2.62E-2	1.1	9.62	1.2	8	0.992	2/91	67	+0.14% ACN
#5D	9.97	2.66E-2	1.1	9.37	1.3	8	0.994	2/91	76	+1.5% ACN
#7A	11.6	2.23E-2	1.3	10.8	2.1	8	0.993	8/91	2	
#7B	11.6	1.93E-2	1.5	10.5	3.9	10	0.998	8/91	4	
#7A-	11.6	1.79E-3	16.1	10.5	25	9	0.998	8/91	25	5 ± 1°C
#7B-	11.6	1.54E-3	18.7	10.1	40	10	0.988	8/91	40	5 ± 1°C
#8A	31.3	3.60E-3	8.0	26.0	20	9	0.993	8/91	109	
#8B	31.4	2.69E-3	11	23.6	20	9	0.982	8/91	109	
Anthrone formation										
#5A		2.1E-2	1.4		5.0	3	0.926	2/91		
#5B		1.5E-2	1.9		5.0	10	0.987	2/91		
#5C		1.8E-2	1.6		5.0	9	0.948	2/91		
#5D		1.8E-2	1.6		5.0	9	0.910	2/91		
#7A		7.4E-3[h]	3.9		1.9	8	0.993	8/91		
#7B		6.9E-3[h]	4.2		3.7	8	0.990	8/91		
#7A-		6.7E-4[h]	43		1-25	8	0.988	8/91		5 ± 1°C
#7B-		5.4E-4[h]	53		4-40	8	0.918	8/91		5 ± 1°C
#8A		9.9E-4	29		10	6	0.959	8/91		
#8B		9.2E-4	31		11	7	0.954	8/91		
Anthrone Loss										
#5A		2.1E-4	137		7-32	4	0.71			
#5B		4.2E-4	67		9-43	4	0.986			
#5C		4.4E-4	64		13-62	5	0.99			
#5D		4.8E-4	60		12-76	6	0.97			
#8A		1.9E-4	150		52-109	6	0.86			
#8B		2.5E-4	110		52-109	6	0.928			

Table 7-2. Data from kinetic experiments, con't

Dye Run/Lake[a]	D_0[b] mg/kg	k hr^{-1}	$t_{1/2}$[c] days	D_i[d] mg/kg	t_r[e] days	n	r^2	Date[f]	t^9_{ex} days	Notes
1-Aminoanthraquinone loss										
#1/H	8.35	1.96E-2	1.5	7.37	3.2		0.988	4/90		
#2	15.4	2.17E-2	1.3	12.2	3.0	10	0.978	6/90		
Solvent Yellow 33 loss										
#1/H	12.5	1.44E-4	200	6.8	48	14	0.39			
#2/O	17.9	2.18E-4	132	4.7	27	8	0.45			
#3/O	14.3	4.83E-4	60	6.3	20	8	0.67			
#4/H	11.3	3.43E-4	84	7.6	27	10	0.51			
#5/H	3.6	4.00E-5	720	2.6	231	15	0.25	6/90		
#6/H	0.55	1.25E-4	230	0.57	224	15	0.57	6/90		
#7/BP	0.69	1.34E-4	214	0.36	200	15	0.78	7/90		
#8/BP	1.2	1.57E-4	184	0.57	277	18	0.90	10/90		
1-Chloroanthraquinone loss										
#1	6.50	4.35E-2	0.66	10.4	2.2	8	0.997	5/90		
#2/H	14.8	1.19E-2	2.4	16.4	6.9	10	0.979	6/90		
#3A	9.88	9.61E-2	0.30	9.09	0.44	9	0.991	11/90		
#3B	10.0	1.10E-1	0.26	9.39	0.27	9	0.991	11/90		
#3D	10.4	3.87E-2	0.75	9.44	0.98	9	0.997	11/90		
#4	10.04	3.53E-2	0.82	8.15	1.25	11	0.988	12/90		
Disperse Violet 1 loss										
		1.60E-3	18				0.84			From (7-16)
		2.21E-3	13				0.969			From (7-16)
		2.05E-3	14				0.929			From (7-16)

Table 7-2. Data from kinetic experiments, con't

Dye Run/Lake[a]	D_o[b] mg/kg	k hr^{-1}	$t_{1/2}$[c] days	D_i[d] mg/kg	t_r[e] days	n	r^2	Date[f]	t^g_{ex} days	Note
Disperse Red 11 loss										
#1/BP	5.8	4.09E-3	7.0		18	17	0.932			
#2/BP	8.5	5.36E-3	5.4		13	12	0.971			
#3/O	9.4	2.83E-3	10		20	17	0.926			
#4/H	8.5	4.02E-2	0.72		3.0	6	0.963			
#5/H	9.2	8.36E-3	3.1		1-14	8	0.902			
#6/O	8.3	2.52E-3	12		20	16	0.76			
#12A/H	8.2	1.42	0.02		0.025	4	0.981		0.04	1st spike
#12B/H	6.9	7.81E-1	0.04		0.029	4	0.998		0.04	2nd spike
#19/BP	9.4	4.22E-3	6.8	5.3	11	14	0.910			
#20A	10.1	6.44E-3	4.5	6.4	14	11	0.990	5/91	100	
#20B	10.05	6.81E-3	4.2	6.4	9	10	0.978	5/91	100	
#21A	12.0	7.51E-3	3.8	7.82	7.9	9	0.986	5/91		27 ± 2°C
#21B	12.2	7.87E-3	3.7	8.11	7.8	9	0.958	5/91		27 ± 2°C
#21A-	12.0	7.59E-4	38	7.70	40	10	0.943	5/91		3.5 ± 1°C
#21B-	12.2	7.02E-4	41	7.62	1-34	10	0.958	5/91	35	3.5 ± 1°C
#22A+	10.7	1.35E-2	2.1	10.1	2.2	9	0.932	6/91		38.4 ±0.1°C
#22B+	10.8	1.33E-2	2.2	10.0	2.2	9	0.947	6/91		38.4 ±0.1°C
#22A	10.7	7.05E-3	4.1	11.6	6.0	9	0.930	6/91		27 ± 2°C
#22B	10.8	6.31E-3	4.6	10.9	6.2	10	0.938	6/91		27 ± 2°C
#23A	30.5	5.43E-3	5.3	23.6	9.3	15	0.941	6/91	105	
#23B	30.4	4.90E-3	5.9	21.9	9.2	15	0.903	6/91	77	
#24A	10.8	1.20E-2	2.4	5.9	4.0	17	0.932	8/91	8	
#24B	10.9	6.22E-3	4.6	3.3	8.0	19	0.971	8/91	8	
#24C	10.4	5.30E-3	5.4	3.4	4.0	14	0.88	8/91	8	+1% phenol
HA43 formation										
#20A		5.1E-3	5.7		4-14	14	0.49	5/91		
#20B		8.4E-3	3.4		4-9	13	0.81	5/91		
#21A		7.4E-3[h]	3.9		1-8	6	0.954	5/91		27 ± 2°C
#21B		8.7E-3[h]	3.3		2-7.8	6	0.946	5/91		27 ± 2°C
#21A-		7.4E-4[h]	39		14-23	4	0.84	5/91		3.5 ± 1°C
#21B-		4.4E-4[h]	56		14-23	5	0.47	5/91		3.5 ± 1°C
#22A+		7.1E-3	4.0		1-2.2	5	0.993	6/91		38.4 ±0.1°C

Table 7-2. Data from kinetic experiments, con't

Dye Run/Lake[a]	D_o[b] mg/kg	k hr^{-1}	$t_{1/2}$[c] days	D_i[d] mg/kg	t_r[e] days	n	r^2	Date[f]	t^9_{ex} days	Notes
HA43 formation (continued)										
#22B+		5.0E-3[h]	5.7		1-2.2	3	0.986	6/91		38.4 ±0.1°C
#22A		2.6E-3[h]	11		2-6	5	0.61	6/91		27 ± 2°C
#22B		5.1E-3[h]	5.6		2-6	5	0.52	6/91		27 ± 2°C
#23A		3.4E-3	8.6		9.3	15	0.910	6/91	105	
#23B		3.5E-3	8.2		9.2	15	0.89	6/91	77	
#24A		3.6E-3[h]	8.1		1.8-7.9	13	0.86	8/91		
#24B		4.7E-3[h]	6.1		1.0-8.0	15	0.980	8/91		
HA43 loss										
#20A		2.0E-4	150		14-100	8	0.74	5/91		
#20B		3.7E-4	78		19-100	7	0.85	5/91		
#23A		4.18E-4	67		34-105	5	0.84	6/91	105	
#23B		6.65E-4	43		34-77	4	0.84	6/91	77	
Sublaprint Blue 70013										
Disperse Blue 3 loss										
#1A	<6	6.27E-4	46.0		15	19	0.416	3/91		
#1B	<6	8.91E-4	32		42	18	0.856	3/91		
#2A	<6	1.31E-3	22		28	17	0.925	3/91		
#2B	<6	1.46E-3	18		36	17	0.861	3/91		
Disperse Blue 14 loss										
#1A	<6	3.18E-3	9		15	19	0.887	3/91		
#1B	<6	1.61E-3	18		42	18	0.762	3/91		
#2A	<6	1.48E-3	20		28	17	0.929	3/91		
#2B	<6	1.32E-3	22		36	17	0.827	3/91		
Disperse Red 1 loss										
		9.3E-2	0.31				0.973			From (7-16)
#1A/H	205	9.36E-2	0.31	153	0.76	4	0.999			1st spike
#1B/H	212	1.63E-2	1.8	208	0.98	6	0.988			2nd spike

Table 7-2. Data from kinetic experiments, con't

Dye Run/Lake[a]	D_0[b] mg/kg	k hr^{-1}	$t_{1/2}$[c] days	D_i[d] mg/kg	t_r[e] days	n	r^2	Date[f]	t^9_{ex} days	Notes
Disperse Red 5 loss										
		3.4E-1					0.982			From (7-16)
		9.5E-2					0.960			From (7-16)
		1.2E-1					0.998			From (7-16)
#1A/H	50.4	1.63E-1	0.18	50	1.0	6	0.997			1st spike
#1B/H	72.7	4.77E-2	0.60	37	5.0	10	0.890			2nd spike
#2A	11.1		<0.08						0.2	
#2B	11.1	1.05E-1	0.27	1.6	0.8	12	0.923		1.0	
#2C	10.4	5.95E-1	<0.08		0.2	6	0.85		0.2	
#2D	10.4	1.21E-1	0.24	3.3	0.9	14	0.958		1.0	
#3	10.6	1.72E+0	<0.08	11.3	0.03	5	0.993		0.11	Not 1st order
#4C	9.9	2.42E-1	0.12	8.0	0.07	8	0.71			
#5	10		<0.08							
#6	9.7		<0.08							
#7	61.5	4.56E-2	0.63	17.5	0.31	9	0.950	12/90	1.8	
#8	62.1	6.53E-2	0.44	51	2.1	12	0.974	12/90		
#9	62.9	6.49E-2	0.44	55	0.96	8	0.945	12/91	1.2	
#10A	11.0	5.10E-1	0.057	8.47	0.20	11	0.991	1/91	0.2	
#10B	11.3	1.95E-1	0.15	10.9	0.30	13	0.994	1/91	0.3	
#10C	10.9	2.7	0.010	0.29	0.015	4	0.996	1/91	0.06	
#10D	10.8	3.1	0.0092	0.27	0.029	5	0.82	1/91	0.03	
#11/H										+phenol
#12									0.2	+$NaNO_2$
Solvent Red 1 loss										
#1A/H	10.0	1.24E-2	2.3	11.0	8.1	11	0.984			
#1A+/H	10.0	4.46E-3	6.4	11.7	12.0	10	0.968			
#1B/H	98.5	4.69E-3	6.1	158	8.3	10	0.74			
#2A	10.7	1.36E-2	2.1	10.2	2.2	10	0.89			
#2B	10.7	5.40E-3	5.3	6.9	9.9	15	0.912			
#2C	10.8	7.43E-3	3.9	8.4	3.9	10	0.78			
#2D	10.8	5.72E-3	5.1	7.8	11	13	0.959			
#3	10.0	3.43E-2	0.8	8.5	0.3	8	0.972			
#4A	23.3	1.23E-2	2.3	20.3	6.1	7	0.992	5/31	22	Not 1st order
#4B	22.9	1.14E-2	2.5	21.1	5.9	7	0.993	5/91	22	Not 1st order

Table 7-2. Data from kinetic experiments, con't

[a]H and BP designate Herrick or Beef Pond lake sediments. All others are from Kingfisher Lake.
[b]Initial concentration.
[c]Halflife or doubling time.
[d]Intercept concentration at zero time.
[e]Time period of regression, same units as respective $t_{1/2}$.
[f]Date of experiment.
[g]Duration of experiment.
[h]Single value calculated from slope of Equation 7-6 using k_3 equal to 3.5E-4 and 4.1E-4 for Disperse Red 9 and Disperse Red 11, respectively.

Table 7-3. Observations and conditions for dye kinetic experiments in Table 1.

Dye/Experiment	Comments
Disperse Red 9	
#2	Stirred 15 min in air before filling vials. Regression is for fast part of the reaction.
#3H	Points not well spaced and much scatter in data.
#4	Stirred 30 min in air before filling vials. Regression less two initial points. Not first order (1°). Most points are during slow part of reaction.
1-aminoanthraquinone	
#1	Stirred 15 min in air before filling vials.
#2	Stirred 30 min in air before filling vials. Product observed to increase by HPLC/Diode Array (see spectra).
1-chloroanthraquinone	
#1	Stirred in air 30 min before filling vials.
#2	Stirred in air 30 min before filling vials.
#3A	Continuously stirred under N_2 during entire experiment.
#3B	Continuously stirred under N_2 during entire experiment.
#3D	Stirred in air 10 min before filling vials.
#4	Duplicate of #3D.
Disperse Red 5	
#1B	Sediment from #1A which has been re-spiked with dye immediately after #1A was completed.
#2A	15 minutes stirring in air after dye addition (before filling vials).
#2B	105 minutes stirring in air after dye addition (before filling vials).
#2C	Same as 2A except with 105 minutes stirring followed by 2 days quiescence prior to dye addition.
#2D	Same as 2B except with 105 minutes stirring in air after dye addition (before filling vials).
#3	Constant stirring in air over entire experiment. Data is not 1°.
#4C	Stirred 25 min in air prior to dye addition.
#5	Kept under N_2 prior to filling vials.
#6	Stirring in air and/or N_2, reaction to fast and/or not 1°.
#7	Stirred 3 hr. under N_2 before added to vials. First sample after 2-2.5 hr.
#8	Stirred 15 min under N_2 before added to vials. First sample after 2-2.5 hr.
#9	Stirred 15 min under N_2 before added to vials. First sample after 2-2.5 hr.
#10A	Stirred in air 45 min prior to dye addition.

Table 7-3. Observations and conditions for dye kinetic experiments in Table 1, cont.

Dye/Experiment	Comments
Disperse Red 5 (continued)	
#10B	Stirred in air 45 min prior to dye addition. Duplicate of 10A.
#10C	Stirred in N_2 45 min prior to dye addition. Otherwise same as #10A & 10B.
#10D	Duplicate of #10C.
#11	Duplicates A & C contained 1% phenol C + D were controls without phenol. Too fast for accurate measurement but results basically the same.
#12	Similar to #11 except containing $NaNO_3$ or ACN. $NaNO_3$ slowed the reaction but still too fast for accurate halflives.
Disperse Red 11	
#1	Stirred in air 30 min before filling vials.
#2	Stirred in air 30 min before filling vials.
#3	Time of air stirring unknown.
#4	Stirred in air 30 min before filling vials.
#5	Stirred in air 80 min before filling vials. Increase of product HA43 detected by HPLC. Regression excludes 1st 3 points.
#6	Stirred in air 90 min before filling vials.
#12B	Double spike experiment. Dye added to sediment from #12A for the second time after 70 min
#19	Stirred in air 15 min before filling vials.
#24A	Stirred in air 90 min before dye addition.
#24B	Under N_2
#24C	Same as 24B but with 1% phenol. Not good 1°. No HA43 formed.
Disperse Red 1	
#1	#1B is a respike with dye of #1A. Dye concentration was too high.
Sublaprint Blue 70013	
	All experiments with commercial dye
Solvent Red 1	
#1A	Stirred in air 15 min prior to filling vials.
#1A	Stirred in air 100 min prior to filling vials. Same sediment as in #1A.
#1B	Stirred in air 24 min prior to filling vials.
#2A	Stirred in air 15 min before filling vials.
#2B	Stirred in air 90 min before filling vials.
#2C	Stirred in air 90 min followed by 2 day quiescence and then 15 min stirring in air before filling vials.
#2D	Same as 2C except 90 min stirring before filling vials.
#3	Under N_2
#4A	Stirred in air 20 min before and after dye added. Not 1°.
#4B	Duplicate of #4A. Not 1°.

Table 7-4. Averages of room temperature rate constants in Table 1

Process	Rate Constant(hr^{-1})*	$t_{1/2}$(days)
Disperse Red 9 loss	1.9E-2±65%	1.5
Anthrone formation	1.1E-2±72%	2.6
Anthrone loss	3.3E-4±39%	88
1-aminoanthraquinone loss	2.1E-2	1.4
Solvent Yellow 33 loss	2.0E-4±70%	140
1-chloroanthraquinone	5.6E-2±69%	0.5
Disperse Violet 1	1.9E-3±16%	15
Disperse Red 11 loss (less exp. 12 and 3)	5.4E-3±35%	3.6
HA43 formation	5.2E-3±42%	5.6
HA43 loss	4.1E-4±40%	70
Disperse Blue 3 loss	1.1E-3±36%	26
Disperse Blue 14 loss	1.9E-3±46%	15
Disperse Red 5 loss (less exp. 10C and 10D)	2.5E-1±150%	0.1
Solvent Red 1 loss	1.1E-2±79%	2.6

* ± Coefficient of variation

Table 7-5. Summary of Disperse Red 9 Kinetic Data

From regression

Run/Lake	k_1(hr^{-1})	k_1(hr^{-1})	k_2(hr^{-1})	k_3(hr^{-1})	k_1/k_2
#2/H	0.045				
#3/H	0.036				
#4	0.015				
#5	0.026[6]*	0.018[14]	0.0084[11]	0.00039[31]	0.7
#7	0.021(7)[b]	0.0072(3)	0.014(9)		0.3
#8	0.0031(15)	0.00095(4)	0.0025	0.00022(14)	0.3
average	0.024[61]	0.0067[99]	0.0083[69]	0.00030[39]	0.4
#7-	0.0017(7)	0.00060(11)	0.0011(4)	(5±1°C)	0.4

From Curvefit

Exp.	D_i	k_1	k_2	k_3	k_1/k_1+k_2
5A	10.6{2}*	1.1E-2{10}	1.3E-2{17}	00000	
5B	10.9{1}	1.4E-2{3}	8.9E-3{9}	5.5E-4{16}	
5C	9.8{2}	1.9E-2{3}	8.5E-3{12}	5.3E-4{13}	
5D	9.6{2}	1.9E-2{4}	8.7E-3{13}	6.1E-4{10}	
average		1.6E-2[25][b]	9.8E-3[22]	5.6E-4[7]	0.6
7A	7.5{15}	2.7E-3*{80}	1.7E-3*{400}	00000	
7B	10.4{1}	7.3E-3{3}	1.1E-2{1}	4.9E-3{20}	
average		5.0E-3(92)	6.4E-3(145)	4.9E-3	0.4
8A	24.5{1}	1.2E-3{4}	2.3E-3{4}	2.1E-4{16}	
8B	23.9{1}	9.2E-4{5}	1.8E-3{5}	2.1E-4{19}	
average		1.1E-3(28)	2.0E-3(25)	2.1E-4(0)	0.3
7A-	10.5{1}	6.2E-4{10}	1.2E-3{5}	9.9E-5*{400}	
7B-	10.2{1}	4.6E-4*{300}	1.1E-3*{118}	00000	
average		5.4E-4(30)	1.2E-3(8)	9.9E-5	0.3

*Value not different from zero at 95% confidence level
[a]Coefficient of variation
[b]Range as percent of mean
[c]Percent asymptotic standard error

Table 7-6. Summary of Kinetic Data for Disperse Red 11 in Kingfisher Lake Sediment

From regression

Exp.	k_2(hr^{-1})	k_1(hr^{-1})	k_2(hr^{-1})	k_3(hr^{-1})	k_1/k_2
20	6.6E-3(3) [a]	6.8E-3(25)	-0.2E-3	2.8E-4(32)	1.0
21	7.7E-3(2)	8.0E-3(8)	-0.3E-3		1.0
22	6.7E-3(6)	3.8E-3(32)	2.9E-3		0.6
23	5.2E-3(5)	3.4E-3(1)	1.8E-3	5.4E-4(22)	0.6
24B	6.2E-3	4.7E-3	1.5E-3		0.8
ave.	6.5E-3[14] [b]	5.3E-3[35]	1.5E-3[36]	4.1E-4(46)	0.8
$t_{1/2}$(days)	4.4	5.4	26	70	
22+	1.3E-2(1)	6.0E-3(17)	1.3E-2(<1)	(38.4°C)	0.5
21-	7.3E-4(4)	5.9E-4(25)	6.4E-4(1)	(3.5°C)	0.8

From curvefit

	D_i				k_1/k_1+k_2
20A	6.9{2} [c]	7.6E-3{3}	000000	2.5E-4{20}	
20B	6.7{6}	6.8E-3{1}	000000	2.9E-4{46}	
Ave.		7.2E-3	------	2.7E-4	1.0
23A	23{5}	3.0E-3{8}	2.0E-3{19}	9.8E-5*{75}	0.6
23B	21{6}	2.9E-3{10}	1.4E-3{45}	6.1E-5*{200}	0.7
Ave.		3.0E-3	1.7E-3	8.0E-5	0.6
Grand Ave.		5.1E-3[49]	1.7E-3[25]	1.7E-4[64]	0.8
$t_{1/2}$(days)		5.6	17	170	

[a] Range from GLBTABL4 as percent of mean
[b] Coefficient of variation
[c] Percent asymptotic standard error
* Value not different from zero at 95% confidence level

Table 7-7. Activation energy for Disperse Red 9 (Runs 7 and 7-) and Disperse Red 11 (Runs 21, 21-, 22 and 22+).

Rate Constant	ΔE_a (KJ/mol)
Disperse Red 9	
k_L	79
k_1	78
k_2	80
Disperse Red 11	
k_L	60
k_1	52

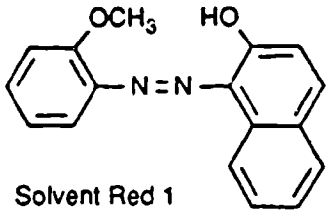

Solvent Red 1

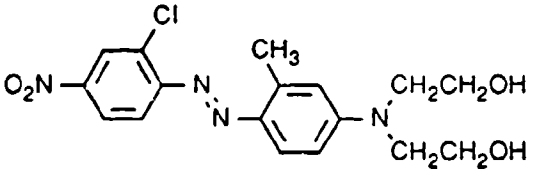

Disperse Red 5

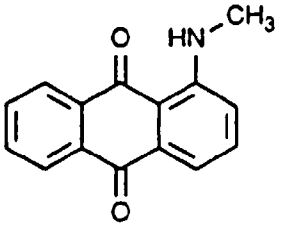

Disperse Red 9

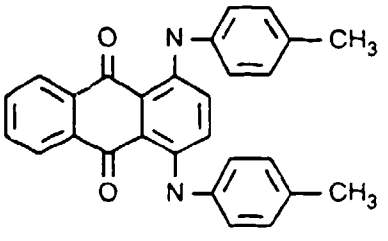

Solvent Green 3

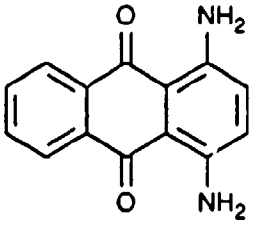

Disperse Violet 1

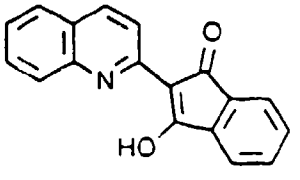

Solvent Yellow 33

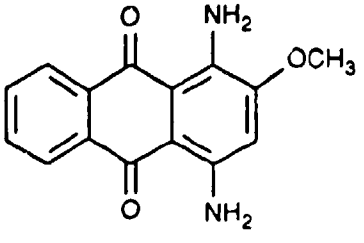

Dispere Red 11

Figure 6-1

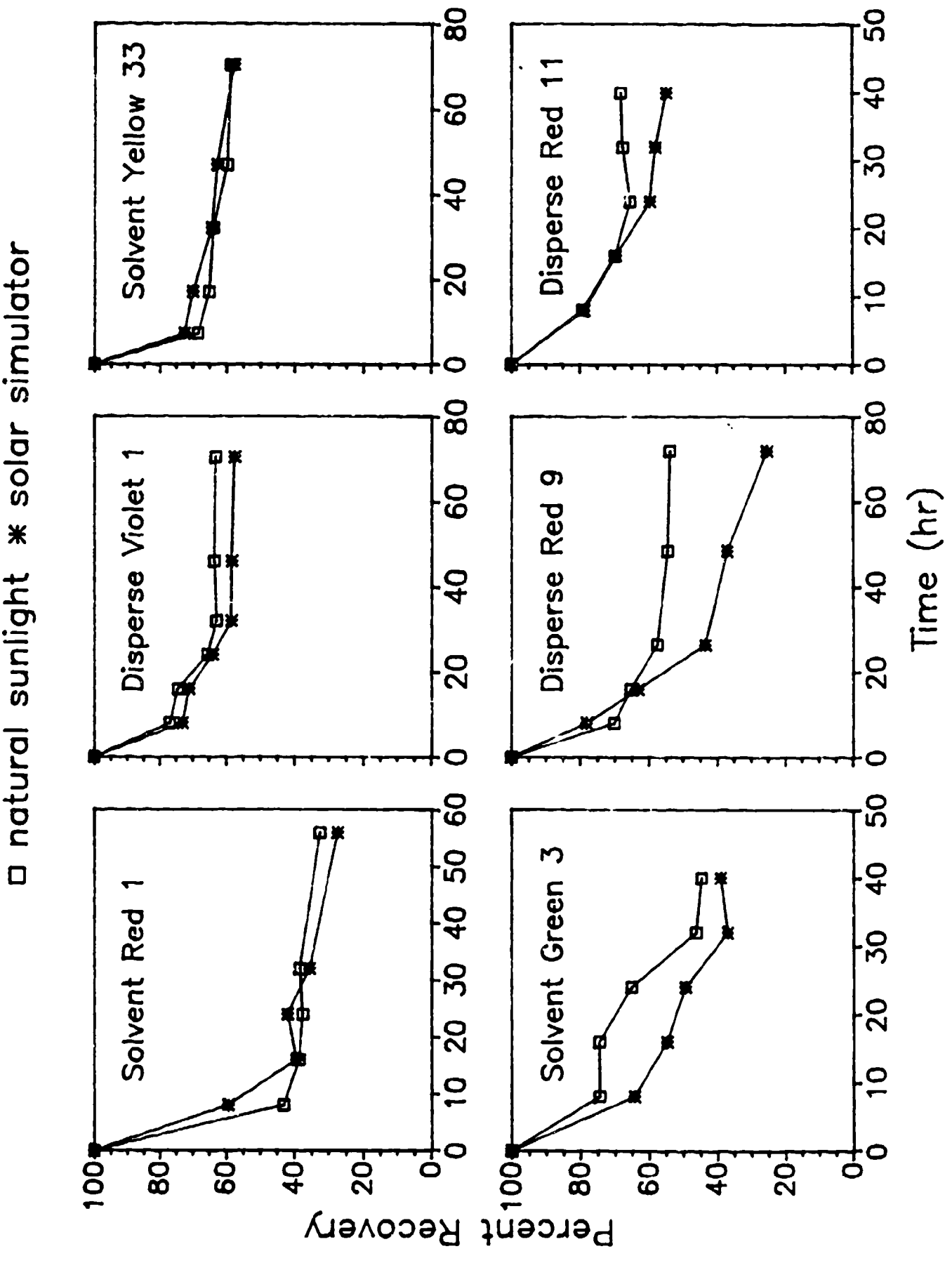
□ natural sunlight * solar simulator
Solvent Red 1
Disperse Violet 1
Solvent Yellow 33
Solvent Green 3
Disperse Red 9
Disperse Red 11
Percent Recovery
Time (hr)

Figure 6-2

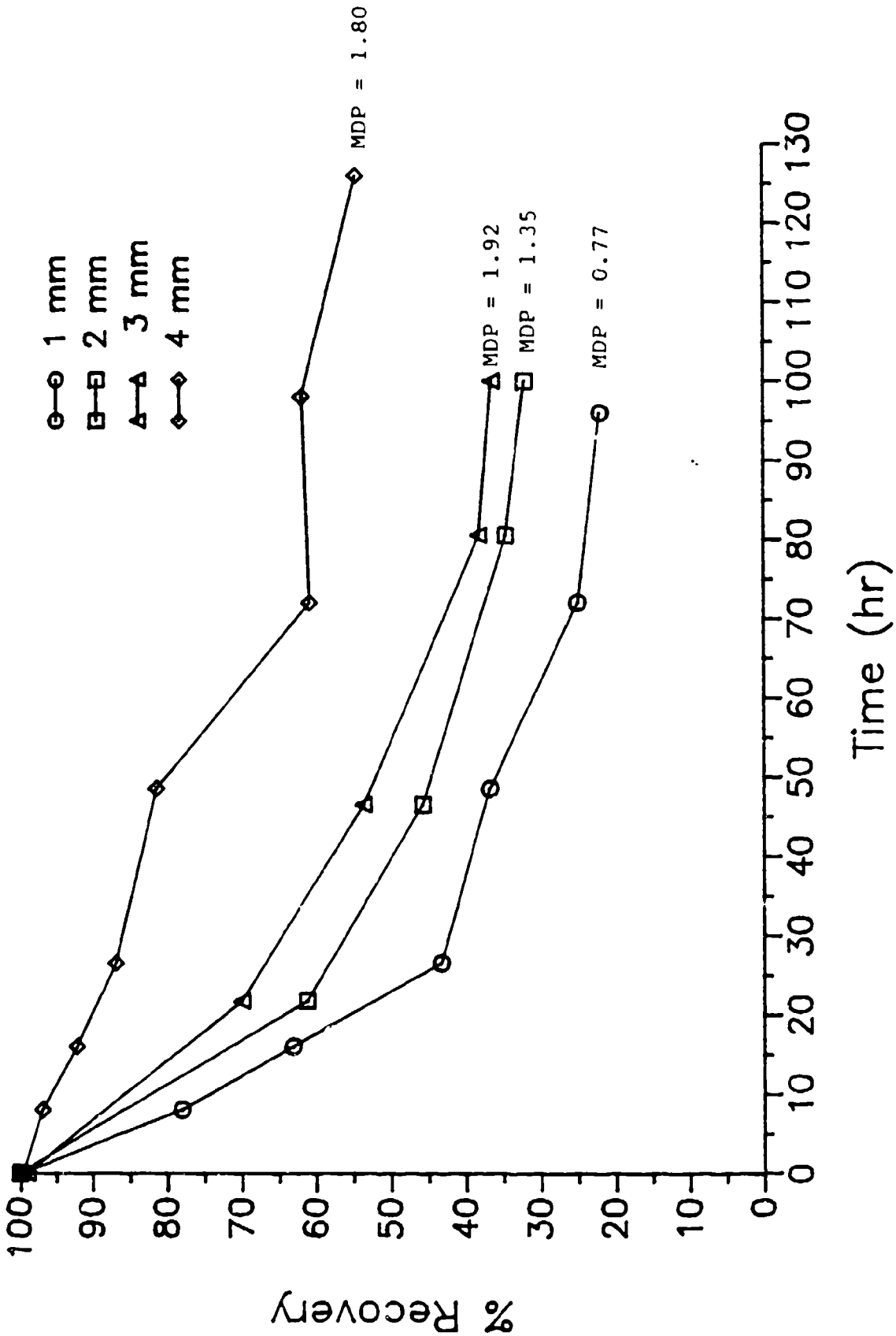
% Recovery
Time (hr)
1 mm
2 mm
3 mm
4 mm
MDP = 1.80
MDP = 1.92
MDP = 1.35
MDP = 0.77
100
90
80
70
60
50
40
30
20
10
0
0
10
20
30
40
50
60
70
80
90
100
110
120
130

Figure 6-3

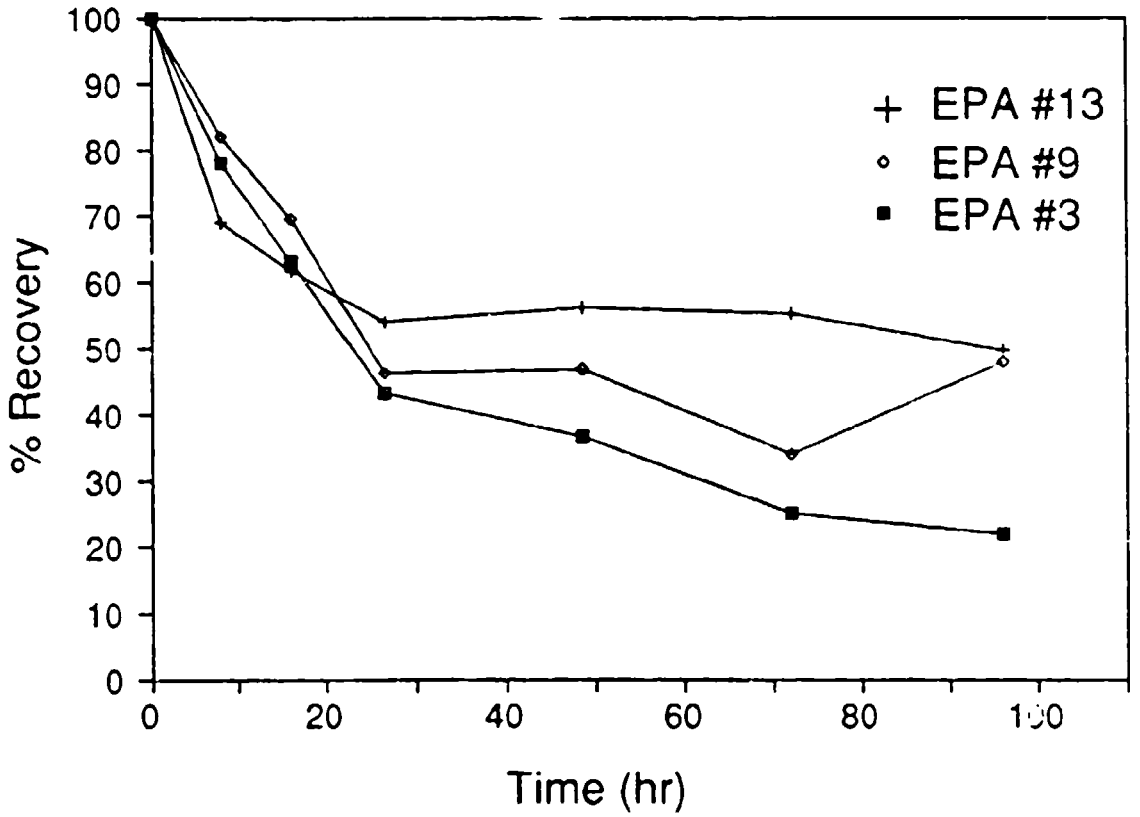
100
90
80
70
60
50
40
30
20
10
0
% Recovery
0
20
40
60
80
100
Time (hr)
+ EPA #13
◇ EPA #9
■ EPA #3

Figure 6-4

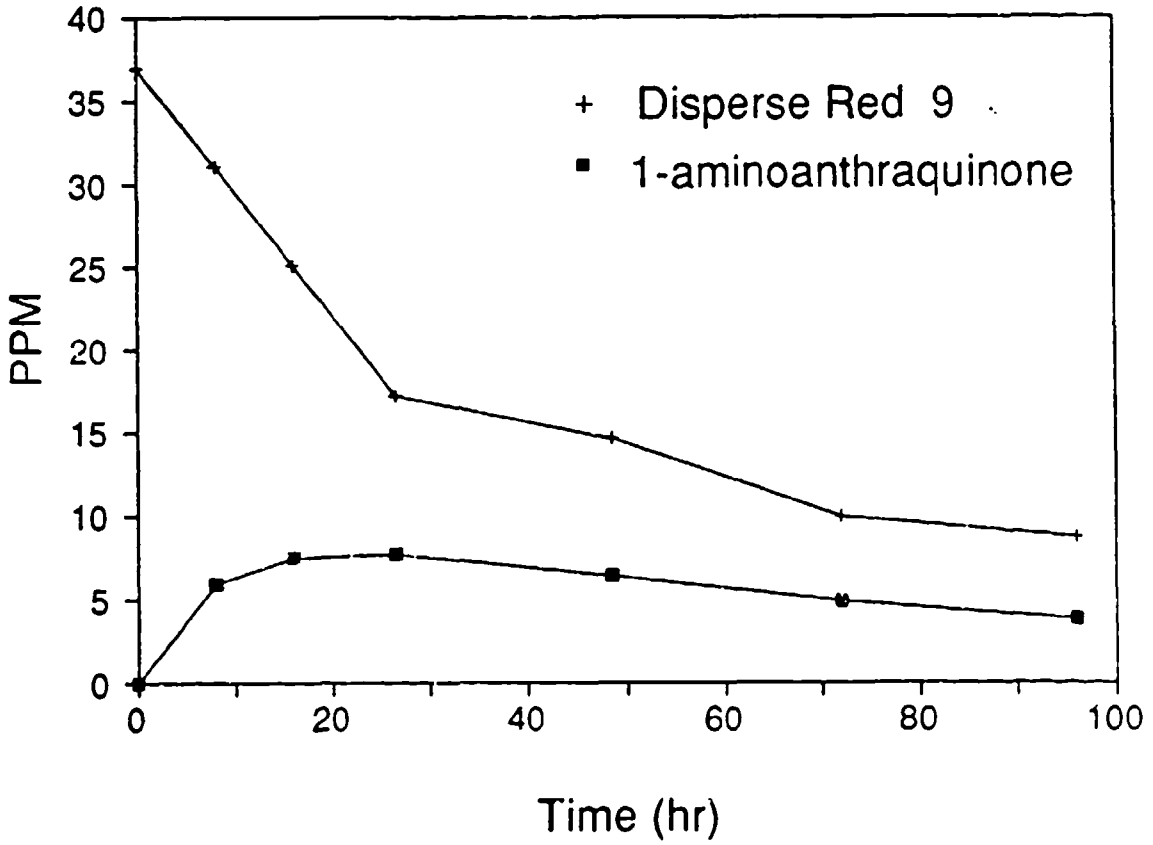
40
35
30
25
20
15
10
5
0
PPM
0
20
40
60
80
100
Time (hr)
+ Disperse Red 9
■ 1-aminoanthraquinone

Figure 6-5

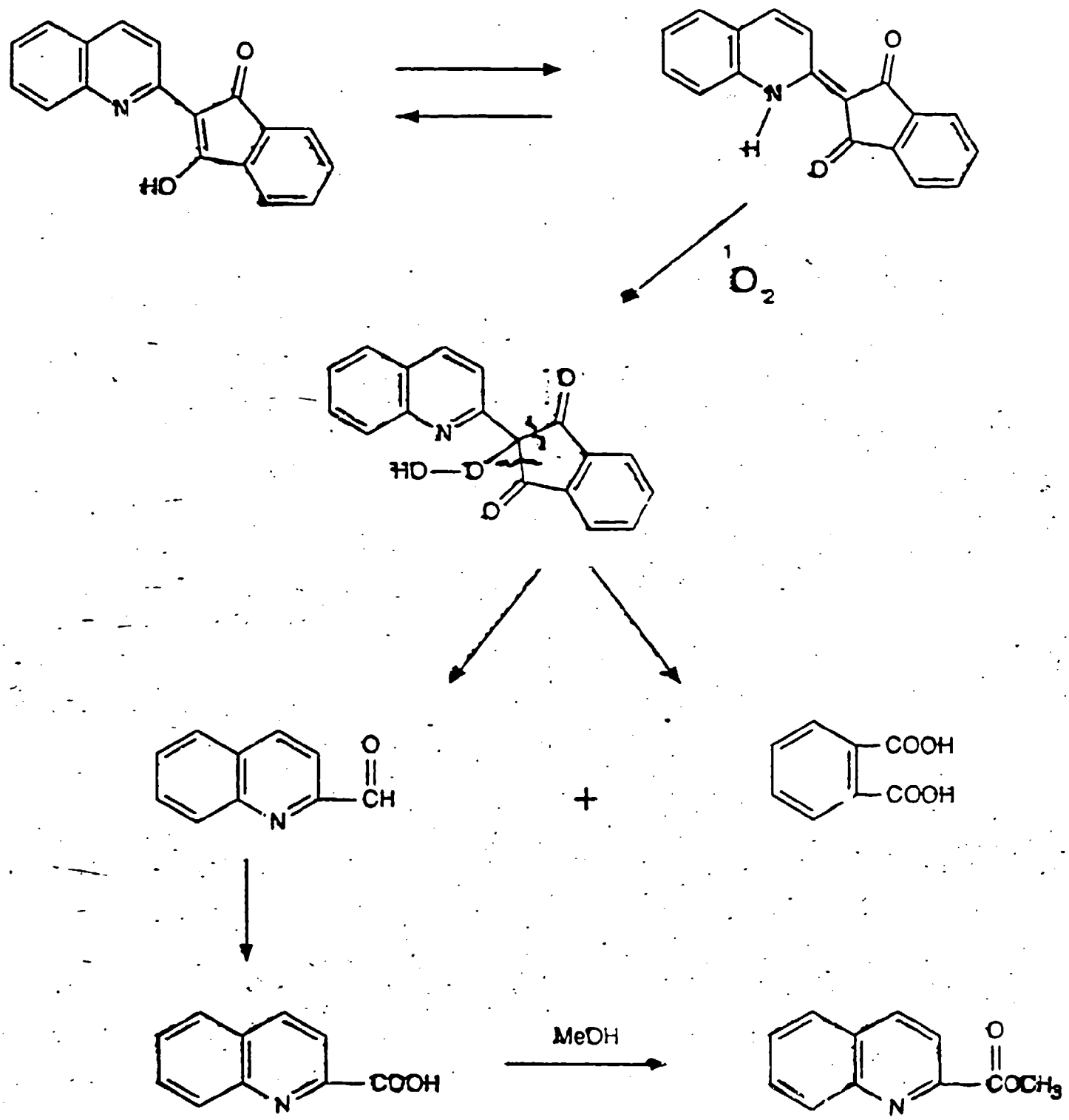

Figure 6-6

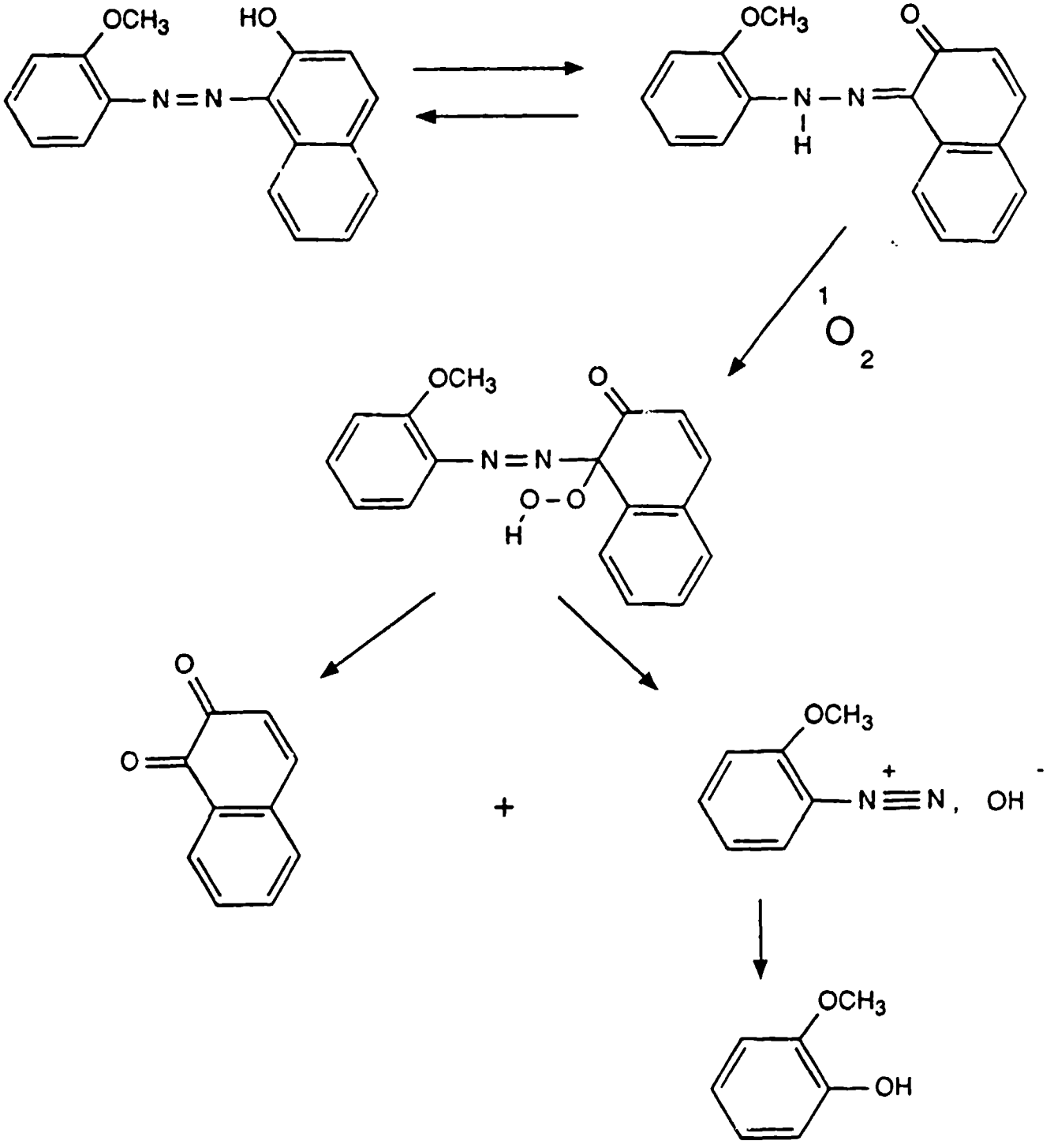

Figure 7-1

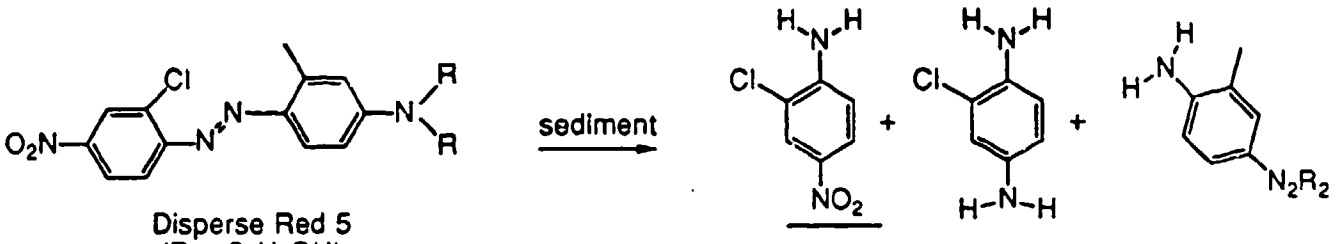

Disperse Red 5
($R = C_2H_4OH$)

Disperse Red 1
($R = Et$, $R_2 = C_2H_4OH$)

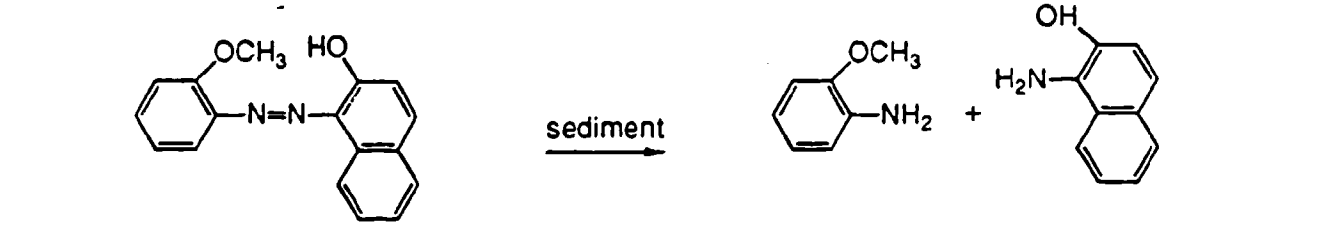

Solvent Red 1

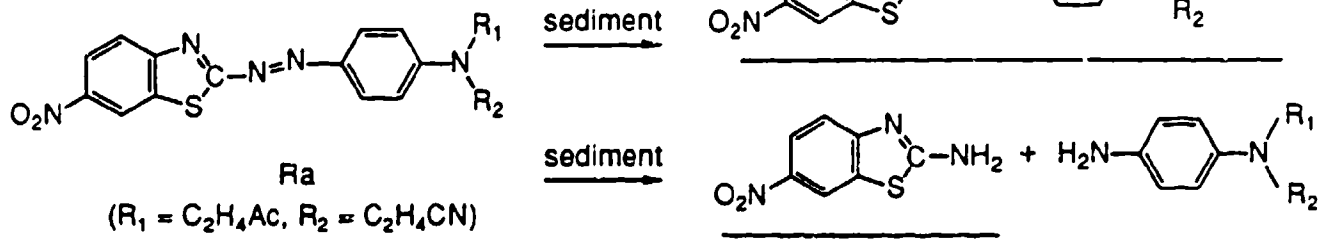

Ra
($R_1 = C_2H_4Ac$, $R_2 = C_2H_4CN$)

Figure 7-2

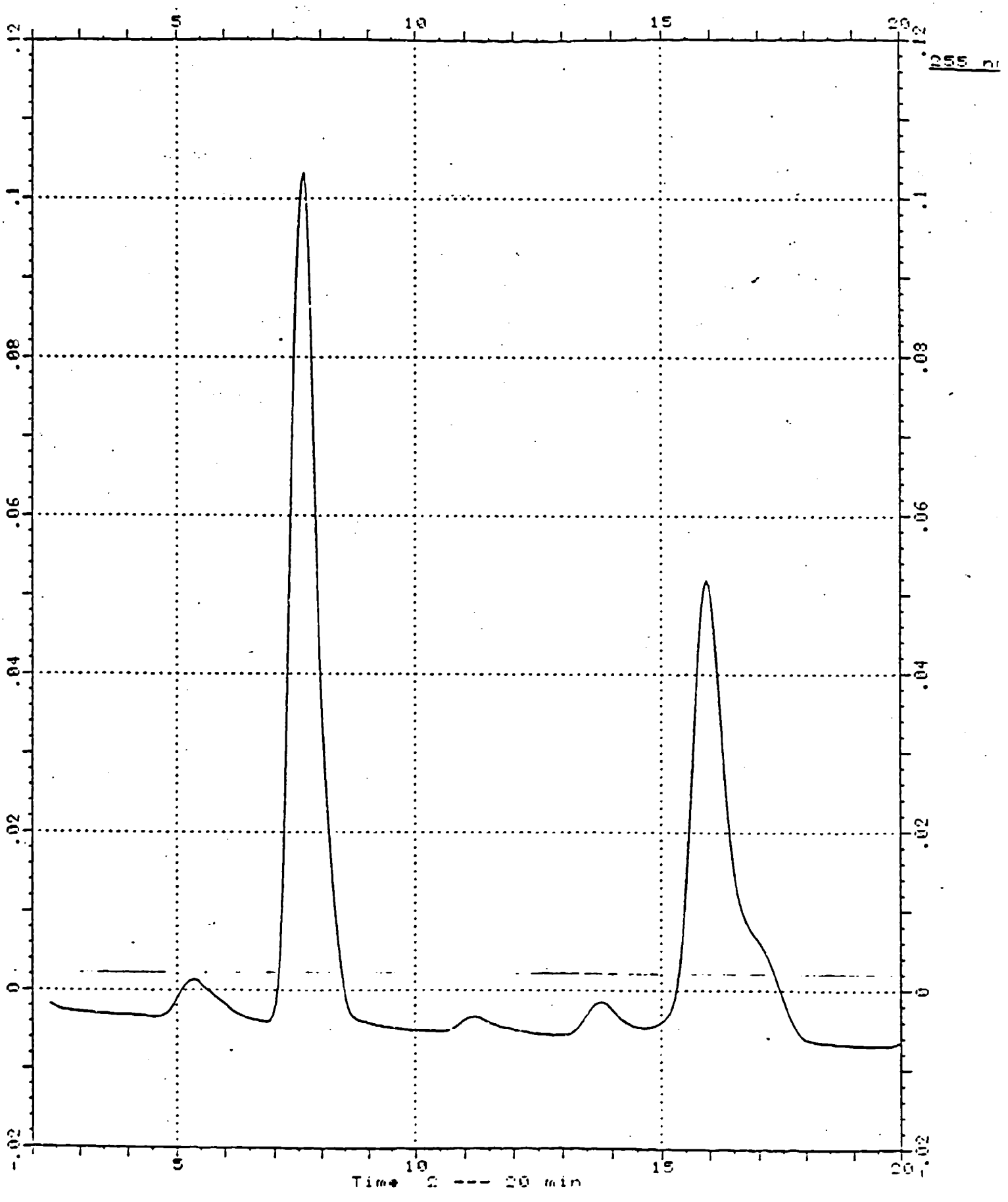

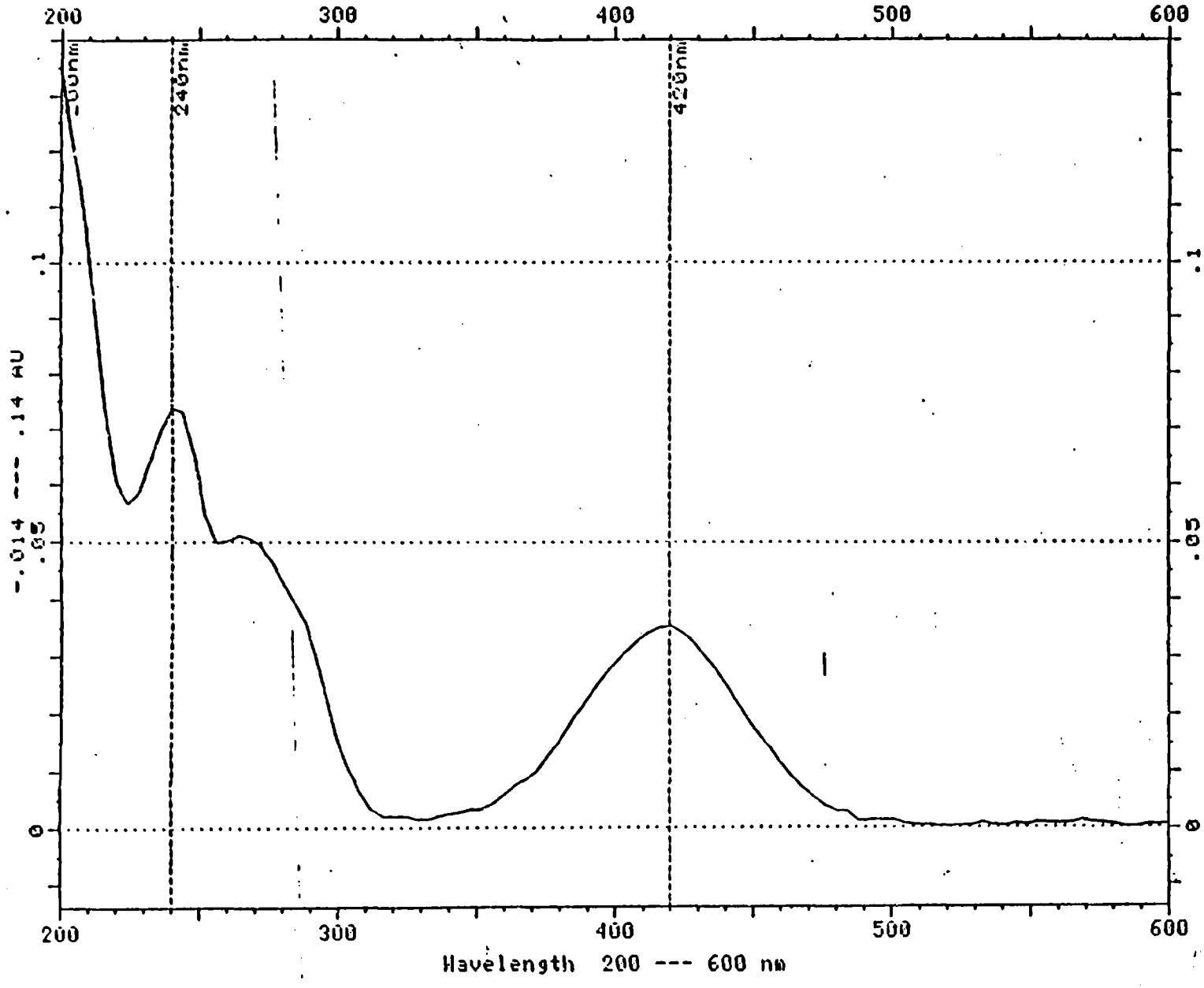

r95.DT3
03-05-1991
14:17:18
Sampling time
31 msec ‡ 17
Y - Scale
.154 AU/FS
Resolution
4 nm
Sample name
redproddr9
16min
Column
mmID ‡ mm
Packing material
Mobile phase
60:40 ACN/H2O
Flow rate
1.0 ml/min
Pressure
285
Waters

Figure 7-3

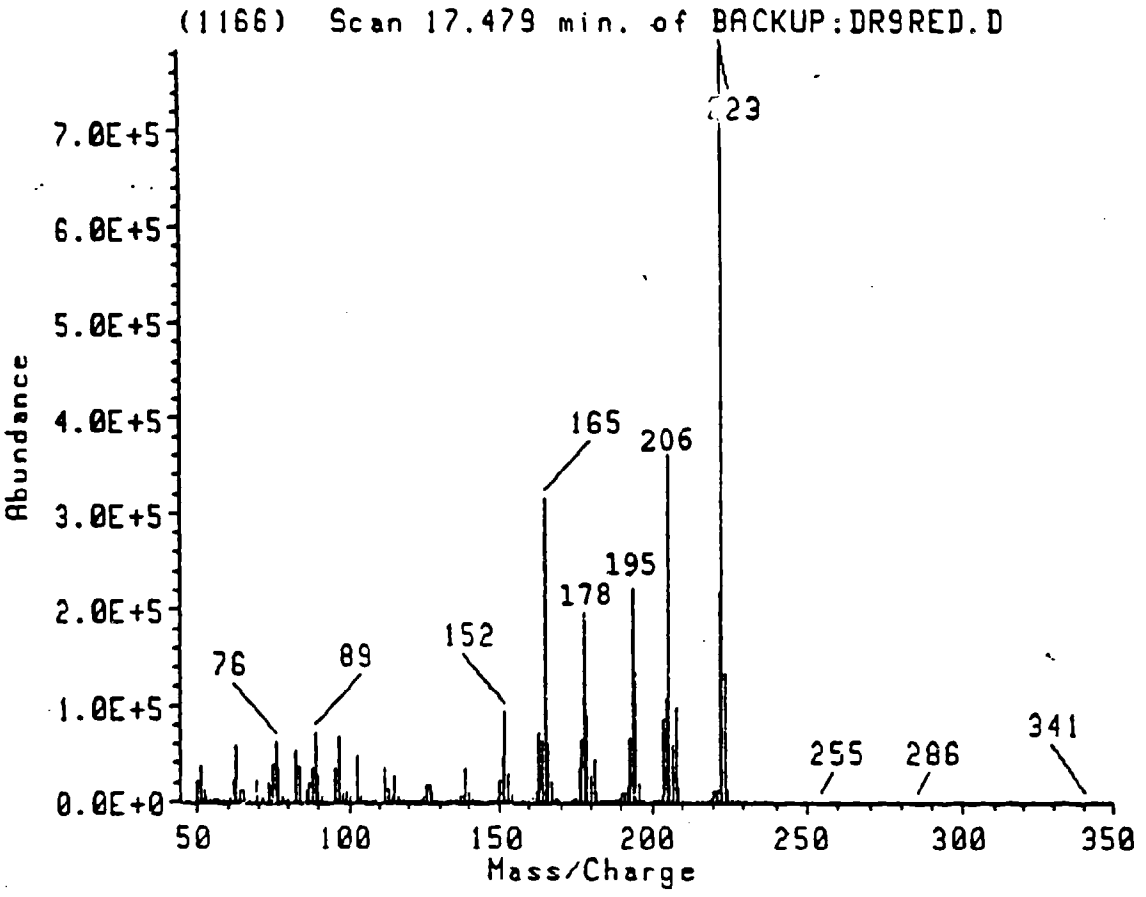
(1166) Scan 17.479 min. of BACKUP:DR9RED.D
Abundance
7.0E+5
6.0E+5
5.0E+5
4.0E+5
3.0E+5
2.0E+5
1.0E+5
0.0E+0
223
165
206
195
178
152
89
76
255
286
341
50
100
150
200
250
300
350
Mass/Charge

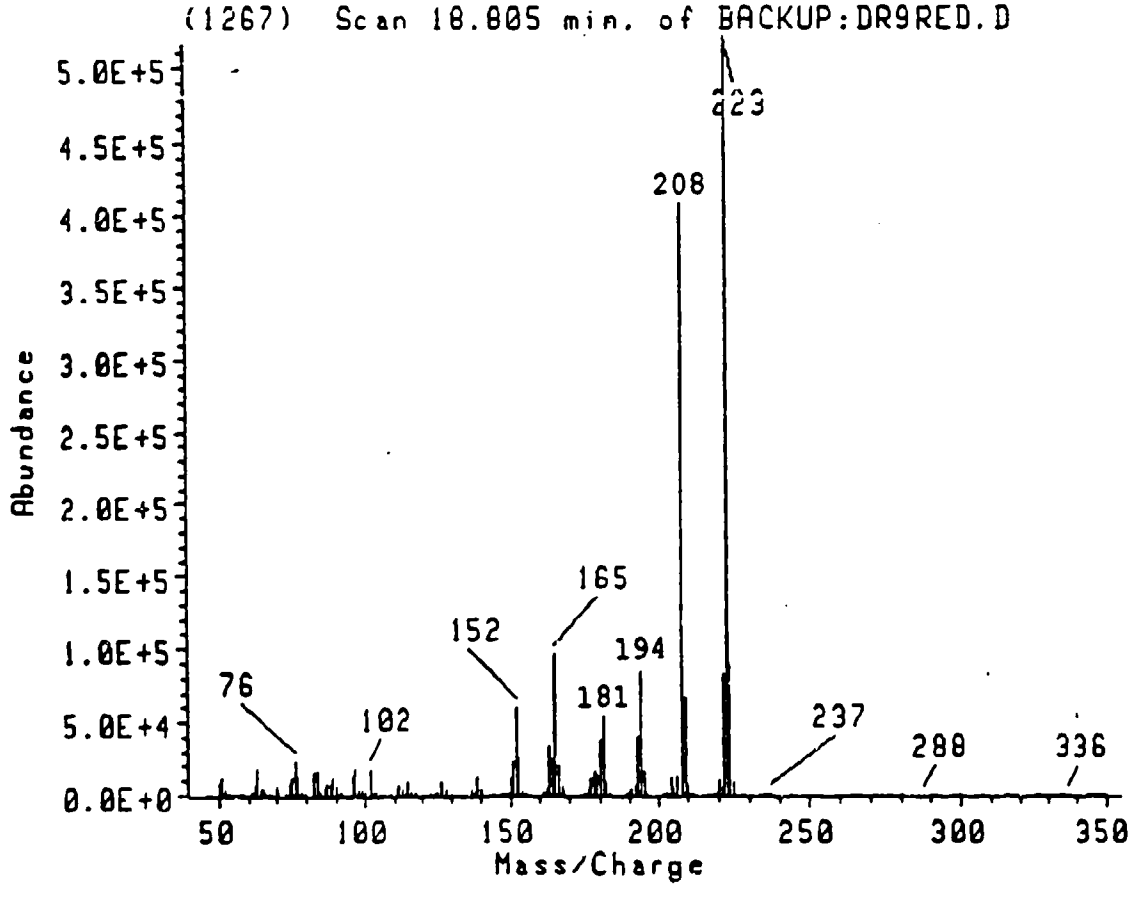
(1267) Scan 18.805 min. of BACKUP:DR9RED.D
Abundance
5.0E+5
4.5E+5
4.0E+5
3.5E+5
3.0E+5
2.5E+5
2.0E+5
1.5E+5
1.0E+5
5.0E+4
0.0E+0
223
208
165
152
194
181
76
102
237
288
336
50
100
150
200
250
300
350
Mass/Charge

Figure 7-5

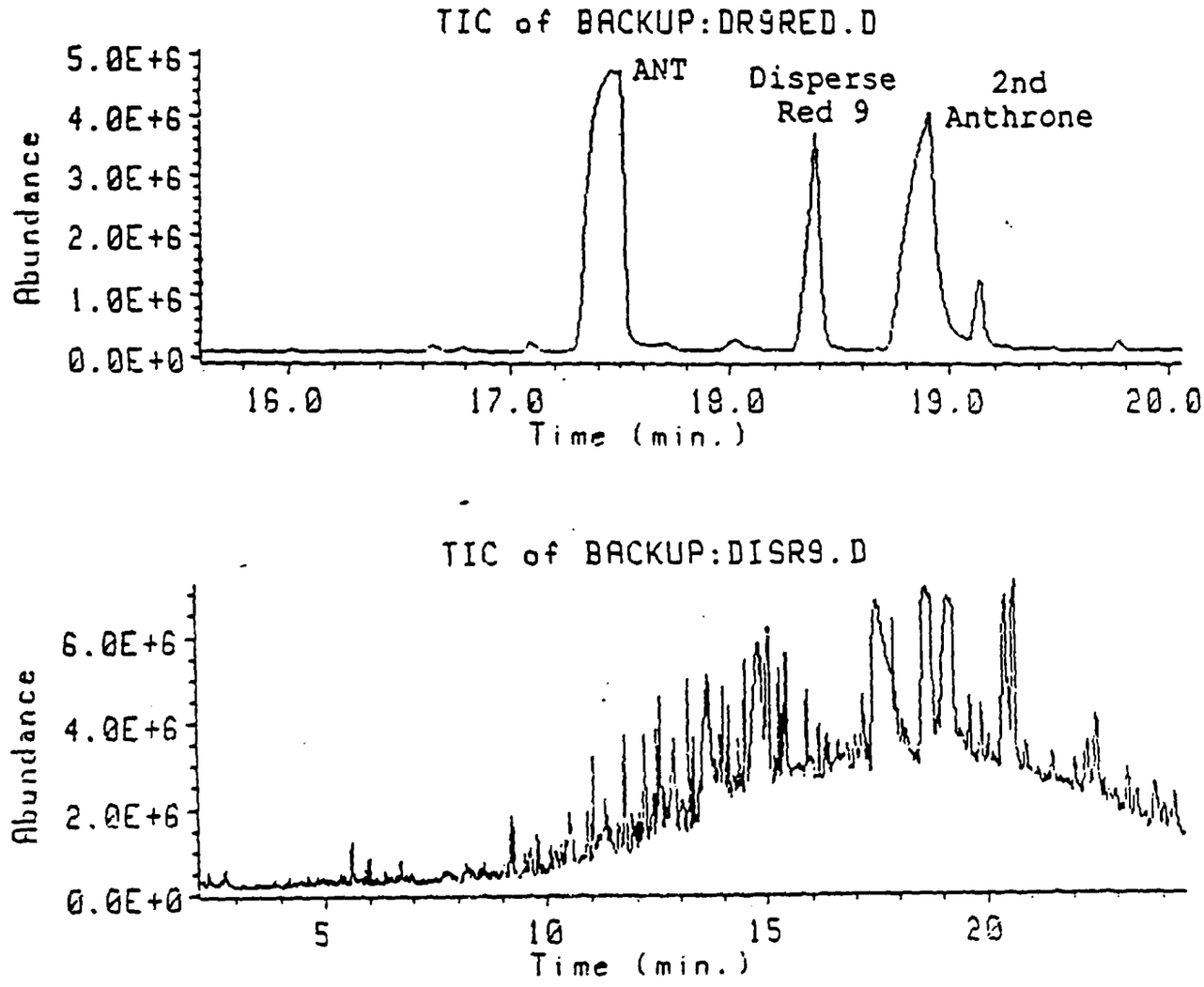
TIC of BACKUP:DR9RED.D
ANT
Disperse
Red 9
2nd
Anthrone
Abundance
5.0E+6
4.0E+6
3.0E+6
2.0E+6
1.0E+6
0.0E+0
16.0
17.0
18.0
19.0
20.0
Time (min.)
TIC of BACKUP:DISR9.D
Abundance
6.0E+6
4.0E+6
2.0E+6
0.0E+0
5
10
15
20
Time (min.)

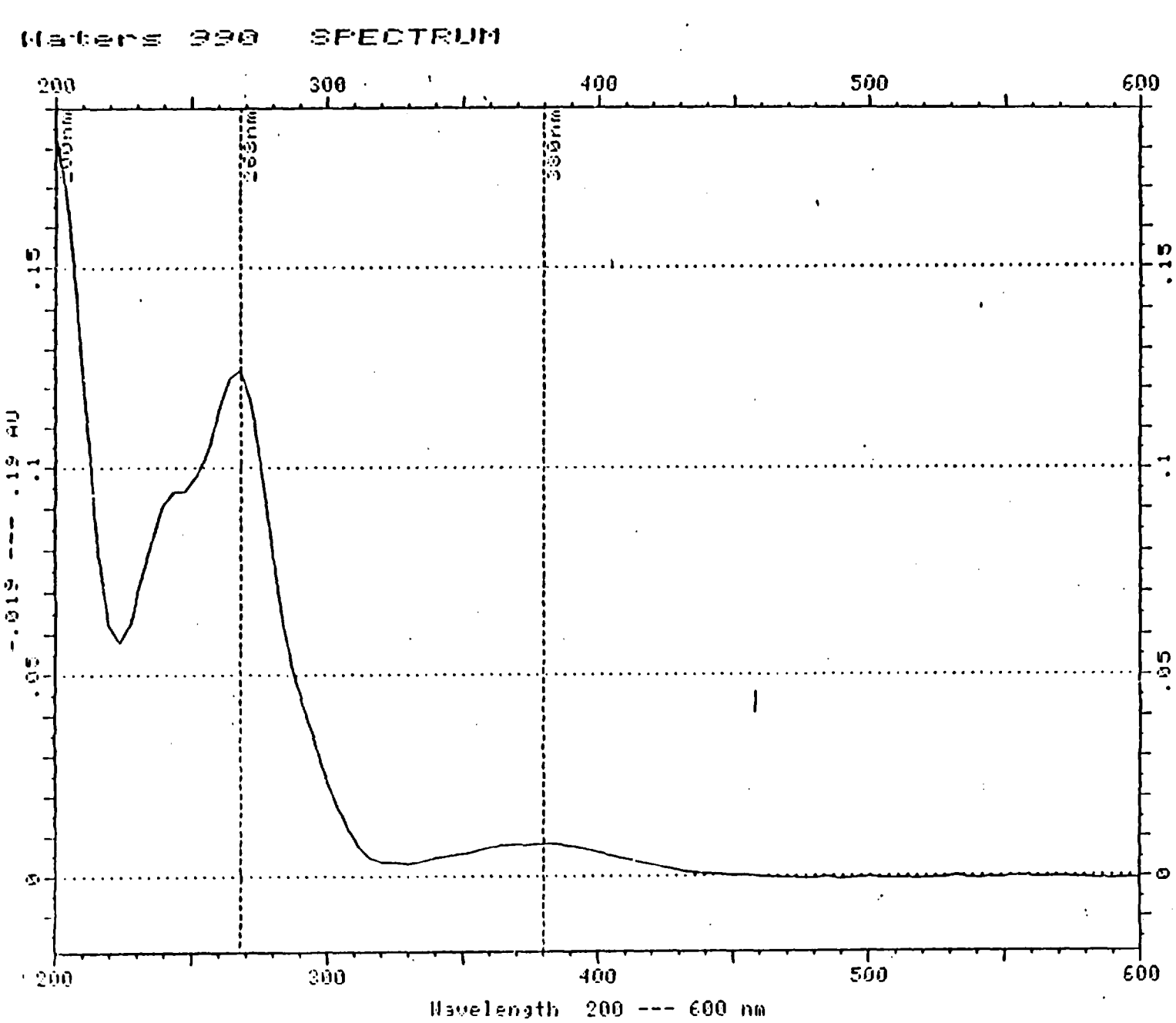

r95.003
03-05-1991
14:17:18
Sampling time
31 msec I 17
Y - Scale
.209 AU/FS
Resolution
4 nm
Sample name
redprodnr9
7.66min
Column
mmID I mm
Packing material
Mobile phase
MeOH/H2O
Flow rate
1.0 ml/min
Pressure
285
Waters

Figure 7-7

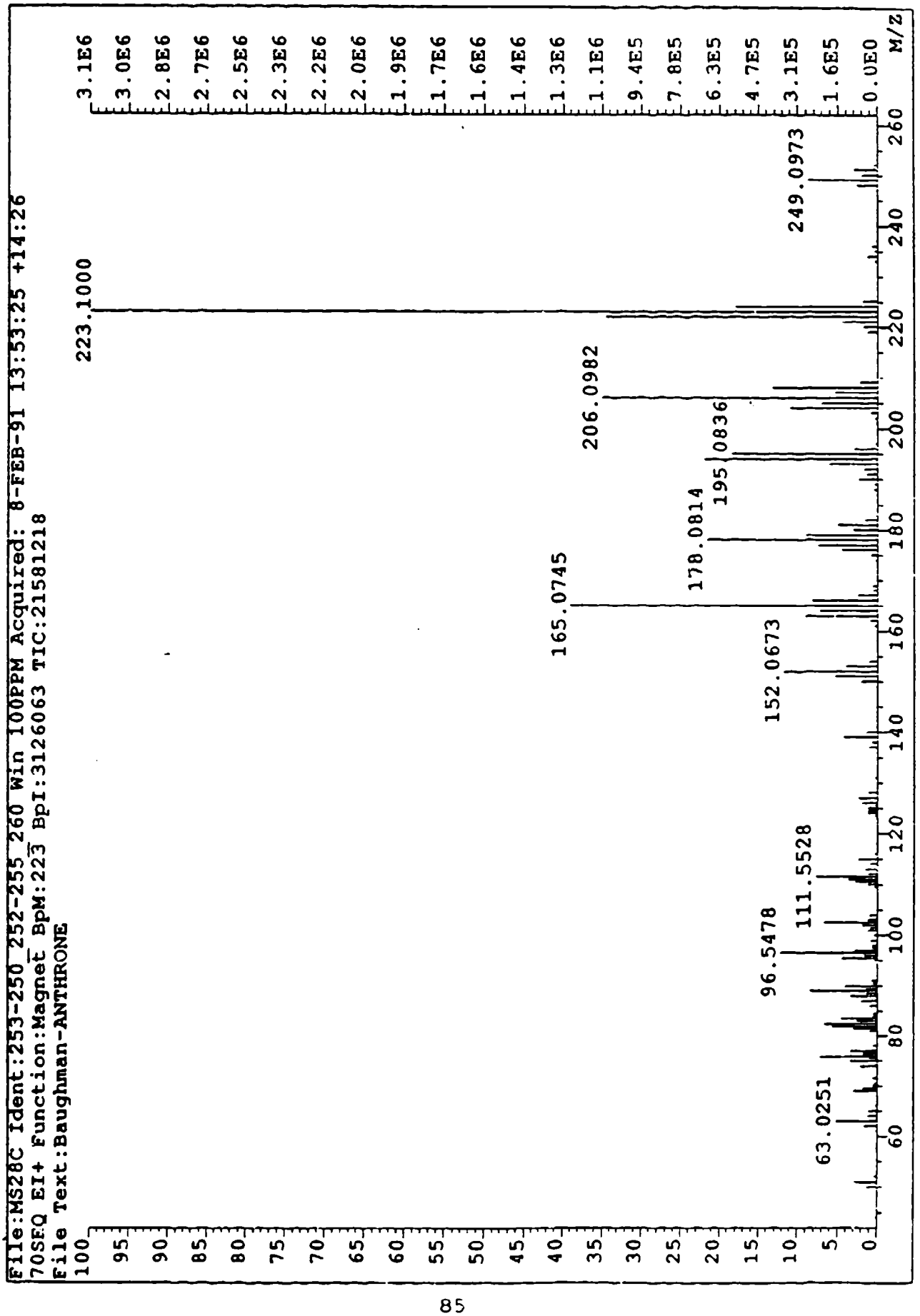
File:MS28C Ident:253-250 252-255 260 Win 100PPM Acquired: 8-FEB-91 13:53:25 +14:26
70SEQ EI+ Function:Magnet BpM:223 BpI:3126063 TIC:21581218
File Text:Baughman-ANTHRONE
223.1000
206.0982
165.0745
178.0814
195.0836
152.0673
249.0973
96.5478
111.5528
63.0251
M/z

Figure 7-8

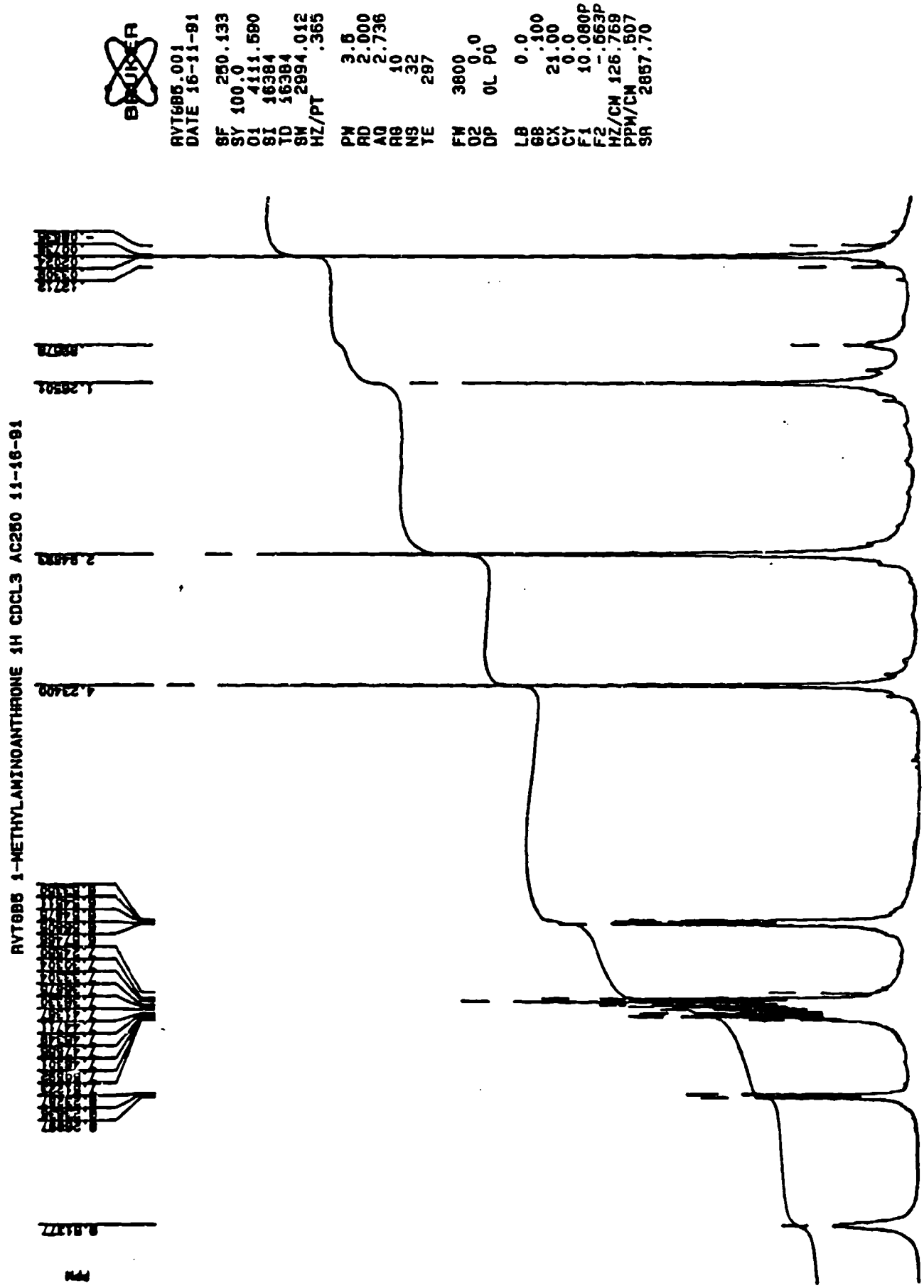
RVT6B5 1-METHYLAMINOANTHRONE 1H CDCL3 AC250 11-16-91
RVT6B5.001
DATE 16-11-91
SF 250.133
SY 100.0
O1 4111.580
SI 16384
TD 16384
SW 2894.012
HZ/PT .365
PW 3.8
RD 2.000
AQ 2.736
RG 10
N3 32
TE 297
FW 3800
O2 0.0
DP OL PO
LB 0.0
GB .100
CX 21.00
CY 0.0
F1 10.080P
F2 -.663P
HZ/CM 126.769
PPM/CM .507
SR 2857.70
PPM

Figure 7-9

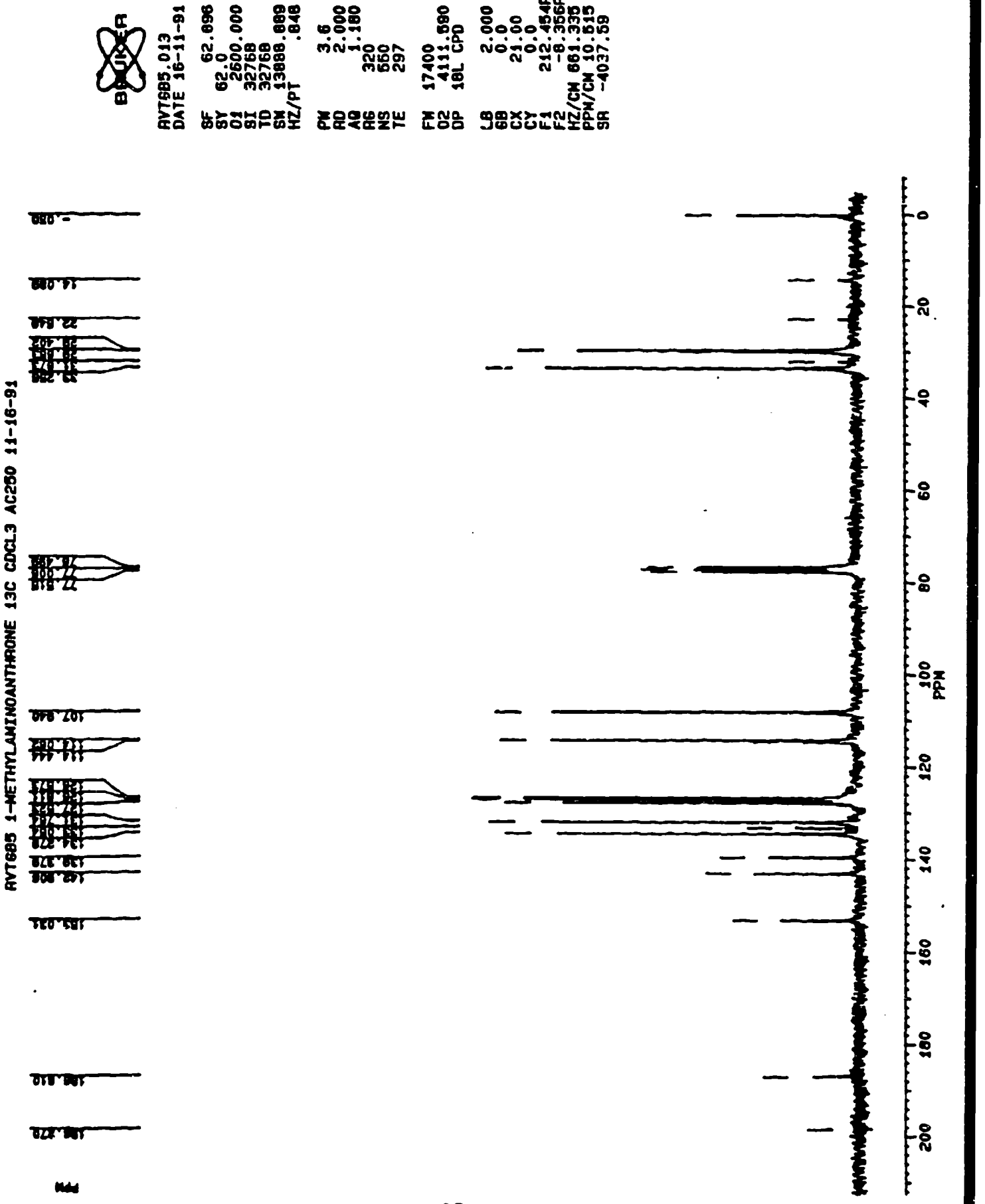
BRUKER
AVT685.013
DATE 16-11-91
SF 62.896
SY 62.0
O1 2600.000
SI 32768
TD 32768
SW 13888.889
HZ/PT .848
PW 3.6
RD 2.000
AQ 1.180
A6 320
NS 550
TE 297
FW 17400
O2 4111.590
DP 18L CPD
LB 2.000
GB 0.0
CX 21.00
CY 0.0
F1 212.454P
F2 -8.356P
HZ/CM 661.335
PPM/CM 10.515
SR -4037.59
AVT685 1-METHYLAMINOANTHRONE 13C CDCL3 AC250 11-16-91
PPM
PPM

Figure 7-10

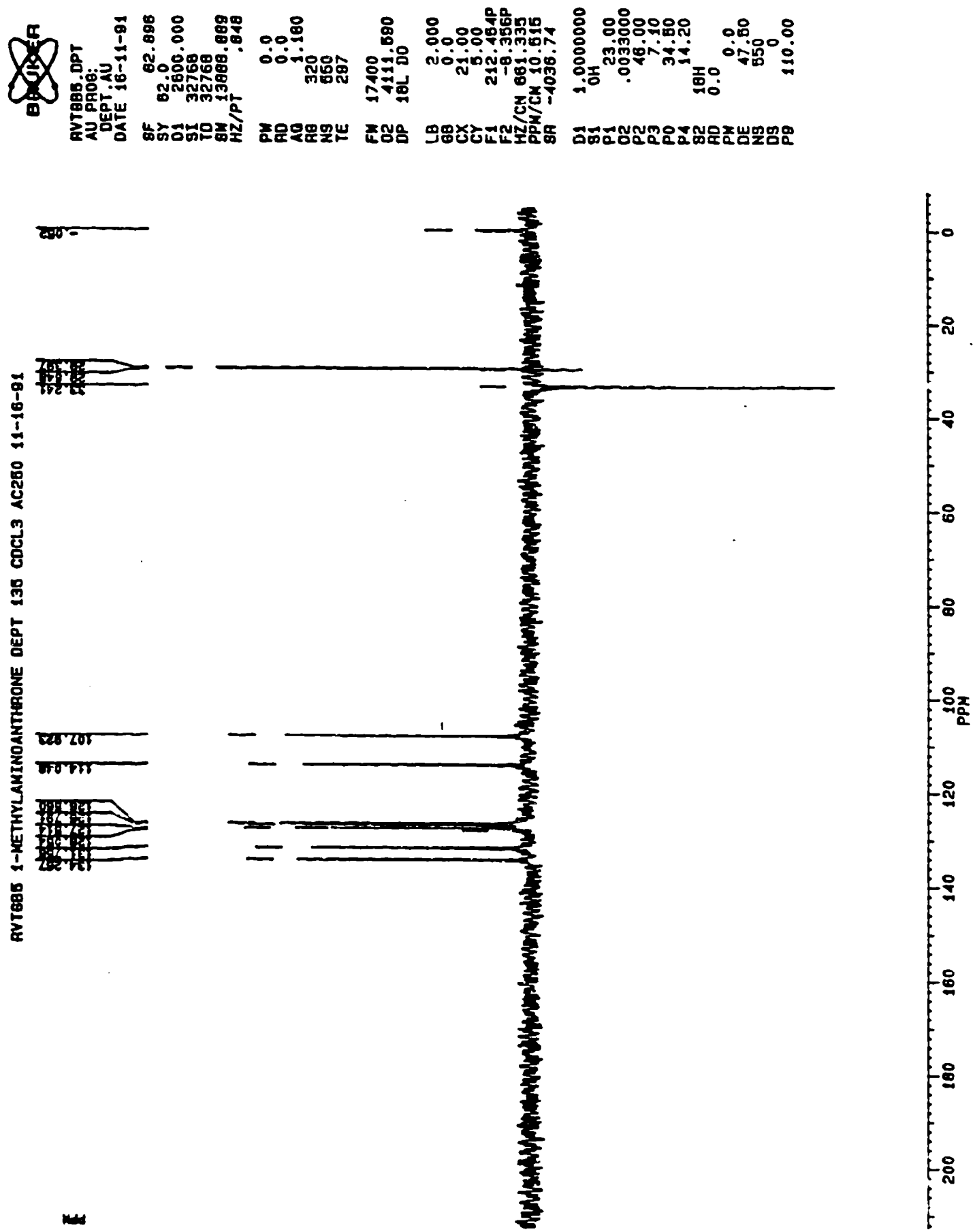
RVT885.DPT
AU PROG:
DEPT.AU
DATE 16-11-91
SF 62.896
SY 62.0
D1 2600.000
SI 32768
TD 32768
SW 13008.889
HZ/PT .848
PW 0.0
RD 0.0
AQ 1.180
RG 320
NS 650
TE 297
FW 17400
O2 4111.590
DP 18L DO
LB 2.000
GB 0.0
CX 21.00
CY 5.00
F1 212.464P
F2 -8.356P
HZ/CN 661.335
PPM/CM 10.615
SR -4036.74
D1 1.0000000
OH
P1 23.00
O2 .0033000
P2 46.00
P3 7.10
P0 34.80
P4 14.20
S2 18H
RD 0.0
PW 0.0
DE 47.80
NS 650
DS 0
PS 110.00
RVT885 1-METHYLANINOANTHRONE DEPT 135 CDCL3 AC250 11-16-91
PPM

Figure 7-11

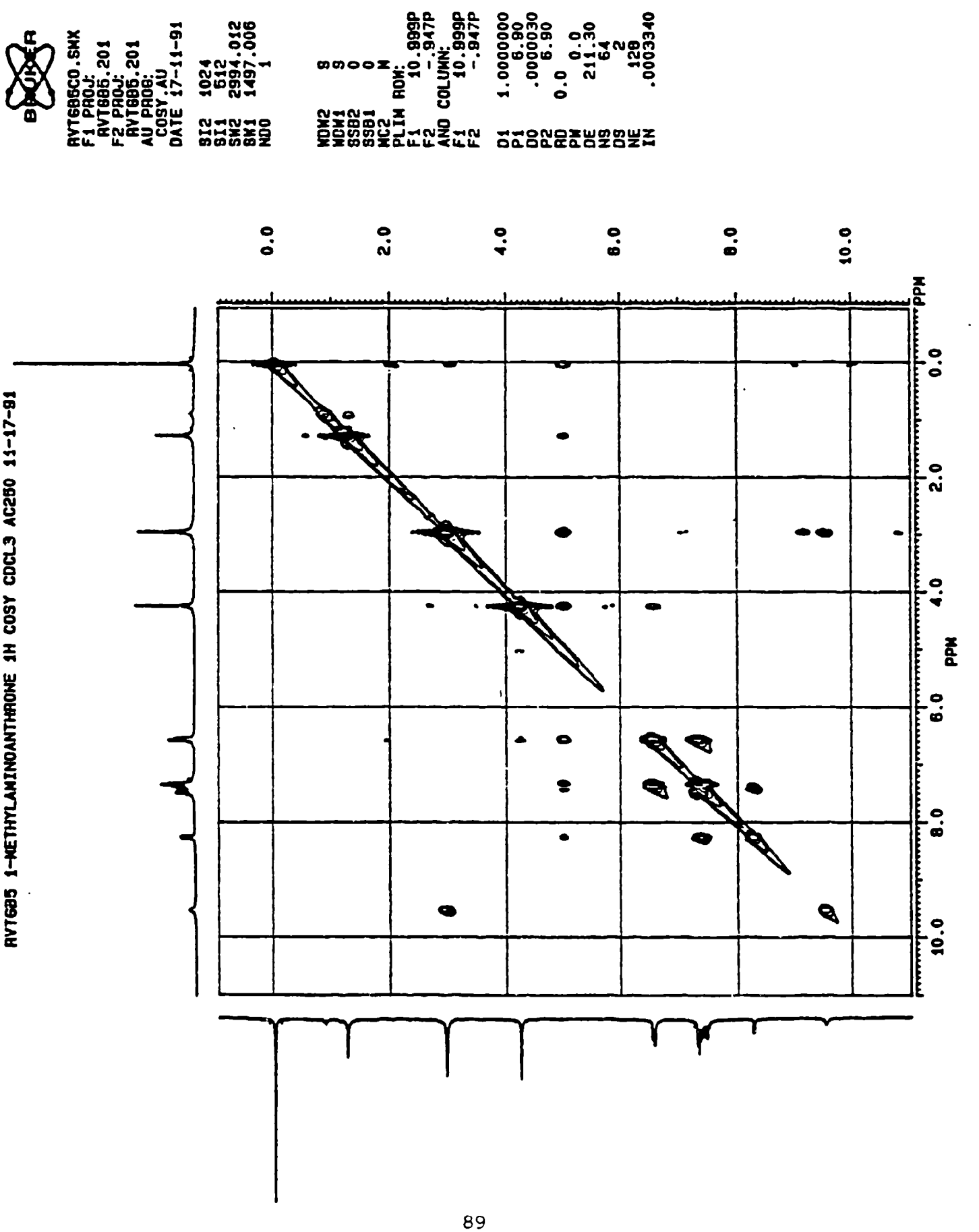
RVT685 1-METHYLAMINOANTHRONE 1H COSY CDCL3 AC250 11-17-91
RVT685CO.SMX
F1 PROJ:
RVT685.201
F2 PROJ:
RVT685.201
AU PROG:
COSY.AU
DATE 17-11-91
SI2 1024
SI1 512
SW2 2994.012
SW1 1497.006
NDO 1
MDW2 8
MDW1 9
SSB2 0
SSB1 0
MC2 N
PLIM ROW:
F1 10.999P
F2 -.947P
AND COLUMN:
F1 10.999P
F2 -.947P
D1 1.0000000
P1 6.80
D0 .0000030
P2 6.90
RD 0.0 0.0
PW 211.30
DE 64
NS 2
DS 128
NE .0003340
IN
0.0
2.0
4.0
6.0
8.0
10.0
PPM

Figure 7-12

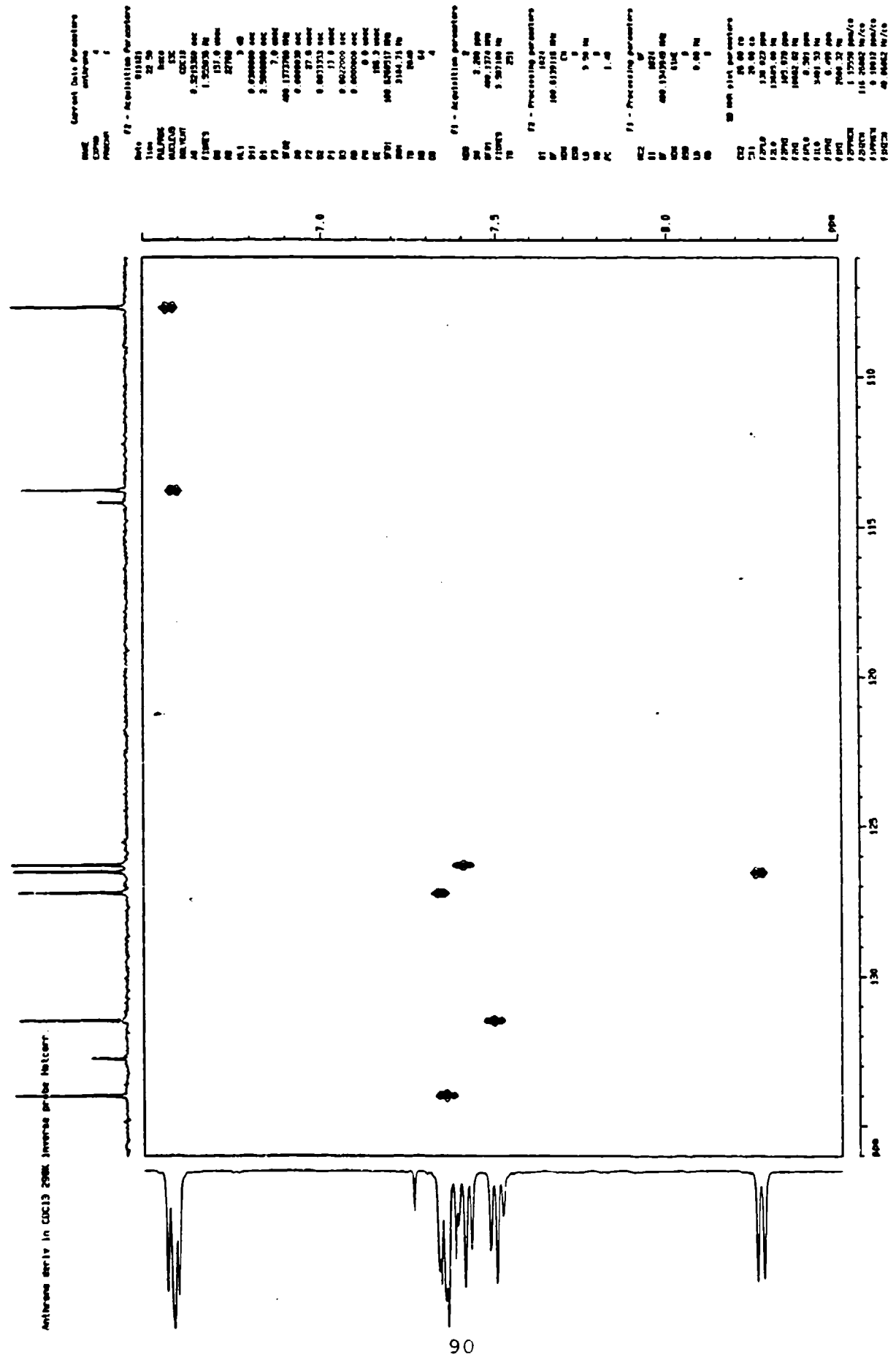
7.0
7.5
8.0
110
115
120
125
130
Anthrone deriv in CDCl3 298K inverse probe Nalcer

Figure 7-13

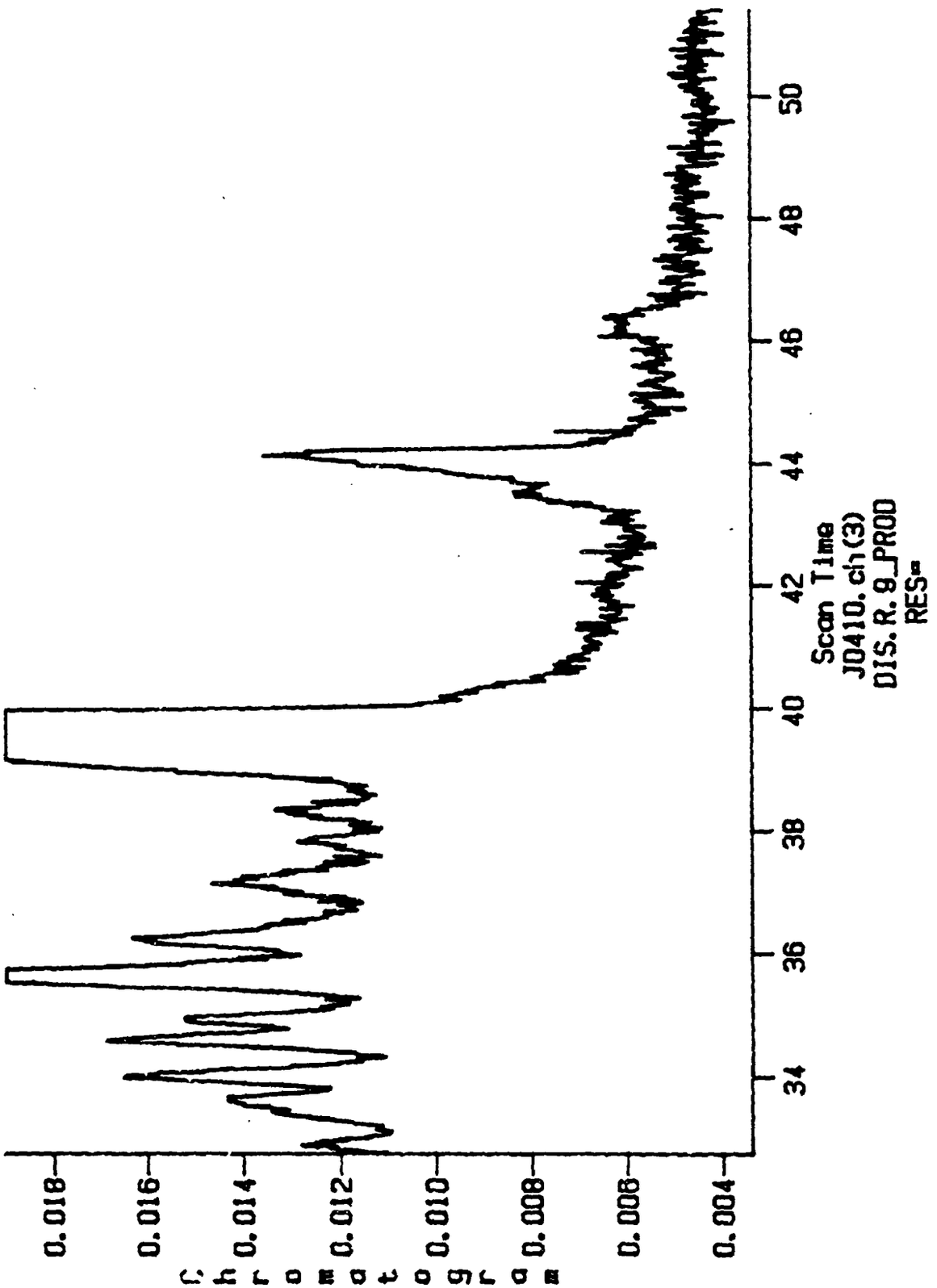
Chromatogram
0.018
0.016
0.014
0.012
0.010
0.008
0.006
0.004
34
36
38
40
42
44
46
48
50
Scan Time
JD410.ch(3)
DIS.R.9_PROD
RES=

Figure 7-14

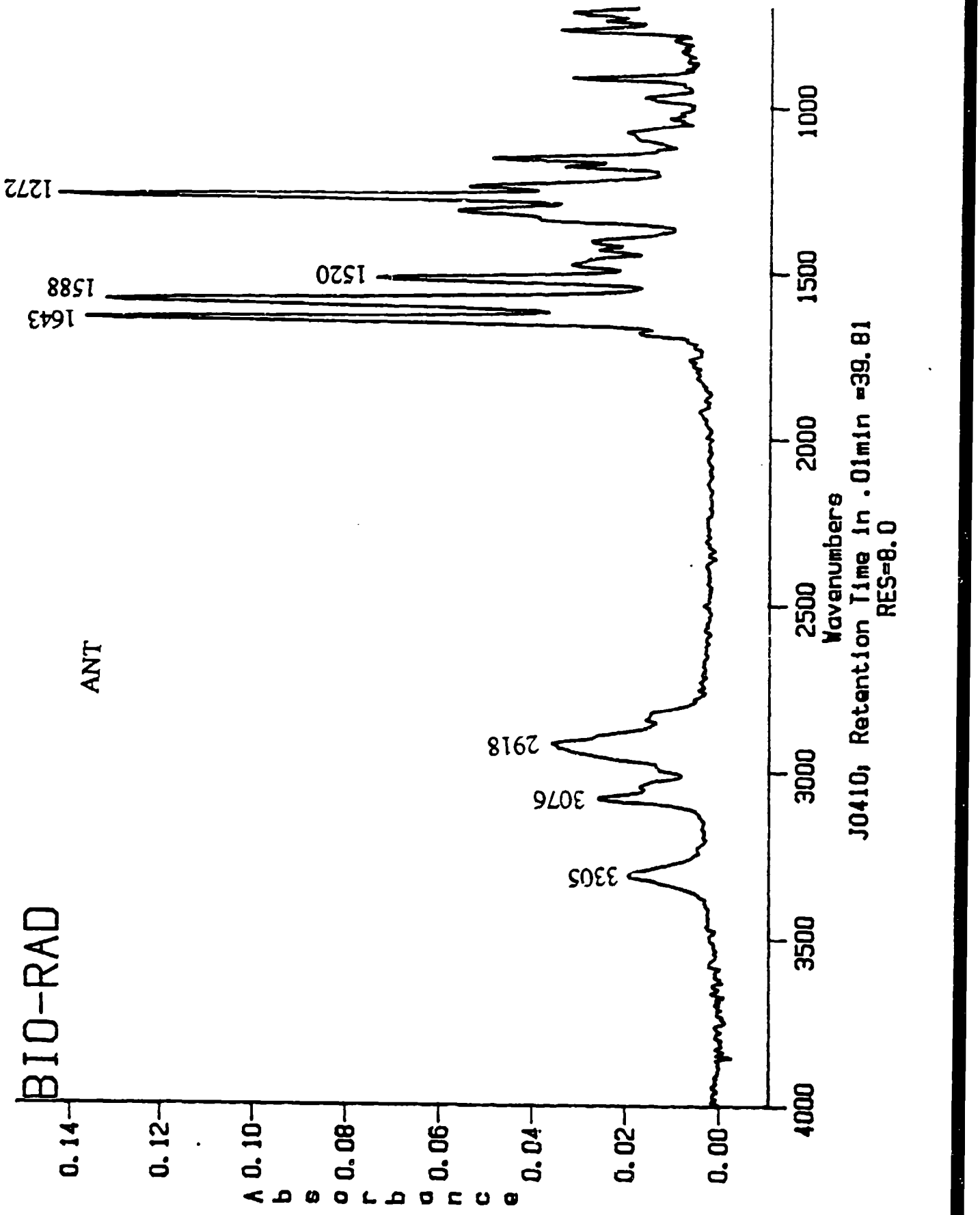
BIO-RAD
ANT
Absorbance
0.14
0.12
0.10
0.08
0.06
0.04
0.02
0.00
4000
3500
3000
2500
2000
1500
1000
Wavenumbers
J0410; Retention Time in .01min =39.81
RES=8.0
3305
3076
2918
1643
1588
1520
1272

Figure 7-15

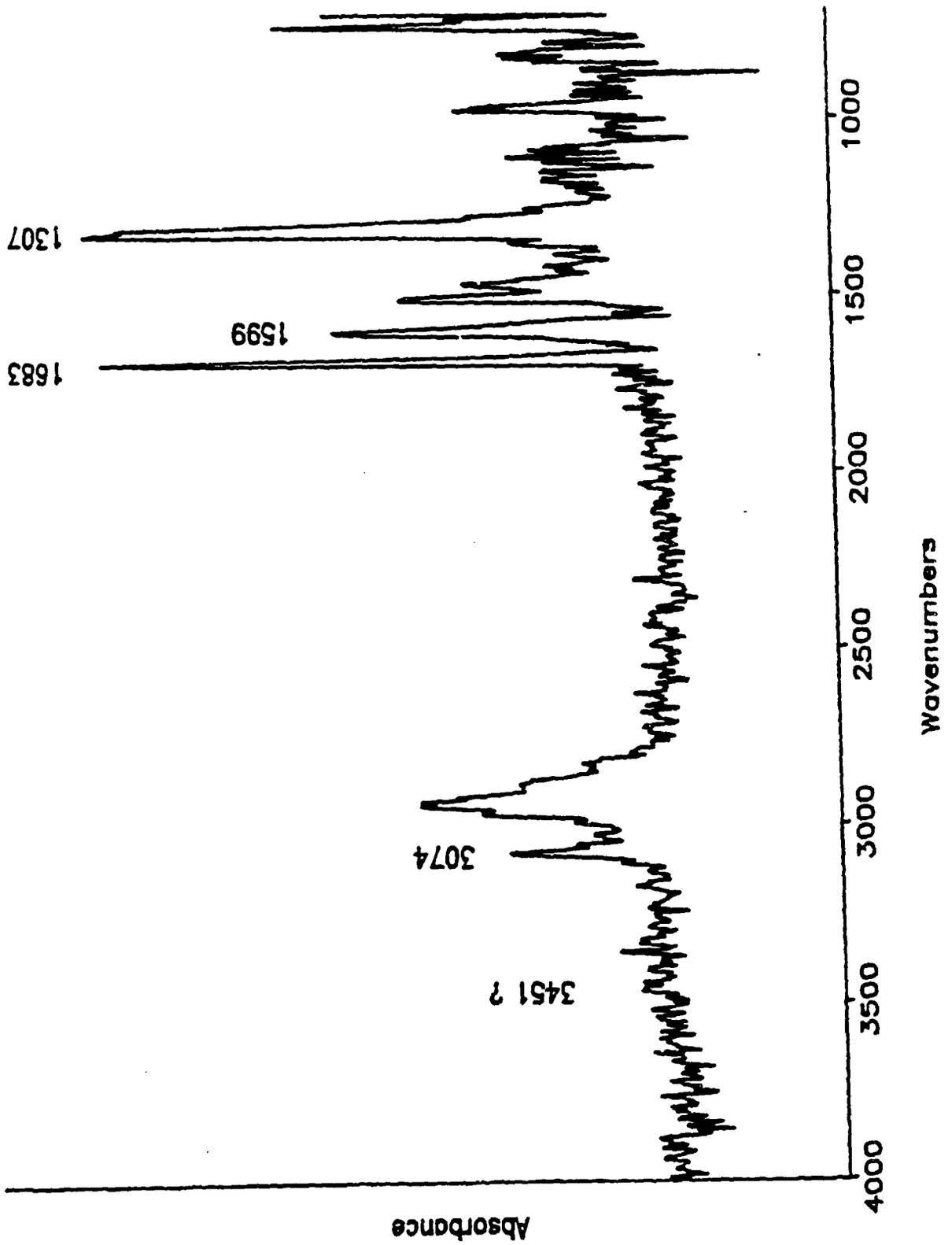
Absorbance
4000
3500
3000
2500
2000
1500
1000
Wavenumbers
3451 ?
3074
1599
1683
1307

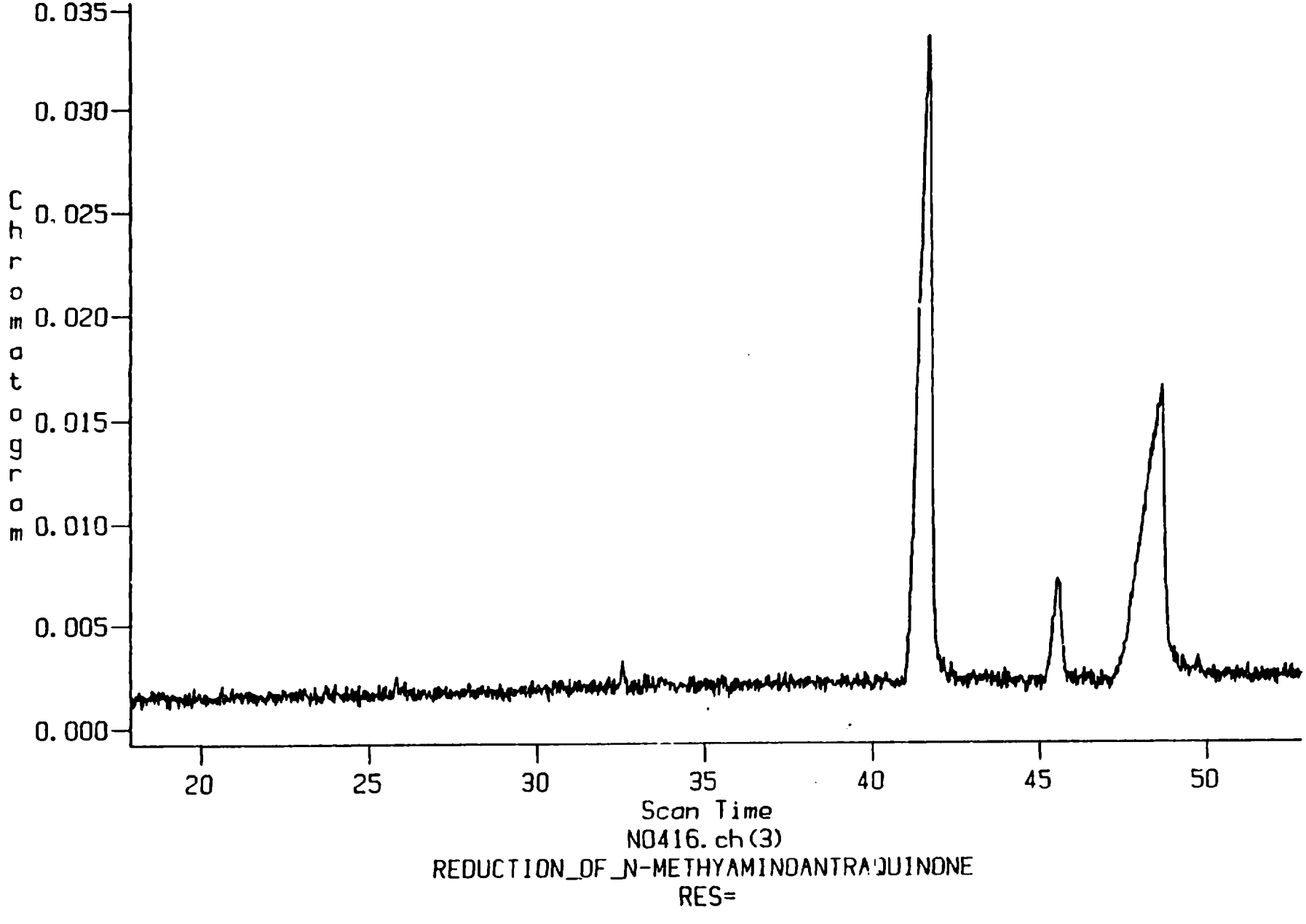
0.035
0.030
0.025
0.020
0.015
0.010
0.005
0.000
Chromatogram
20
25
30
35
40
45
50
Scan Time
N0416.ch(3)
REDUCTION_OF_N-METHYAMINOANTRAQUINONE
RES=

Figure 7-16

Figure 7-17

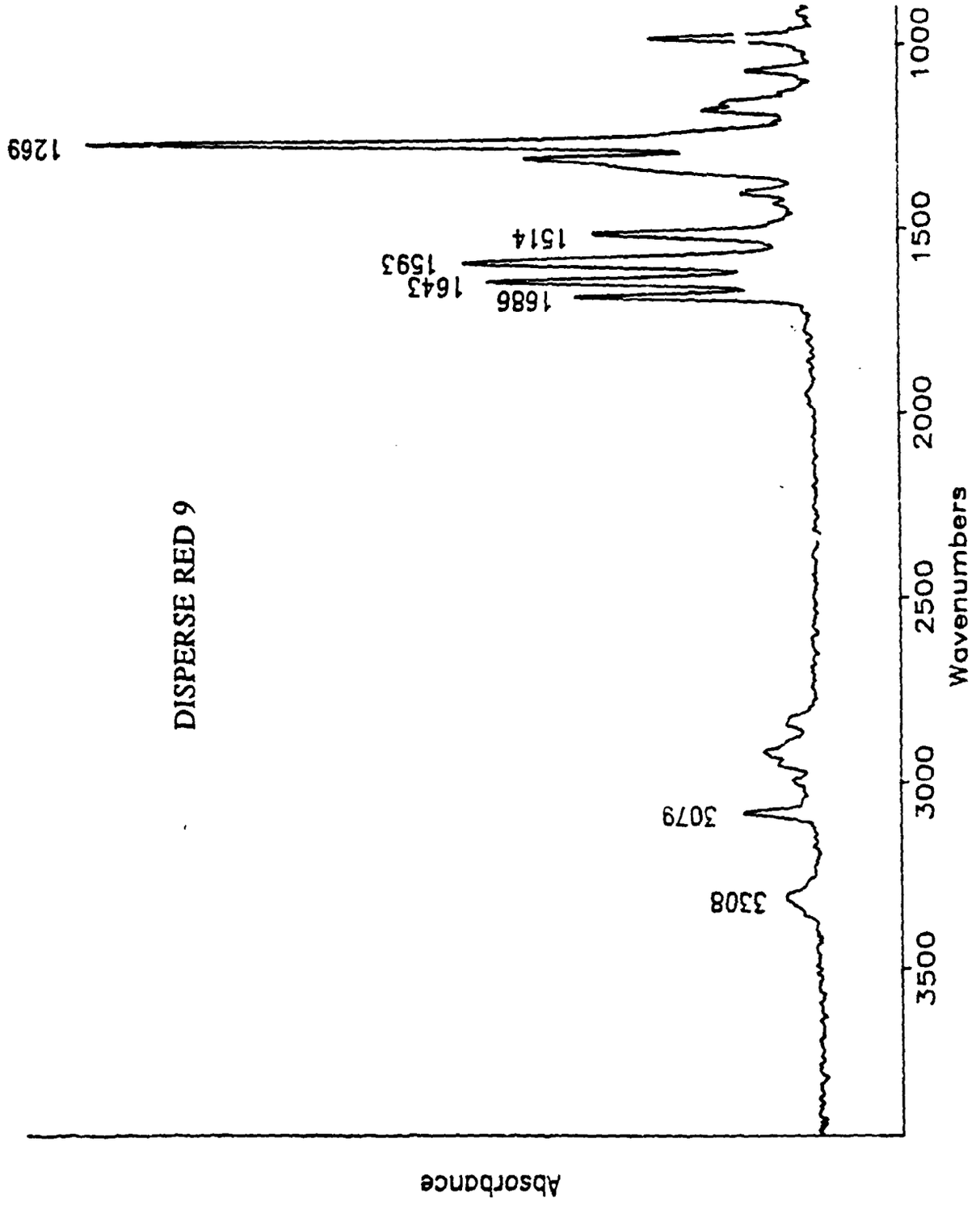
DISPERSE RED 9
Absorbance
Wavenumbers
1000
1500
2000
2500
3000
3500
1269
1514
1593
1643
1686
3079
3308

Figure 7-18

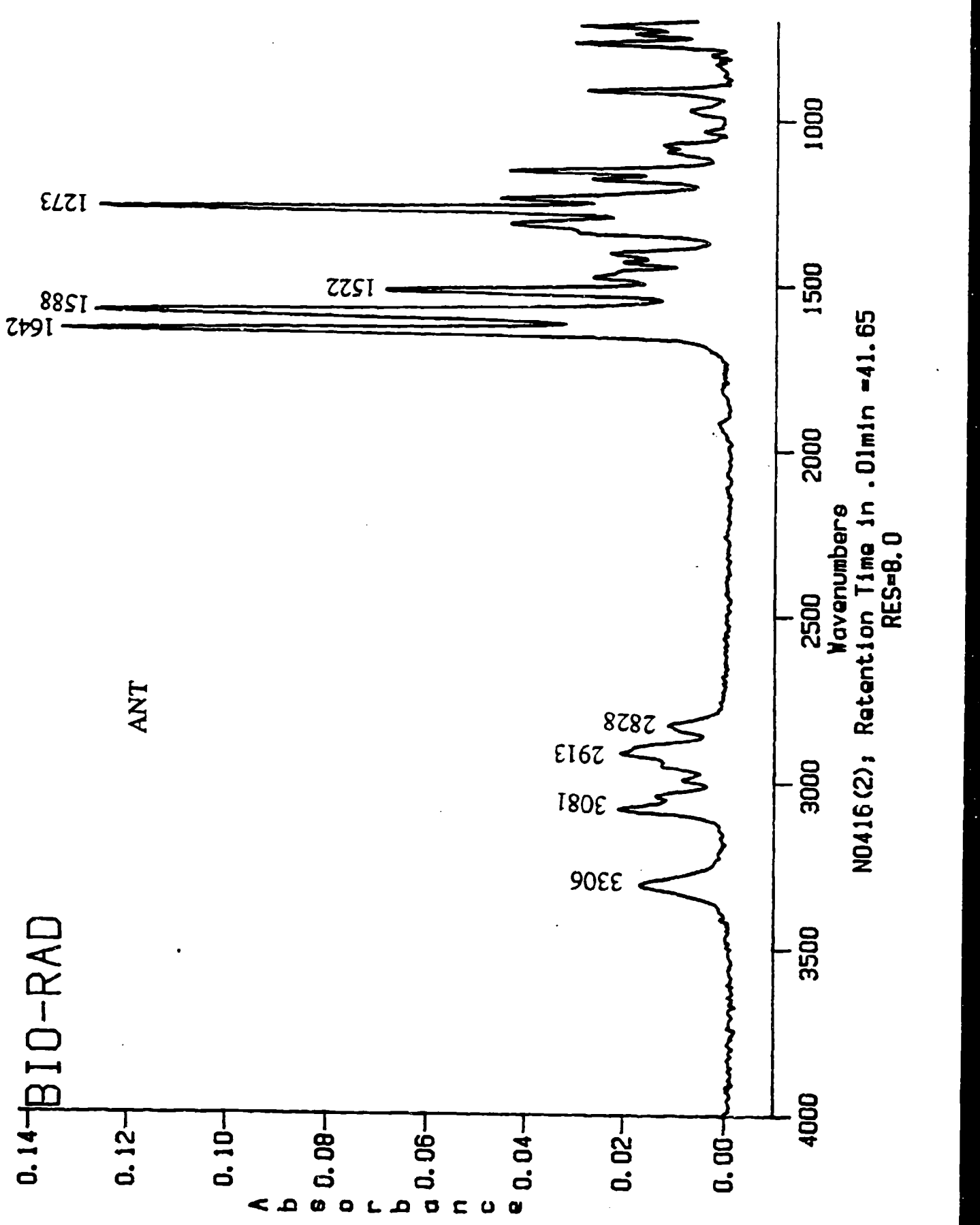
BIO-RAD
ANT
Absorbance
0.14
0.12
0.10
0.08
0.06
0.04
0.02
0.00
4000
3500
3000
2500
2000
1500
1000
Wavenumbers
N0416(2); Retention Time in .01min =41.65
RES=8.0
1273
1522
1588
1642
2828
2913
3081
3306

Figure 7-19

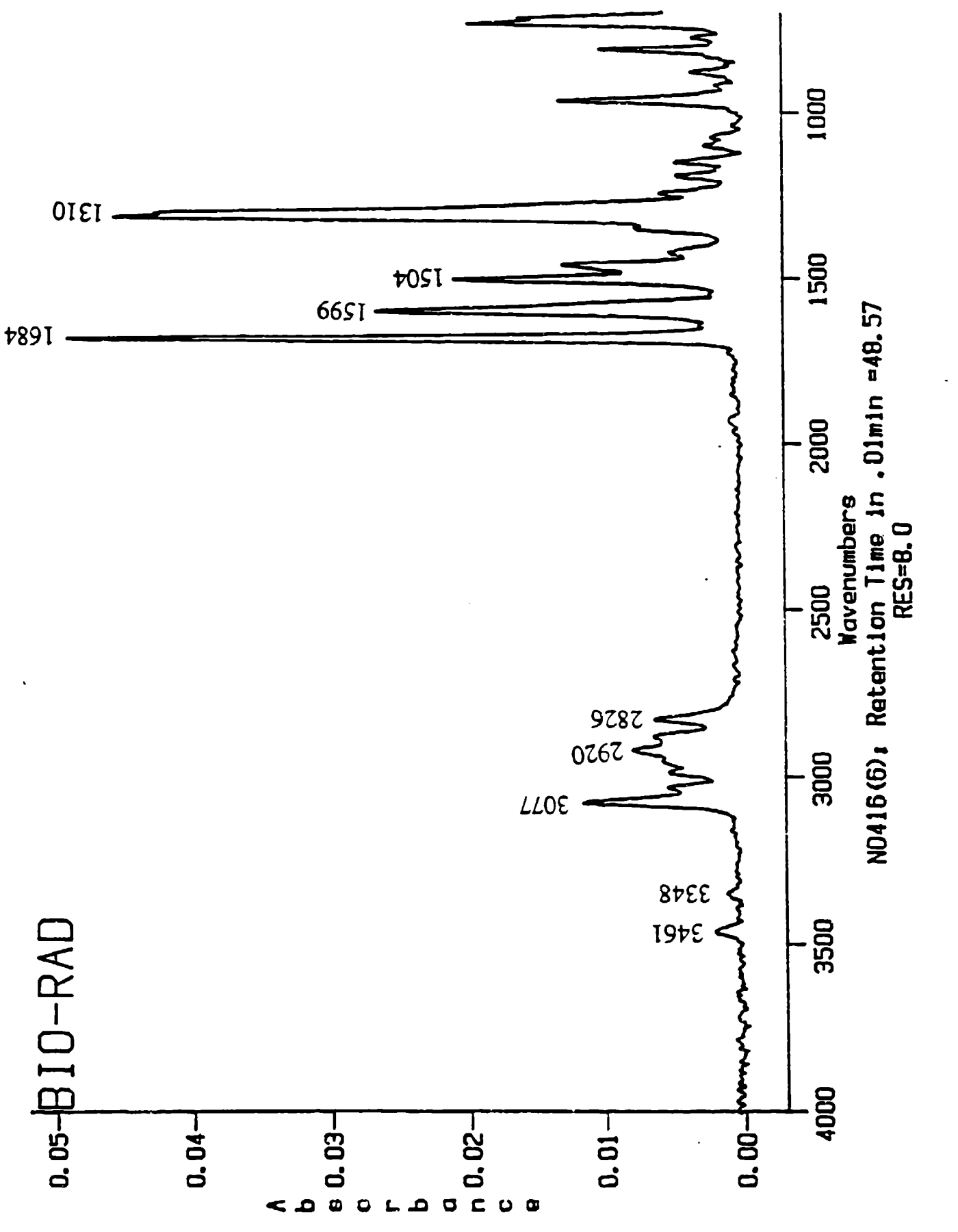
BIO-RAD
Absorbance
0.05
0.04
0.03
0.02
0.01
0.00
4000
3500
3000
2500
2000
1500
1000
Wavenumbers
ND416(6): Retention Time in .01min =48.57
RES=8.0
3461
3348
3077
2920
2826
1684
1599
1504
1310

Figure 7-20

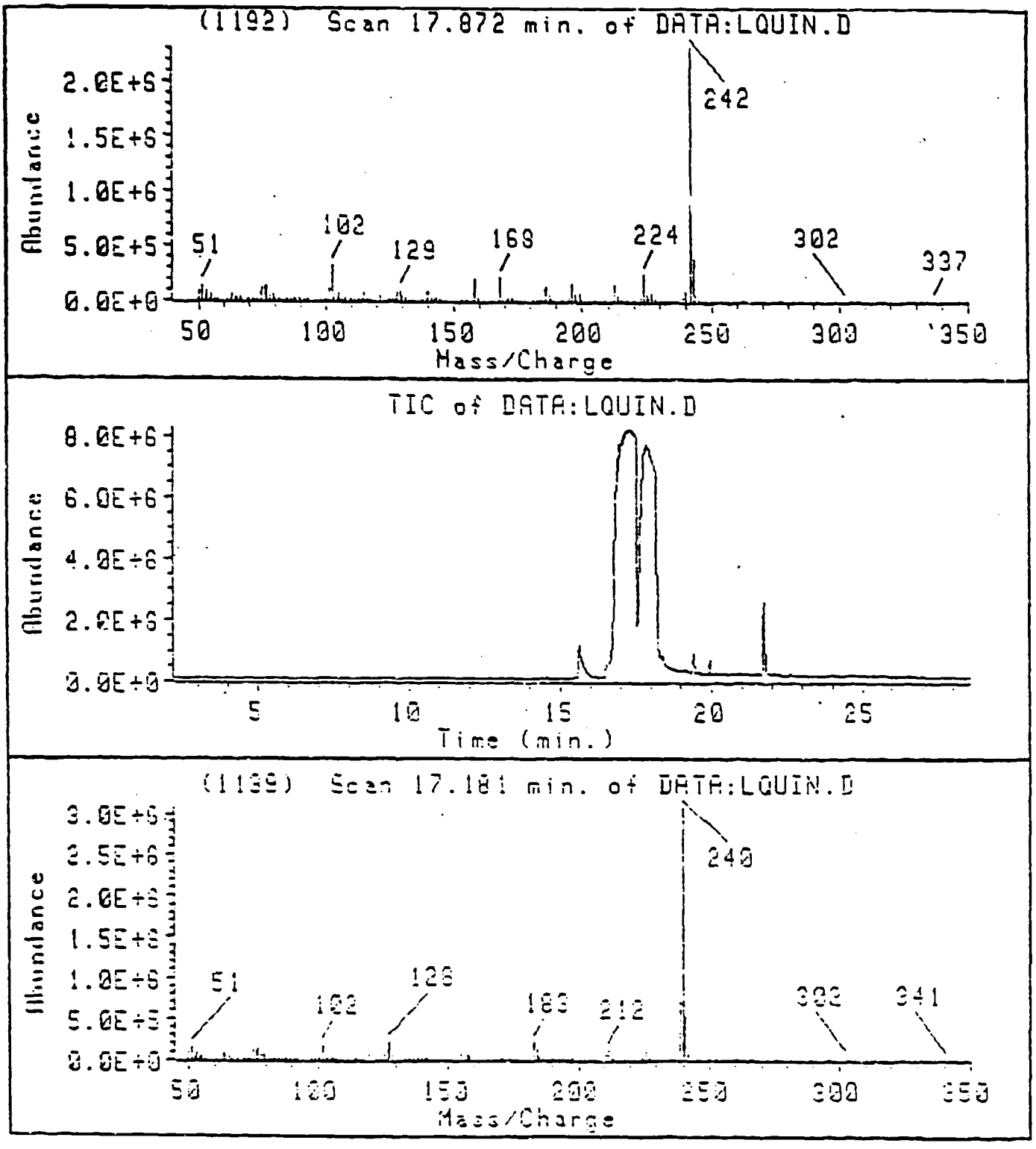
(1192) Scan 17.872 min. of DATA:LQUIN.D
Abundance
2.0E+6
1.5E+6
1.0E+6
5.0E+5
0.0E+0
242
102
51
129
168
224
302
337
50
100
150
200
250
300
350
Mass/Charge
TIC of DATA:LQUIN.D
Abundance
8.0E+6
6.0E+6
4.0E+6
2.0E+6
0.0E+0
5
10
15
20
25
Time (min.)
(1139) Scan 17.181 min. of DATA:LQUIN.D
Abundance
3.0E+6
2.5E+6
2.0E+6
1.5E+6
1.0E+6
5.0E+5
0.0E+0
240
51
126
102
183
212
302
341
50
100
150
200
250
300
350
Mass/Charge

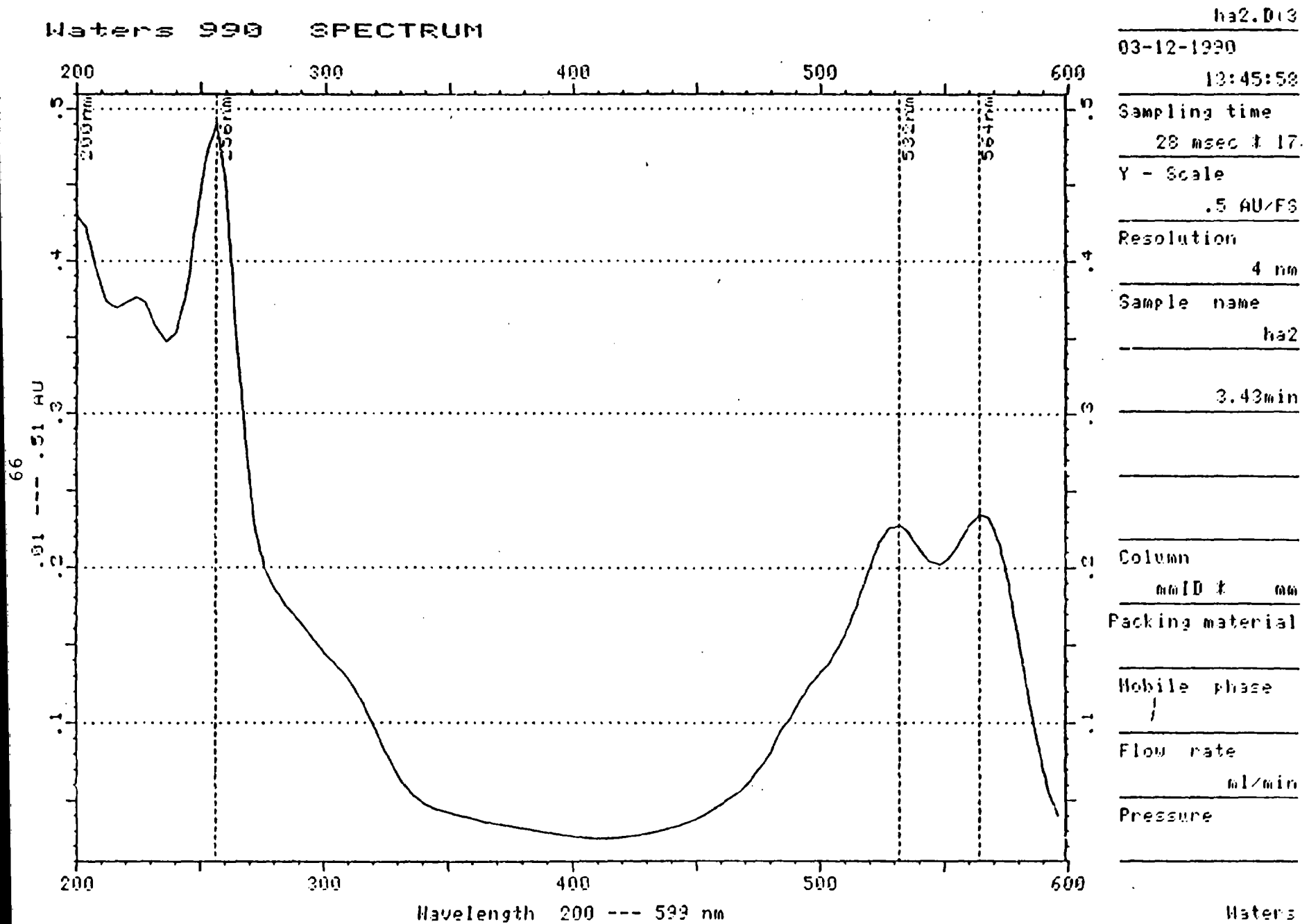
Waters 990 SPECTRUM
ha2.D03
03-12-1990
13:45:58
Sampling time
28 msec # 17
Y - Scale
.5 AU/FS
Resolution
4 nm
Sample name
ha2
3.43min
Column
mmID # mm
Packing material
Mobile phase
Flow rate
ml/min
Pressure
Waters
200
300
400
500
600
.5
.4
.3
.2
.1
0
.51 AU
.01 ---
66
Wavelength 200 --- 599 nm

Figure 7-21

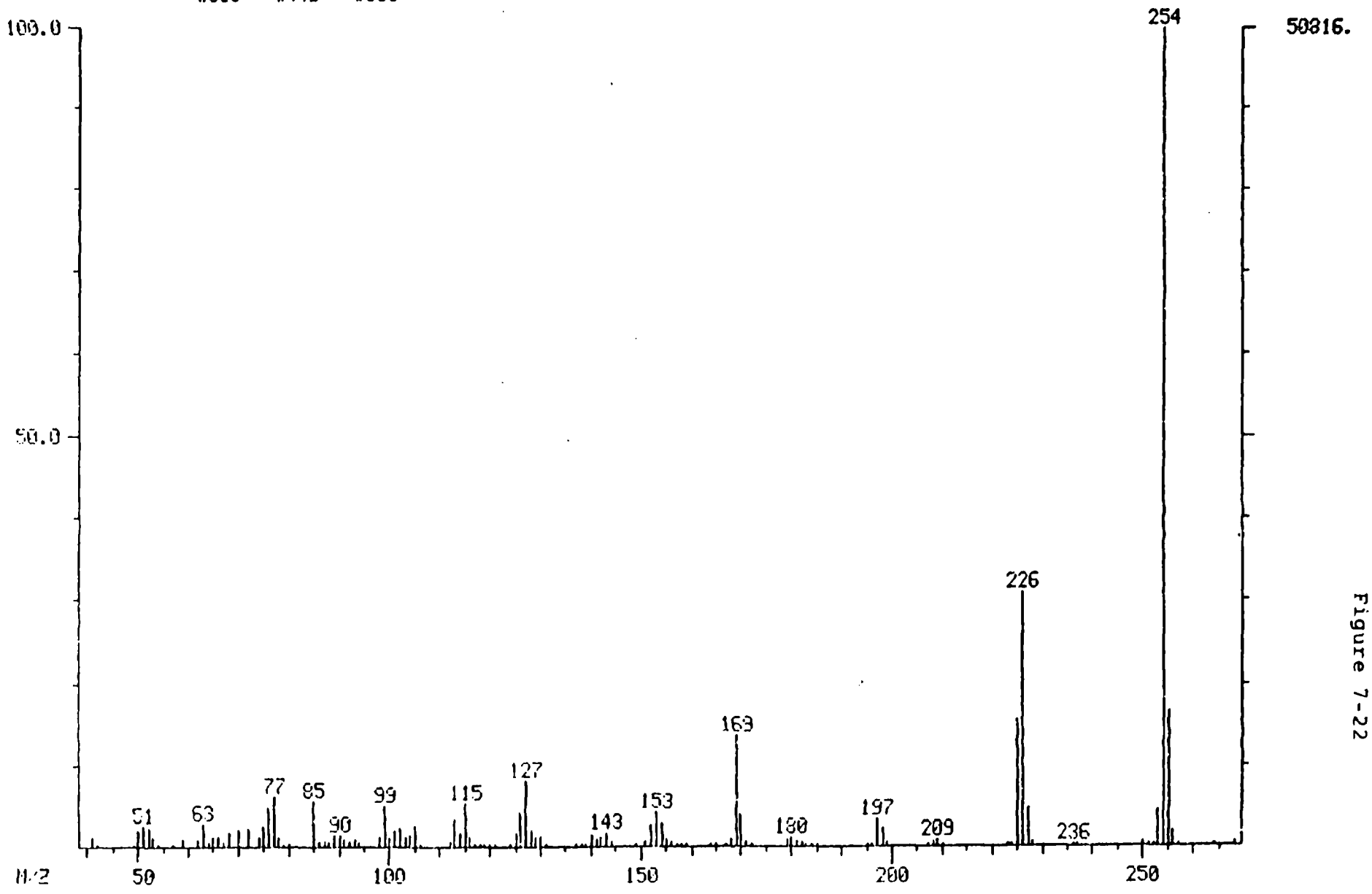
MASS SPECTRUM
09/11/90 10:09:00 + 8:50
SAMPLE: HA4-F GEO. BAUGHMAN (DIAMINOHYROXANTHRA)
CONDS.: EI/PROBE
GC TEMP: 284 DEG. C
#530 - #443 - #603
DATA: HA4F #530
CALI: C911 #3
BASE M/Z: 254
RIC: 169728.
100.0
50.0
100
50816.
254
226
163
127
77
85
99
115
153
51
63
90
143
180
197
209
236
M/Z
50
100
150
200
250

Figure 7-22

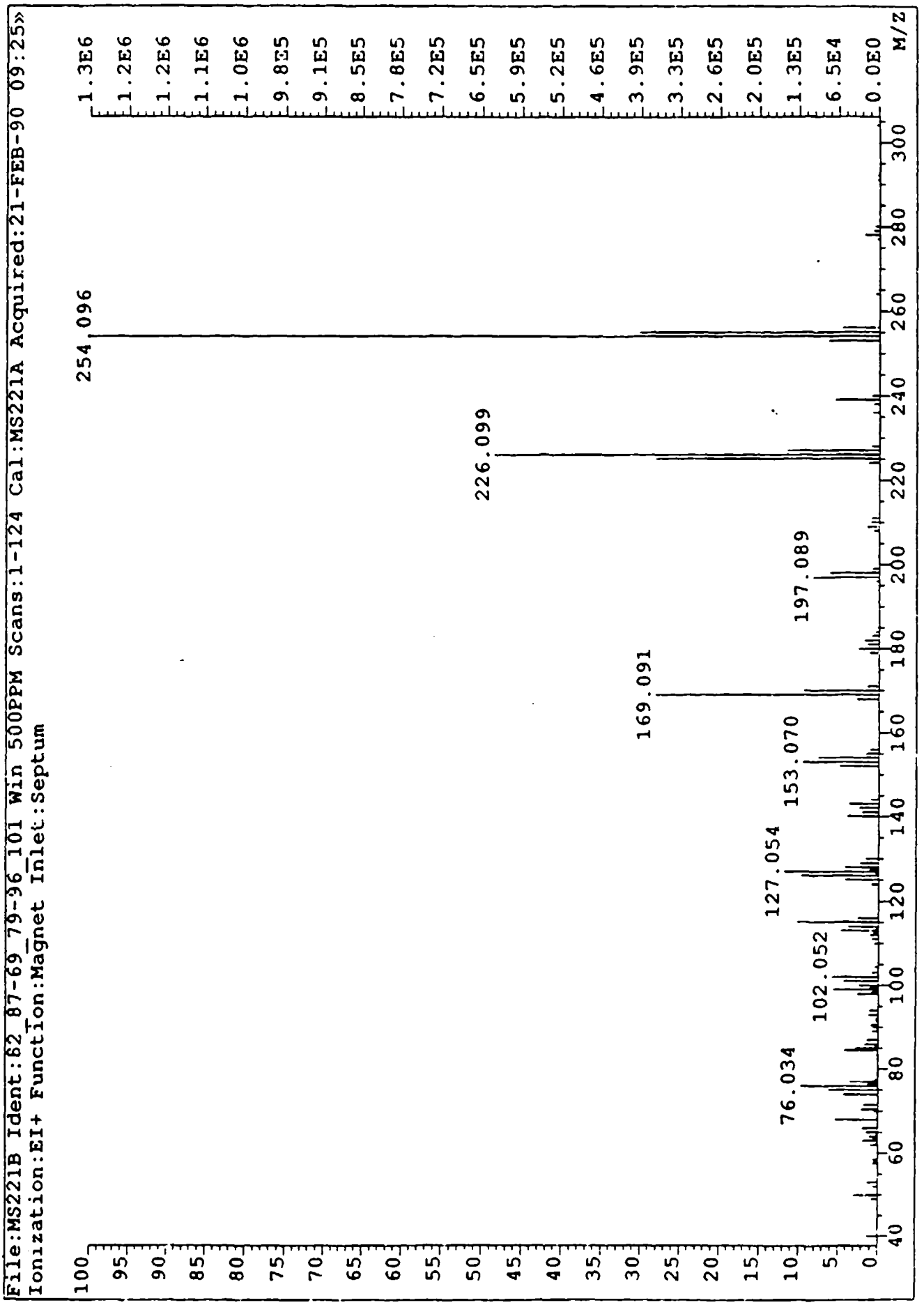
File:MS221B Ident:62_87-69_79-96_101 Win 500PPM Scans:1-124 Cal:MS221A Acquired:21-FEB-90 09:25»
Ionization:EI+ Function:Magnet Inlet:Septum
254.096
226.099
197.089
169.091
153.070
127.054
102.052
76.034
M/Z

Figure 7-24

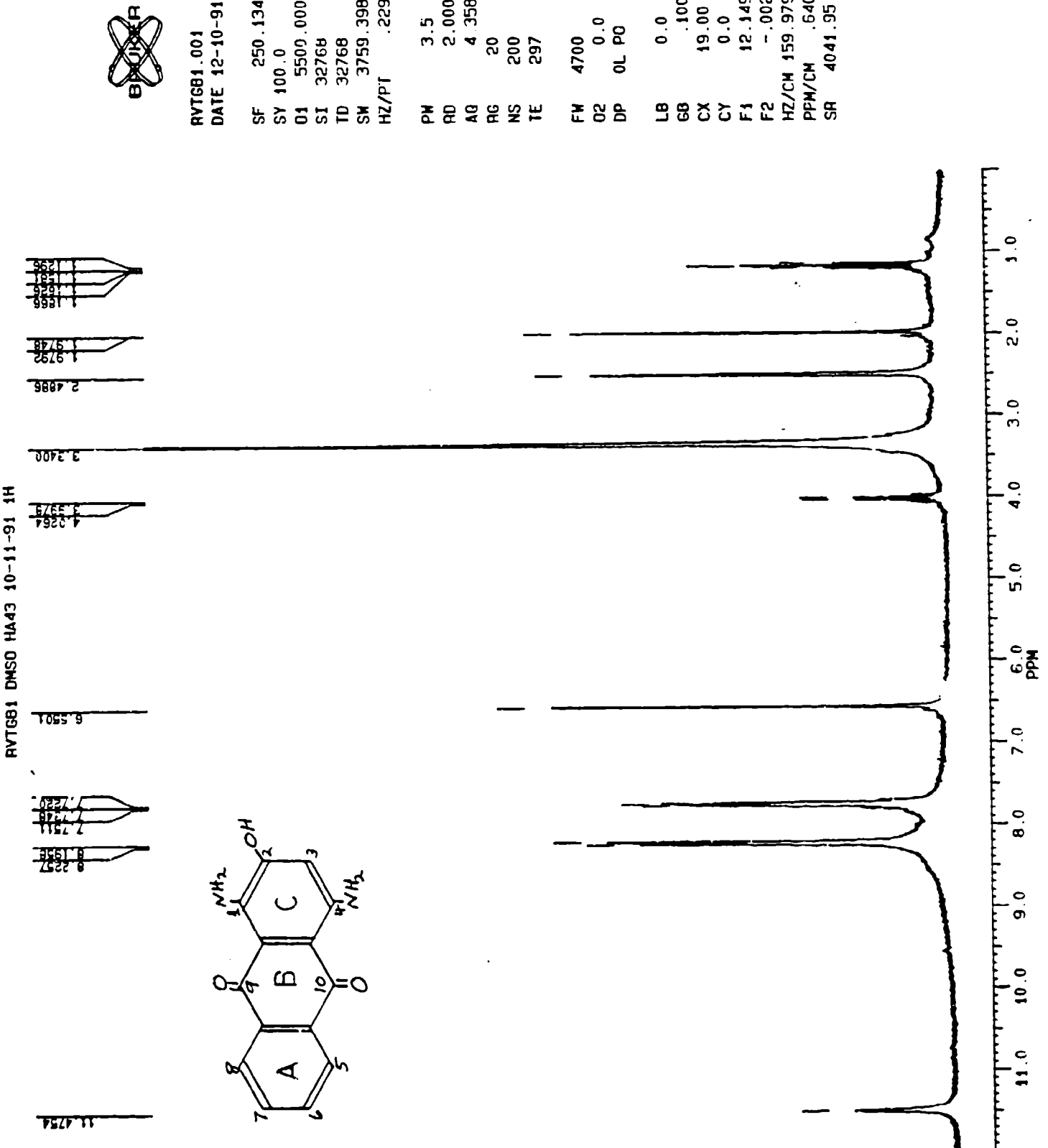
RVTGB1.001
DATE 12-10-91
SF 250.134
SY 100.0
O1 5500.000
SI 32768
TD 32768
SW 3759.398
HZ/PT .229
PW 3.5
RD 2.000
AQ 4.358
RG 20
NS 200
TE 297
FW 4700
O2 0.0
DP OL PO
LB 0.0
GB .100
CX 19.00
CY 0.0
F1 12.149P
F2 -.002P
HZ/CM 159.979
PPM/CM .640
SR 4041.95
RVTGB1 DMSO HA43 10-11-91 1H
PPM

Figure 7-25

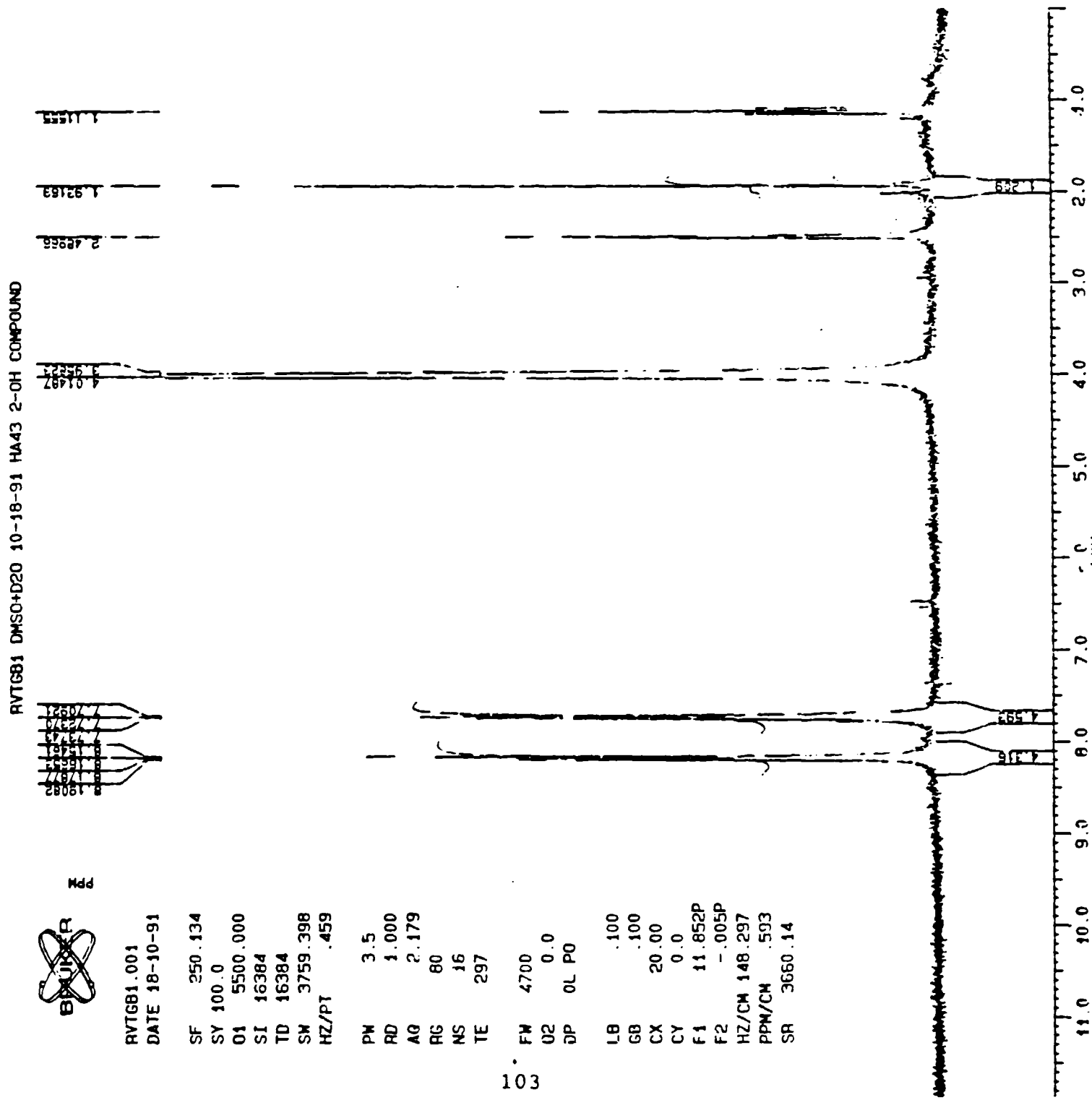
RVTGB1 DMSO+D20 10-18-91 HA43 2-OH COMPOUND
PPM
BRUKER
RVTGB1.001
DATE 18-10-91
SF 250.134
SY 100.0
O1 5500.000
SI 16384
TD 16384
SW 3759.398
HZ/PT .459
PW 3.5
RD 1.000
AQ 2.179
RG 80
NS 16
TE 297
FW 4700
U2 0.0
DP OL PO
LB .100
GB .100
CX 20.00
CY 0.0
F1 11.852P
F2 -.005P
HZ/CM 148.297
PPM/CM .593
SR 3660.14

Figure 7-26

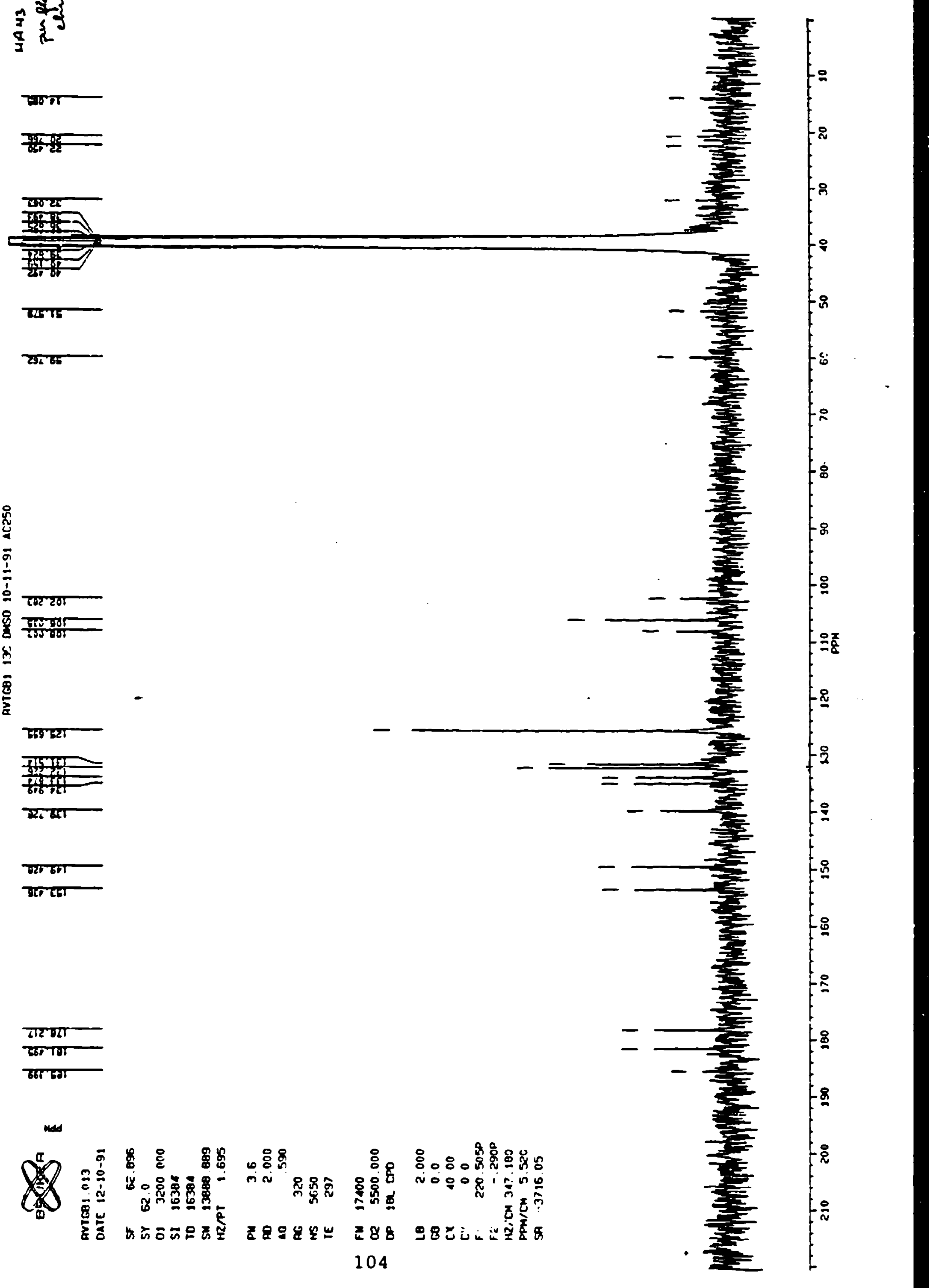
RVTGB1 13C DMSO 10-11-91 AC250
185.199
181.493
178.217
153.438
149.428
139.728
125.695
102.283
59.762
51.578
32.063
22.450
20.766
14.089
PPM
RVTGB1.013
DATE 12-10-91
SF 62.896
SY 62.0
O1 3200.000
SI 16384
TD 16384
SW 13888.889
HZ/PT 1.695
PW 3.6
RD 2.000
AQ .590
RG 320
NS 5650
TE 297
FW 17400
O2 5500.000
DP 18L CPD
LB 2.000
GB 0.0
CX 40.00
CY 0.0
F1 220.505P
F2 -.290P
HZ/CM 347.180
PPM/CM 5.520
SR -3716.05

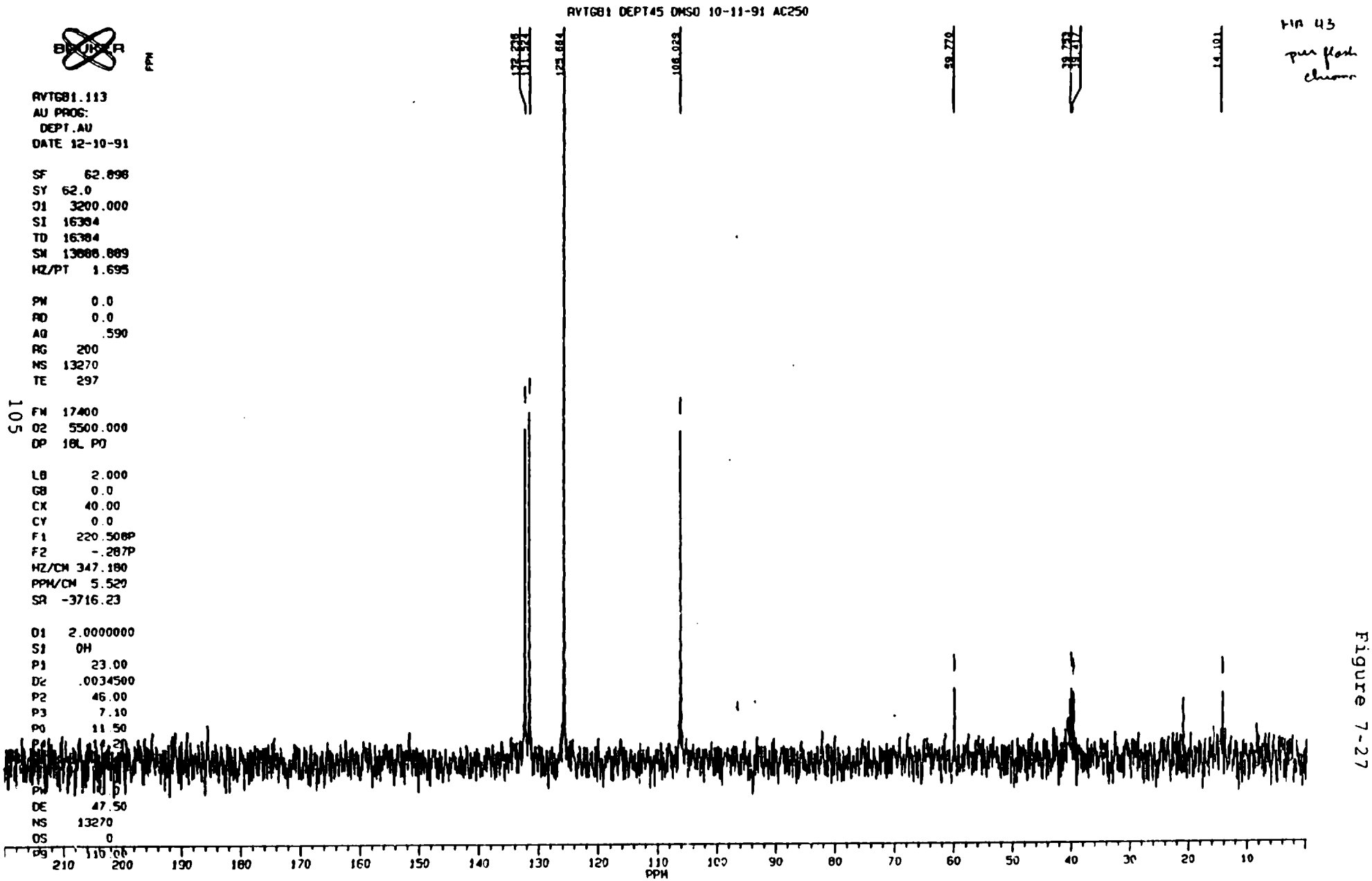

105

Figure 7-27

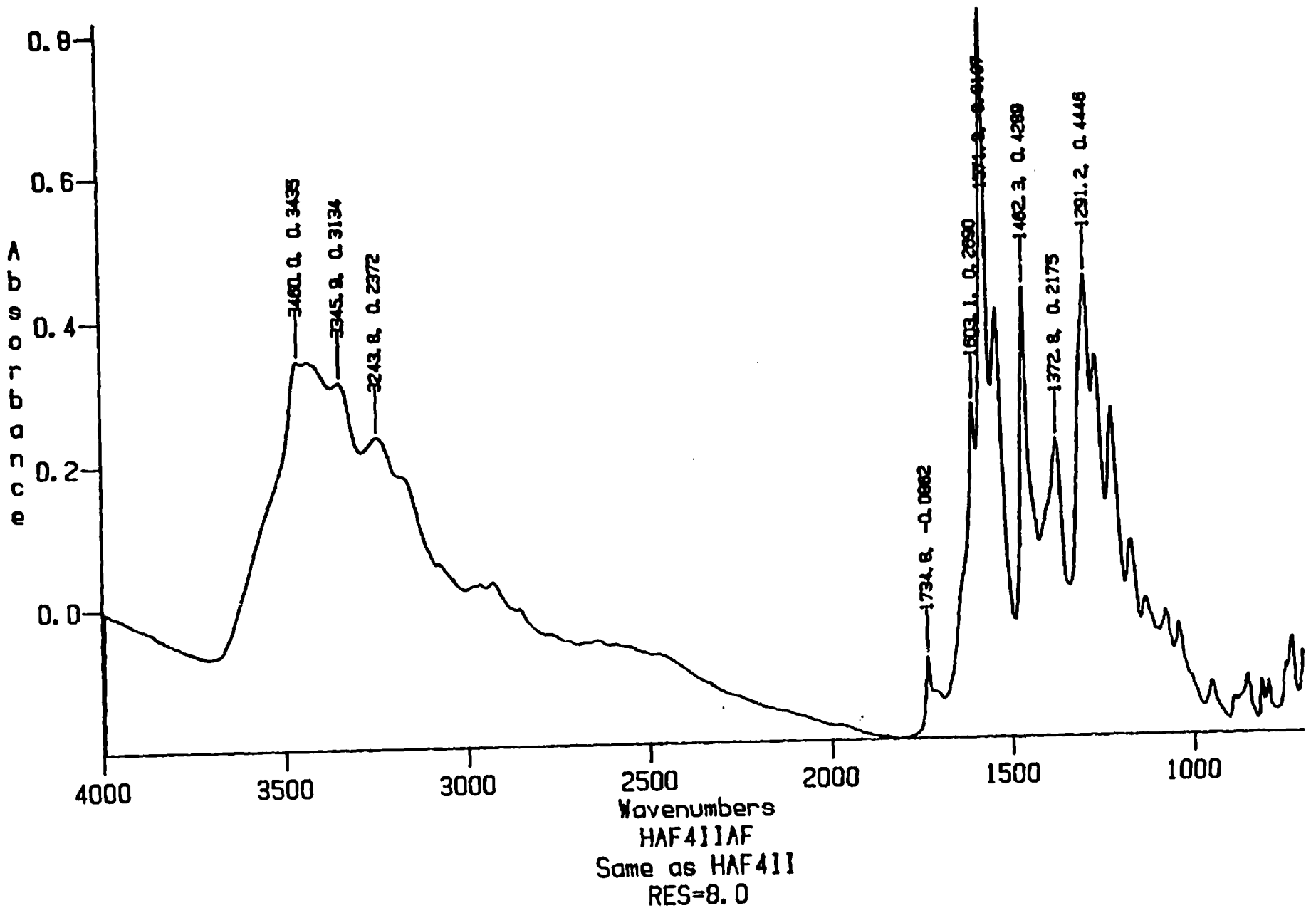
0.8
0.6
0.4
0.2
0.0
Absorbance
3460.0, 0.3435
3345.9, 0.3134
3243.8, 0.2372
1734.8, -0.0862
1603.1, 0.2690
1462.3, 0.4289
1372.8, 0.2175
1291.2, 0.4446
4000
3500
3000
2500
2000
1500
1000
Wavenumbers
HAF411AF
Same as HAF411
RES=8.0

Figure 7-26

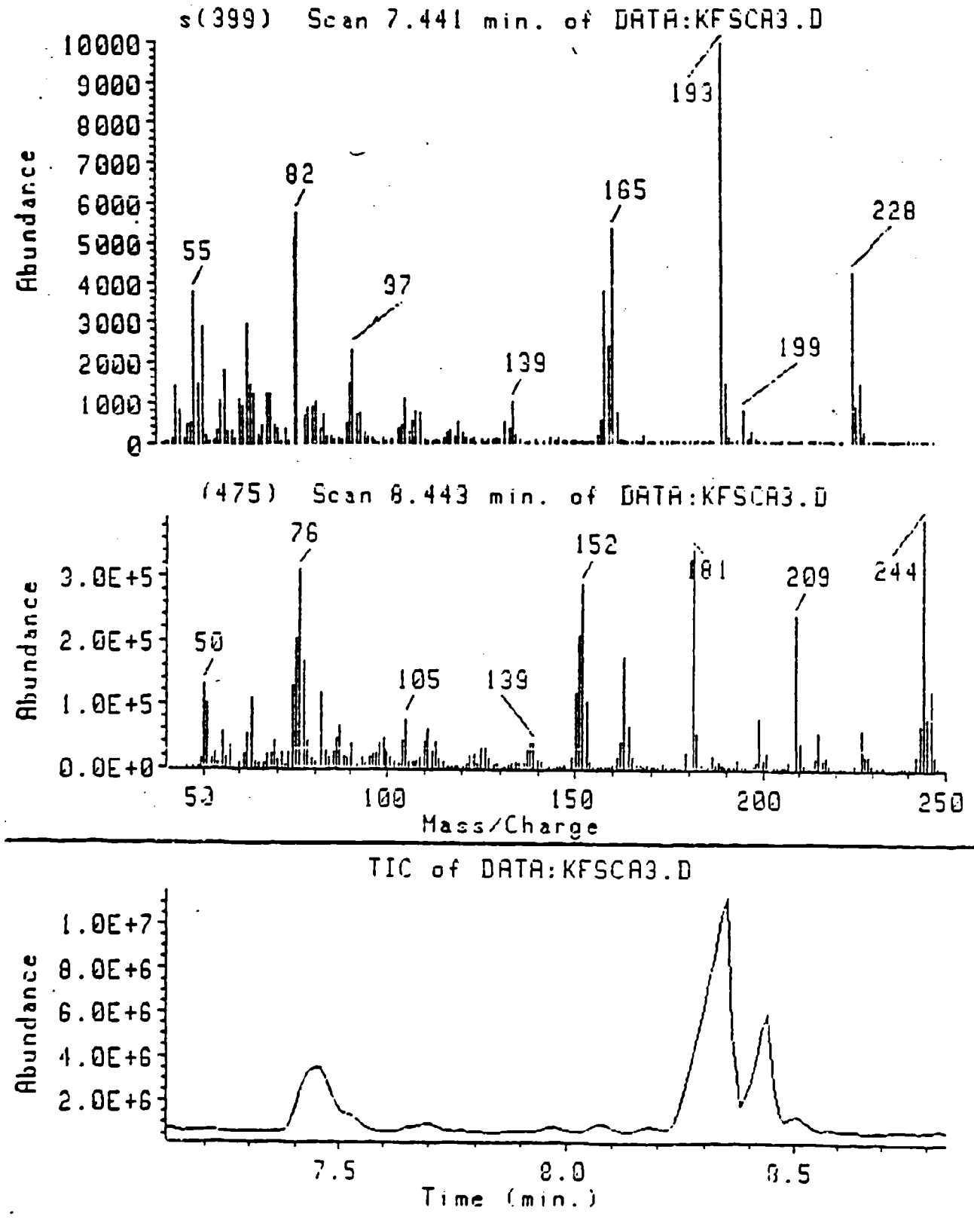
s(399) Scan 7.441 min. of DATA:KFSCA3.D
Abundance
10000
9000
8000
7000
6000
5000
4000
3000
2000
1000
0
55
82
97
139
165
193
199
228
(475) Scan 8.443 min. of DATA:KFSCA3.D
Abundance
3.0E+5
2.0E+5
1.0E+5
0.0E+0
50
76
105
139
152
181
209
244
50
100
150
200
250
Mass/Charge
TIC of DATA:KFSCA3.D
Abundance
1.0E+7
8.0E+6
6.0E+6
4.0E+6
2.0E+6
7.5
8.0
8.5
Time (min.)

Figure 7-30

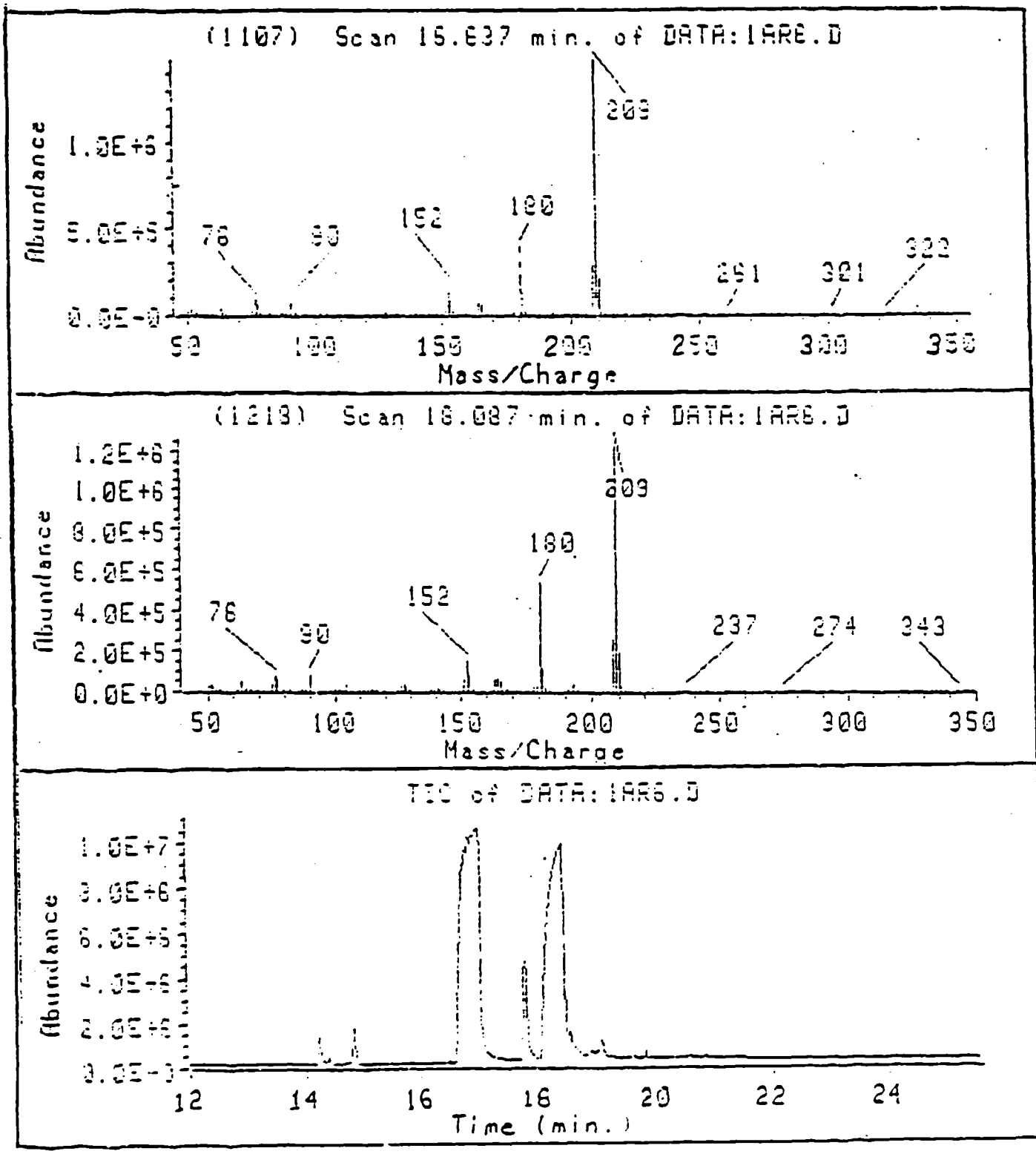
(1107) Scan 15.637 min. of DATA:1AR6.D
Abundance
1.0E+6
5.0E+5
0.0E-0
76
90
152
180
209
291
301
322
50
100
150
200
250
300
350
Mass/Charge
(1218) Scan 18.087 min. of DATA:1AR6.D
Abundance
1.2E+6
1.0E+6
8.0E+5
6.0E+5
4.0E+5
2.0E+5
0.0E+0
76
90
152
180
209
237
274
343
50
100
150
200
250
300
350
Mass/Charge
TIC of DATA:1AR6.D
Abundance
1.0E+7
12
14
16
18
20
22
24
Time (min.)

Figure 7-31

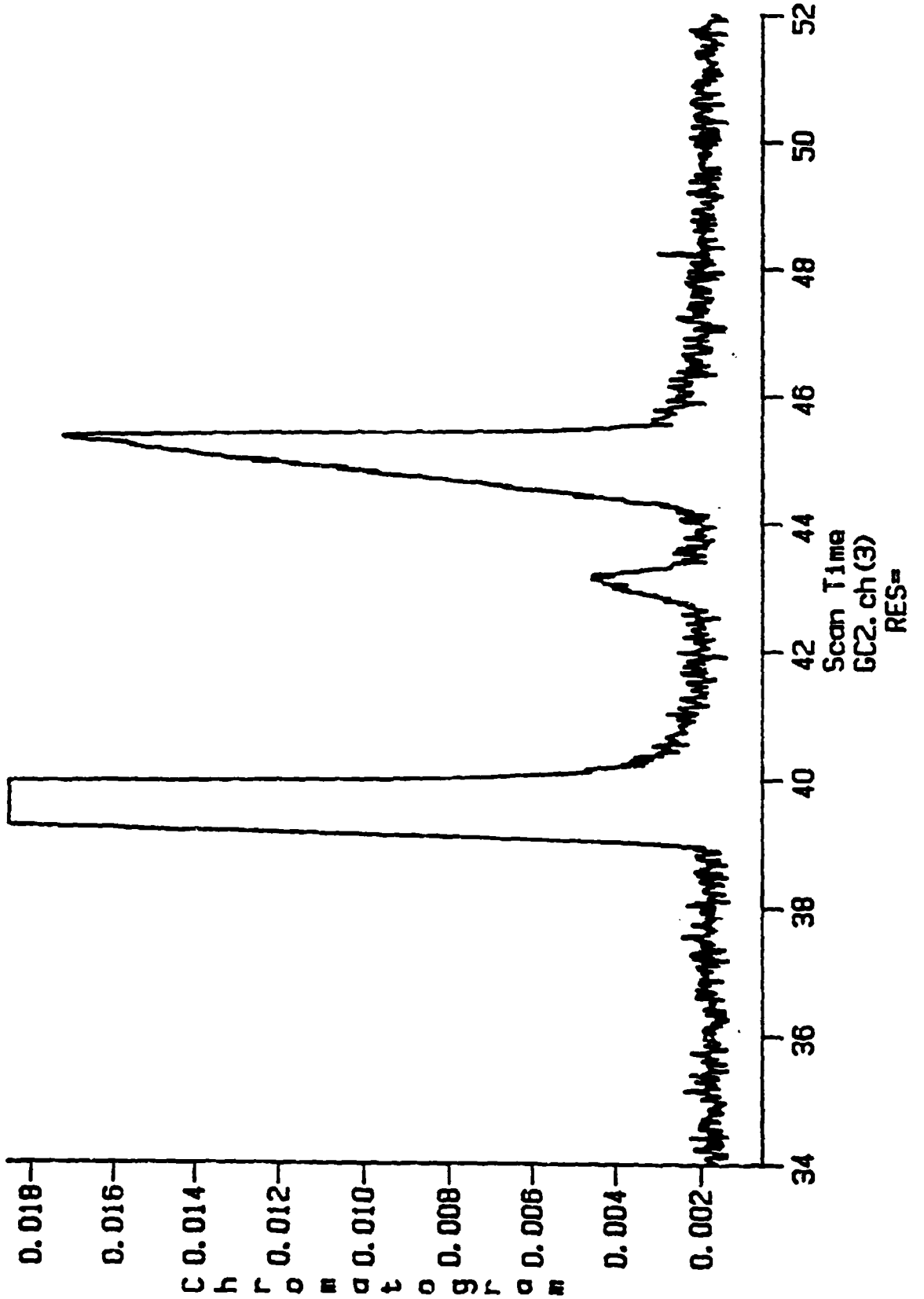
0.018
0.016
0.014
0.012
0.010
0.008
0.006
0.004
0.002
Chromatogram
34
36
38
40
42
44
46
48
50
52
Scan Time
GC2.ch(3)
RES=

Figure 7-32

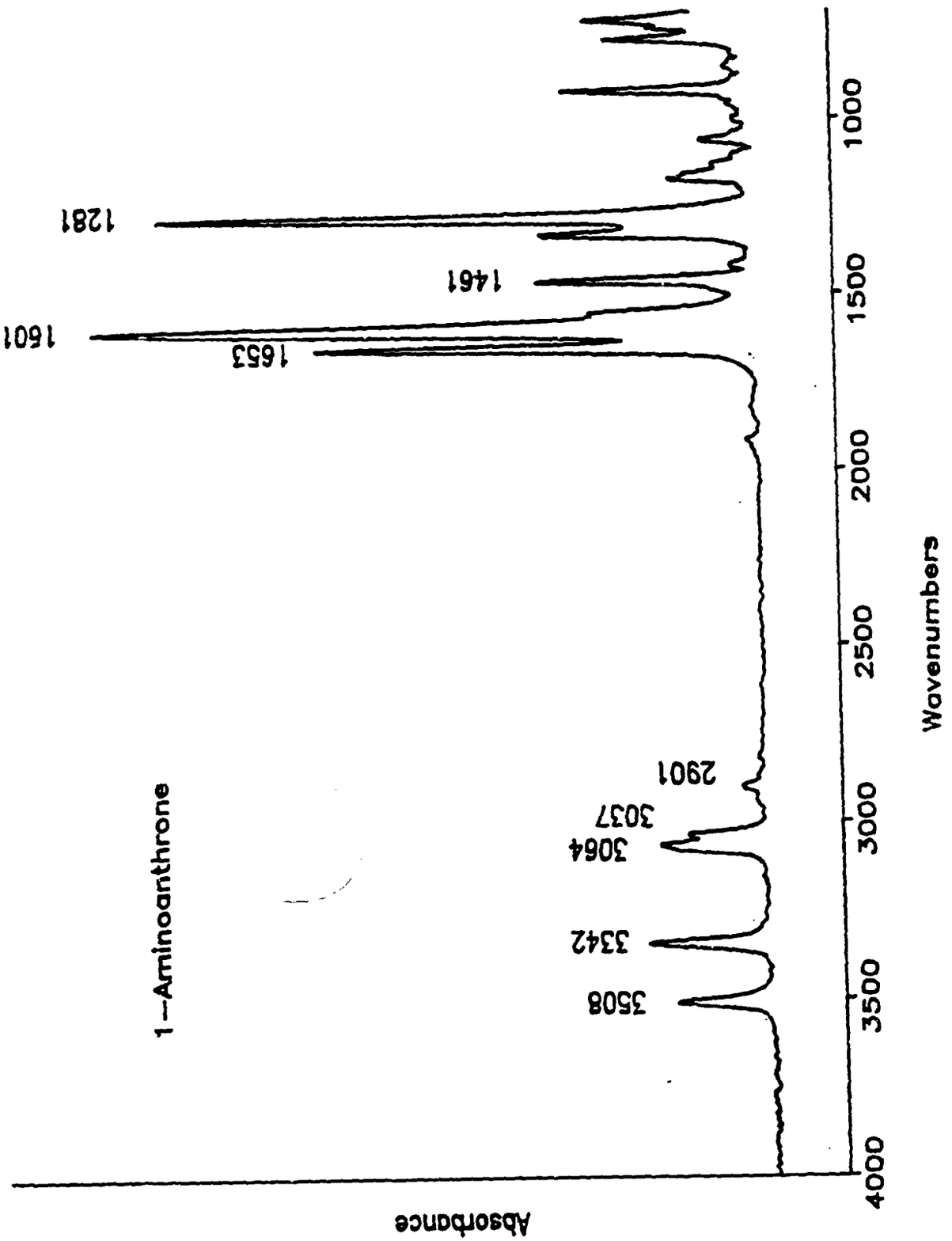
1-Aminoanthrone
Absorbance
Wavenumbers
4000
3500
3000
2500
2000
1500
1000
3508
3342
3064
3037
2901
1653
1601
1461
1281

Figure 7-33

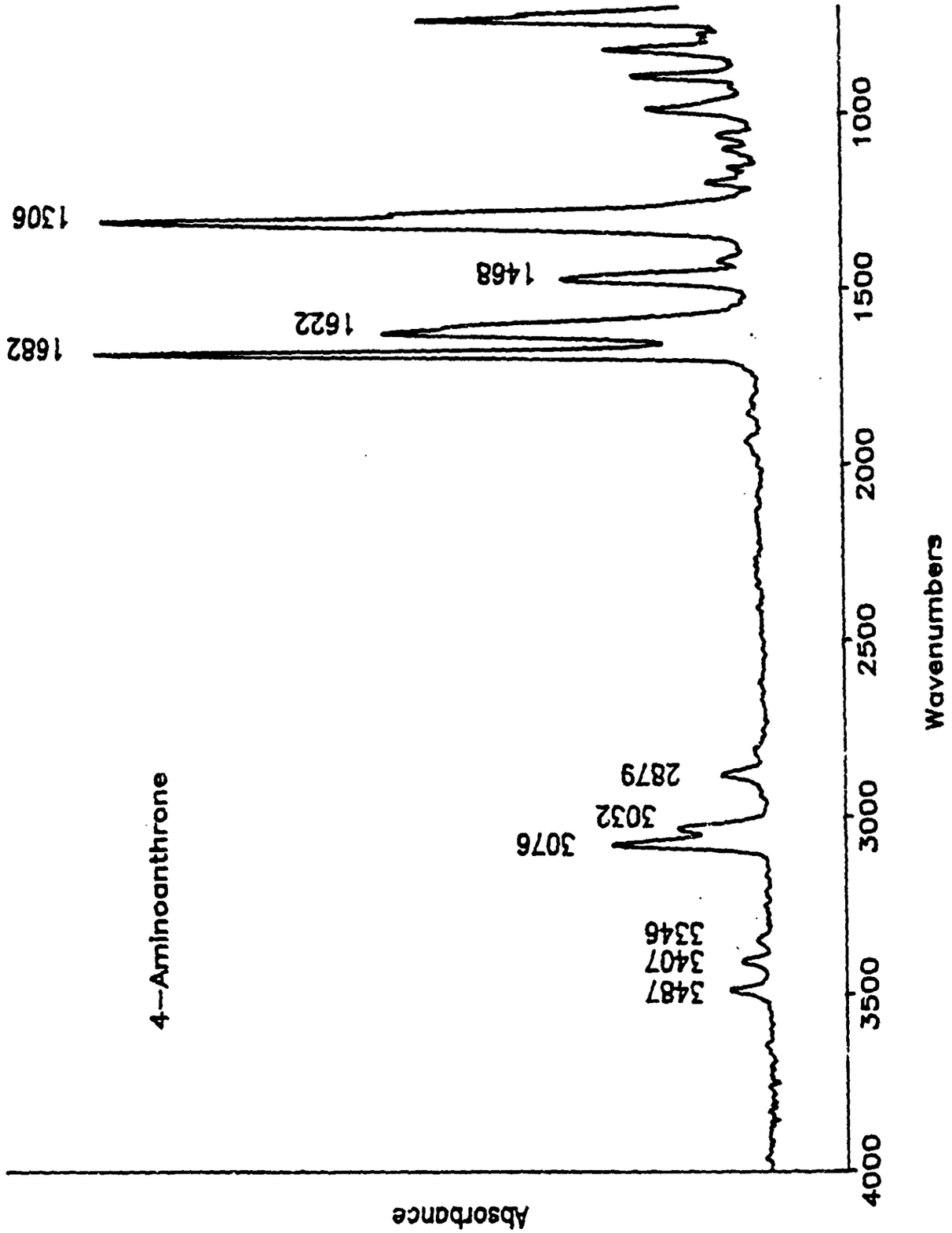
4—Aminoanthrone
Absorbance
Wavenumbers
4000
3500
3000
2500
2000
1500
1000
3487
3407
3346
3076
3032
2879
1682
1622
1468
1306

Figure 7-34

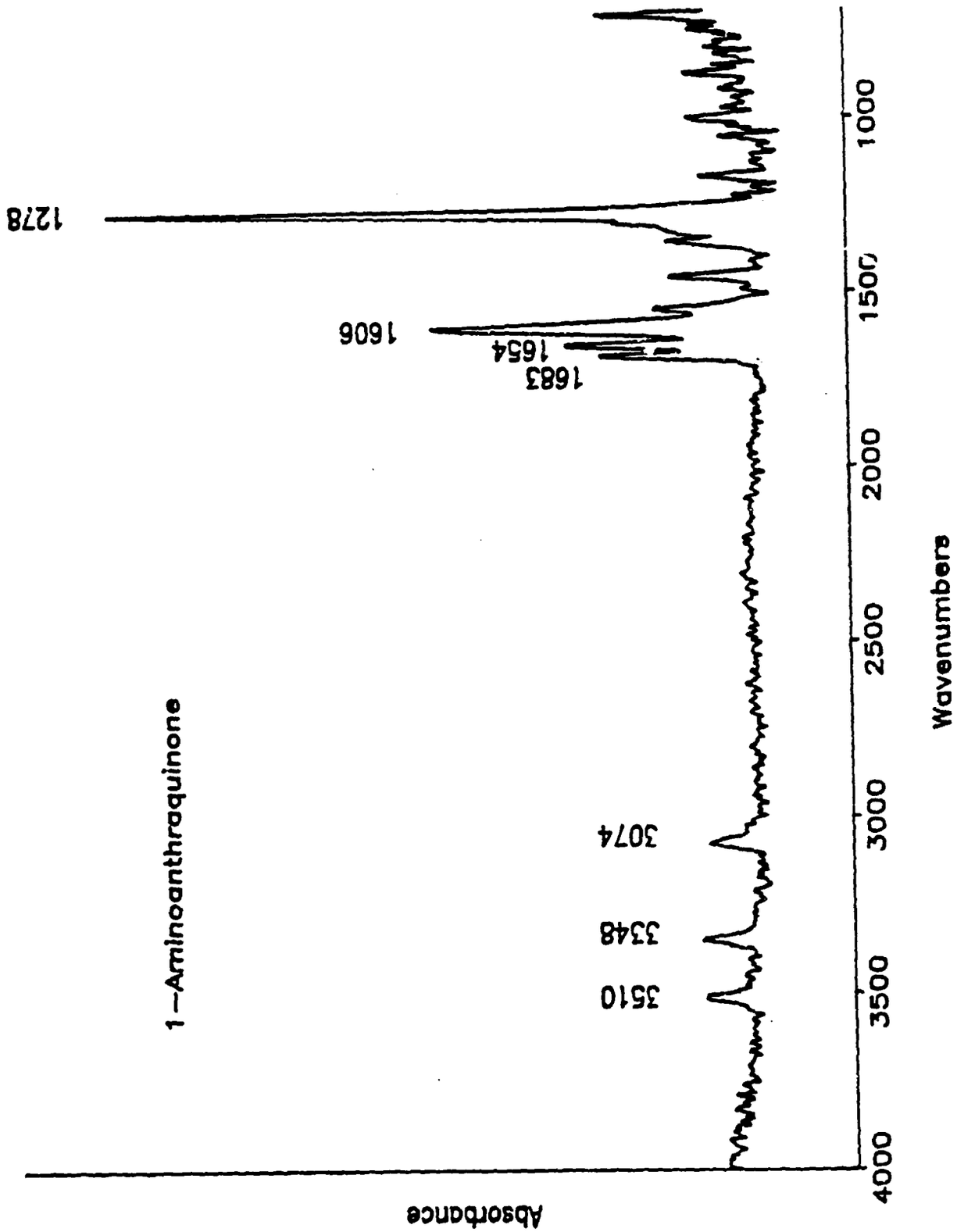
1—Aminoanthraquinone
Absorbance
Wavenumbers
4000
3500
3000
2500
2000
1500
1000
3510
3348
3074
1683
1654
1606
1278

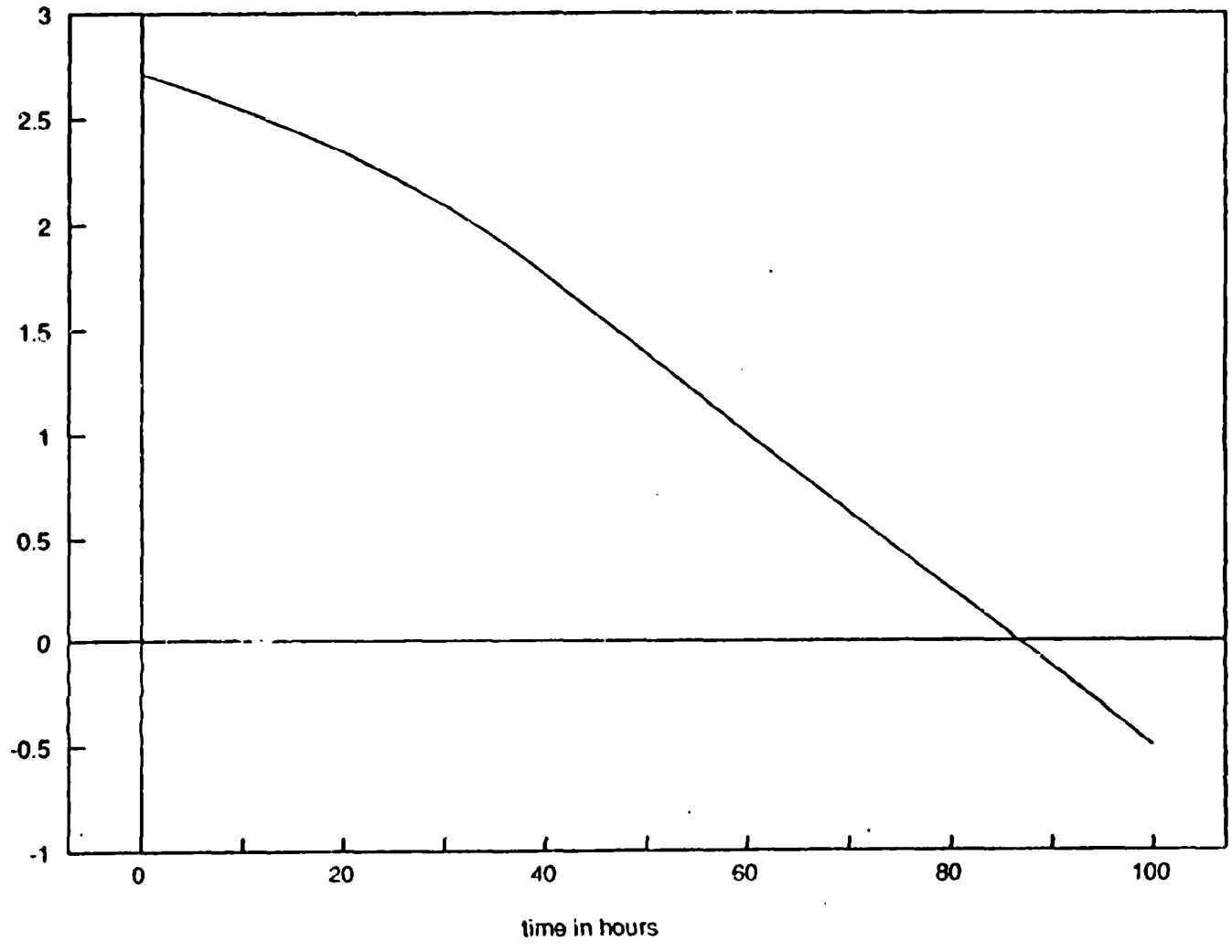
ln Ct vs time
3
2.5
2
1.5
1
0.5
0
-0.5
-1
ln Ct
0
20
40
60
80
100
time in hours

Figure 7-35

Figure 7-36

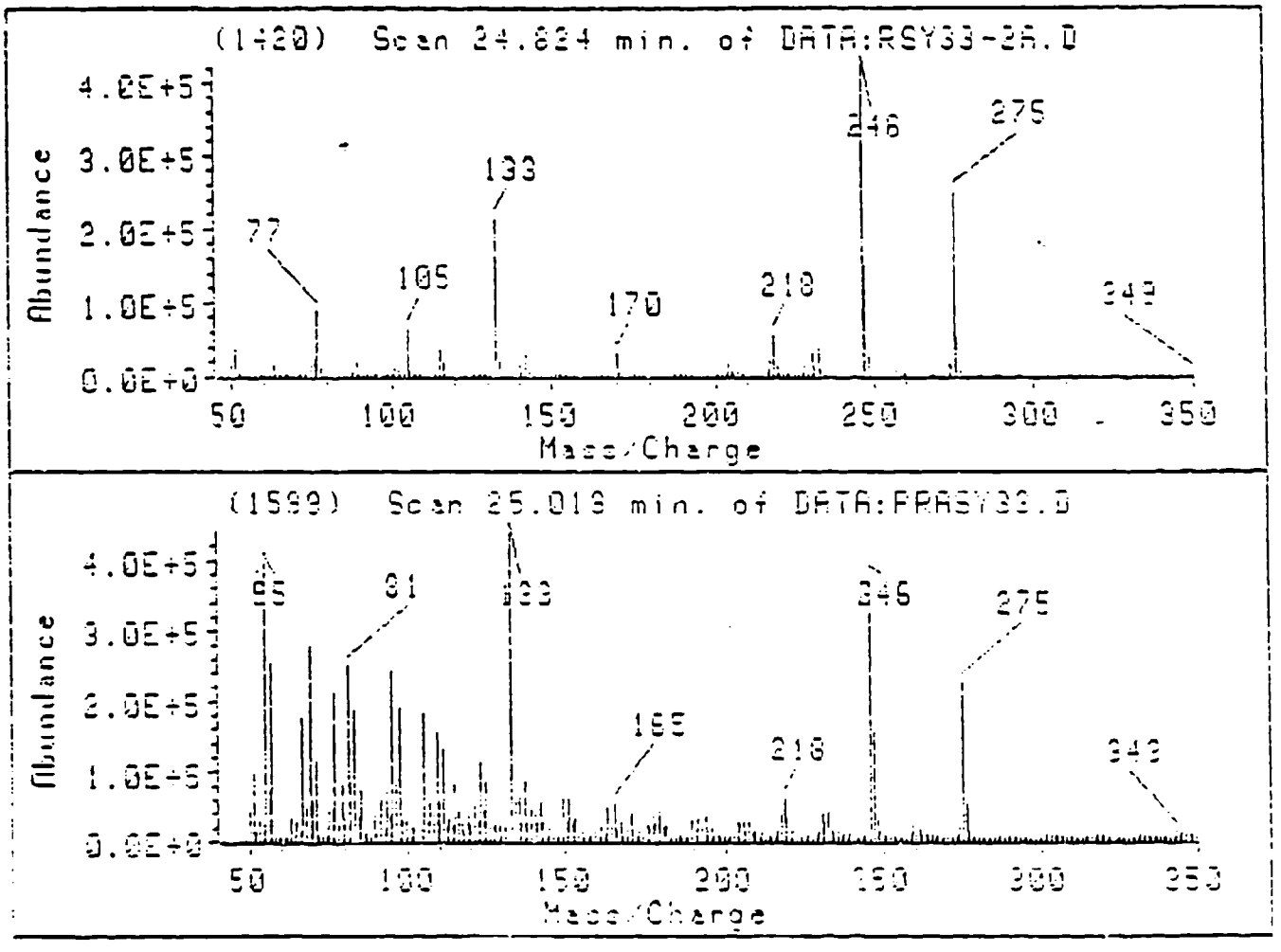
(1+20) Scan 24.824 min. of DATA:RSY33-2A.D
Abundance
4.0E+5
3.0E+5
2.0E+5
1.0E+5
0.0E+0
77
105
133
170
218
246
275
349
50
100
150
200
250
300
350
Mass/Charge
(1599) Scan 25.019 min. of DATA:PRRSY33.D
Abundance
4.0E+5
3.0E+5
2.0E+5
1.0E+5
0.0E+0
65
81
133
195
218
246
275
349
50
100
150
200
250
300
350
Mass/Charge

Figure 7-37

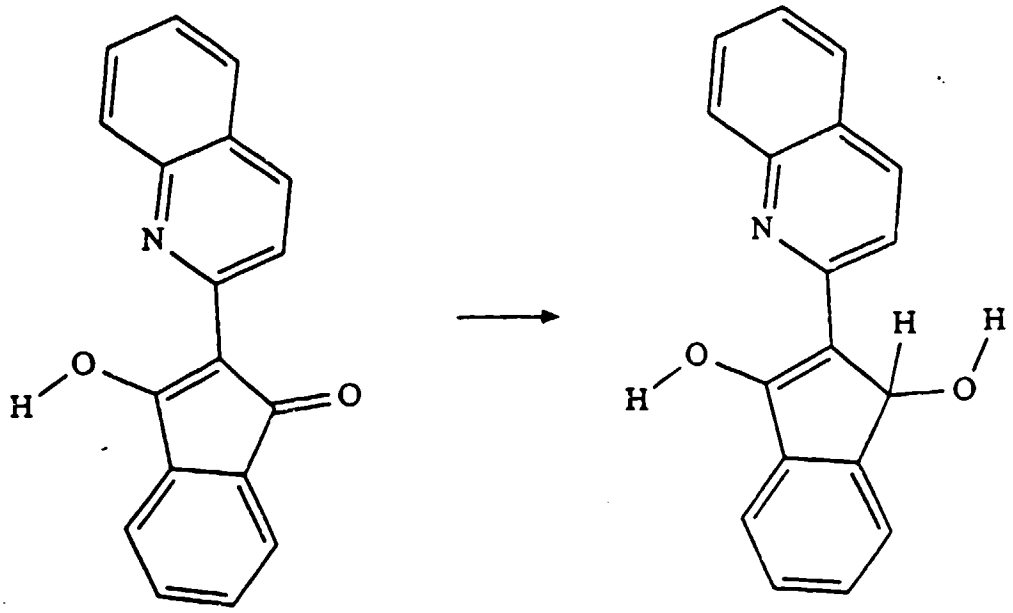

Solvent Yellow 33
MW 273

Proposed Product
MW 275

Figure 7-38

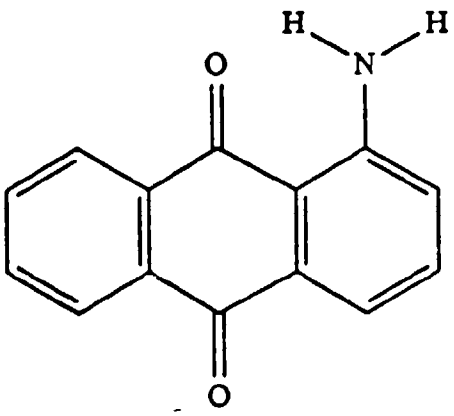

MW 223

1-aminoanthraquinone

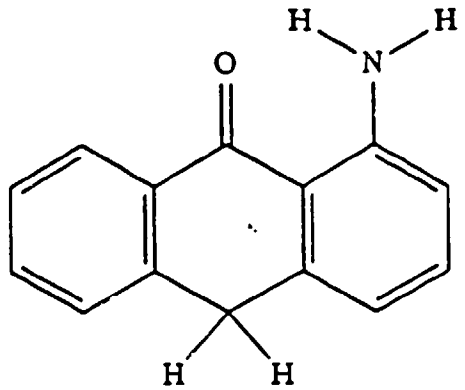

MW 219

+

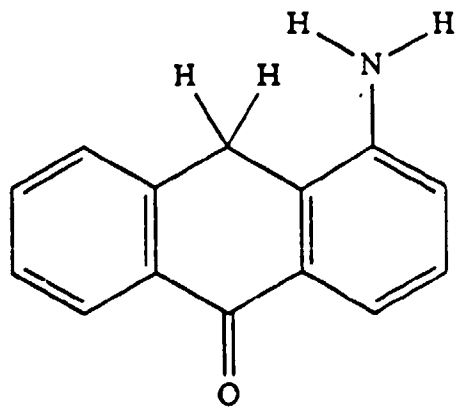

MW 219

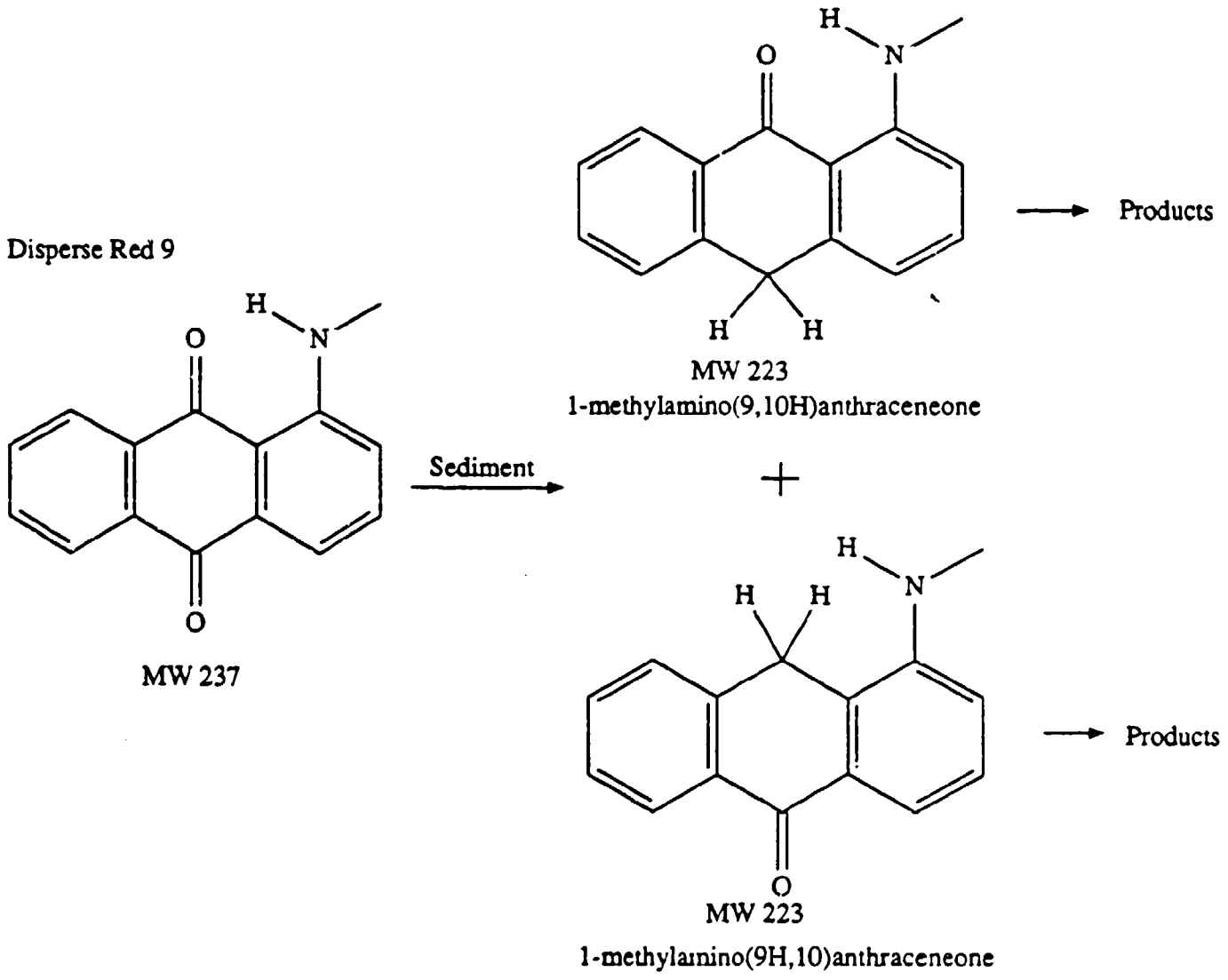
Disperse Red 9
MW 237
Sediment
MW 223
1-methylamino(9,10H)anthraceneone
Products
MW 223
1-methylamino(9H,10)anthraceneone
Products

Figure 7-40

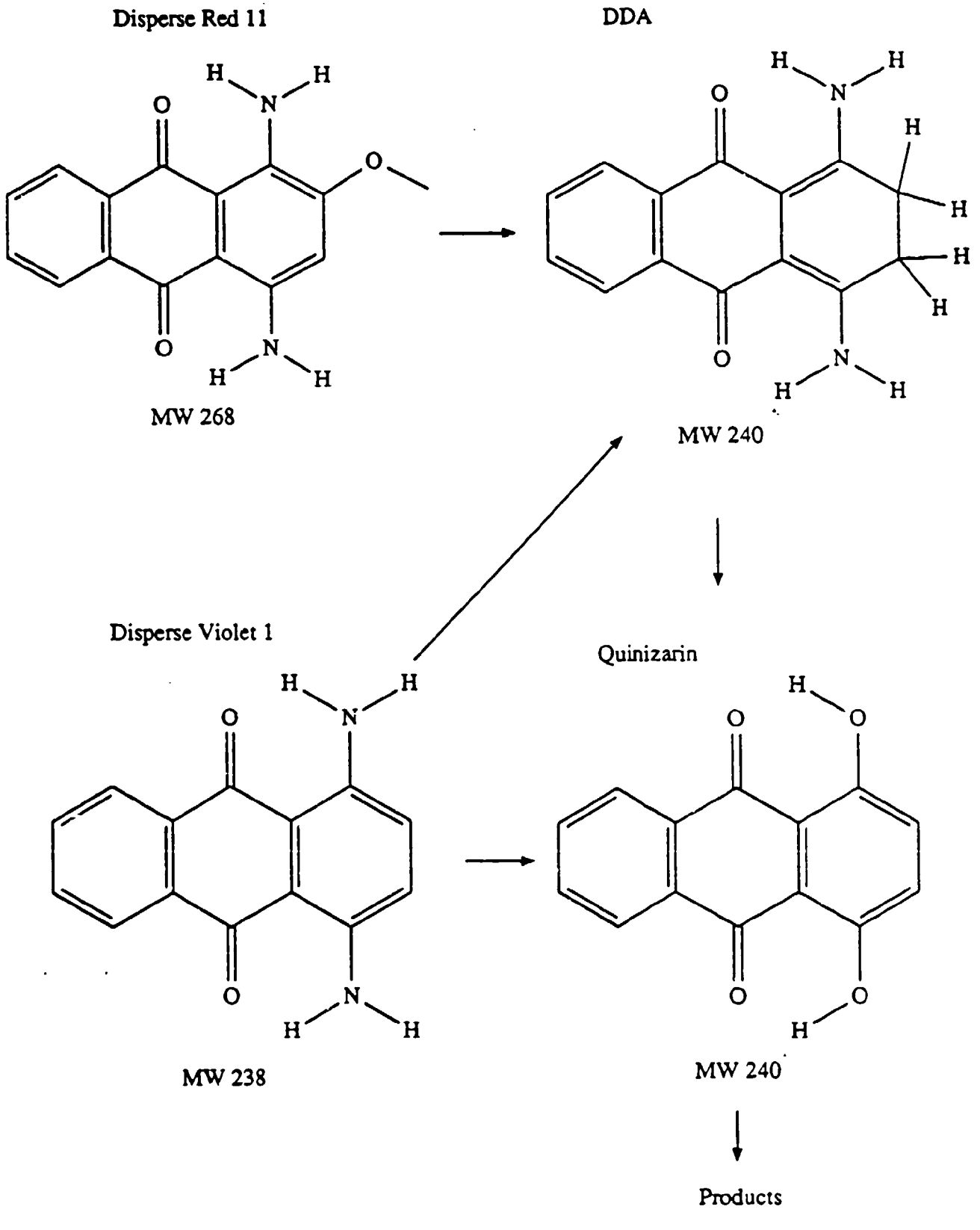
Disperse Red 11
DDA
MW 268
MW 240
Disperse Violet 1
Quinizarin
MW 238
MW 240
Products

Figure 7-41

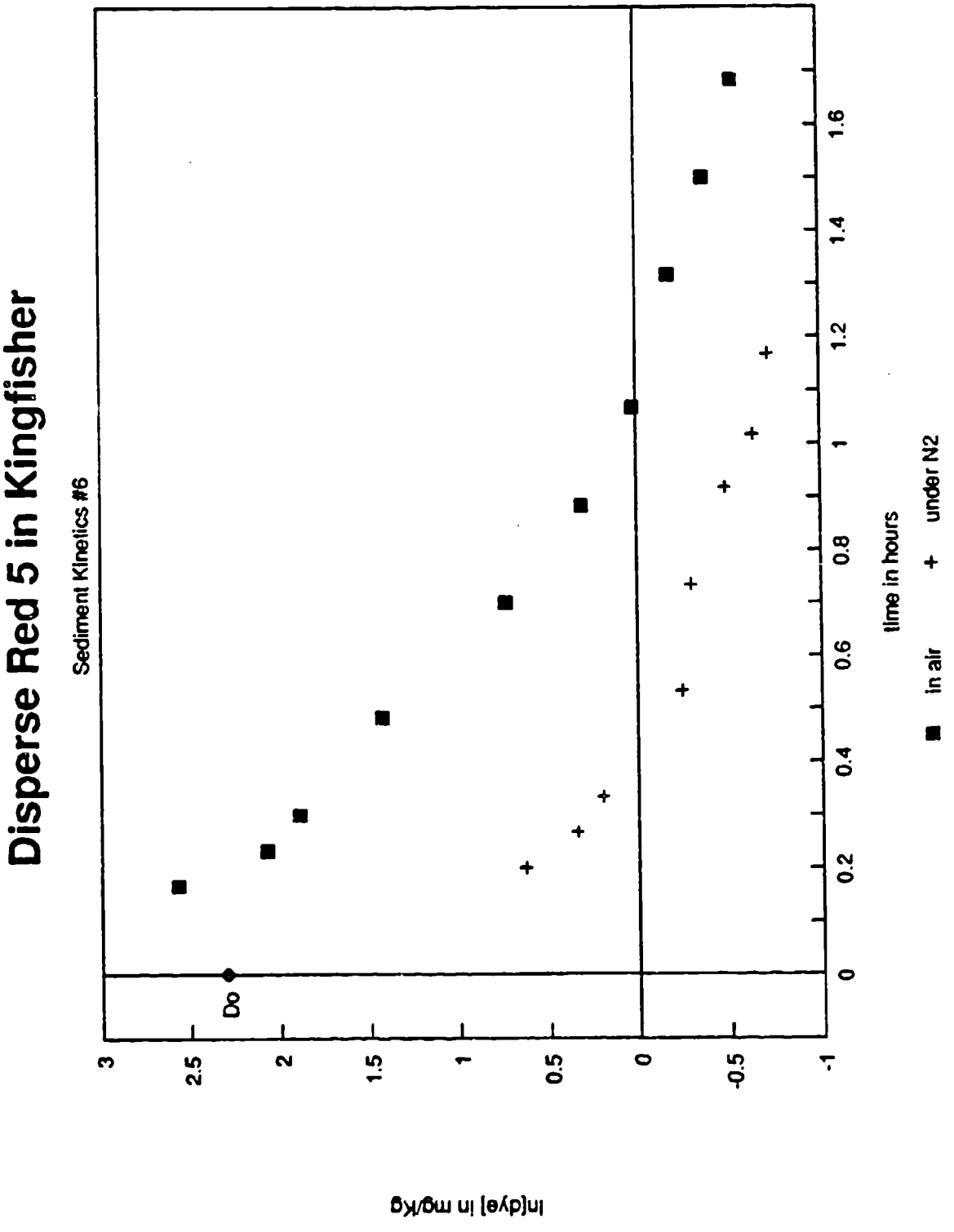
Disperse Red 5 in Kingfisher
Sediment Kinetics #6
Do
3
2.5
2
1.5
1
0.5
0
-0.5
-1
0
0.2
0.4
0.6
0.8
1
1.2
1.4
1.6
ln[dye] in mg/kg
time in hours
in air
under N2

Figure 7-42

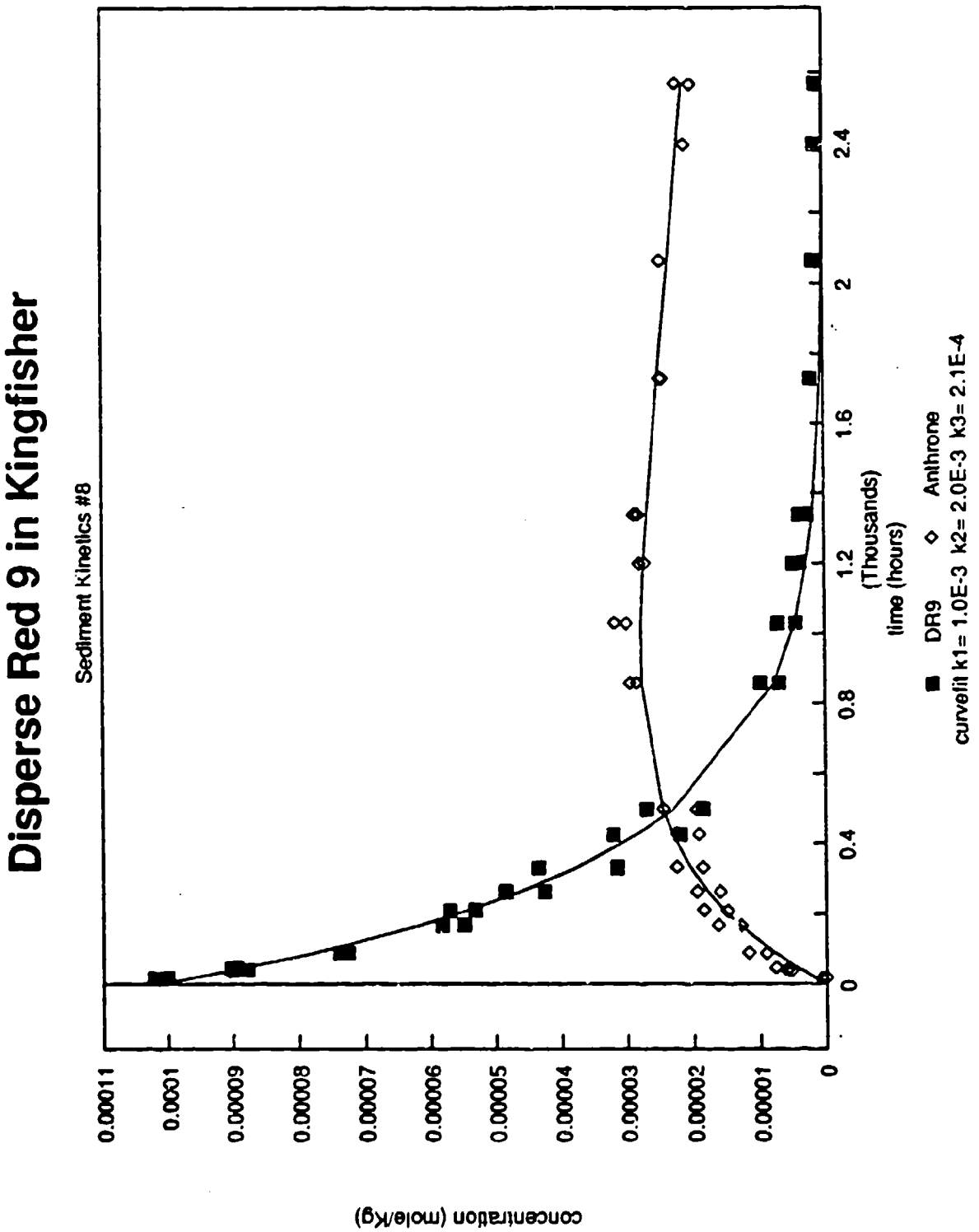
Disperse Red 9 in Kingfisher
Sediment Kinetics #8
concentration (mole/kg)
0.00011
0.0001
0.00009
0.00008
0.00007
0.00006
0.00005
0.00004
0.00003
0.00002
0.00001
0
0
0.4
0.8
1.2
1.6
2
2.4
(Thousands)
time (hours)
DR9
Anthrone
curvefit k1= 1.0E-3 k2= 2.0E-3 k3= 2.1E-4

Figure 7-43

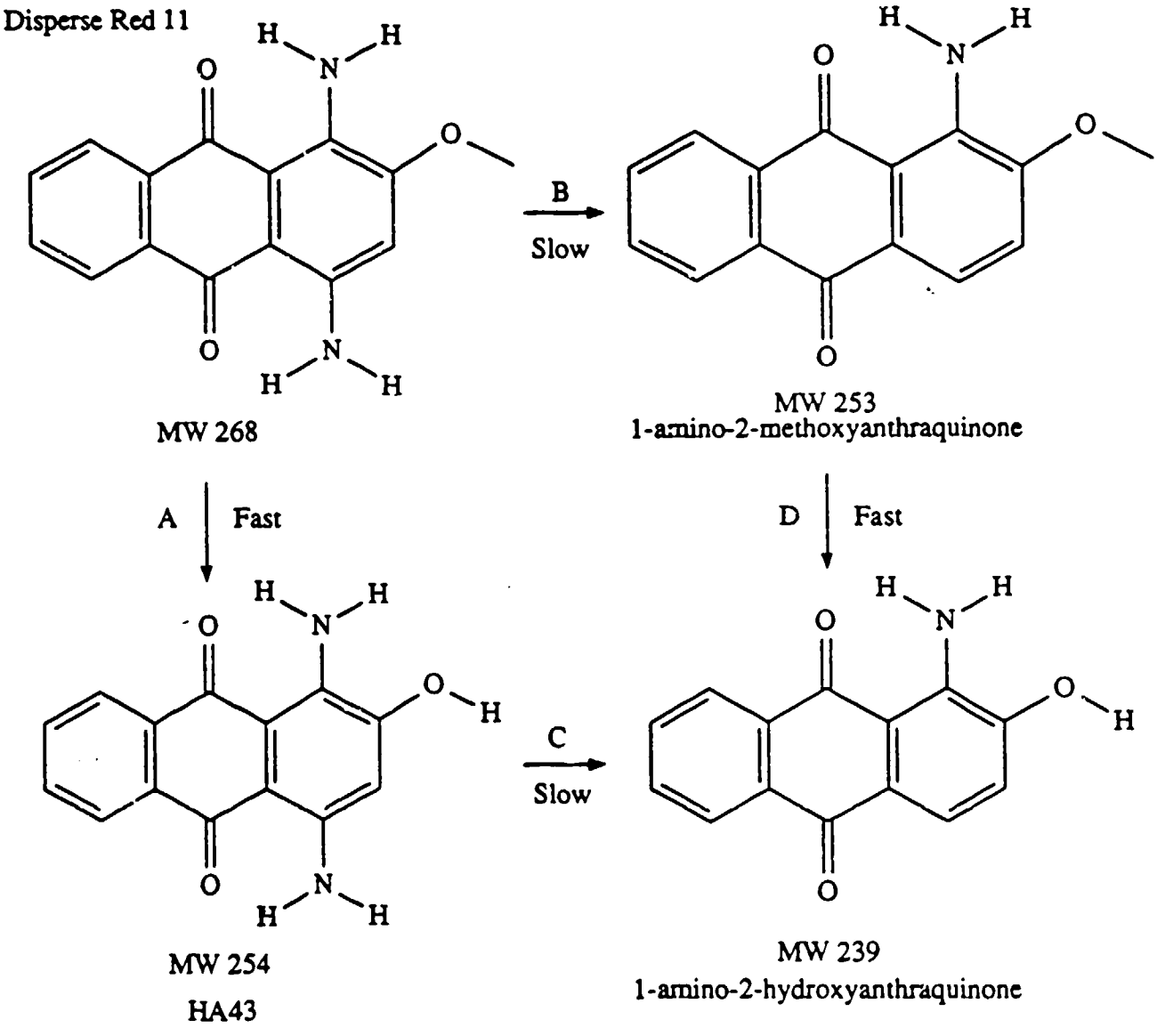
Disperse Red 11
MW 268
B
Slow
MW 253
1-amino-2-methoxyanthraquinone
A
Fast
D
Fast
C
Slow
MW 254
HA43
MW 239
1-amino-2-hydroxyanthraquinone

Figure 8-1

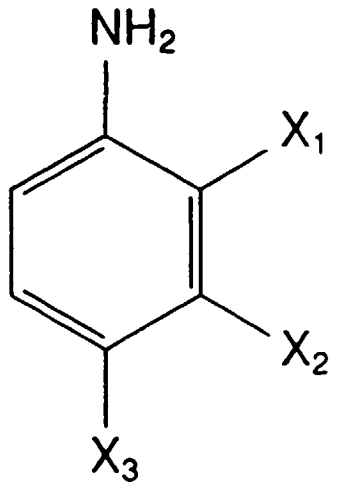

pKa's of Monosubstituted Anilines

	X_1	X_2	X_3
OCH_3	4.52	4.21	5.34
CH_3	4.45	4.72	5.10
H	4.60	4.60	4.60
Cl	2.64	3.50	3.98
Br	2.53	3.54	3.86
CF_3	----	3.49	2.54
$COCH_3$	2.22	3.59	2.19
CN	0.95	2.76	1.74

Figure 8-2

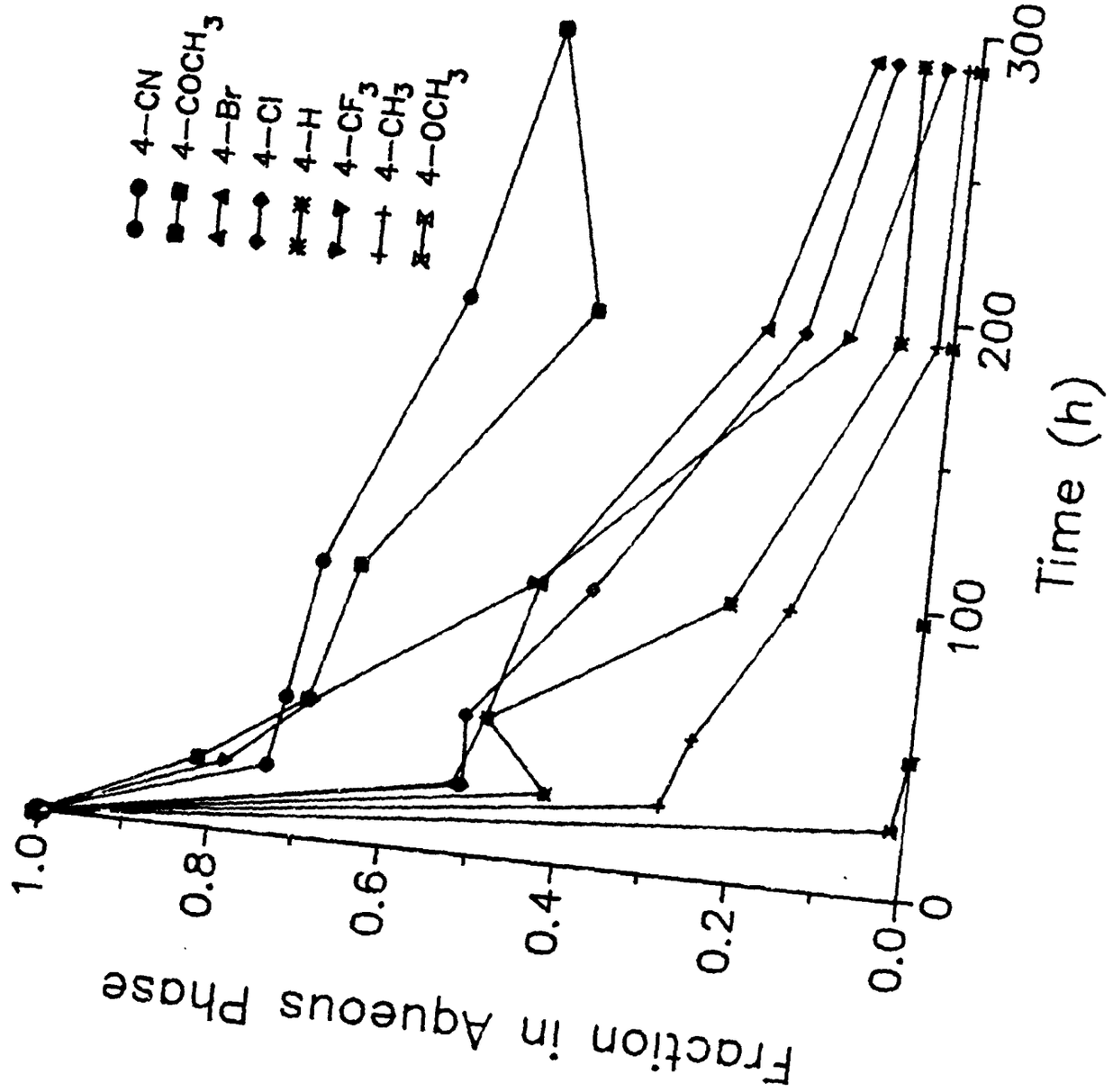
4—CN
4—COCH3
4—Br
4—Cl
4—H
4—CF3
4—CH3
4—OCH3
1.0
0.8
0.6
0.4
0.2
0.0
Fraction in Aqueous Phase
0
100
200
300
Time (h)

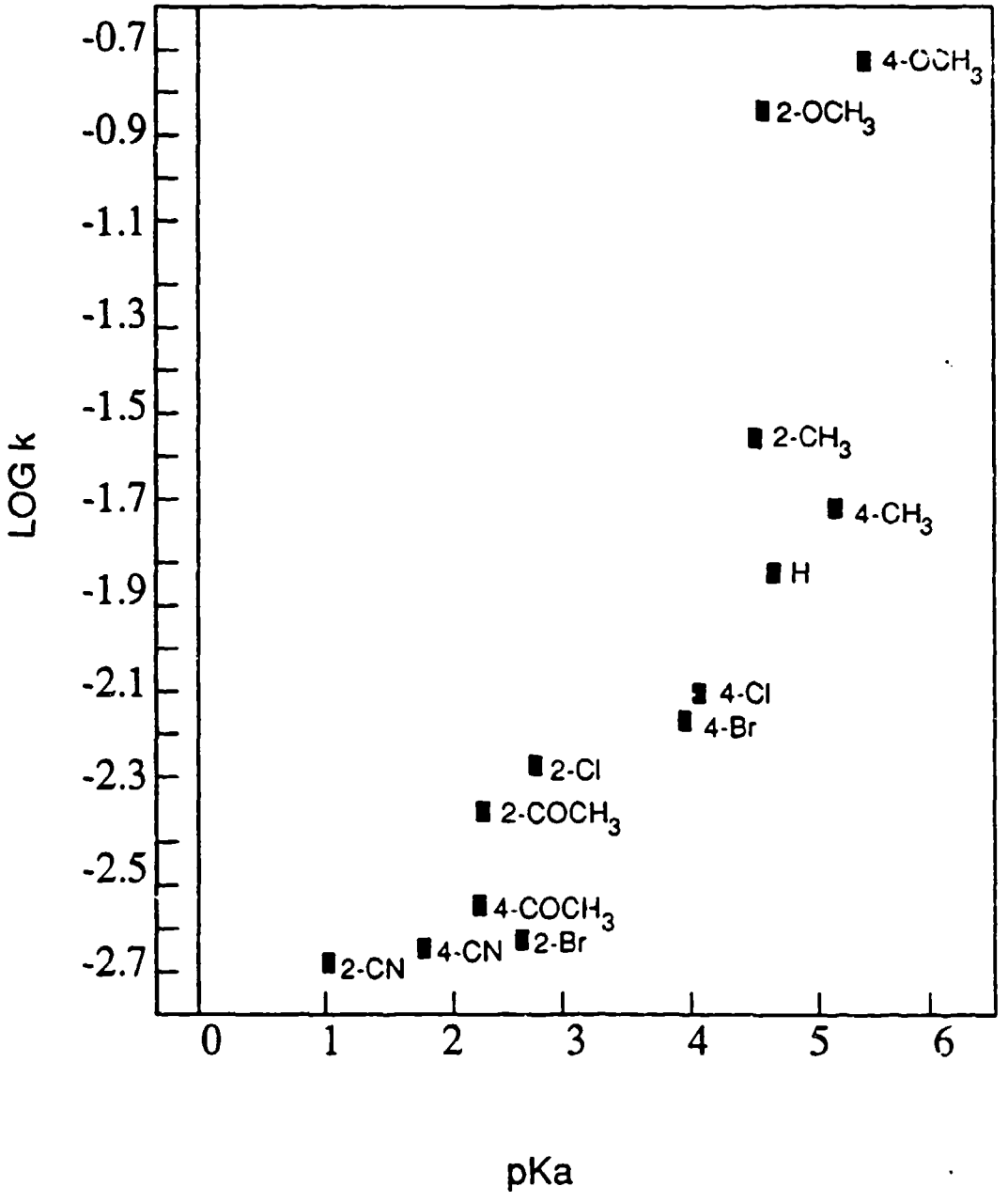
LOG k
-0.7
-0.9
-1.1
-1.3
-1.5
-1.7
-1.9
-2.1
-2.3
-2.5
-2.7
0
1
2
3
4
5
6
pKa
4-OCH3
2-OCH3
2-CH3
4-CH3
H
4-Cl
4-Br
2-Cl
2-COCH3
4-COCH3
2-Br
4-CN
2-CN

Figure 8-4

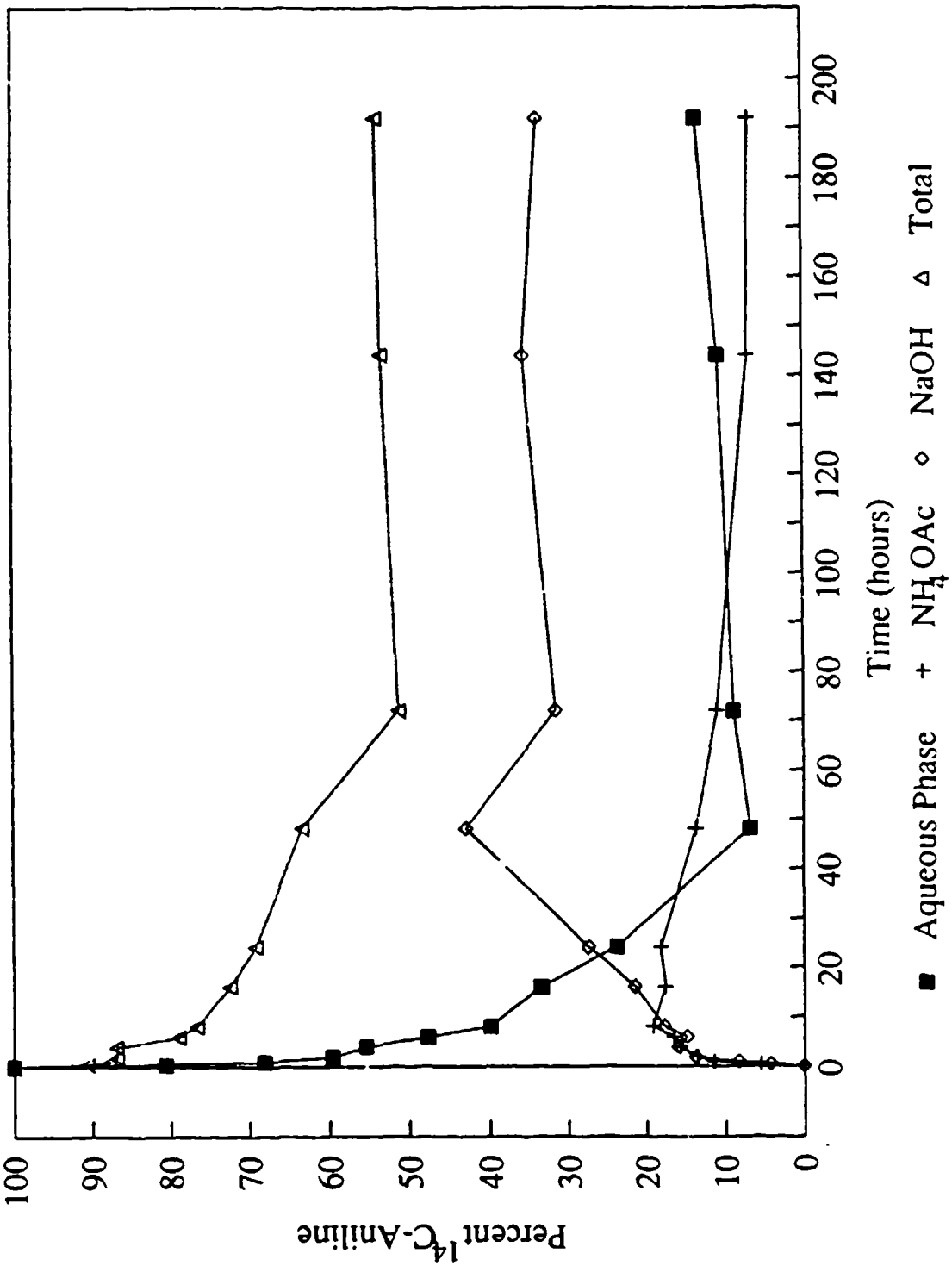
Percent ^{14}C-Aniline
0
10
20
30
40
50
60
70
80
90
100
0
20
40
60
80
100
120
140
160
180
200
Time (hours)
■ Aqueous Phase + NH_4OAc ◇ NaOH △ Total

Figure 8-5

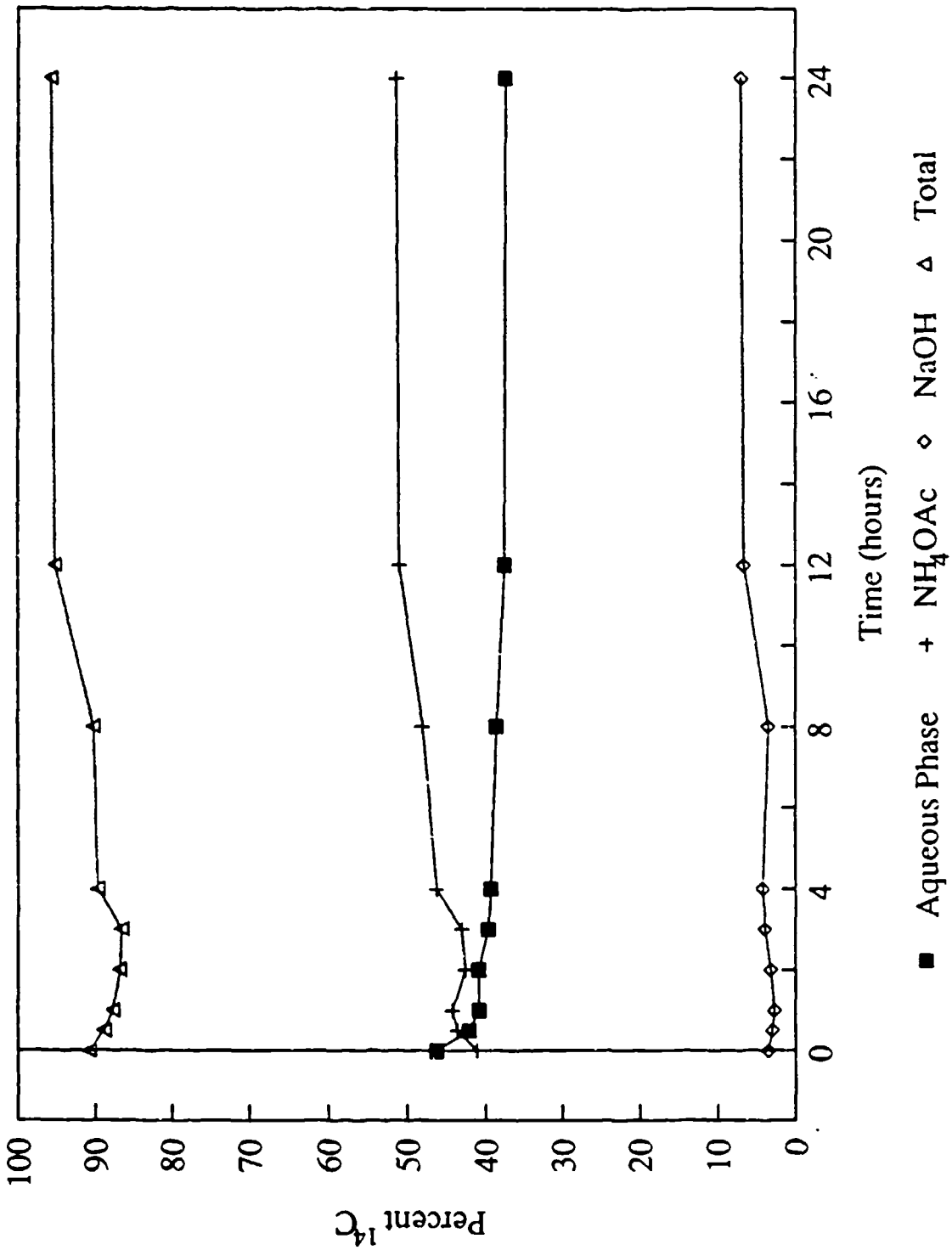
Percent ^{14}C
100
90
80
70
60
50
40
30
20
10
0
0
4
8
12
16
20
24
Time (hours)
■ Aqueous Phase + NH_4OAc ◇ NaOH △ Total

Figure 8-6

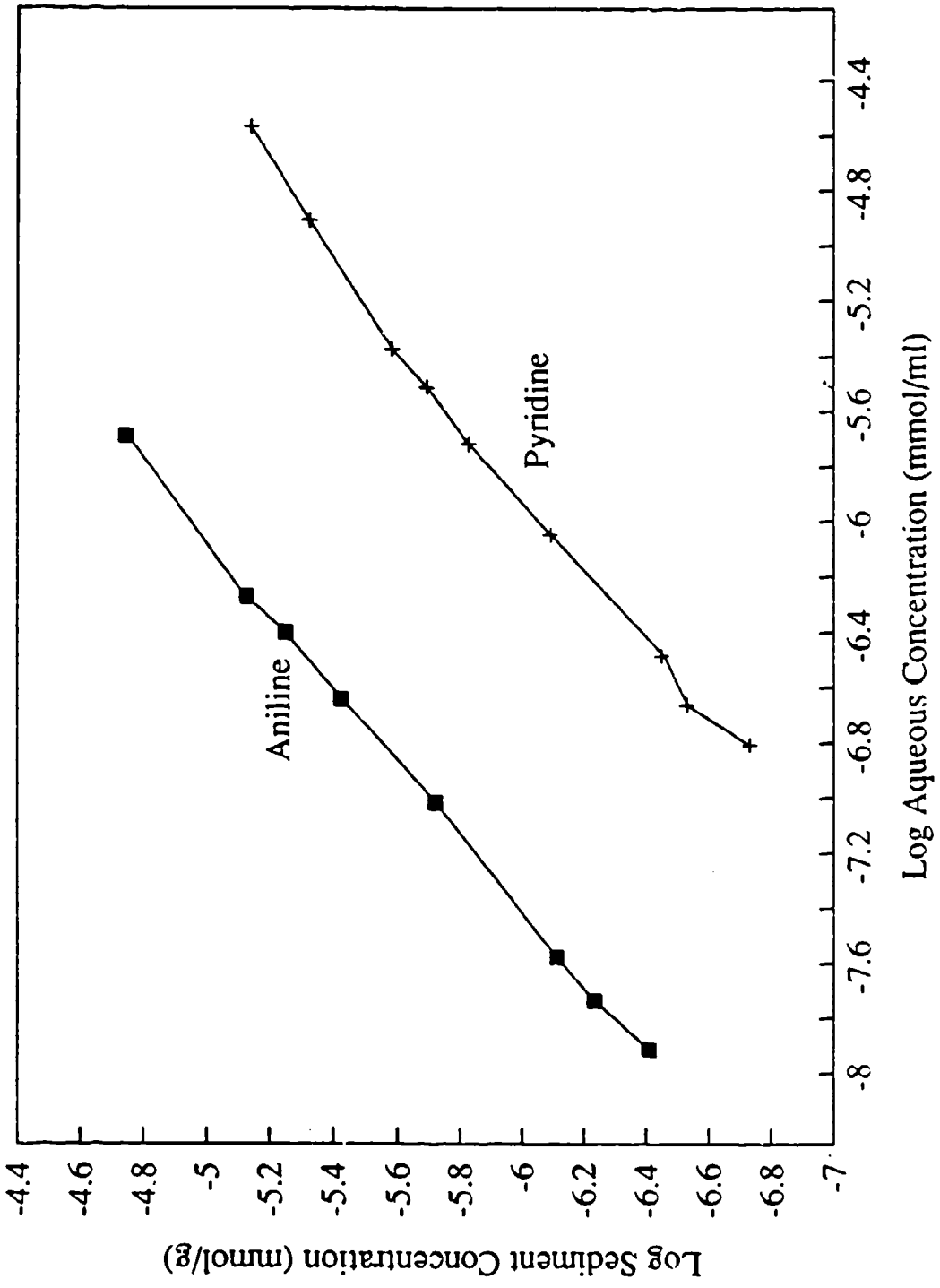
Log Sediment Concentration (mmol/g)
-4.4
-4.6
-4.8
-5
-5.2
-5.4
-5.6
-5.8
-6
-6.2
-6.4
-6.6
-6.8
-7
Log Aqueous Concentration (mmol/ml)
-8
-7.6
-7.2
-6.8
-6.4
-6
-5.6
-5.2
-4.8
-4.4
Aniline
Pyridine

Figure 8-7

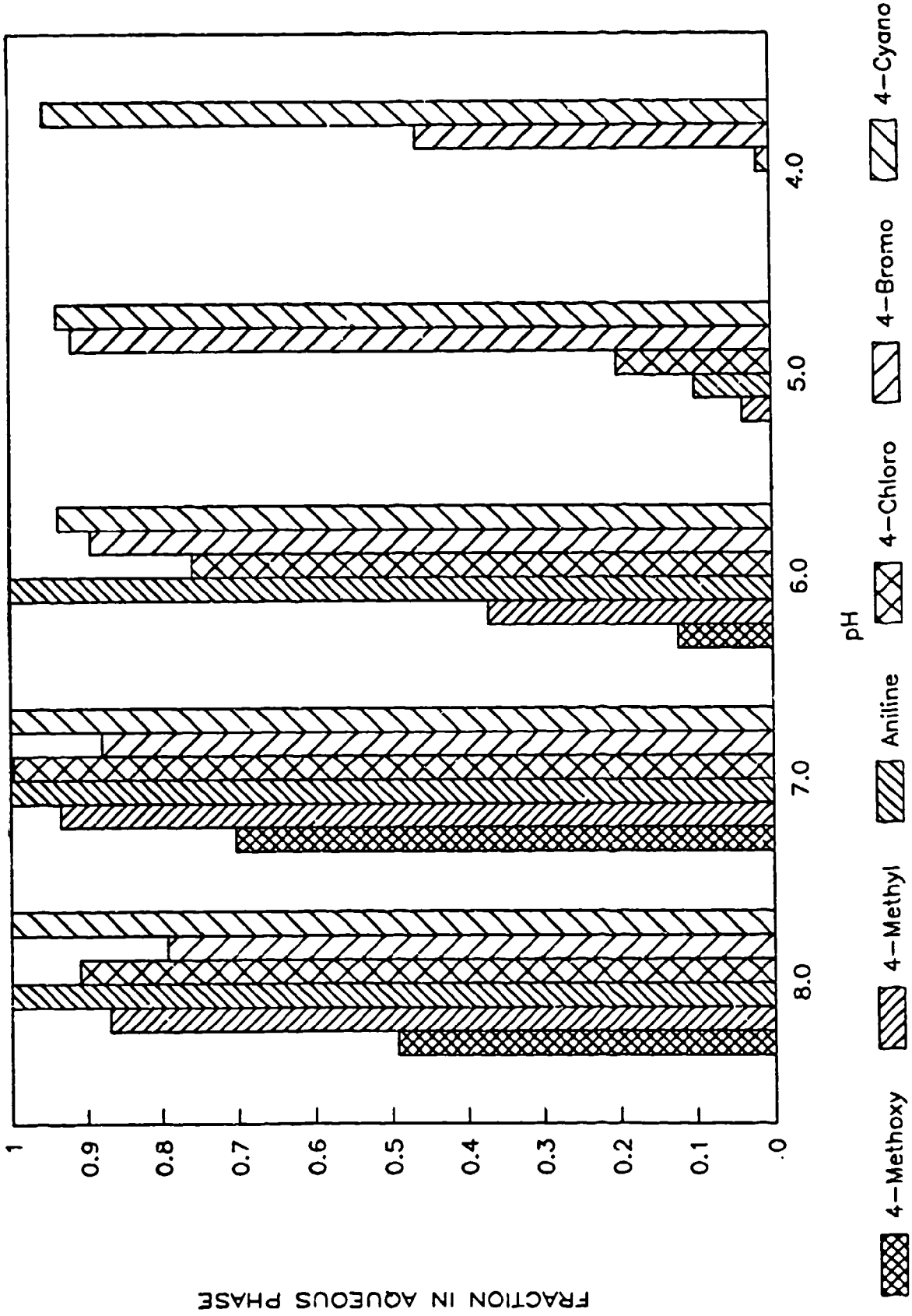
FRACTION IN AQUEOUS PHASE
1
0.9
0.8
0.7
0.6
0.5
0.4
0.3
0.2
0.1
0
4.0
5.0
6.0
7.0
8.0
pH
4-Methoxy
4-Methyl
Aniline
4-Chloro
4-Bromo
4-Cyano

Figure 8-8

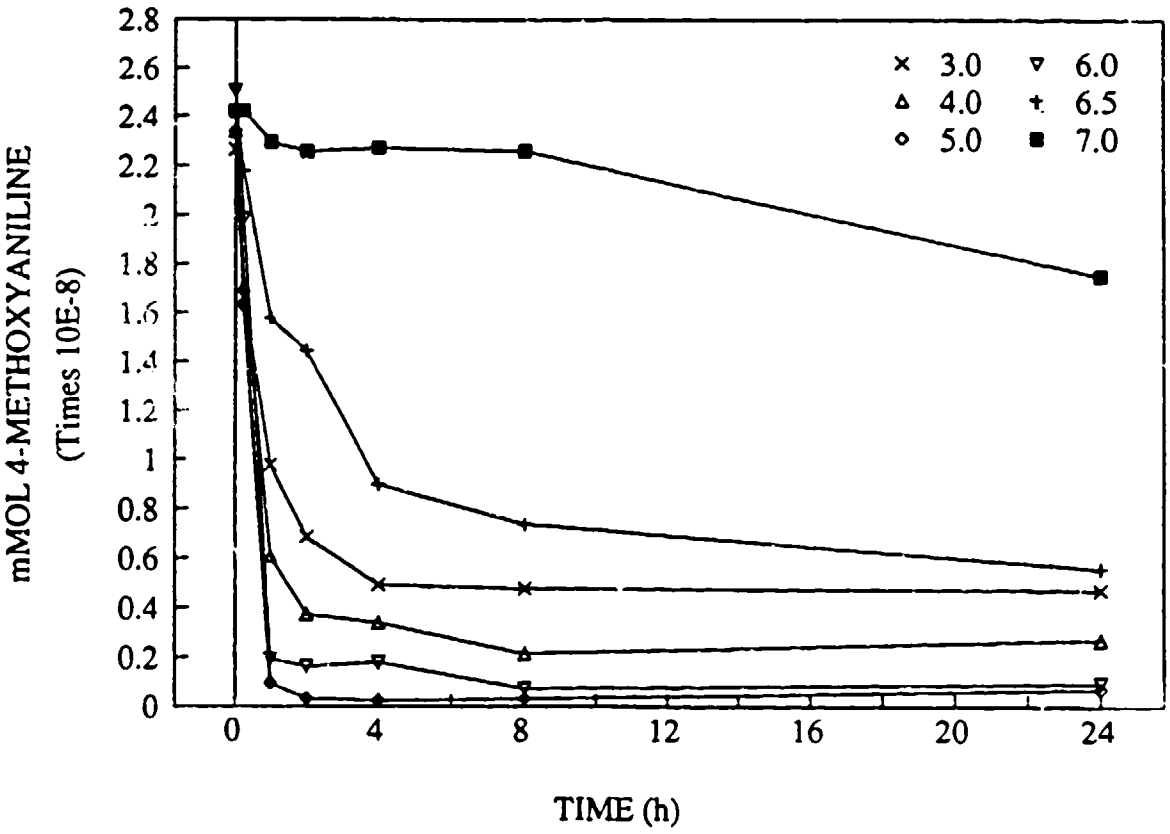
mMOL 4-METHOXYANILINE
(Times 10E-8)
2.8
2.6
2.4
2.2
1.8
1.6
1.2
1
0.8
0.6
0.4
0.2
0
0
4
8
12
16
20
24
TIME (h)
3.0
4.0
5.0
6.0
6.5
7.0

Figure 8-9

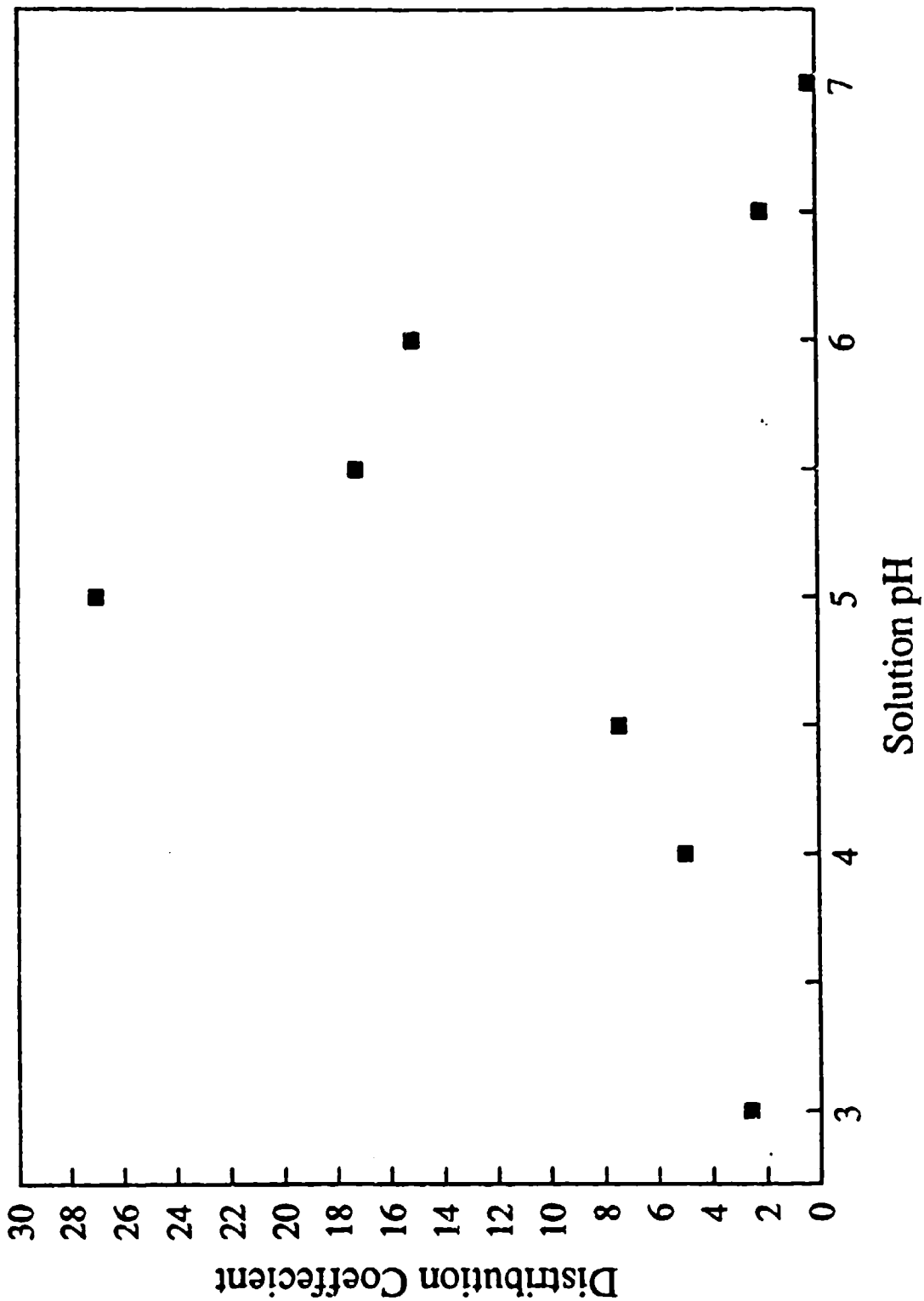
Distribution Coefficient
0
2
4
6
8
10
12
14
16
18
20
22
24
26
28
30
3
4
5
6
7
Solution pH

Figure 8-10

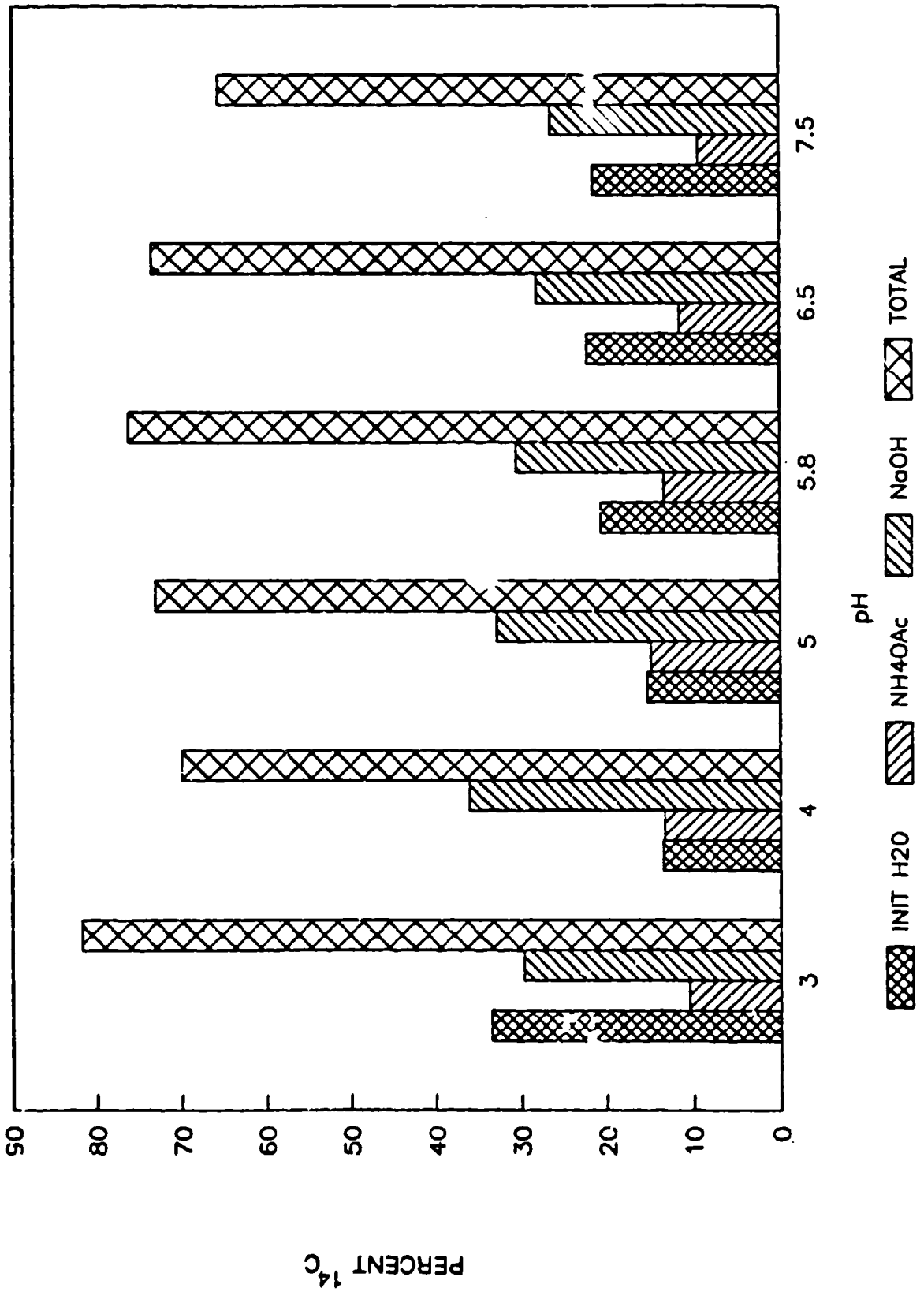
PERCENT ^{14}C
0
10
20
30
40
50
60
70
80
90
3
4
5
5.8
6.5
7.5
pH
INIT H2O
NH4OAc
NaOH
TOTAL

Figure 8-11

SO3Na
R2
-O
R1
Bisulfite Adduct
NHPh(NO2)2
N
R2
R1
Hydrazone
OH
N
R2
R1
Oxime

Figure 8-12

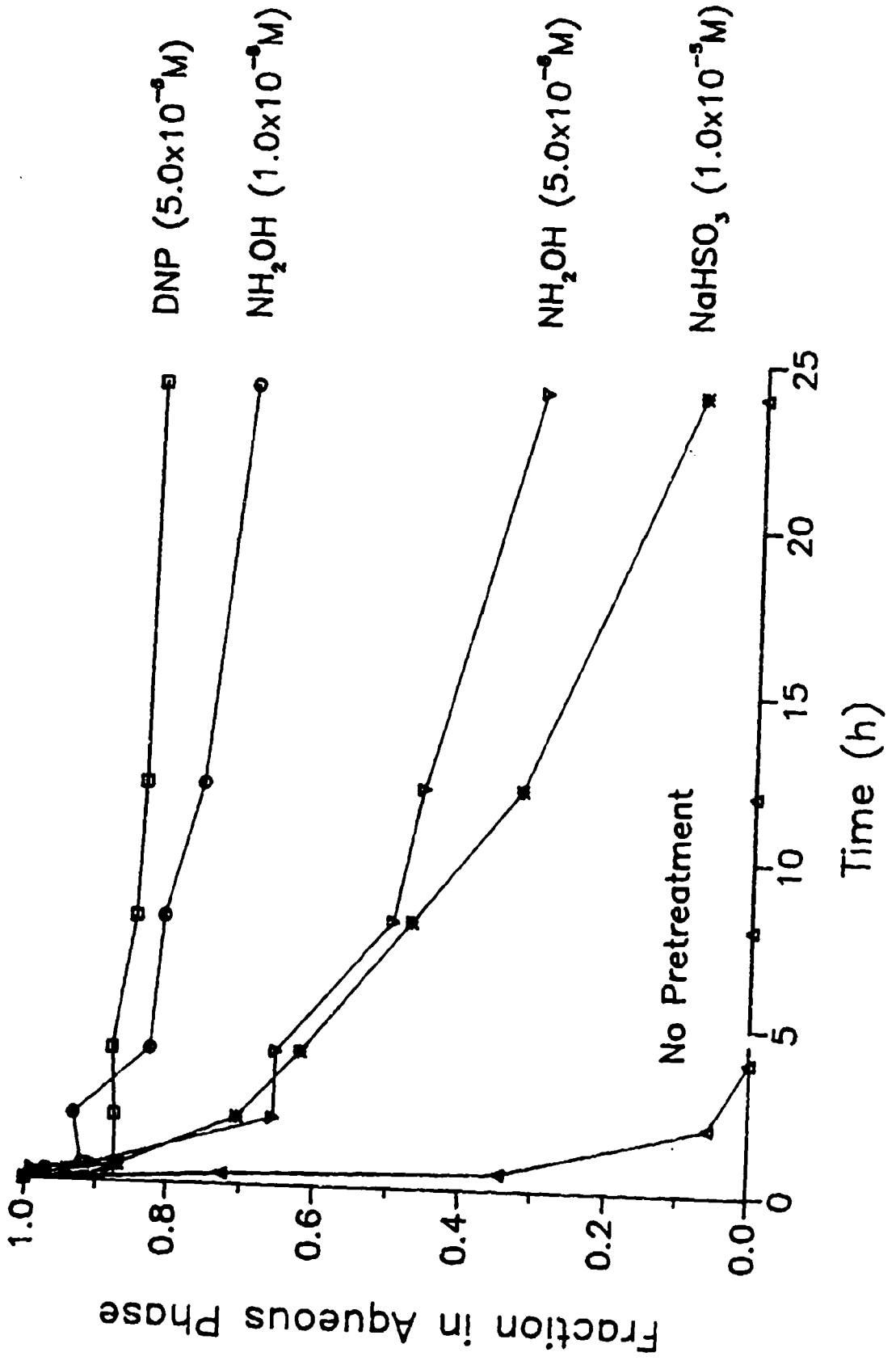
DNP (5.0x10⁻⁶M)
NH₂OH (1.0x10⁻⁶M)
NH₂OH (5.0x10⁻⁶M)
NaHSO₃ (1.0x10⁻³M)
No Pretreatment
Fraction in Aqueous Phase
Time (h)
0.0
0.2
0.4
0.6
0.8
1.0
0
5
10
15
20
25

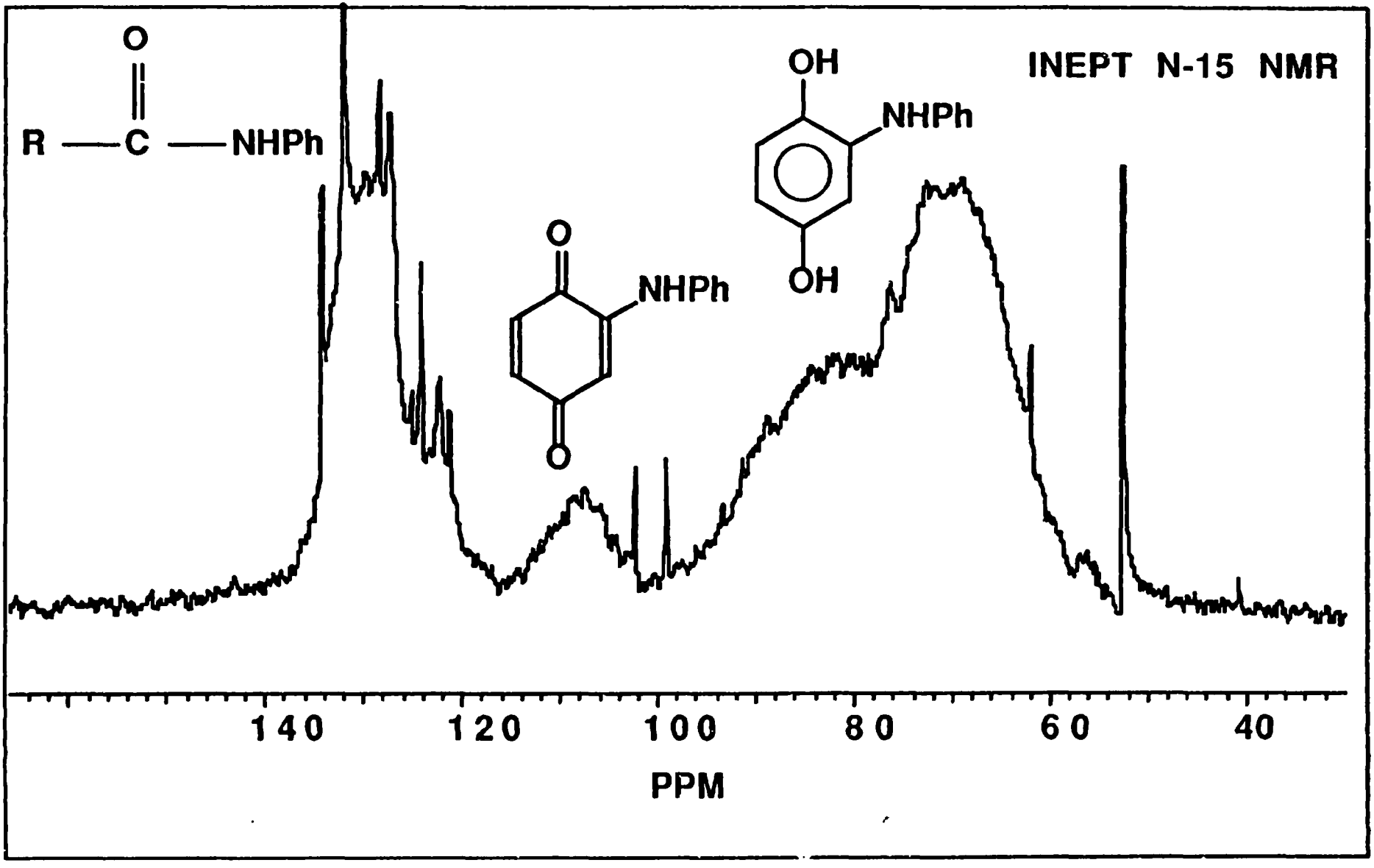

SUWANNEE FULVIC ACID REACTED WITH N-15 ANILINE (MeOH/Reflux)

Figure 8-13

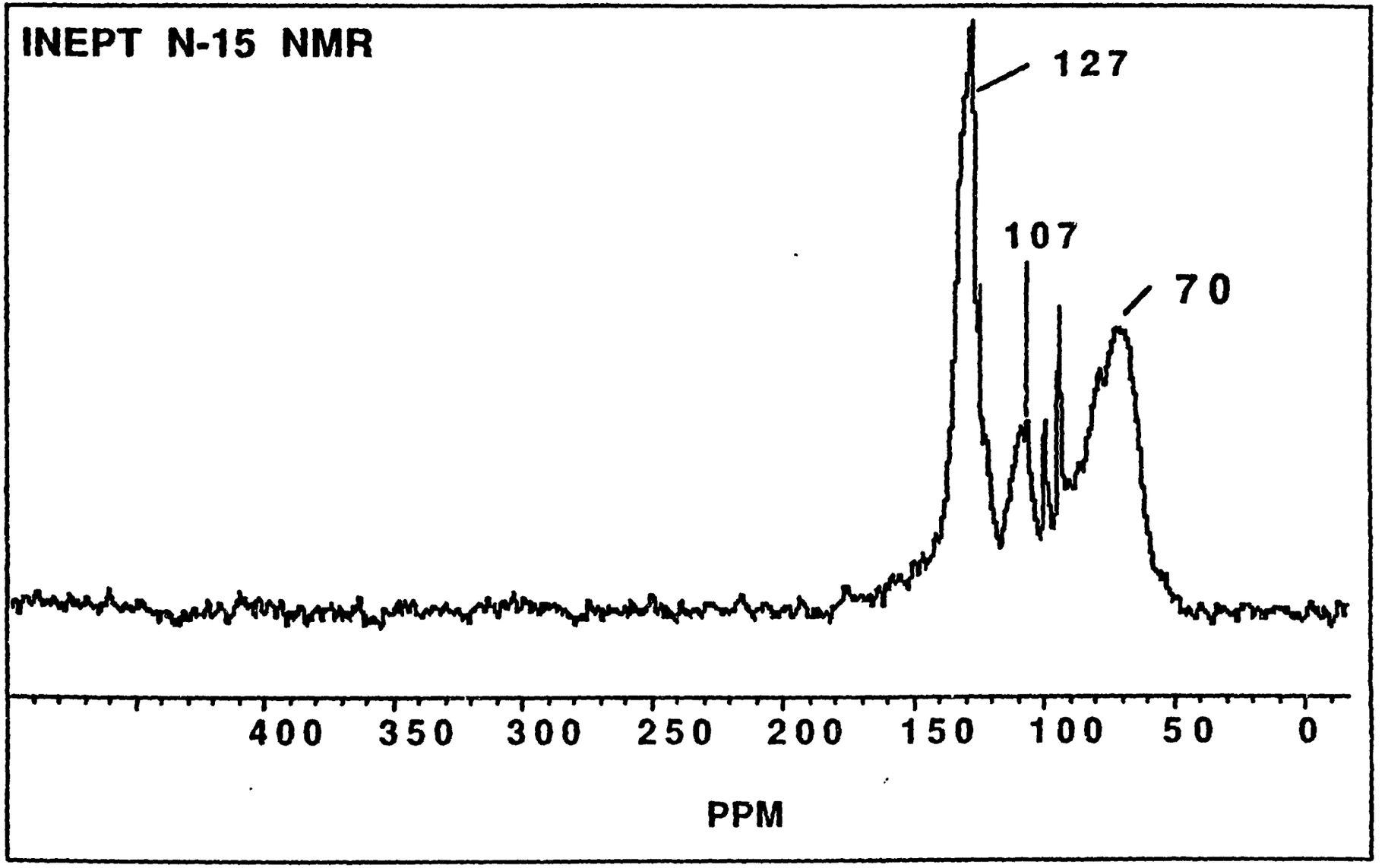

Figure 8-14

Suwannee Fulvic Acid Reacted with N-15 Aniline (Aq/RT/pH 6)

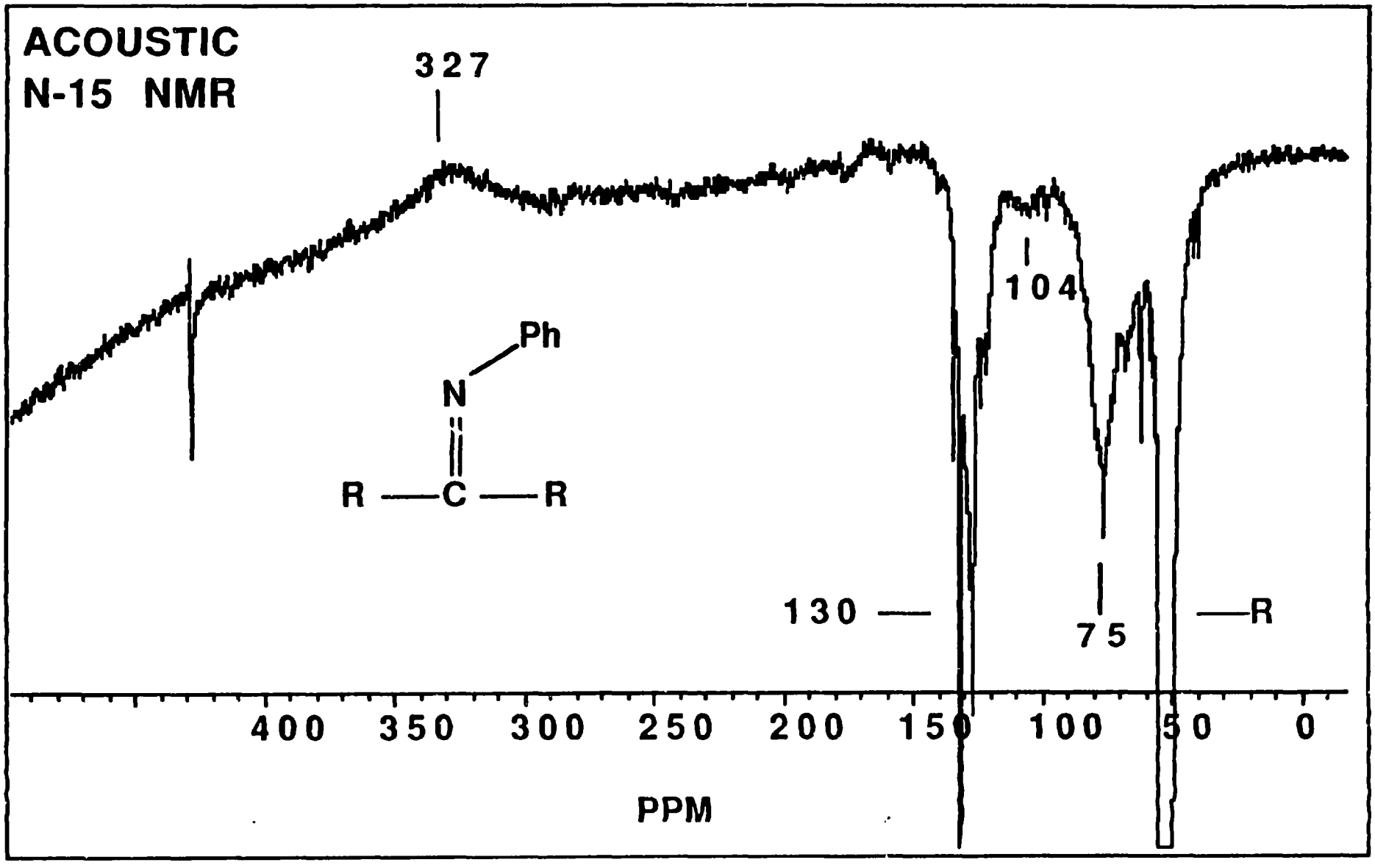

Suwannee Fulvic Acid Reacted with N-15 Aniline (MeOH/Reflux)

Figure 8-15

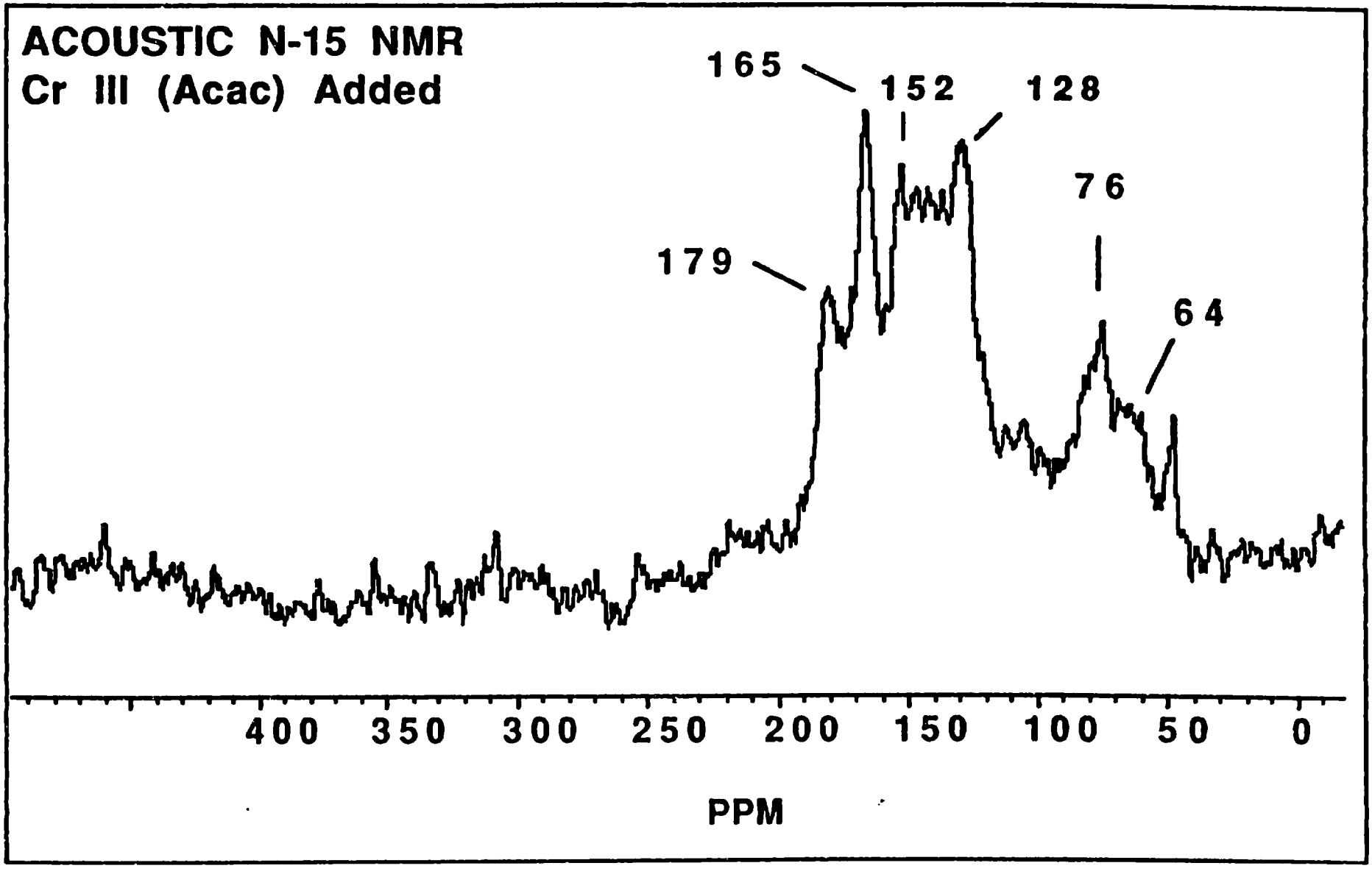

Suwannee Fulvic Acid Reacted with N-15 Aniline (Aq/RT/pH 6)

^{15}N NMR Chemical Shifts of Model Aniline Adducts

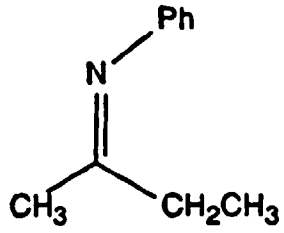

323 ppm

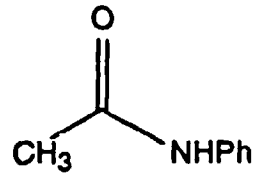

132 ppm

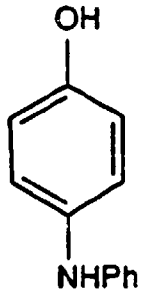

85 ppm

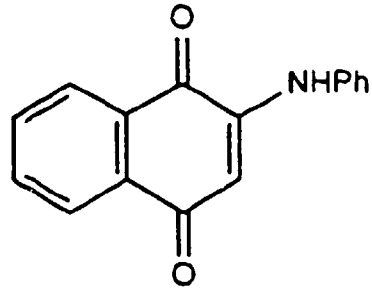

103 ppm

Summary of Assingments

340 - 290 ppm	Imine
190 - 140 ppm	Heterocyclic
140 - 155 ppm	Anilide
115 - 110 ppm	Anilino-quinone
100 - 60 ppm	Anilino-hydroquinone

Appendix A. Mass Spectra of Smoke Dyes

MASS SPECTRUM
12/07/88 14:01:00 + 5:33
SAMPLE: SOLVENT GREEN 3 #RA1-0057W
CONDS.: GC/MS
ENHANCED (S 15B 2N 0T)

DATA: GREEN3 #333
CALI: C127 #3

BASE M/Z: 418
RIC: 301568.

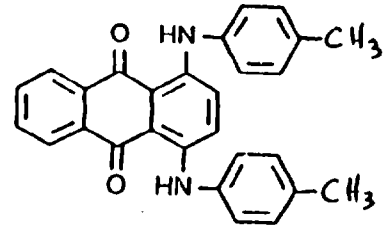

Solvent Green 3

139

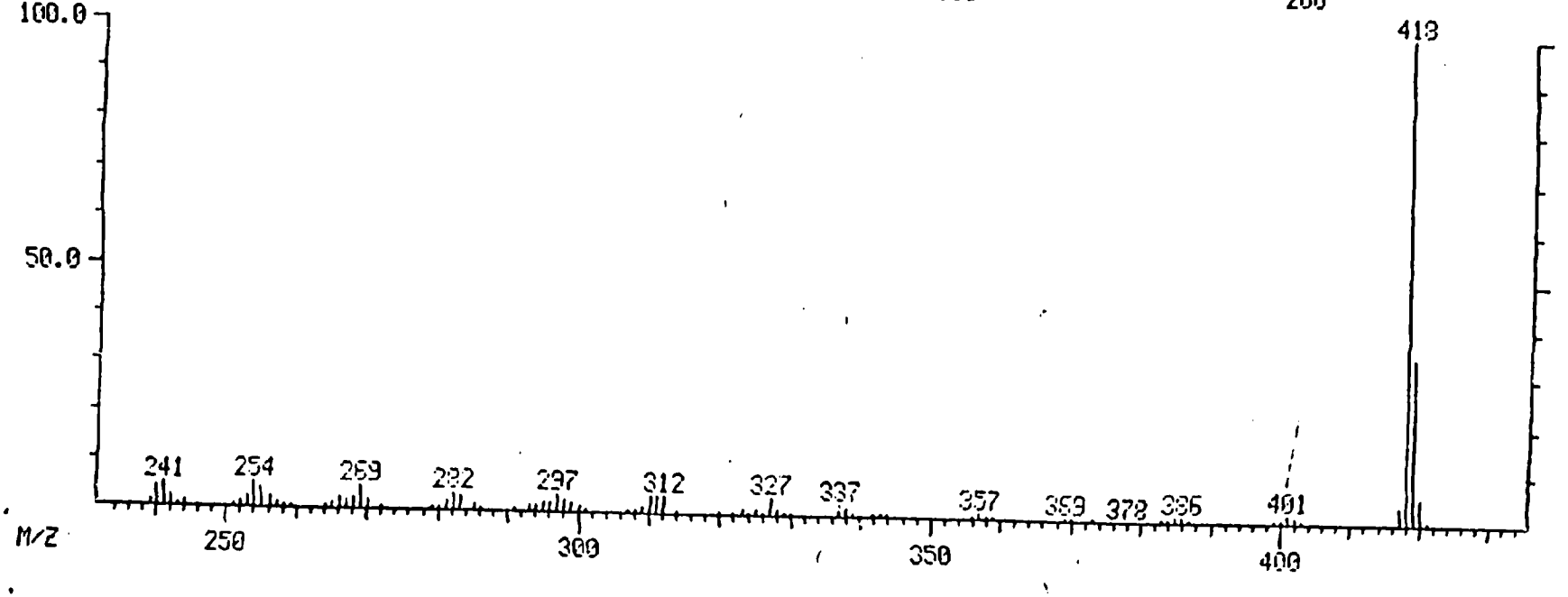

MASS SPECTRUM
01/04/89 9:48:00 + 7:57
SAMPLE: DISPERSE RED5 #RA1-0010 REBECCA ADAMS
CONDS.: PROBE
#477 - #390 - #493 TO #499

DATA: DRED5 #477
CALI: C14 #5

BASE M/Z: 347
RIC: 1366010.

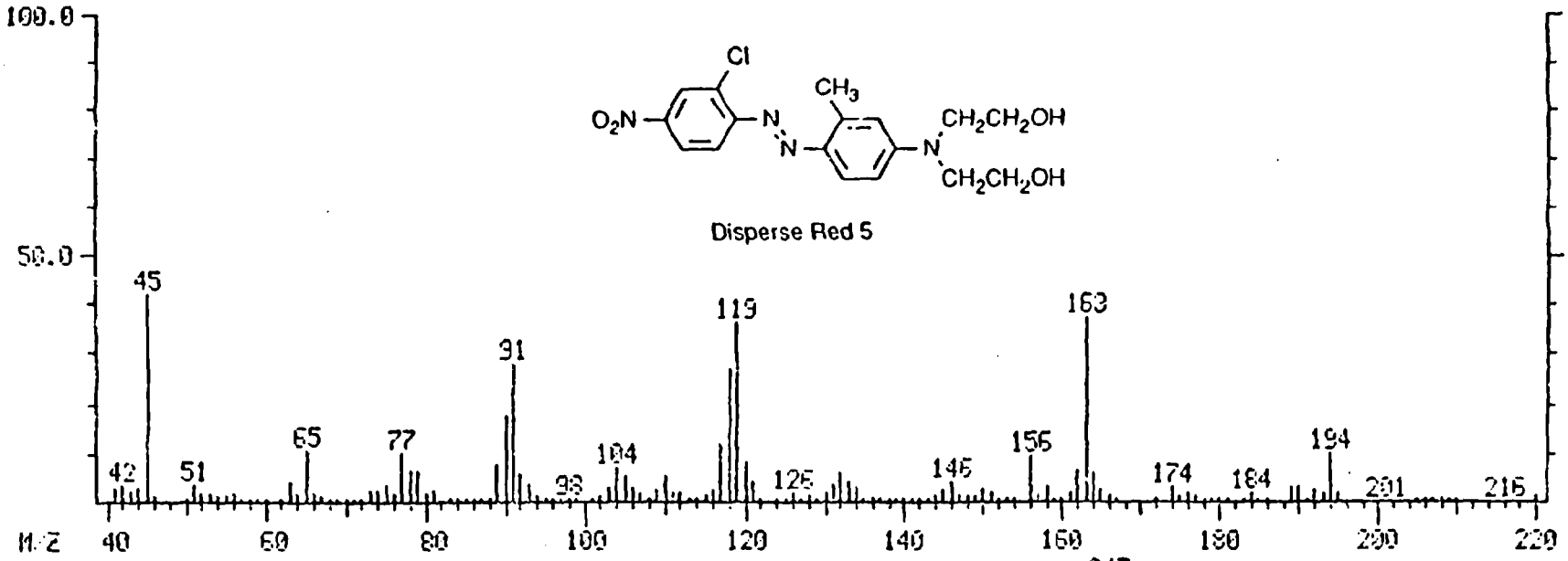

Disperse Red 5

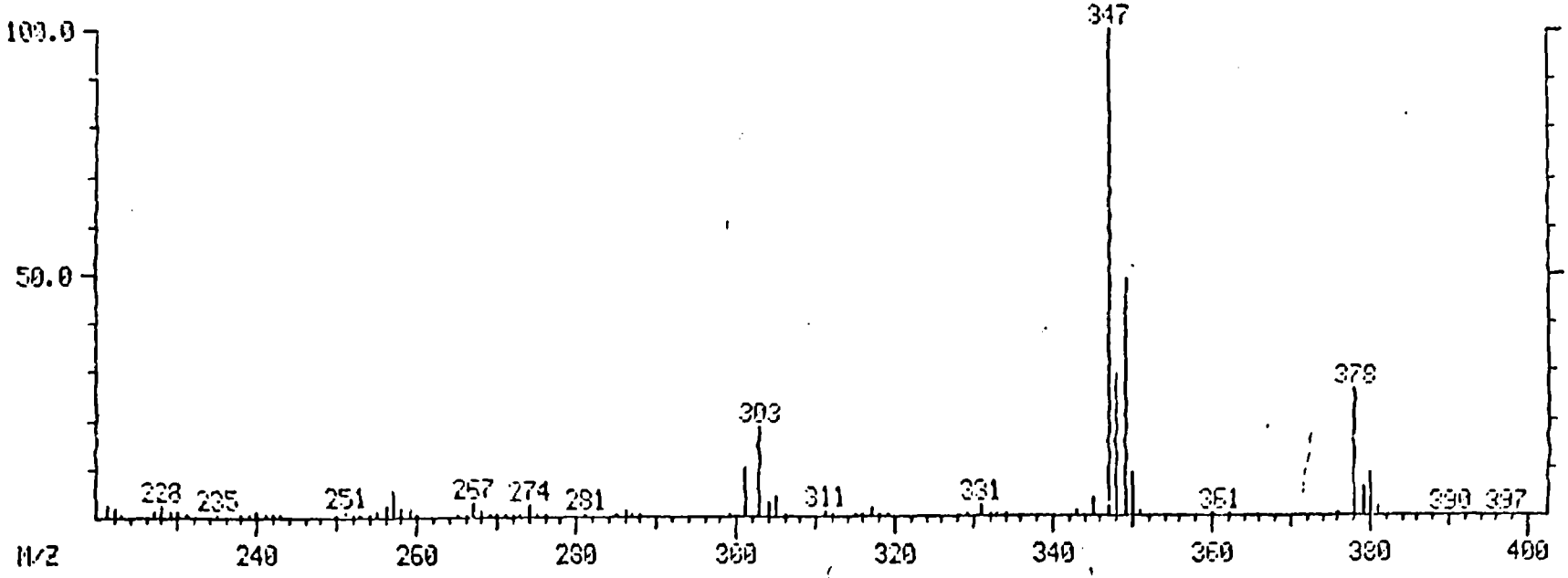

140

MASS SPECTRUM
12/07/93 13:24:00 + 4:47
SAMPLE: DISPERSE RED 9 #RA1-0011W
CONDS.: GC/MS
#287 - #112 - #314 TO #329

DATA: RED9 #287
CALI: C127 #3

BASE M/Z: 237
RIC: 232704.

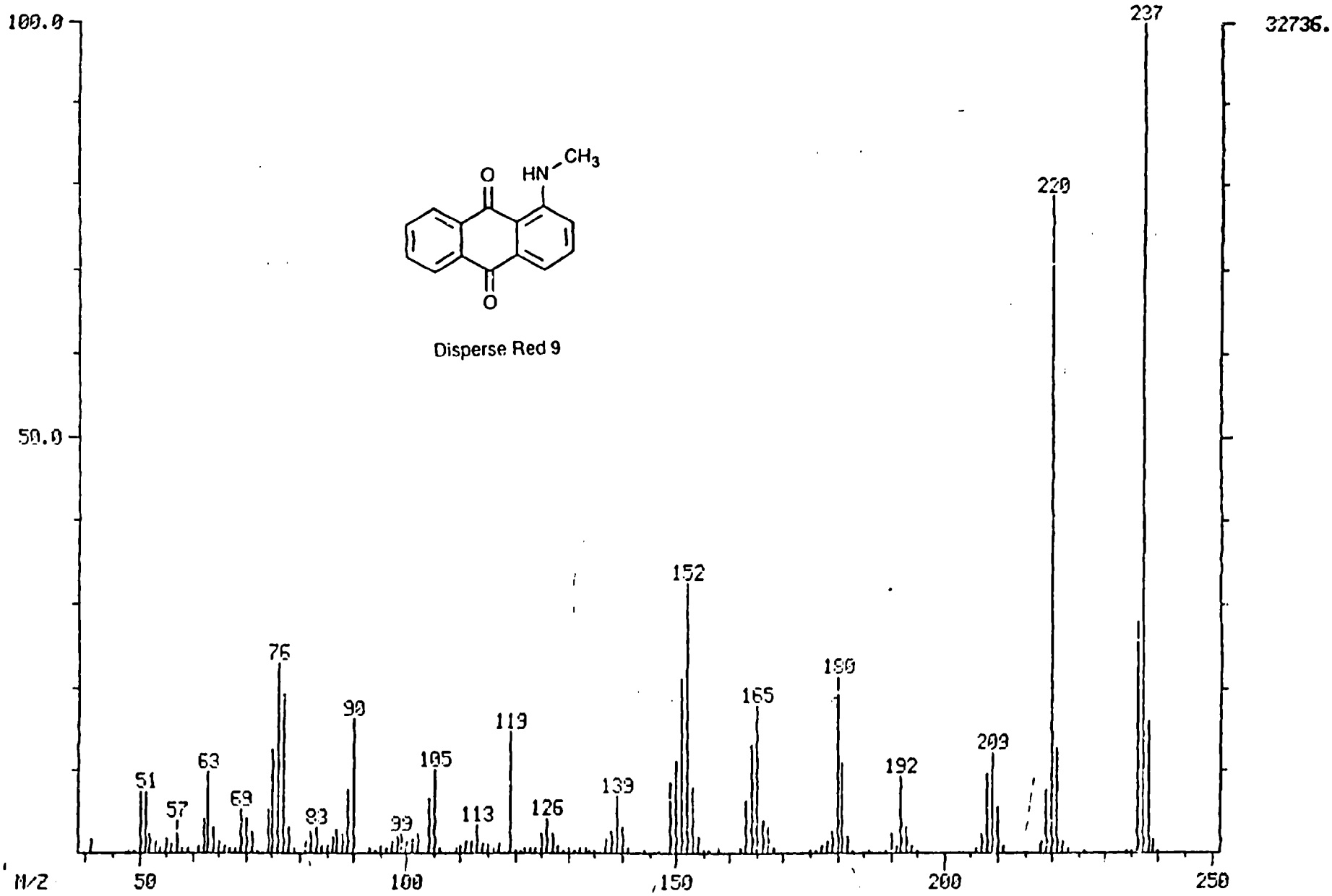

Disperse Red 9

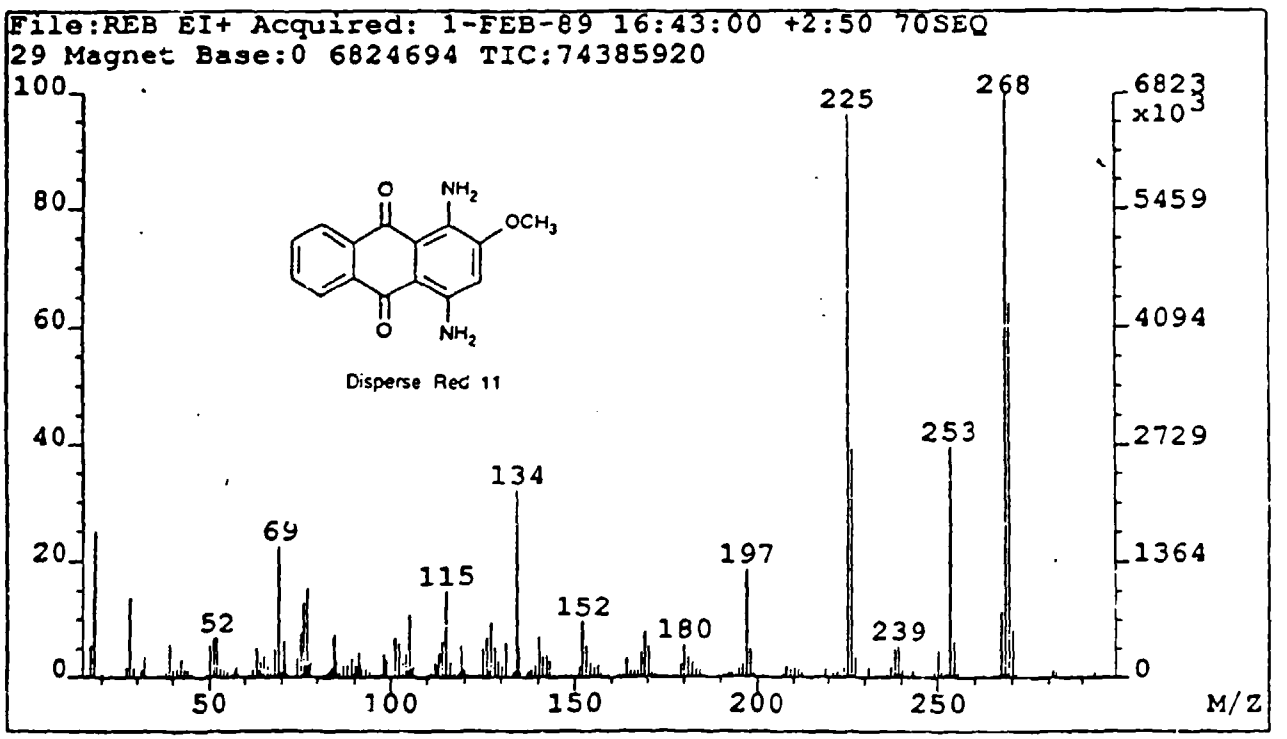
File:REB EI+ Acquired: 1-FEB-89 16:43:00 +2:50 70SEQ
29 Magnet Base:0 6824694 TIC:74385920
100
80
60
40
20
0
6823
x10 3
5459
4094
2729
1364
0
225
268
253
134
69
115
197
152
180
239
52
50
100
150
200
250
M/Z
O
NH2
OCH3
O
NH2
Disperse Red 11

MASS SPECTRUM
01/12/89 15:24:00 + 2:51
SAMPLE: NEG CI/CH4 DISPERSE VIOLET 1 RA1-0008 EM VOLTS 1000 EE 70
CONDS.: PROG PROBE
GC TEMP: 174 DEG. C

DATA: DIV1 #171
CALI: C112 #3

BASE M/Z: 238
RIC: 49984.

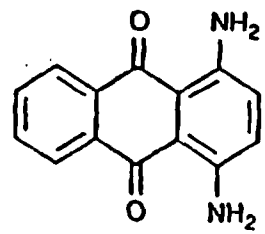

Disperse Violet 1

143

NASS SPECTRUM
12/07/88 10:18:00 + 3:02
SAMPLE: SOLVENT RED 1
CONDS.: GC/MS
#182 - #120 - #305

DATA: RED1 #182
CALI: C127 #3

BASE M/Z: 143
RIC: 631000.

75648.

100.0

50.0

144

143
278
77
115
92
51
65
101
128
171
247
263
156
219
235
178
189
205
282

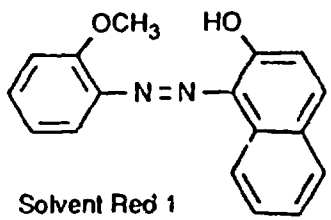

Solvent Red 1

M/Z

50
100
150
200
250
300

MASS SPECTRUM
12/13/88 10:38:00 + 4:38
SAMPLE: SOLVENT YELLOW 33 RA1-0071
CONDS.: GC/MS
#278 - #238 - #304

DATA: YEL33 #278
CALI: C1213 #3

BASE M/Z: 273
RIC: 423424.

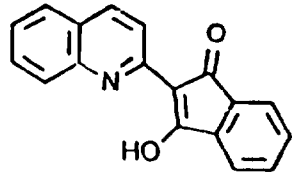

Solvent Yellow 33

145

Appendix B. IR Spectra of Smoke Dyes

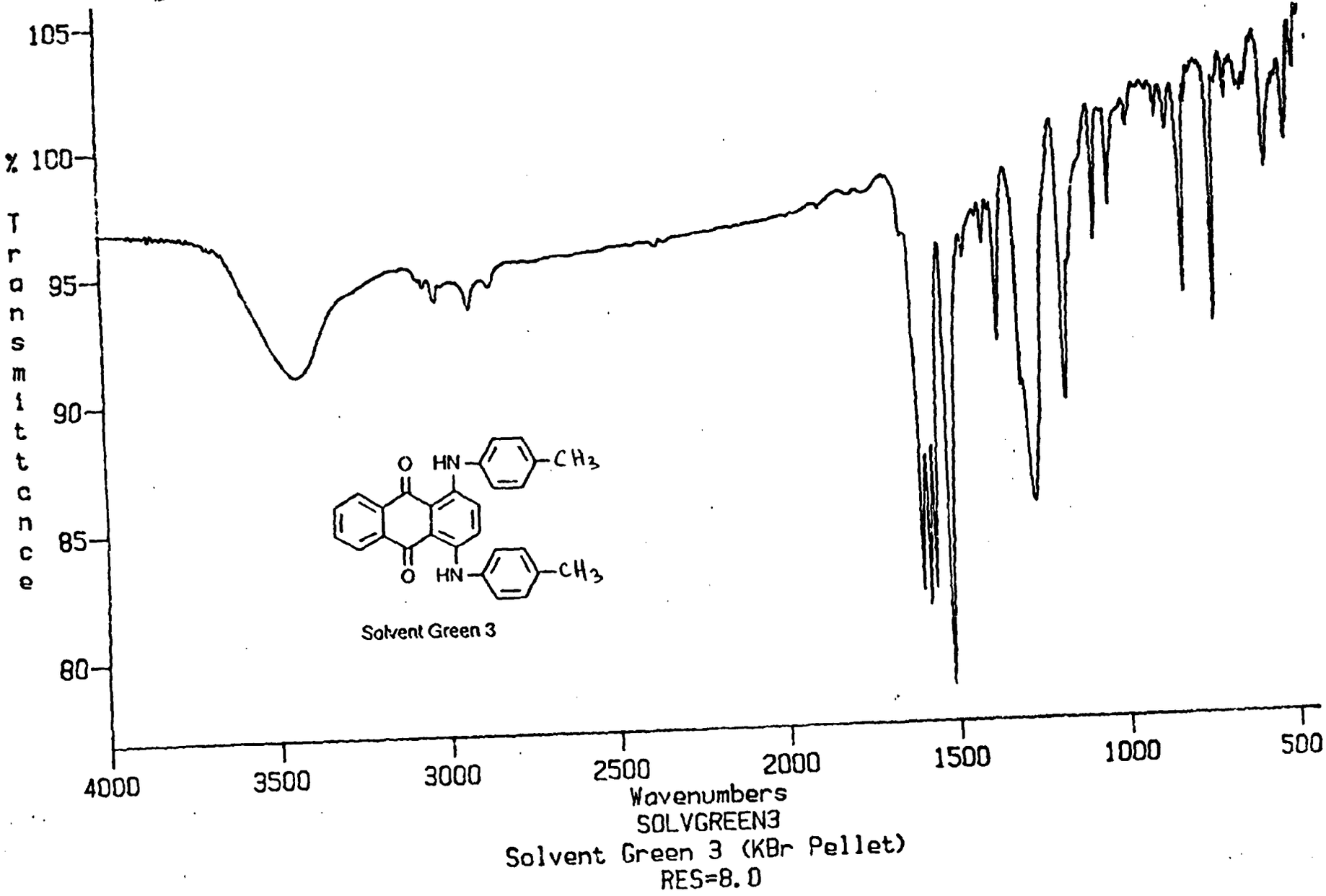

Solvent Green 3

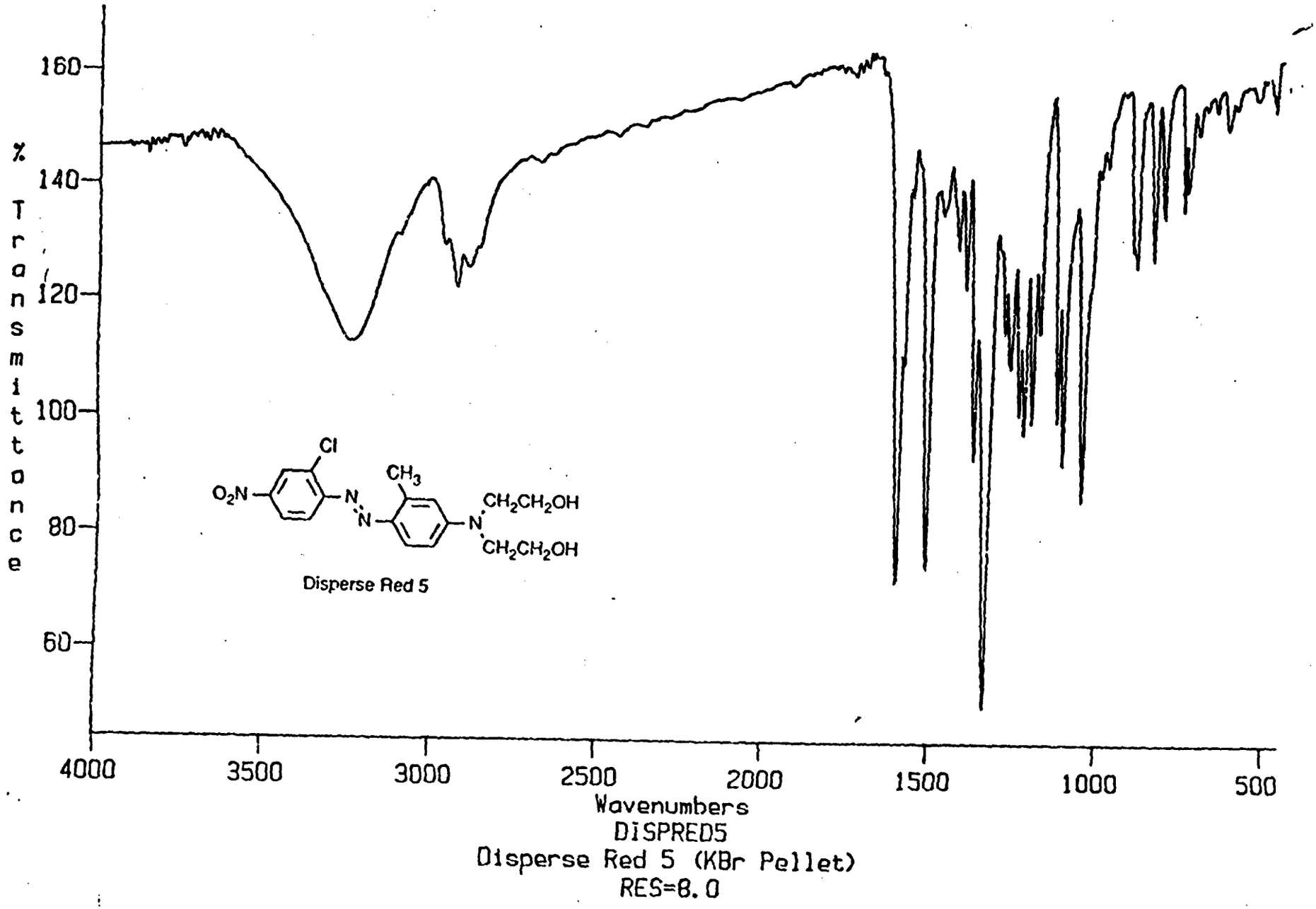
160
140
120
100
80
60
% Transmittance
4000
3500
3000
2500
2000
1500
1000
500
Wavenumbers
DISPRED5
Disperse Red 5 (KBr Pellet)
RES=8.0
Cl
O_2N
CH_3
N
N
CH_2CH_2OH
N
CH_2CH_2OH
Disperse Red 5

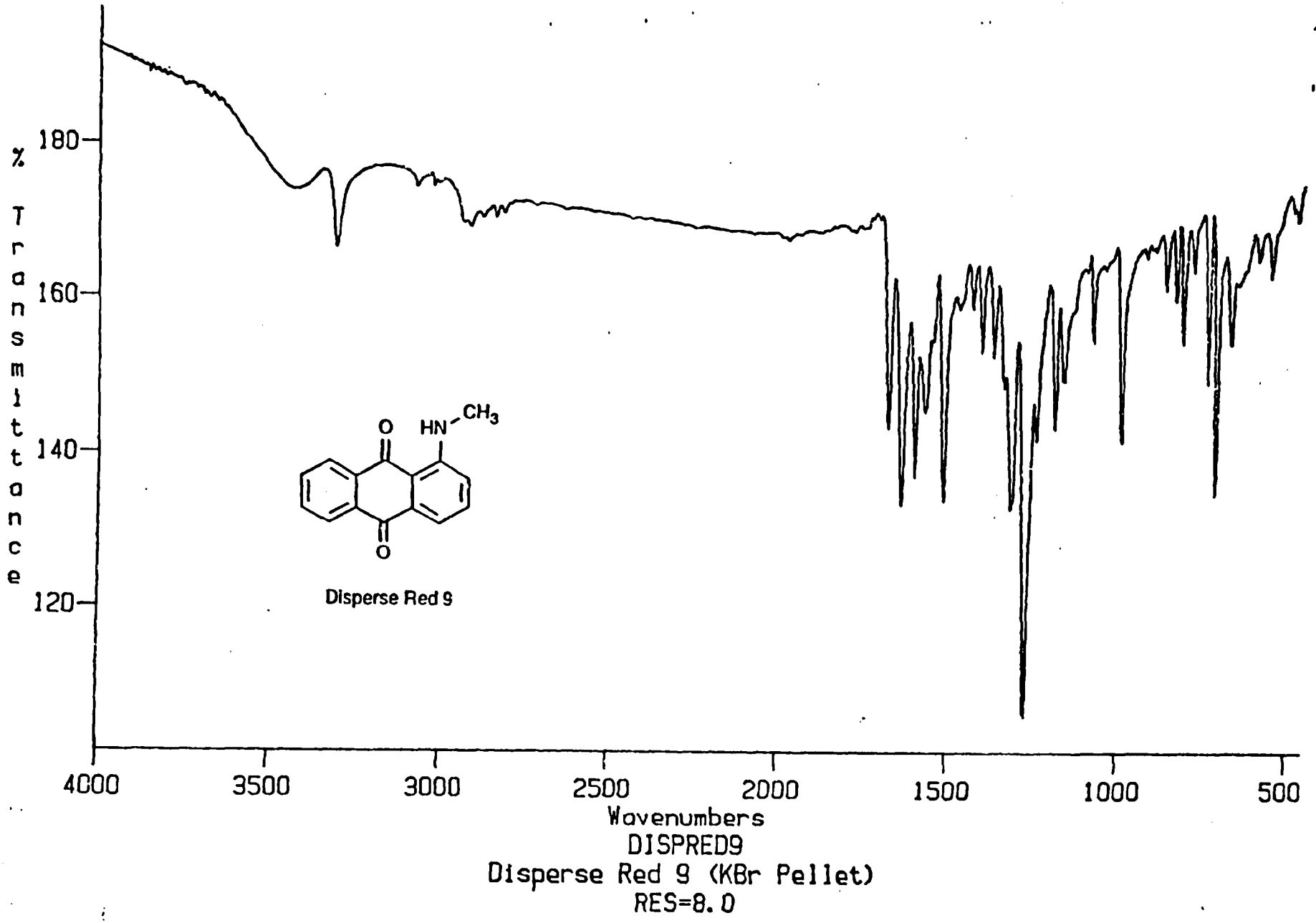
% Transmittance
180
160
140
120
4000
3500
3000
2500
2000
1500
1000
500
Wavenumbers
O
HN
CH3
O
Disperse Red 9
DISPRED9
Disperse Red 9 (KBr Pellet)
RES=8.0

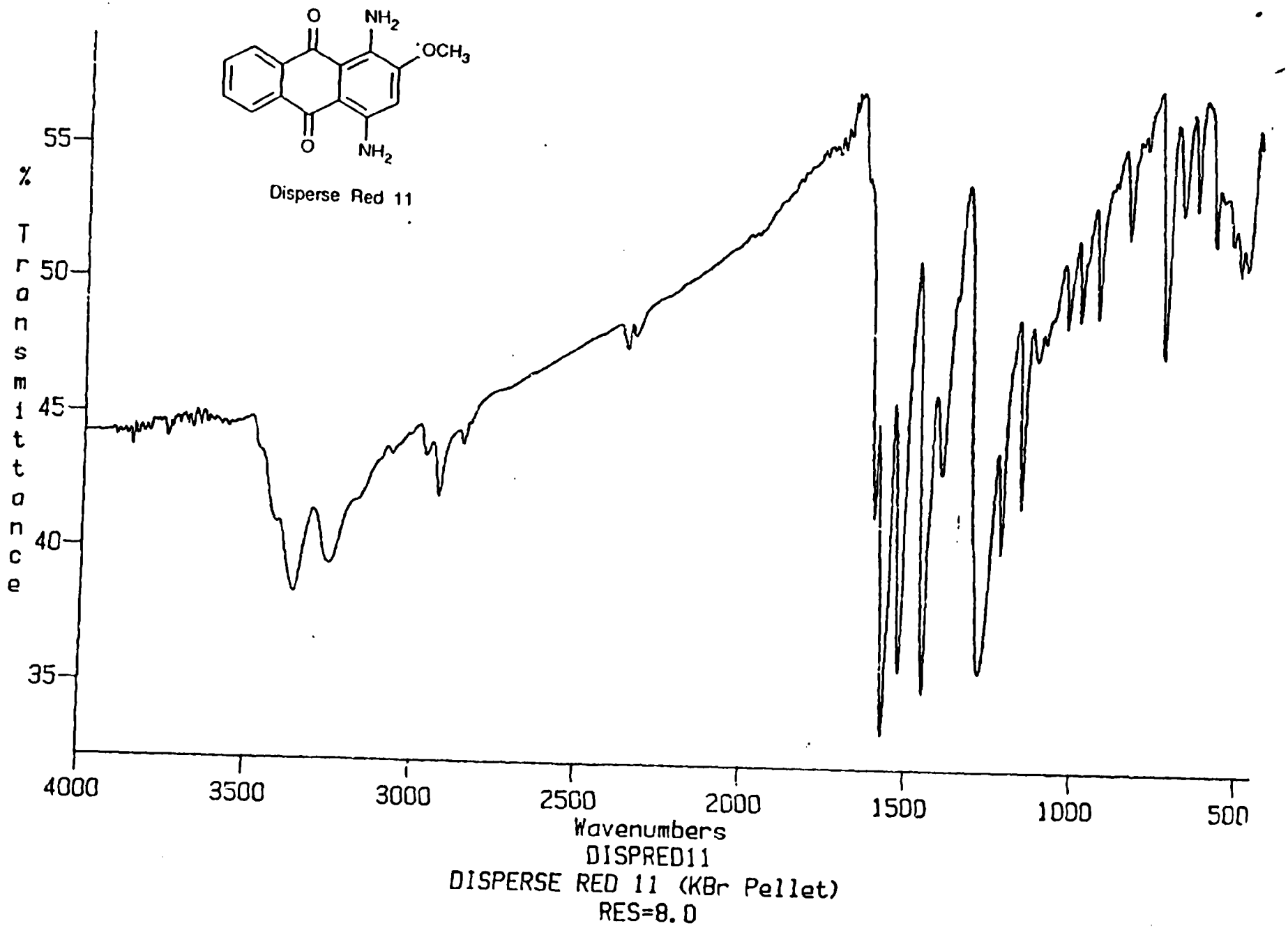
O
NH2
OCH3
O
NH2
Disperse Red 11
% Transmittance
55
50
45
40
35
4000
3500
3000
2500
2000
1500
1000
500
Wavenumbers
DISPRED11
DISPERSE RED 11 (KBr Pellet)
RES=8.0

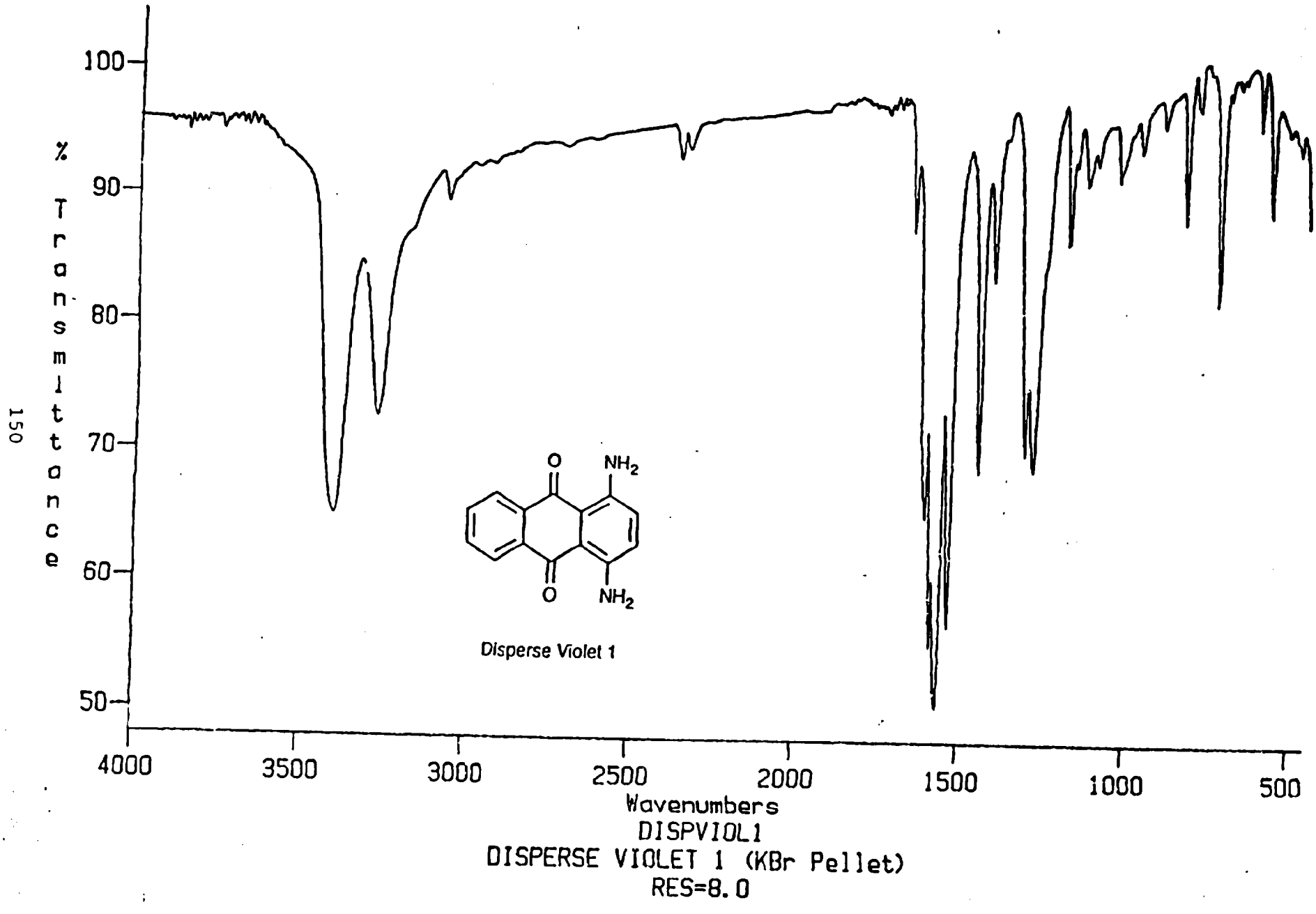
100
90
80
70
60
50
% Transmittance
150
4000
3500
3000
2500
2000
1500
1000
500
Wavenumbers
O
NH2
O
NH2
Disperse Violet 1
DISPVIOL1
DISPERSE VIOLET 1 (KBr Pellet)
RES=8.0

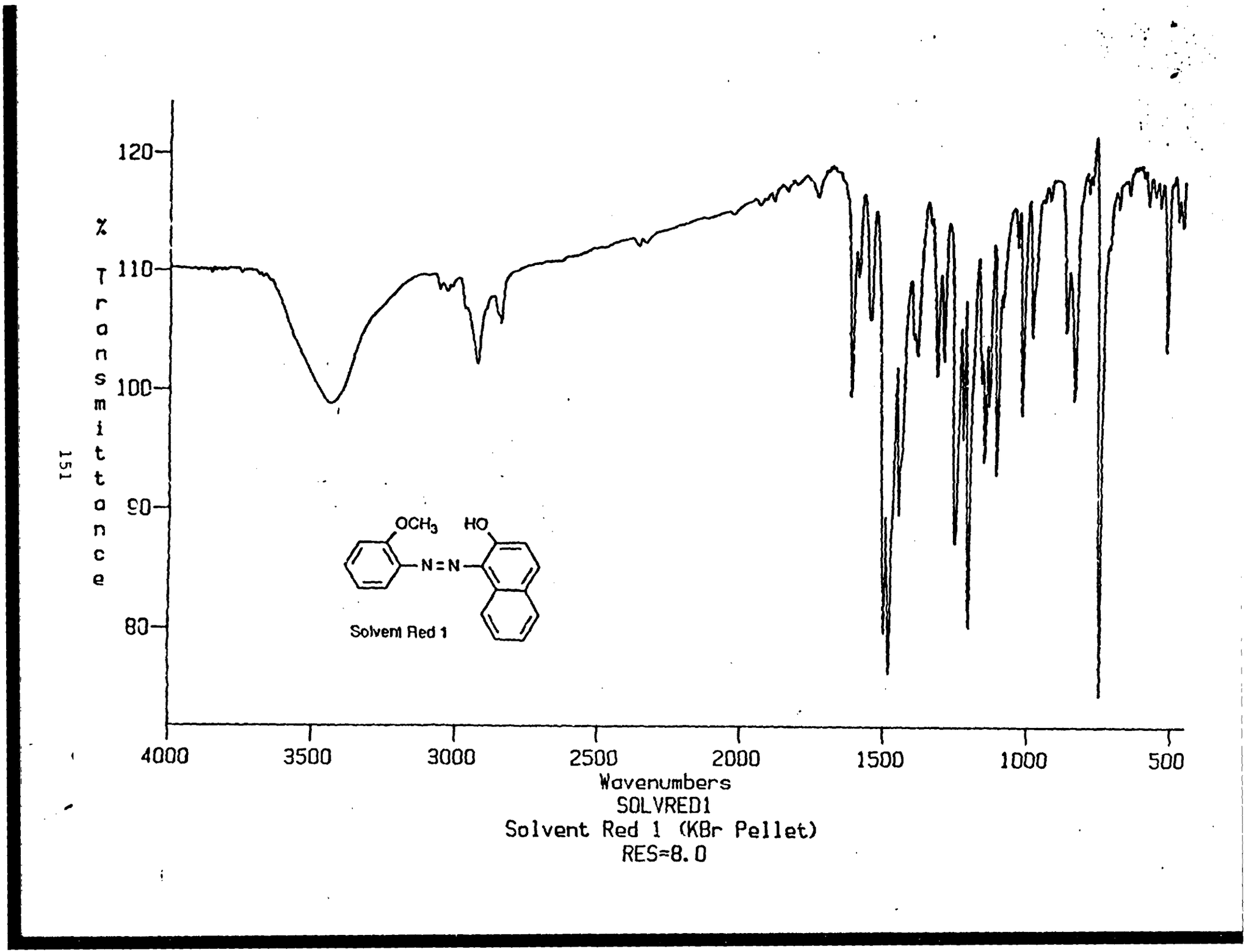
120
110
100
90
80
% Transmittance
OCH3
HO
N=N
Solvent Red 1
4000
3500
3000
2500
2000
1500
1000
500
Wavenumbers
SOLVRED1
Solvent Red 1 (KBr Pellet)
RES=8.0

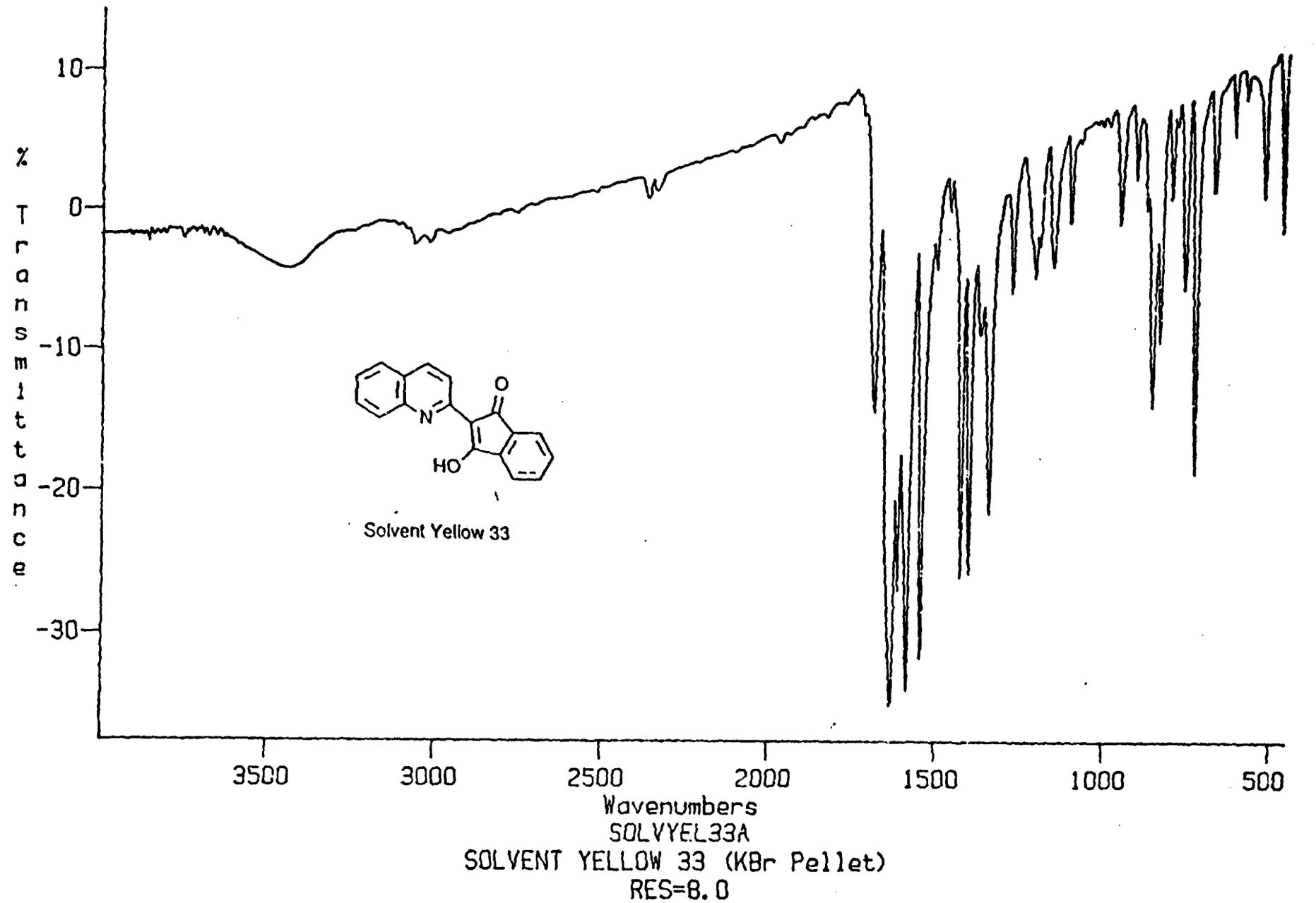
10
0
-10
-20
-30
% Transmittance
3500
3000
2500
2000
1500
1000
500
Wavenumbers
SOLVYEL33A
SOLVENT YELLOW 33 (KBr Pellet)
RES=8.0
O
N
HO
Solvent Yellow 33

Appendix C. UV-VIS Spectra of Smoke Dyes

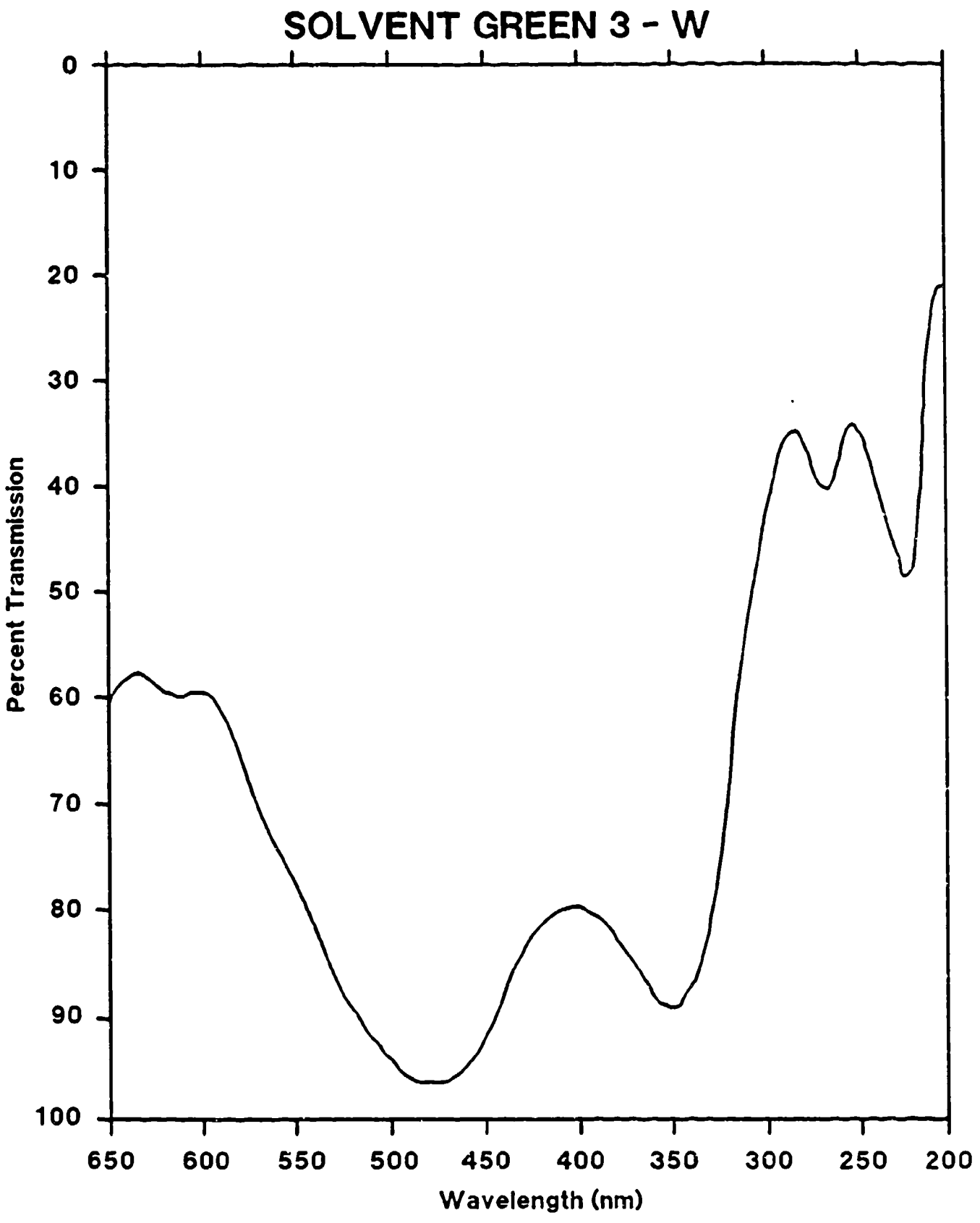
SOLVENT GREEN 3 - W
0
10
20
30
40
50
60
70
80
90
100
Percent Transmission
650
600
550
500
450
400
350
300
250
200
Wavelength (nm)

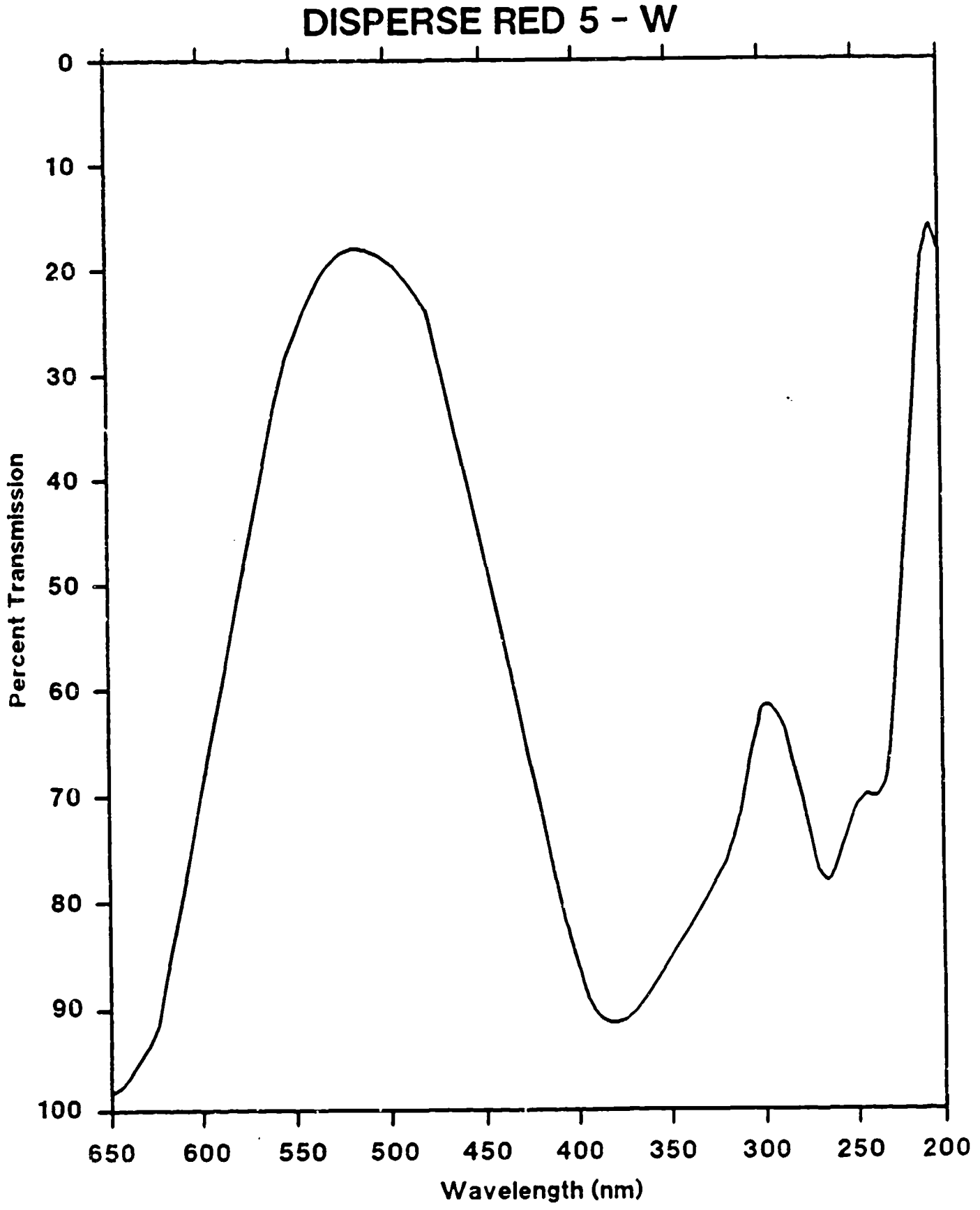
DISPERSE RED 5 - W
0
10
20
30
40
50
60
70
80
90
100
Percent Transmission
650
600
550
500
450
400
350
300
250
200
Wavelength (nm)

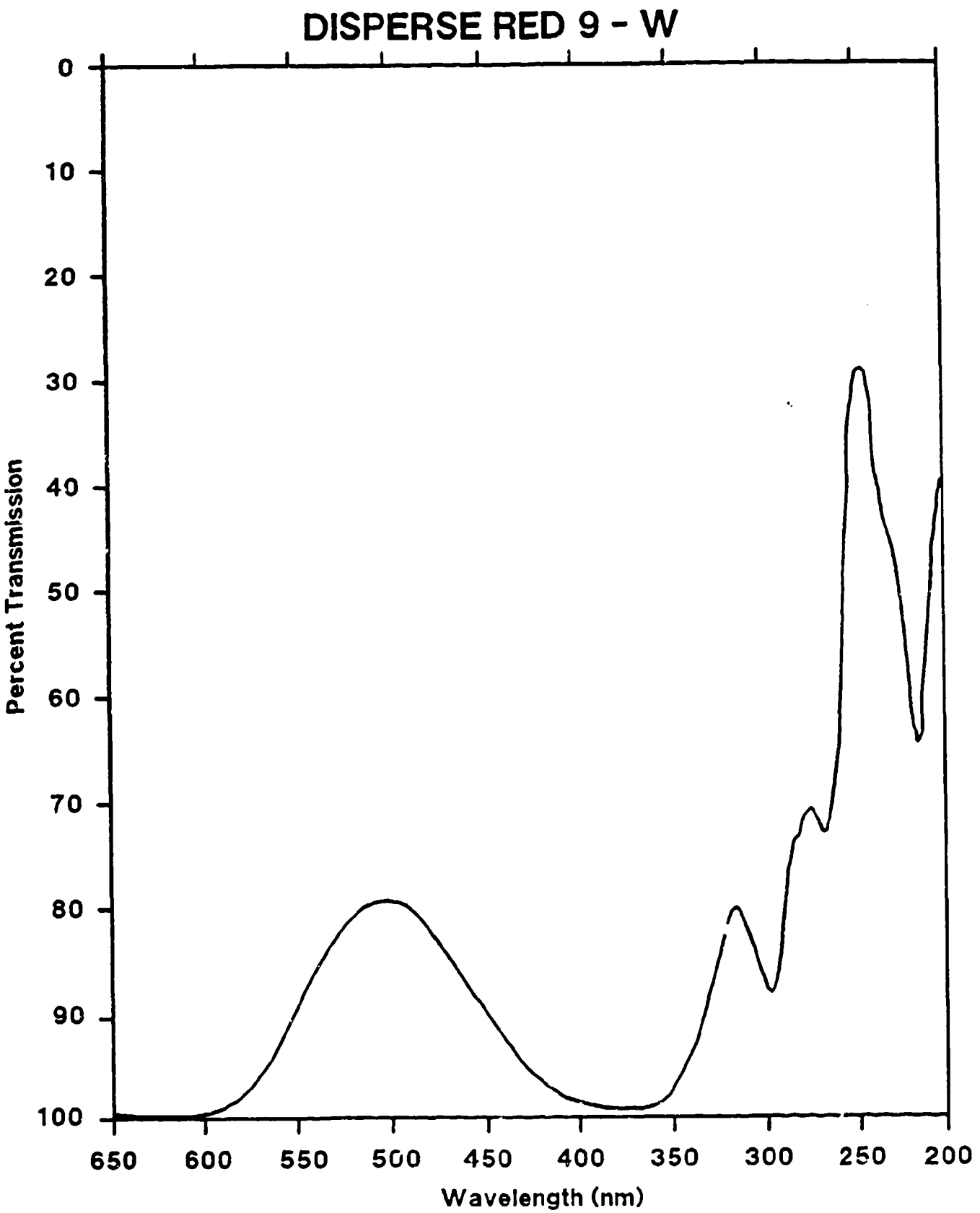
DISPERSE RED 9 - W
Percent Transmission
0
10
20
30
40
50
60
70
80
90
100
650
600
550
500
450
400
350
300
250
200
Wavelength (nm)

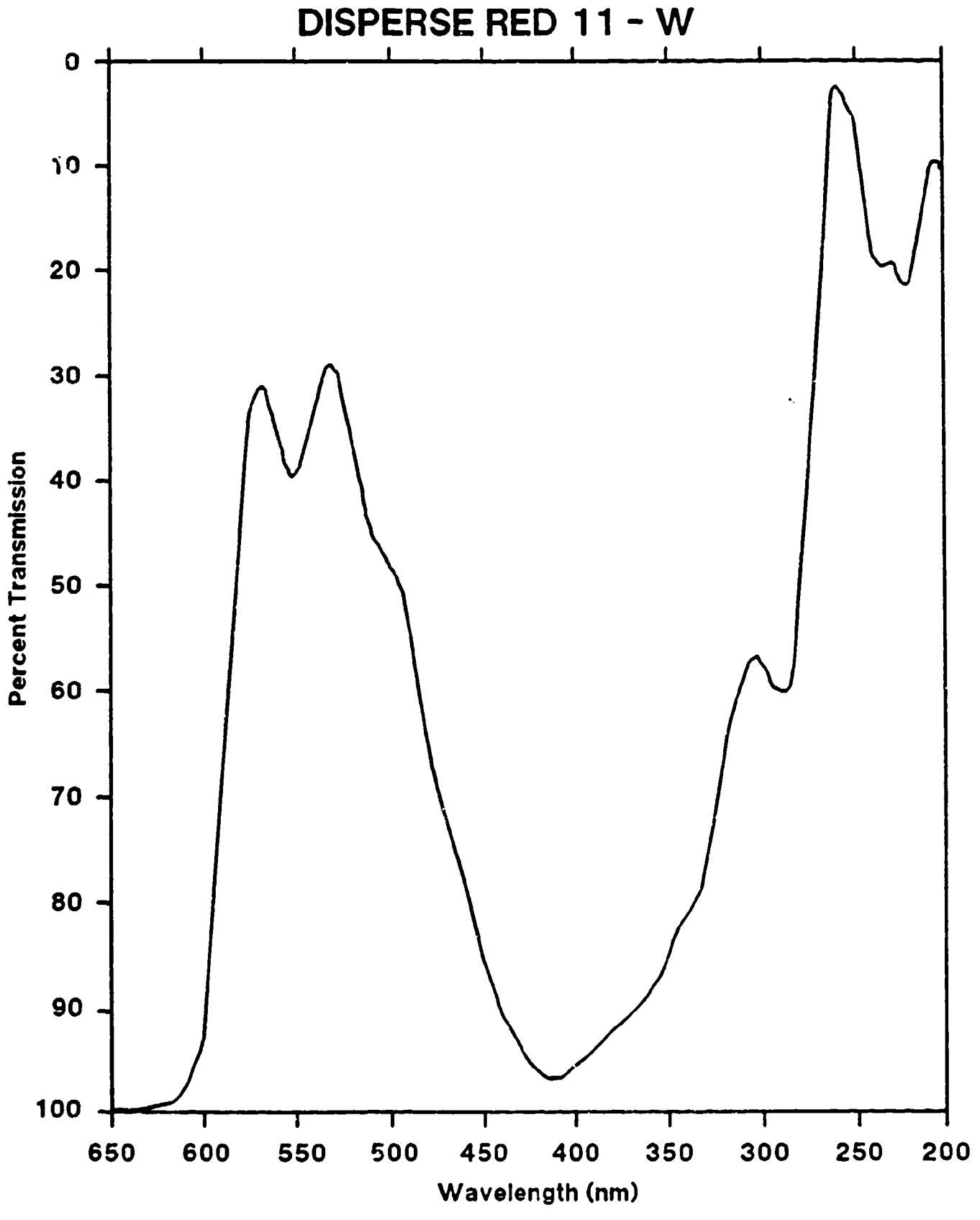
DISPERSE RED 11 - W
0
10
20
30
40
50
60
70
80
90
100
Percent Transmission
650
600
550
500
450
400
350
300
250
200
Wavelength (nm)

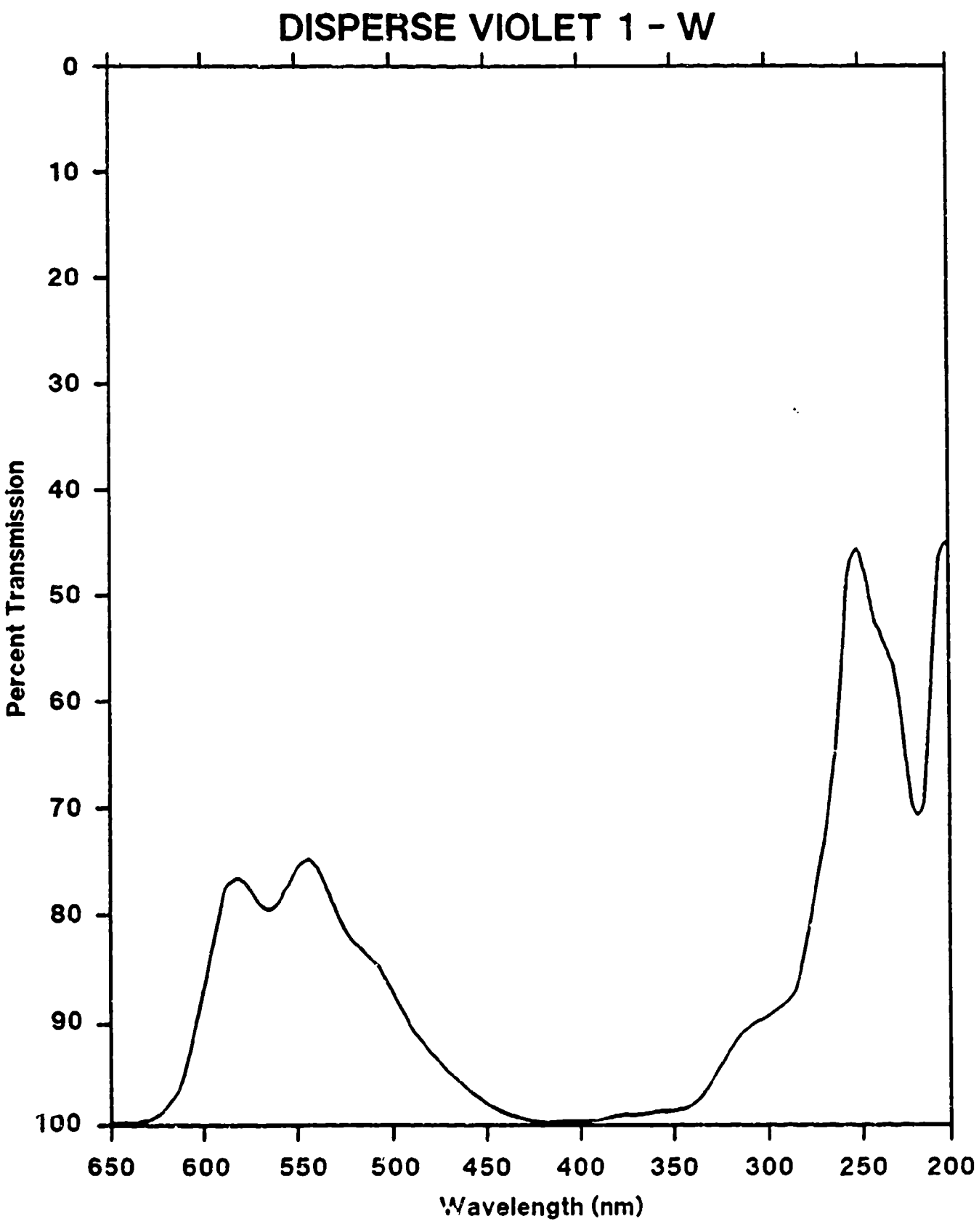
DISPERSE VIOLET 1 - W
Percent Transmission
0
10
20
30
40
50
60
70
80
90
100
650
600
550
500
450
400
350
300
250
200
Wavelength (nm)

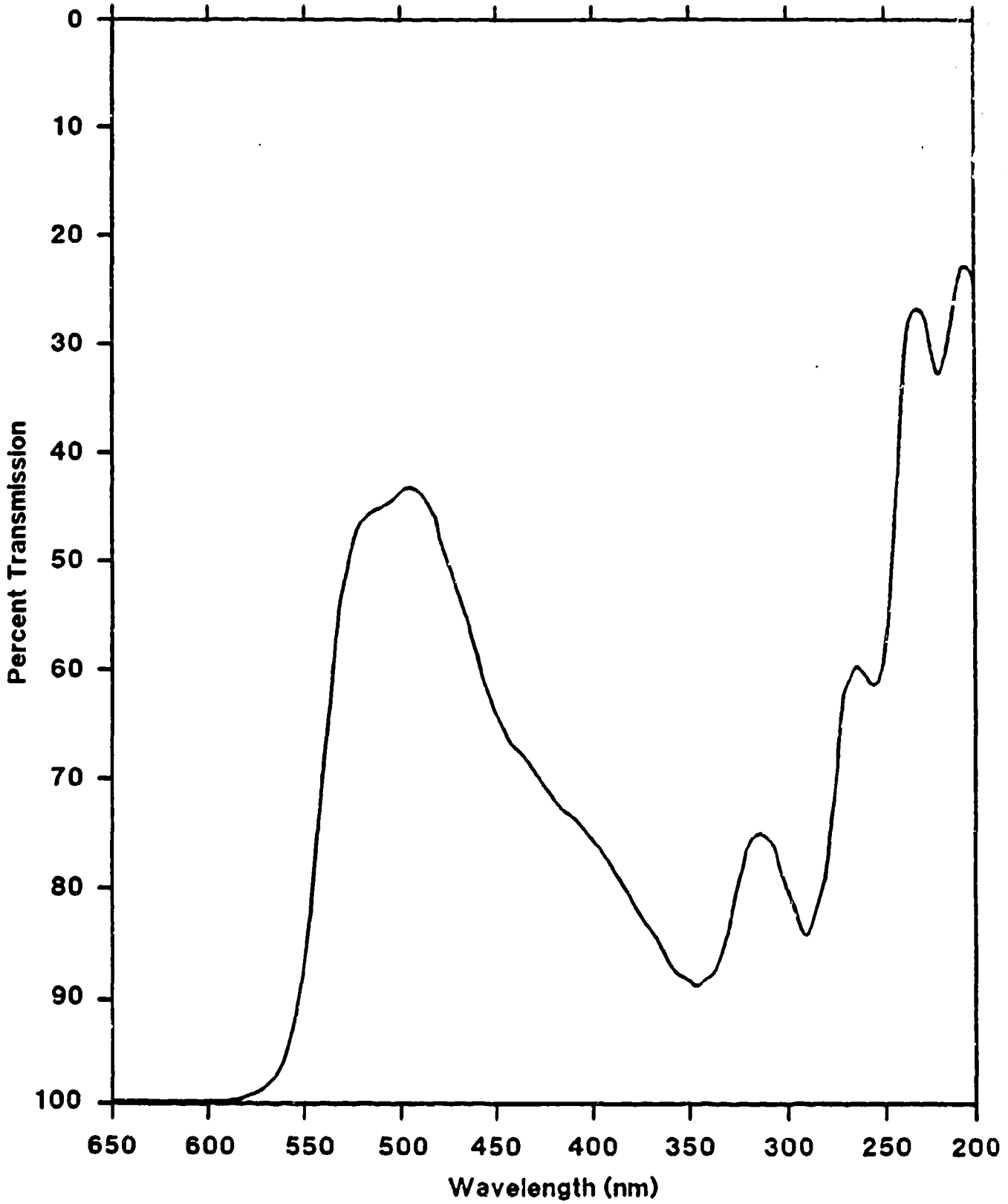
SOLVENT RED 1 - W
0
10
20
30
40
50
60
70
80
90
100
Percent Transmission
650
600
550
500
450
400
350
300
250
200
Wavelength (nm)

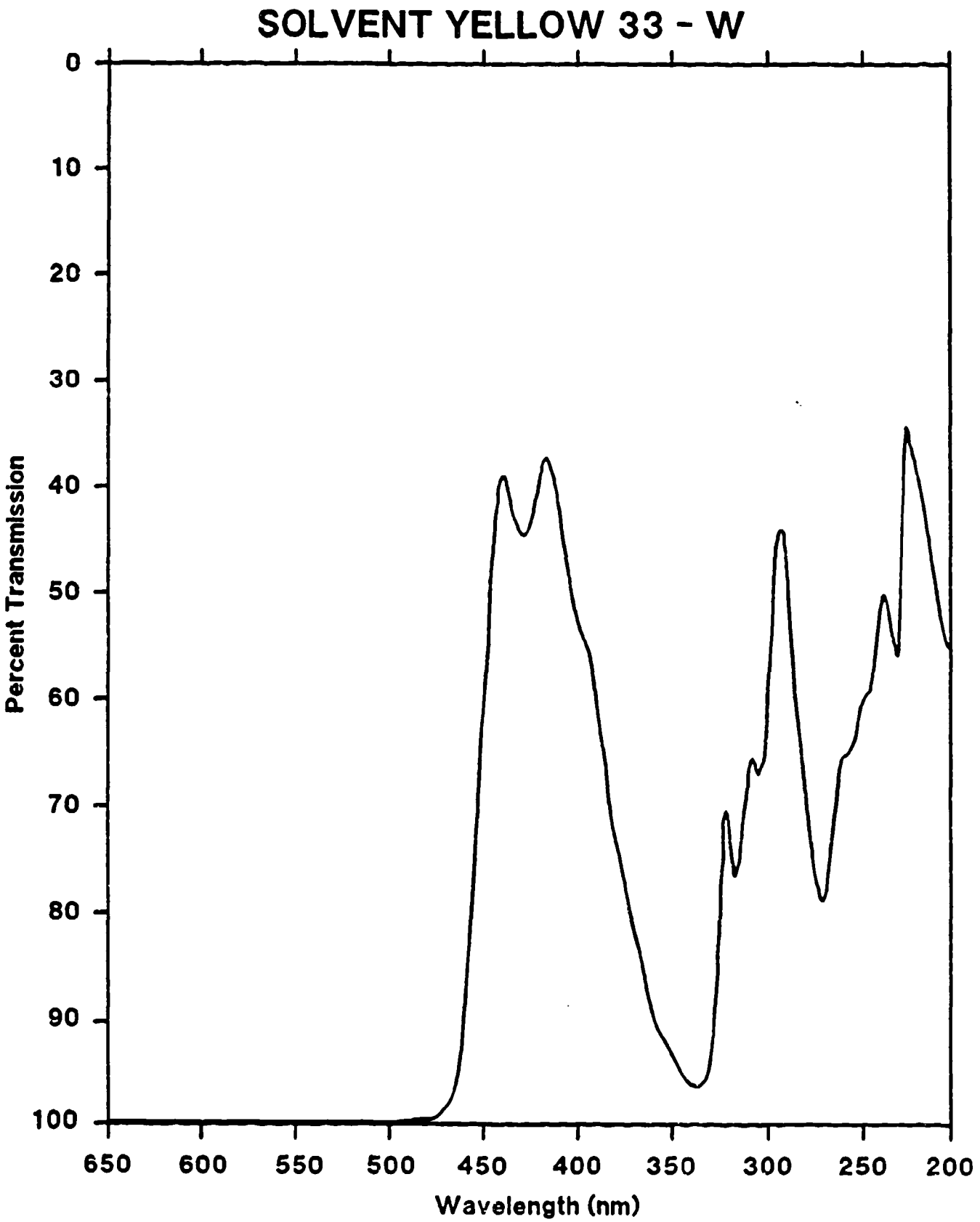
SOLVENT YELLOW 33 - W
Percent Transmission
0
10
20
30
40
50
60
70
80
90
100
650
600
550
500
450
400
350
300
250
200
Wavelength (nm)

Appendix D. Kinetic Data

Disperse Red 9 in Kingfisher

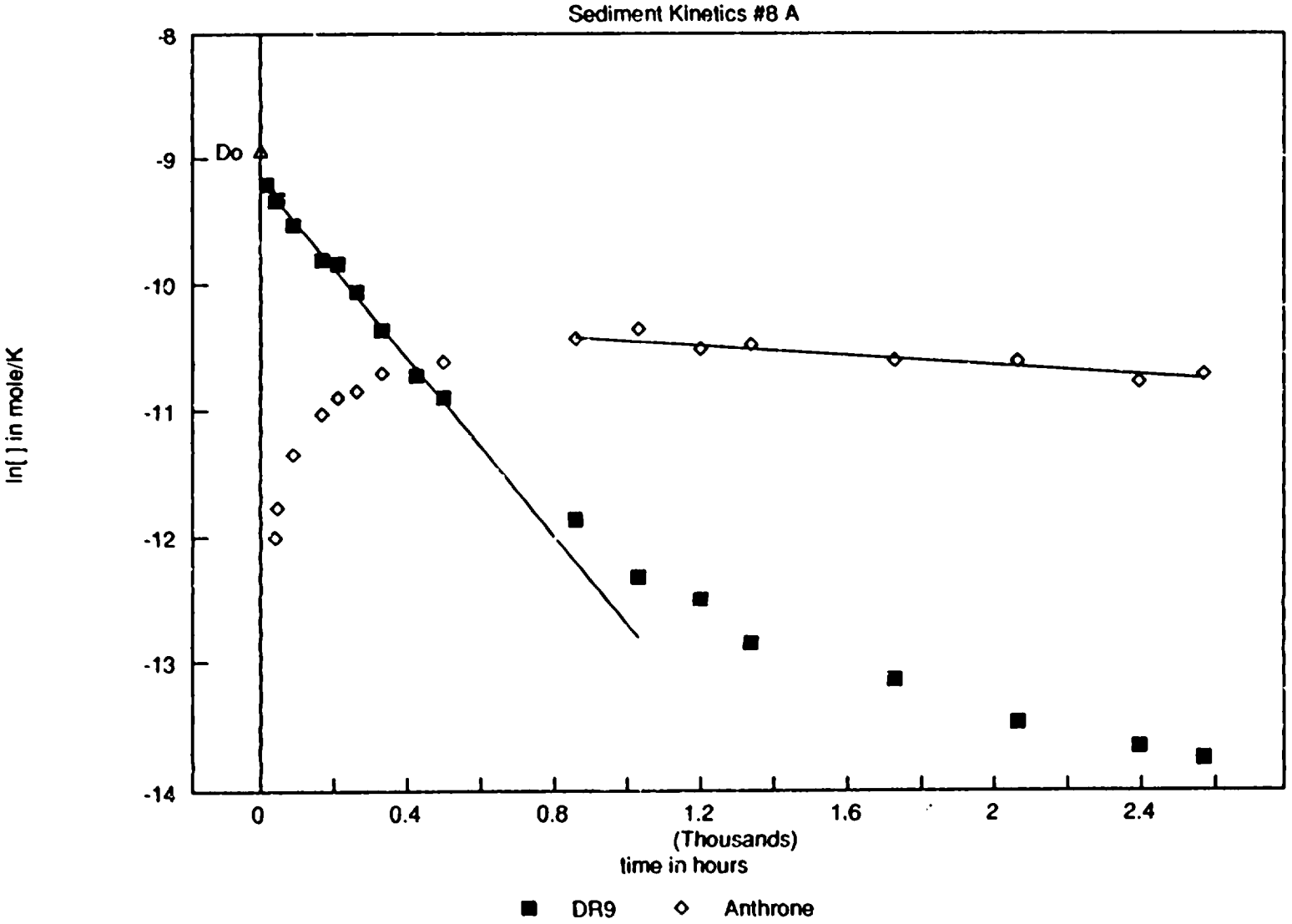

Disperse Red 11 in Kingfisher

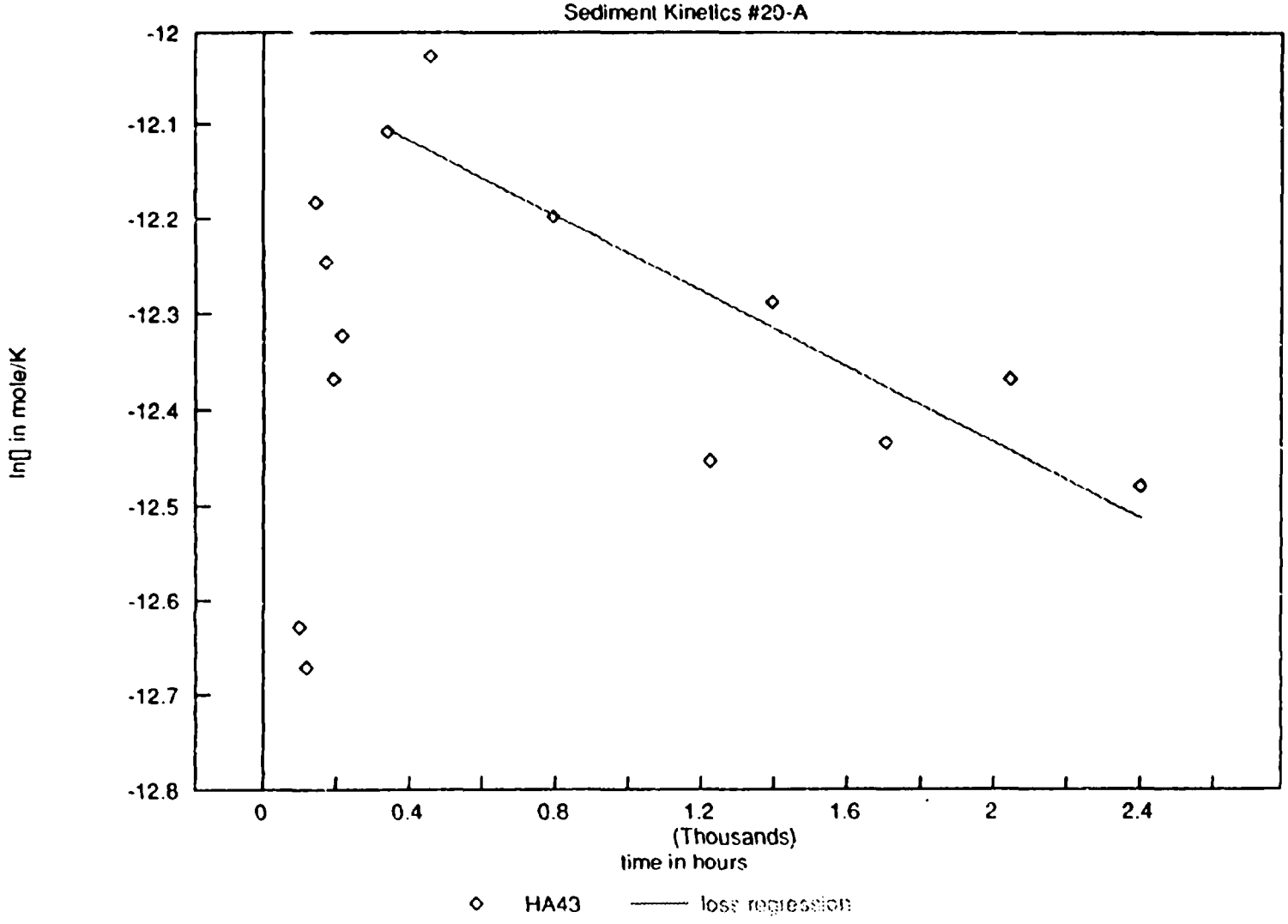

Disperse Red 11 in Kingfisher

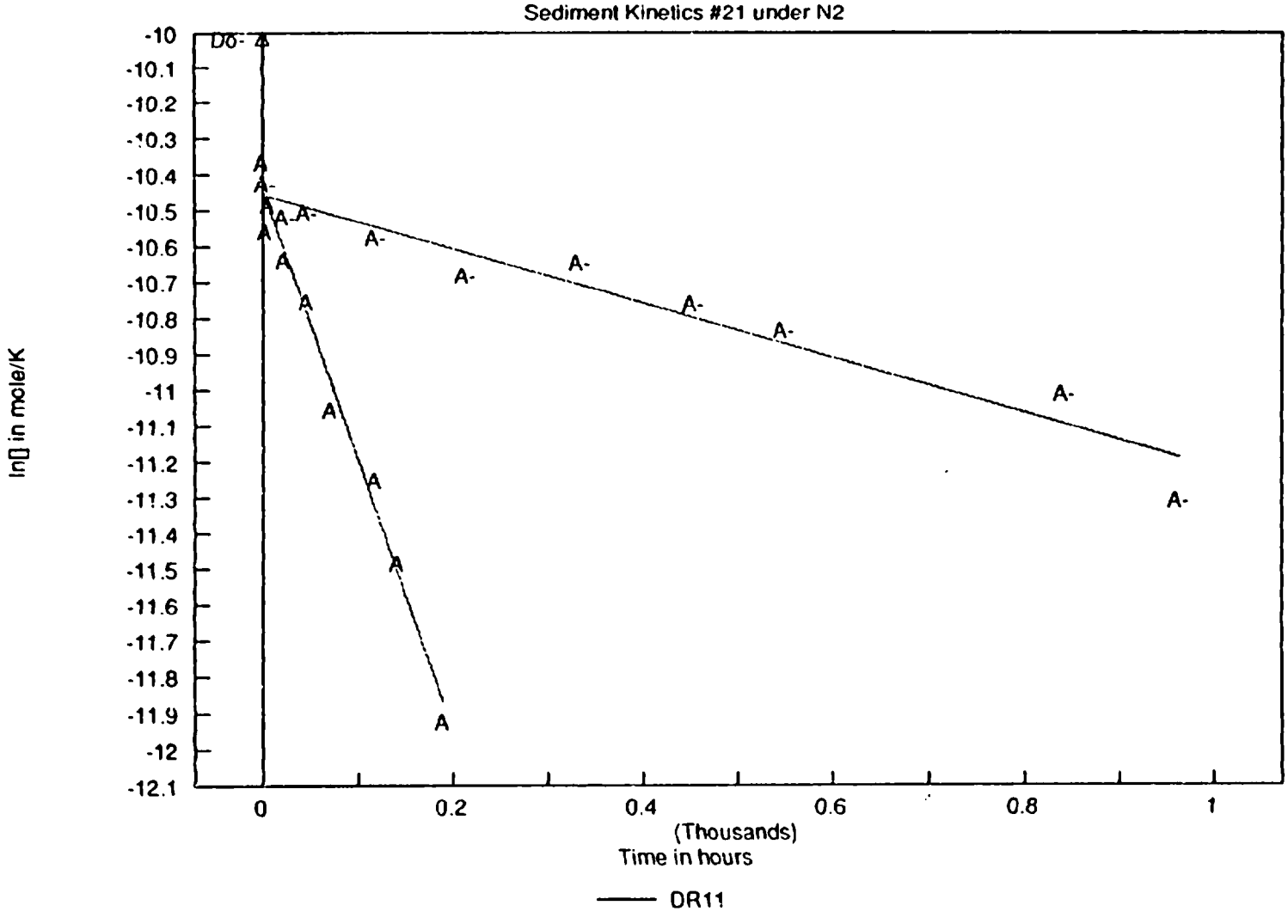

Disperse Red 11 in Kingfisher

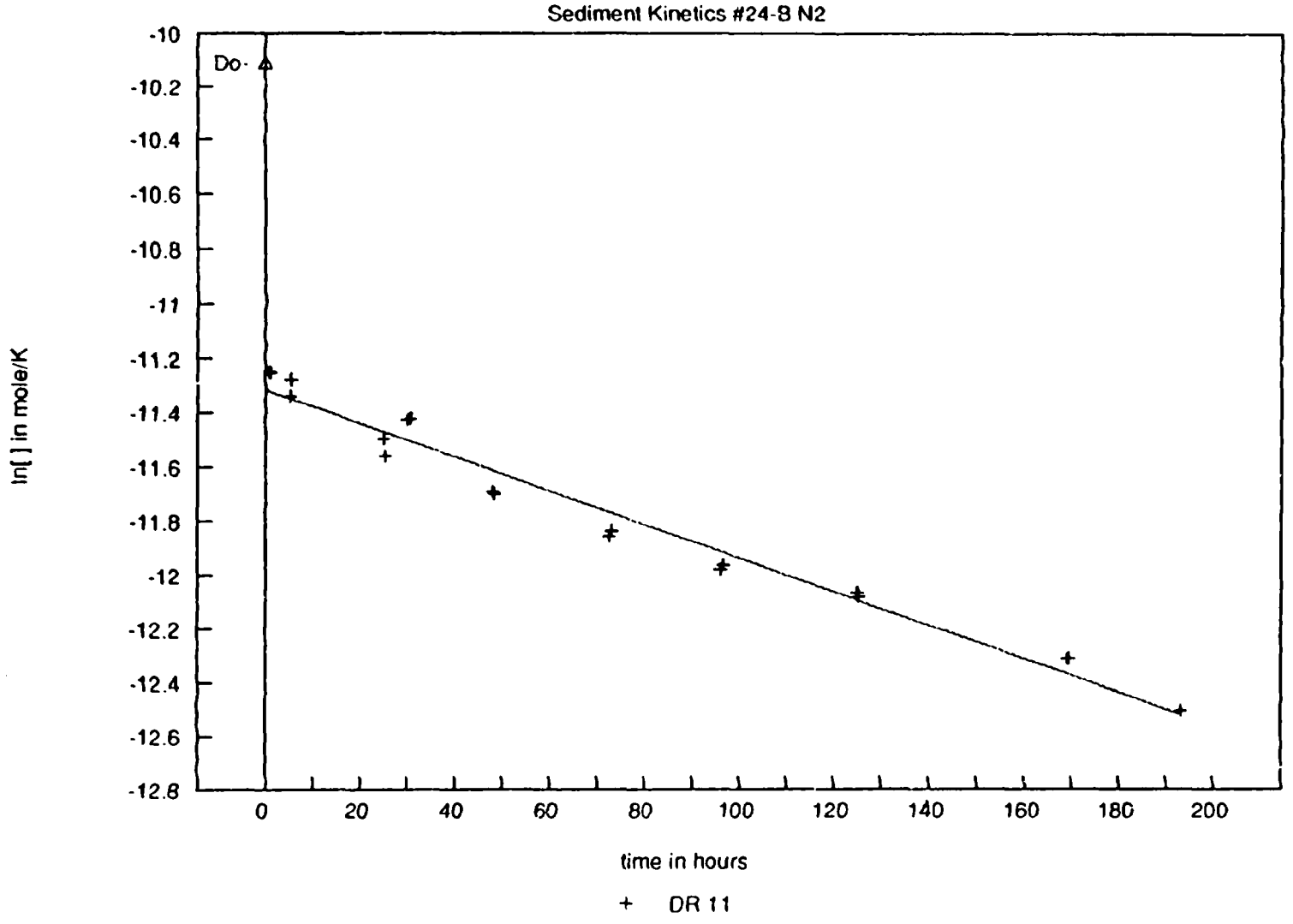

Disperse Red 9 in Kingfisher

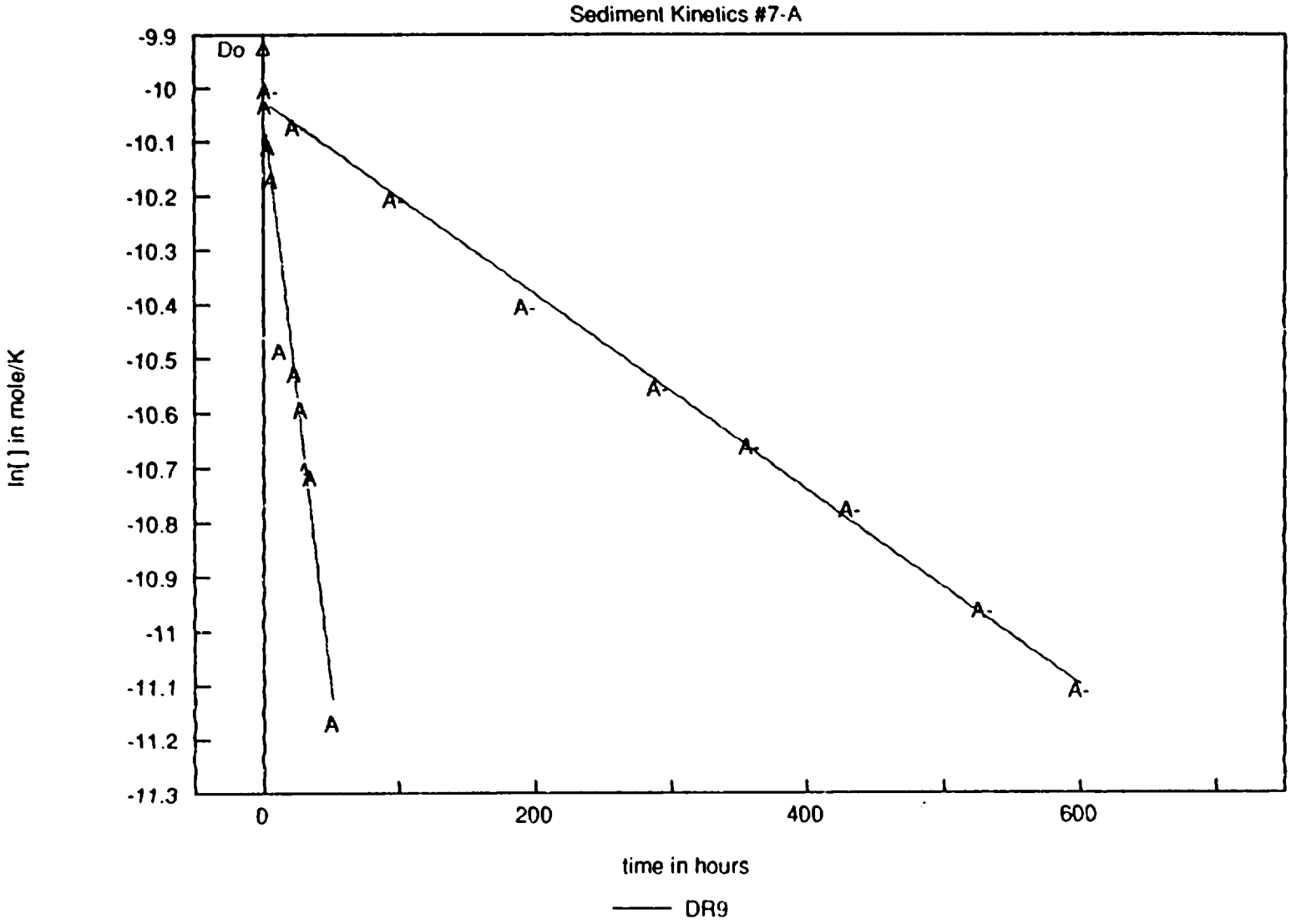

1—Aminoanthraquinone in Herrick #1

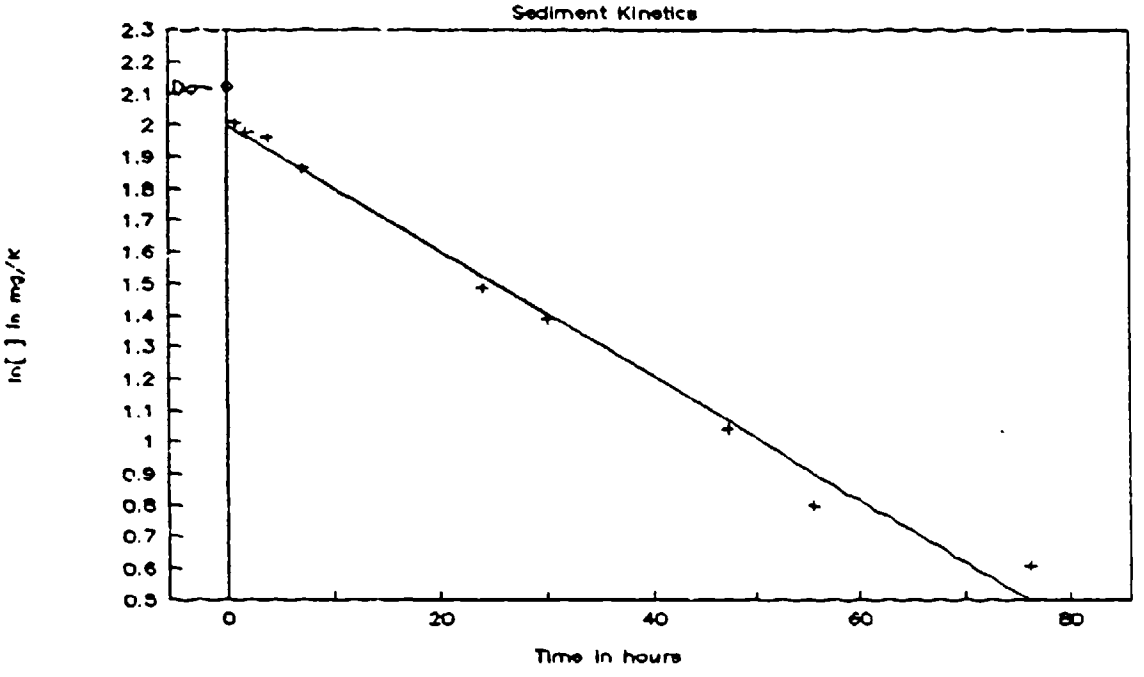

1—Chloroanthraquinone in Herrick

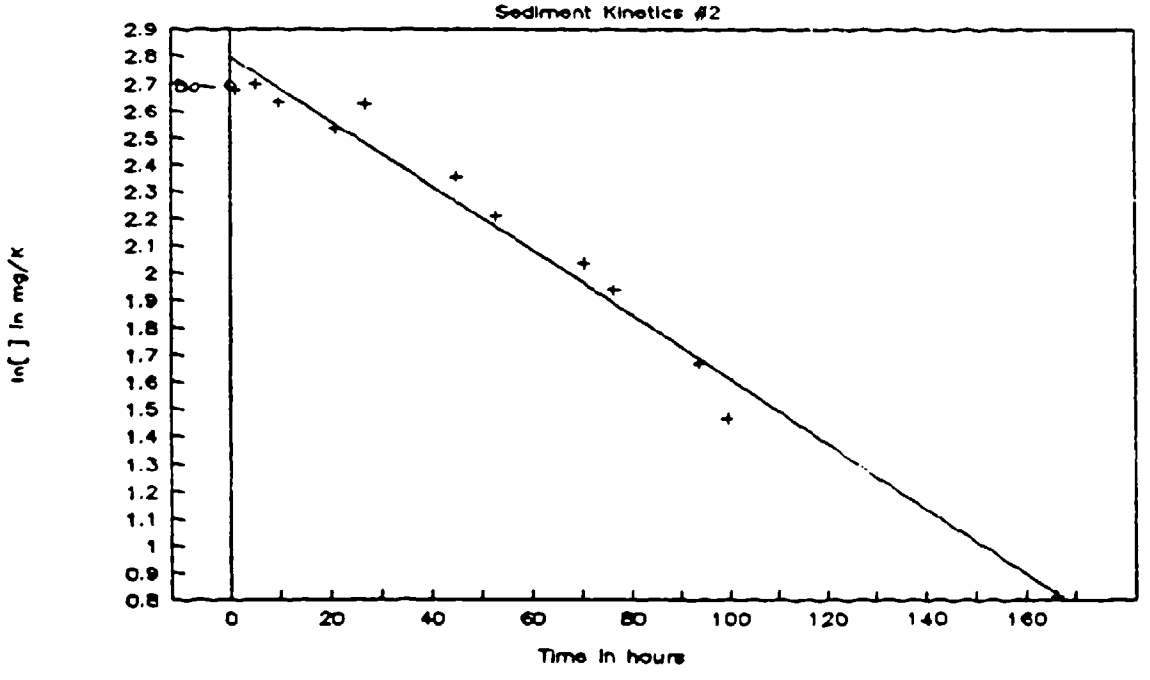

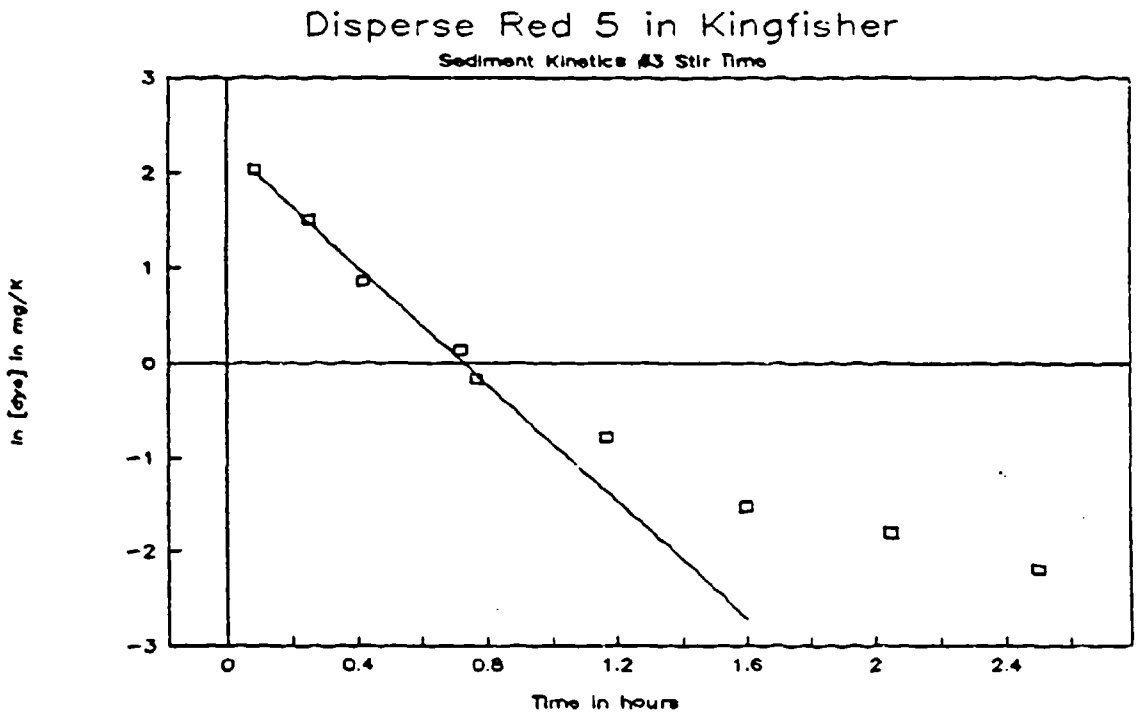
Disperse Red 5 in Kingfisher
Sediment Kinetics #3 Stir Time
ln [dye] in mg/K
Time in hours
3
2
1
0
-1
-2
-3
0
0.4
0.8
1.2
1.6
2
2.4

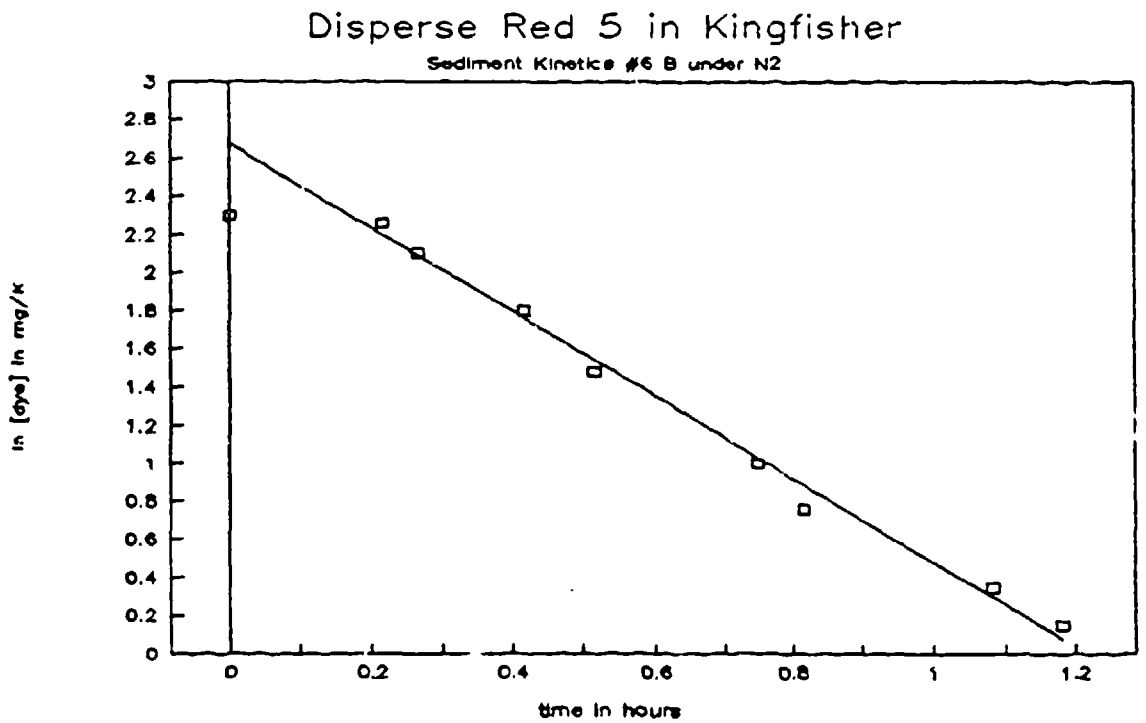
Disperse Red 5 in Kingfisher
Sediment Kinetics #6 B under N2
ln [dye] in mg/K
time in hours
3
2.8
2.6
2.4
2.2
2
1.8
1.6
1.4
1.2
1
0.8
0.6
0.4
0.2
0
0
0.2
0.4
0.6
0.8
1
1.2

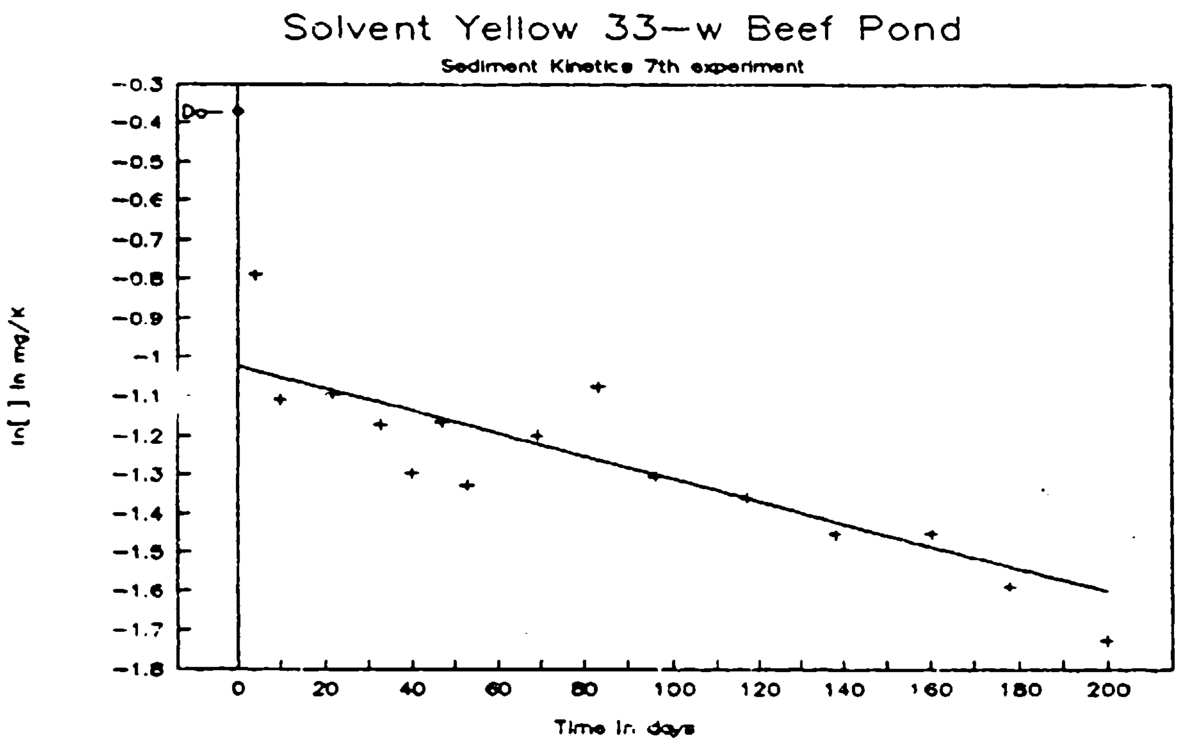
Solvent Yellow 33—w Beef Pond
Sediment Kinetics 7th experiment
ln[ ] ln mg/K
Time in days
Do

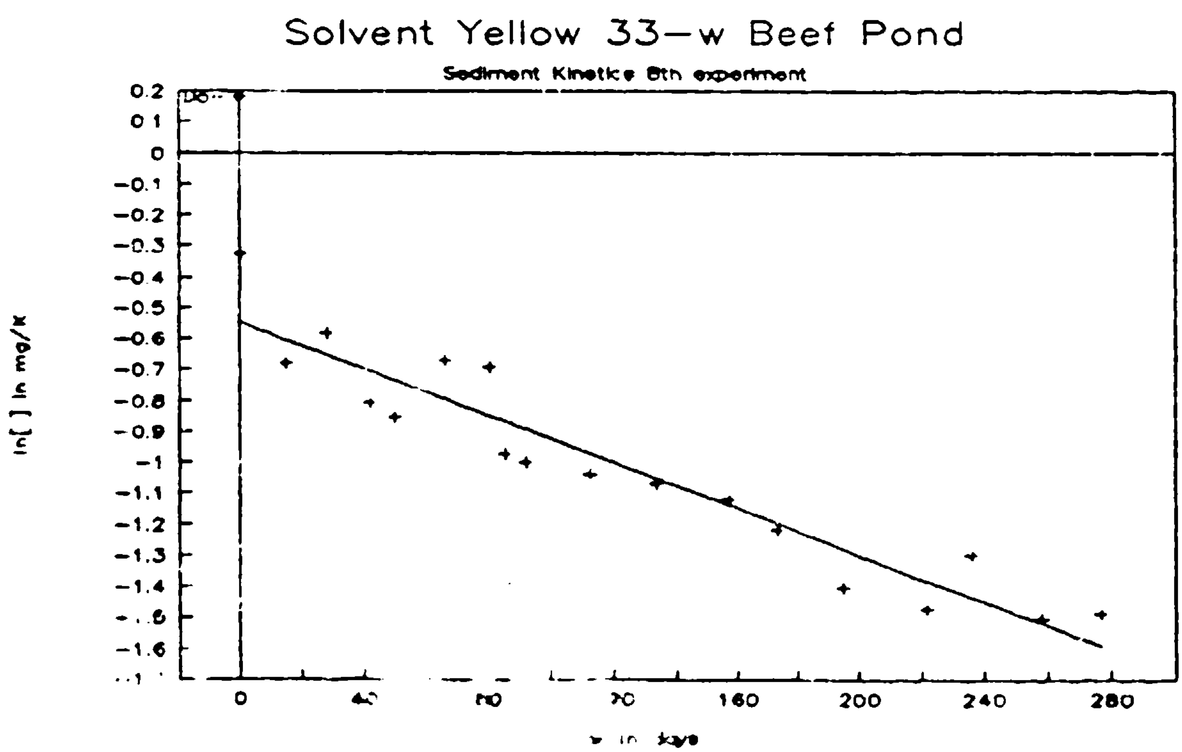
Solvent Yellow 33—w Beef Pond
Sediment Kinetics 8th experiment
ln[ ] ln mg/K

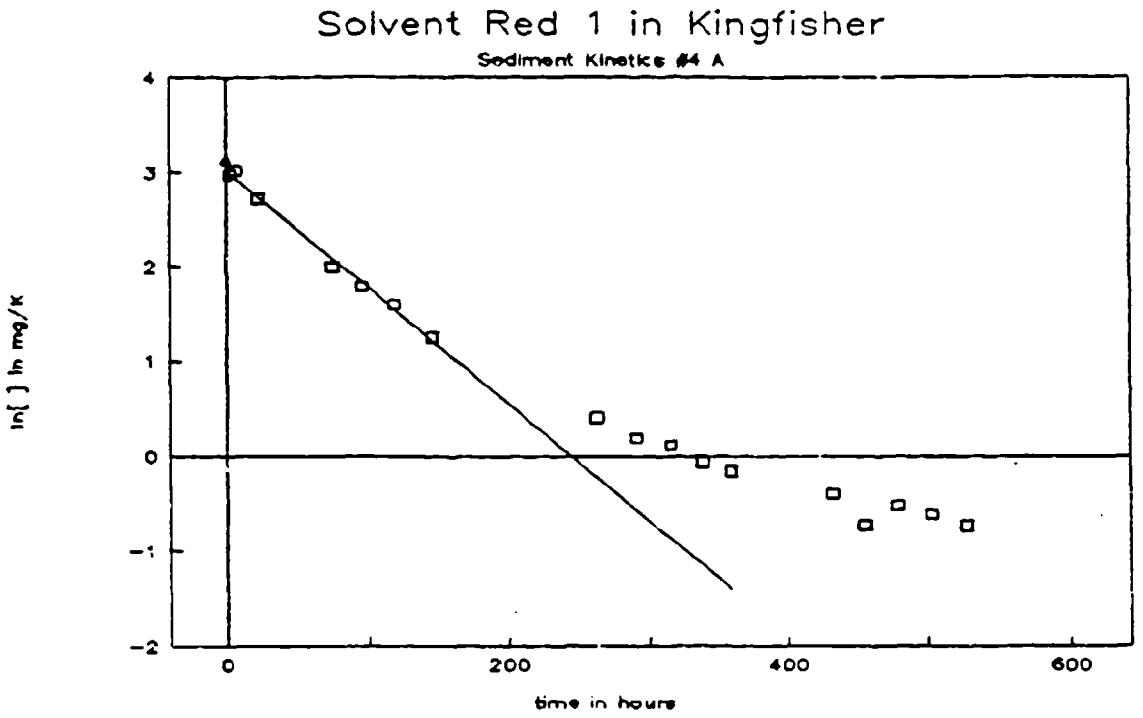
Solvent Red 1 in Kingfisher
Sediment Kinetics #4 A
ln[ ] ln mg/K
4
3
2
1
0
-1
-2
0
200
400
600
time in hours

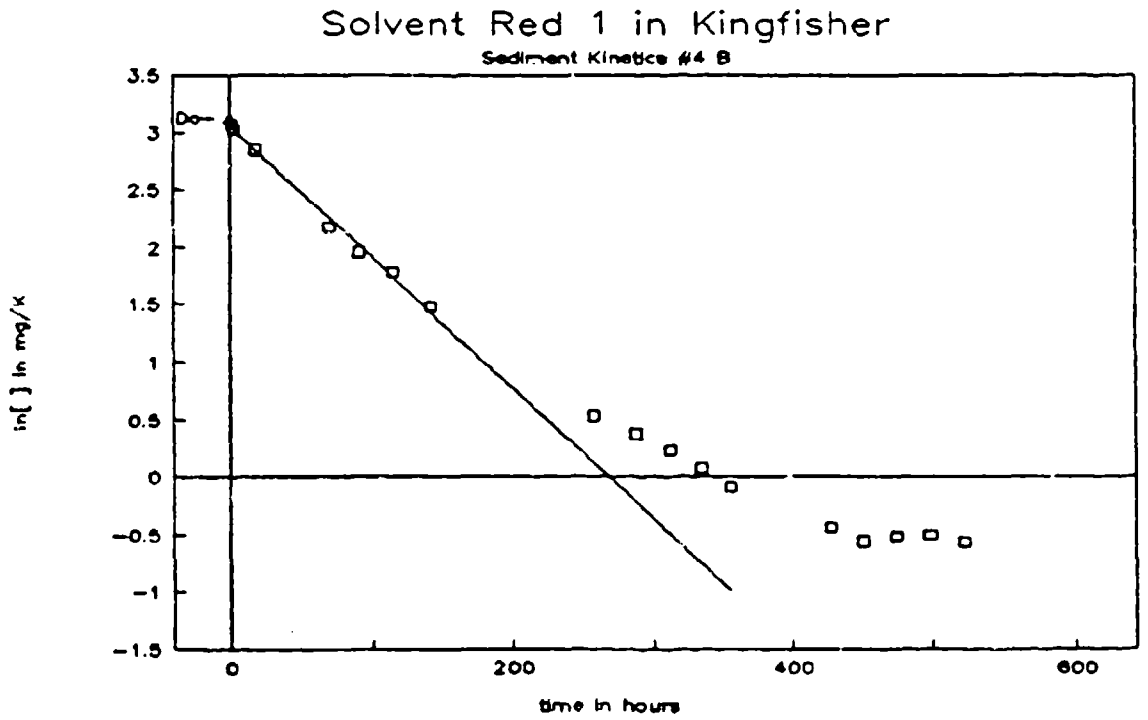
Solvent Red 1 in Kingfisher
Sediment Kinetics #4 B
ln[ ] ln mg/K
3.5
3
2.5
2
1.5
1
0.5
0
-0.5
-1
-1.5
0
200
400
600
time in hours

Solvent Red 1 in Herrick